

**This document was too large to scan  
as a single document. It has  
been divided into smaller sections.**

**Section 2 of 5**

<b>Document Information</b>			
<b>Document #</b>	ISO-100	<b>Revision</b>	
<b>Title</b>	WASTE MANAGEMENT TECHNICAL MANUAL		
<b>Date</b>	08/31/1967		
<b>Originator</b>	J.S. BUCKINGHAM	<b>Originator Co.</b>	ISOCHEM
<b>Recipient</b>		<b>Recipient Co.</b>	
<b>References</b>			
<b>Keywords</b>			
<b>Projects</b>			
<b>Other Information</b>			

BEST AVAILABLE COPY

FIGURESPage

IV-57	Rare Earth Solubility in the Presence of Varying Concentrations of Sulfate and Complexant as a Function of pH -----	4126
IV-58	Chemical Flowsheet for Washing D2EHPA Extractant -----	4132
IV-59	Sodium Operating Diagram - 1S Column PAW Flowsheet Conditions -----	4149
IV-60	Calculation of the Number of Transfer Units ( $N_t$ ) by Graphical Integration -----	4150
IV-61	Effect of Silver and Persulfate Concentration on Cerium Loss to the LCP -----	4178
IV-62	Typical Strontium Semiworks Chemical Flowsheet for Purification of Strontium -----	4182
IV-63	D2EHPA Extraction of Np-Pu from PAS Solution -----	4190
IV-64	Kinetics of Destruction of Oxalic Acid with $HNO_3$ -----	4197
IV-65	Chemical Flowsheet for Recovery of Neptunium and Plutonium from Purex Acid Sludge - Recovery Cycle -----	4198
IV-66	Chemical Flowsheet for Recovery of Neptunium and Plutonium from Purex Acid Sludge - Purification Cycle --	4199
IV-67	Log - Probability Plot of Breakthrough Curves Showing the Effect of the Parameter "A" -----	4208
IV-68	Cumulative Percent Breakthrough Loss as a Function of A and the Throughput Ratio, $n/n_0$ -----	4211
IV-69	Cumulative Breakthrough Loss as a Function of A and $C/C_0$ -----	4211
IV-70	$n_1/n_0$ as a Function of A -----	4212
IV-71	Cross-Plot of Figure IV-67 -----	4212
IV-72	Cesium Recovery from Purex Alkaline Supernate by Linde AW-500 Zeolite Ion Exchange -----	4219
IV-73	Cesium Recovery from Redox Alkaline Supernate by Duolite C-3 Ion Exchange -----	4220
IV-74	Mass Action Quotients for the Exchange of Cesium with Sodium, Potassium, Rubidium, Ammonium and Hydrogen-Based Clinoptilolite -----	4223

<u>FIGURES</u>	<u>Page</u>
IV-75 Mass Action Quotients for the Exchange of Cesium with Sodium, Potassium, Rubidium, and Ammonium-Based Linde AW-400 -----	4224
IV-76 Mass Action Quotients for the Exchange of Cesium with Sodium, Potassium, Rubidium, and Ammonium-Based Linde AW-500 -----	4224
IV-77 Equilibrium Cs/Na Ratios in Zeolite and Solution Phases -----	4225
IV-78 Equilibrium Cesium Loading on Zeolites from Cesium-Sodium Solutions -----	4225
IV-79 Effect of Particle Size on Cesium Breakthrough Curves -----	4228
IV-80 Cesium Breakthrough Curves for Several Zeolites -----	4228
IV-81 Comparison of Cesium Breakthrough from Purex and Redox Supernatants -----	4229
IV-82 Effect of Loading Temperature on Cesium Breakthrough -----	4229
IV-83 Effect of Superficial Flow Rate on Cesium Breakthrough -----	4230
IV-84 Effect of Column Volumes per Hour on Cesium Breakthrough -----	4230
IV-85 Effect of Column Volumes/Hour on the Constant "A" -----	4231
IV-86 Removal of Sodium from Clinoptilolite with Various "Scrub" Solutions -----	4232
IV-87 Removal of Sodium from Linde AW-400 with Various "Scrub" Solutions -----	4232
IV-88 Cesium Loss from Clinoptilolite During Scrubbing for Two Cesium Breakthrough Levels -----	4233
IV-89 Elution of Cesium-137 from Clinoptilolite by Various $2N$ Ammonium Salts -----	4234
IV-90 Elution of Cesium from Clinoptilolite by Three Concentrations of $(NH_4)_2CO_3-NH_4OH$ Solutions -----	4236
IV-91 Cesium Elution from Several Exchangers with $(NH_4)_2CO_3-NH_4OH$ Solutions -----	4237

<u>FIGURES</u>	<u>Page</u>
IV-92 Elution of Cesium from Duolite C-3 with $2M (NH_4)_2CO_3$ -----	4240
IV-93 Effect of Flow Rate on Elution of Cesium from Clinoptilolite with $4N (NH_4)_2CO_3$ Solution -----	4240
IV-94 Cesium Breakthrough Curves for Cesium Product Concentrate -----	4241
IV-95 Cesium Waste Packaging -----	4242
IV-96 Cesium Extraction from Purex Acid Waste -----	4243
IV-97 Effect of Flow Rate on Cesium Breakthrough with Purex Acid Waste -----	4244
IV-98 Effect of Cesium Concentration on Cesium Breakthrough with Purex Acid Waste -----	4244
IV-99 Removal of ZrNb-95 from Clinoptilolite by Four Solutions -----	4244
IV-100 Strontium Waste Packaging Flowsheet -----	4245
IV-101 Variation of Mass Action Quotients with Solution Normality Ratios for the Exchange Reaction $2Na_{Zeolite} + Sr_{Solution} = Sr_{Zeolite} + 2Na_{Solution}$ -----	4247
IV-102 Variation of Mass Action Quotients with Solution Normality Ratios for the Exchange Reaction $Ca_{Zeolite} + Sr_{Solution} = Sr_{Zeolite} + Ca_{Solution}$ -----	4247
IV-103 Variation of Mass Action Quotients with Solution Normality Ratios for the Exchange Reaction $Ca_{Zeolite} + 2Na_{Solution} = 2Na_{Zeolite} + Ca_{Solution}$ -----	4247
IV-104 Effect of Particle Size on the Strontium Breakthrough Curves at 25 C -----	4248
IV-105 Effect of Flow Rate on Strontium Breakthrough Curve -----	4249
IV-106 Effect of Temperature on Strontium Breakthrough Curves -----	4249
IV-107 Technetium Recovery from Purex Alkaline Supernate -----	4250
IV-108 Technetium Distribution on IRA 401 Resin as a Function of $(H^+)$ at Constant $7.5M$ Nitrate -----	4254

FIGURESPage

IV-109	Technetium Distribution on Dowex 1 x 8 from Nitric Acid Solutions -----	4254
IV-110	Technetium Breakthrough Curves -----	4255
IV-111	Elution of Technetium from IRA 401 with 8M HNO <sub>3</sub> -----	4255
IV-112	Cesium Phosphotungstate Flowsheet -----	4260
IV-113	Nickel Ferrocyanide Process - Purex Plant Test I. Cesium Precipitation II. Silver Metathesis -----	4263
IV-114	Optimized Cesium Nickel Ferrocyanide Process -----	4264
IV-115	Effect of Solvent Irradiation on Strontium and Cerium(IV) Extraction -----	4269
IV-116	Hydrogen Ion Complexing by Ligands -----	4280
IV-117	Persulfate Stability in Silver-Free ICX -----	4283

LIST OF TABLES

<u>TABLES</u>		<u>Page</u>
IV-1	Typical Purex Waste Compositions Used in Laboratory and Pilot Plant Strontium Precipitation Studies ---	423
IV-2	Effect of Digestion Time on Strontium Losses -----	427
IV-3	Strontium and Cerium Losses Obtained During Sulfate Cake Washing Studies -----	430
IV-4	Lead, Strontium, and Cerium Dissolution During Metathesis of Lead Sulfate Cake with Carbonate-Hydroxide Mixtures -----	432
IV-5	Strontium and Cerium Losses Obtained During Metathesized-Cake Washing -----	433
IV-6	Effect of Hold-up Time and Centrifugal Force on Centrifugation of Lead Sulfate-Strontium Sulfate Slurries -----	434
IV-7	Settling Rates for Lead Sulfate and Carbonate Precipitates -----	435
IV-8	Approximate Synthetic Waste Compositions Used in Laboratory Studies -----	464
IV-9	Distribution Ratios as a Function of Complexing Agents -----	465
IV-10	Effect of Complexant Type and pH on Distribution Ratios, 25 C -----	466
IV-11	Effect of Complexant Type and pH on Distribution Ratios, 60 C -----	472
IV-12	Effect of Feed HEDTA Concentration on Distribution Ratios -----	474
IV-13	Effect of Feed Citrate Concentration on Distribution Ratios -----	474
IV-14	Extraction Kinetics: Citrate and Tartrate Feeds -----	475
IV-15	Effect of Feed Impurities on the Extraction of Strontium and Cerium from Citrate-Complexed Feeds -----	484
IV-16	Effect of Citrate Concentration on Partition Column Distribution Ratios -----	493
IV-17	Composition of Impure Strontium Fractions -----	4111

<u>TABLES</u>	<u>Page</u>
IV-18 Comparison of Complexing Agents -----	4113
IV-19 1B Column Distribution Ratios -----	4116
IV-20 Estimated Composition of Rare Earth - Americium Fraction -----	4122
IV-21 NaOH-Complexant Solvent Washes -----	4129
IV-22 Multiple Batch Washing of Strontium Semiworks Solvent -----	4129
IV-23 HNO <sub>3</sub> -KMnO <sub>4</sub> Washing of D2EHPA Solvents -----	4130
IV-24 B-Plant Pulse Column Specifications -----	4158
IV-25 Nozzle Plate Cartridge Used in CSW Runs -----	4158
IV-26 Typical "Cold" Semiworks LAF Compositions -----	4159
IV-27 1A Column Capacity Summary -----	4160
IV-28 Effect of Temperature and Interface Position on Cerium Extraction -----	4162
IV-29 Effect of Frequency on 1A Column Performance -----	4163
IV-30 1A Column Performance with ZAW Feed -----	4164
IV-31 Effect of Feed pH on Europium Extraction -----	4166
IV-32 Effect of Temperature and Interface Position on Europium Extraction -----	4167
IV-33 1S Column Capacity Summary -----	4168
IV-34 1S Column Sodium Scrubbing Performance -----	4169
IV-35 Nickel Extraction and Scrubbing Behavior -----	4170
IV-36 1B Column Capacity Summary -----	4170
IV-37 Calcium and Cerium Decontamination Performance -----	4172
IV-38 1C Column Capacity Studies -----	4174
IV-39 Cerium Stripping Efficiency Studies -----	4175
IV-40 Threshold Conditions for Precipitation of Rare Earth Sulfates in the LCP -----	4179

<u>TABLES</u>	<u>Page</u>
IV-41 Summary of Typical Strontium Semiworks Experience in Purifying Strontium Crudes -----	4181
IV-42 PAW Flowsheet Demonstration Run Summary - Promethium Process Test No. 4 -----	4183
IV-43 Over-all Promethium, Cerium, and Strontium Material Balances for Promethium Process Test No. 2 ----	4184
IV-44 ZAW Flowsheet Demonstration Run Summary -----	4185
IV-45 D2EHPA Extraction of Neptunium and Plutonium from PAS Solution -----	4191
IV-46 Oxalic Acid Stripping of Plutonium and Neptunium -----	4192
IV-47 Extraction Contact-Decontamination Performance -----	4193
IV-48 Strip Contact-Decontamination Performance -----	4193
IV-49 Purification Cycle Extraction Contact -----	4194
IV-50 Solvent Washing Studies -----	4195
IV-51 Zeolite Properties -----	4204
IV-52 Ion Exchange Resin Properties -----	4206
IV-53 Empirical Constants for Determining Pressure Drops in Beds of Ion Exchange Material -----	4216
IV-54 Synthetic Alkaline Supernate Waste Compositions Used in Column Loading Studies -----	4226
IV-55 Effect of Temperature and Ammonia Concentrations on Gassing of $(\text{NH}_4)_2\text{CO}_3$ Solutions -----	4235
IV-56 Technetium Distribution from Simulated Purex Waste Supernates at Various Dilutions -----	4251
IV-57 Effect of Anion Composition on Technetium $K_d$ at pH 10 -----	4252
IV-58 Selected Physical Properties of D2EHPA -----	4267
IV-59 G Values and Irradiation Parameters for D2EHPA Study -----	4268
IV-60 Properties of Irradiated D2EHPA - TBP - Diluent Solvents -----	4270

TABLESPage

IV-61	Selected Physical Properties of TBP -----	4273
IV-62	Material Balance Data and G Values for TBP Irradiation -----	4274
IV-63	Properties of Diluents -----	4275
IV-64	Physical Properties of Complexants -----	4278
IV-65	Physical Properties of Complexants -----	4278
IV-66	Selected Acid Dissociation Constants -----	4279
IV-67	Selected Formation Constants -----	4281
IV-68	Selected Physical Properties of Aqueous Hydrogen Peroxide Solutions -----	4285

<u>TABLES</u>	<u>Page</u>
IV-41 Summary of Typical Strontium Semiworks Experience in Purifying Strontium Crudes -----	4181
IV-42 PAW Flowsheet Demonstration Run Summary - Promethium Process Test No. 4 -----	4183
IV-43 Over-all Promethium, Cerium, and Strontium Material Balances for Promethium Process Test No. 2 ----	4184
IV-44 ZAW Flowsheet Demonstration Run Summary -----	4185
IV-45 D2EHPA Extraction of Neptunium and Plutonium from PAS Solution -----	4191
IV-46 Oxalic Acid Stripping of Plutonium and Neptunium -----	4192
IV-47 Extraction Contact-Decontamination Performance -----	4193
IV-48 Strip Contact-Decontamination Performance -----	4193
IV-49 Purification Cycle Extraction Contact -----	4194
IV-50 Solvent Washing Studies -----	4195
IV-51 Zeolite Properties -----	4204
IV-52 Ion Exchange Resin Properties -----	4206
IV-53 Empirical Constants for Determining Pressure Drops in Beds of Ion Exchange Material -----	4216
IV-54 Synthetic Alkaline Supernate Waste Compositions Used in Column Loading Studies -----	4226
IV-55 Effect of Temperature and Ammonia Concentrations on Gassing of $(\text{NH}_4)_2\text{CO}_3$ Solutions -----	4235
IV-56 Technetium Distribution from Simulated Purex Waste Supernates at Various Dilutions -----	4251
IV-57 Effect of Anion Composition on Technetium $K_d$ at pH 10 -----	4252
IV-58 Selected Physical Properties of D2EHPA -----	4267
IV-59 G Values and Irradiation Parameters for D2EHPA Study -----	4268
IV-60 Properties of Irradiated D2EHPA - TBP - Diluent Solvents -----	4270

TABLES

	<u>Page</u>
IV-61 Selected Physical Properties of TBP -----	4273
IV-62 Material Balance Data and G Values for TBP Irradiation -----	4274
IV-63 Properties of Diluents -----	4275
IV-64 Physical Properties of Complexants -----	4278
IV-65 Physical Properties of Complexants -----	4278
IV-66 Selected Acid Dissociation Constants -----	4279
IV-67 Selected Formation Constants -----	4281
IV-68 Selected Physical Properties of Aqueous Hydrogen Peroxide Solutions -----	4285

DECLASSIFIED

CHAPTER IV: PROCESS CHEMISTRY AND ENGINEERING

A. SCOPE AND ARRANGEMENT OF CHAPTER

This chapter describes and discusses the process chemistry and engineering of those waste management precipitation, solvent extraction, and ion exchange processes performed in the B-Plant proper. Because of the broad spectrum of subjects treated, this chapter is a very lengthy one. It is appropriate, therefore, to sketch for the reader in a general fashion what is covered in each of the sections of this chapter.

Section B describes head-end processes for preparing suitable feedstocks for subsequent solvent extraction operations. Specifically discussed are removal and leaching of solids from Purex Acid Waste and lead sulfate carrier precipitation of a strontium-rare earth fraction from Purex Acid Sludge solution.

Section C treats in detail the theory and application of D2EHPA solvent extraction processes to the recovery and purification of strontium, rare earths, and americium from the various waste solutions.

Engineering concepts of solvent extraction and solvent extraction equipment are discussed in Section D. Pulse column demonstration runs of several of the B-Plant solvent extraction processes are also described in this section.

Purex Acid Sludge solutions contain considerable quantities of neptunium and plutonium. A batch D2EHPA extraction process suitable for recovery of these actinides has been developed and is discussed in Section E.

Ion exchange processes for recovery of Cs-137 and Tc-99 from alkaline waste supernate solutions form the subject matter for Section F. The theory of zeolite exchange systems and their application in storing purified Sr-90 and Cs-137 fractions is also covered in this section.

Two alternate precipitation schemes for recovering Cs-137 from various waste solutions - the cesium phosphotungstate and the cesium nickel ferrocyanide processes - are discussed in Section G.

Finally, in Section H are tabulated and discussed selected chemical and physical properties of many of the chemicals used in the waste management solvent extraction processes.

DECLASSIFIED

B. HEAD-END PROCESSES

1. Clarification of PAW Solution

1.1 Source and Characterization of Solids

Purex Acid Waste (PAW) solution is made by sugar denitration of Purex LWW solution<sup>(4)</sup>. Purex LWW solution is known to contain at least 4 vol % solids. The most significant and comprehensive examination of the LWW solids is that of Van Tuyl<sup>(13)</sup>. His data indicate the solids are largely  $Zr_3(PO_4)_4 \cdot xH_2O$  (30 vol %) and  $SiO_2 \cdot xH_2O$  (60 vol %); metal silicates,  $BaSO_4$ , and  $PbSO_4$  account for the other 10 vol %. Van Tuyl found the solids to be gelatinous but readily centrifugable. No single chemical reagent tested completely dissolved the solids, but successive leaches with 7M  $HNO_3$ , 0.5M oxalic acid, 1-2M  $NaOH$ , and 0.5M sodium tartrate in 1M  $NaOH$  dissolved the major portion. These leaching experiments indicated that as much as 75% of the zirconium and 90% of the niobium in the LWW solution are probably adsorbed on these solids. Much smaller amounts of other nuclides (Ce-144, Sr-90, etc) appear to be present on these solids.

Laboratory and Purex plant tests in progress as this manual was written demonstrate additional solids can precipitate, depending on conditions, during sugar denitration of LWW solution. For example, in laboratory experiments with plant LWW solution (concentrated to a volume equivalent to 50 gal of waste per ton of uranium processed), dense, black, crystalline solids precipitated when sugar was added to adjust the acidity to about 1M<sup>(10)</sup>. X-ray diffraction analyses tentatively identify them as sulfates. Limited Purex plant experience with centrifugation of denitrated LWW solution appears to be in agreement with the laboratory work<sup>(8)</sup>. The plant experience indicates denitrated LWW contains 10 to 20 vol % solids. Also, plant results indicate about 60% of the Sr-90, about 70% of the Ce-144, about 50% of the Sb-125, and 90-100% of the ZrNb-95 activity in the LWW are associated with these solids.

A significant laboratory observation is that little or no sulfate solids precipitate when 75 gal/ton LWW is denitrated to about 1M acid. Obviously, if further laboratory and plant tests confirm that sulfate solids do not precipitate at 75 gal/ton, dilution to this volume before denitration would appear to be a highly efficient way of avoiding, or at least minimizing, a difficult problem.

1.2 Leaching Procedures

As this manual was written only one Purex plant test of leaching of solids produced during denitration of LWW solution had been conducted with inconclusive results<sup>(8)</sup>. In this test, solids from 1750 gal of denitrated LWW were leached at 80 C successively with about 400 gal of 4 M  $HNO_3$  and 450 gal of 2M  $NaOH$ -0.1M tartrate. The  $HNO_3$  leach removed about 25% of the Sr-90 and about 50% of the Ce-144. The efficiency of the  $NaOH$ -tartrate leach could not be established because of analytical difficulties.

DECLASSIFIED

420

1.3 Chemical Flowsheet

A chemical flowsheet for the centrifugation and leaching of Purex Acid Waste solids is given in Figure IV-1<sup>(11)</sup>. In view of the present (mid-1966) inadequate knowledge of the formation, composition, and leach properties of PAW solids, the flowsheet should be regarded as conceptual only.

2. Lead Sulfate Carrier Precipitation Process

2.1 Introduction

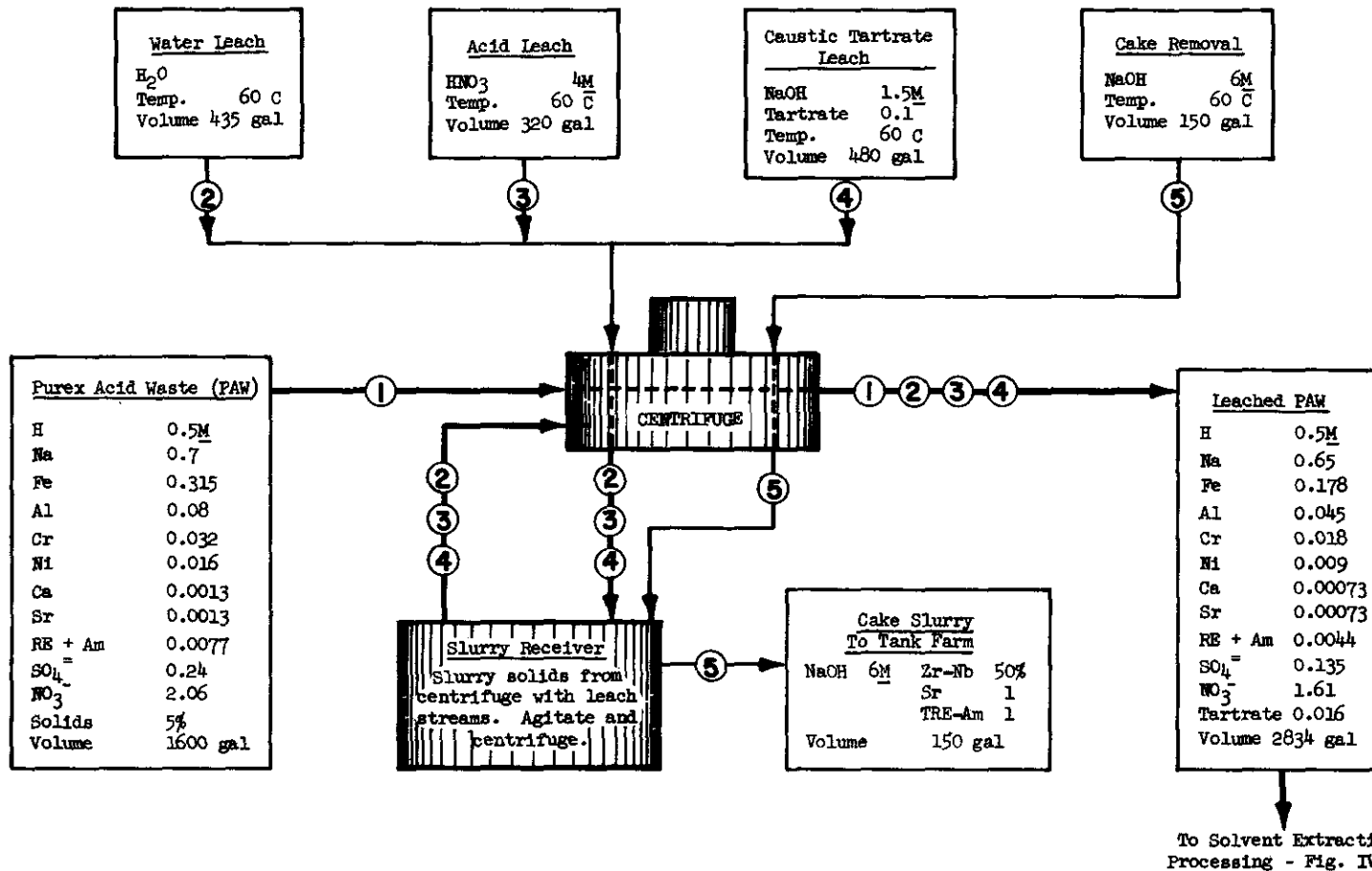
A lead sulfate carrier precipitation process was developed in 1960 for recovering Sr-90 from Purex high level waste (LHW)<sup>(2,6,7,14)</sup>. The process, shown in Figure IV-2, has the following steps:

1. Add hydroxyacetic acid (originally tartaric acid) to complex iron.
2. Adjust the sulfate concentration to about 1M by the addition of  $\text{Na}_2\text{SO}_4$ .
3. Neutralize the solution to pH 0.7 to 2 with NaOH.
4. Heat to 90 C and digest 30 min to precipitate the double salt  $\text{Na}_2\text{SO}_4 \cdot \text{RE}_2(\text{SO}_4)_3 \cdot 2\text{H}_2\text{O}$ <sup>(15)</sup>.
5. Add  $\text{Pb}(\text{NO}_3)_2$  to 0.02M to co-precipitate lead and strontium sulfates.
6. Digest the precipitate about 30 min at 90 C.
7. Centrifuge and wash the precipitate cake with 1M  $\text{Na}_2\text{SO}_4$  (pH 1). Most of the undesired components (iron, sodium, aluminum, magnesium, manganese, chromium, nickel, calcium, zirconium-niobium, ruthenium, and cesium) are discarded in this step.
8. Metathesize the precipitate in the centrifuge with a mixture of NaOH and  $\text{Na}_2\text{CO}_3$  to convert the sulfate cake to a carbonate cake.
9. Wash the sulfate from the cake with dilute  $\text{Na}_2\text{CO}_3$ .
10. Dissolve the carbonate precipitate in  $\text{HNO}_3$ .

The strontium and rare earths are further separated by selective precipitation of the rare earth oxalates (not shown). Over 90% recovery of strontium and rare earths have been demonstrated with this process in the Purex plant and in B-Plant Phase I operations.

DECLASSIFIED

DECLASSIFIED

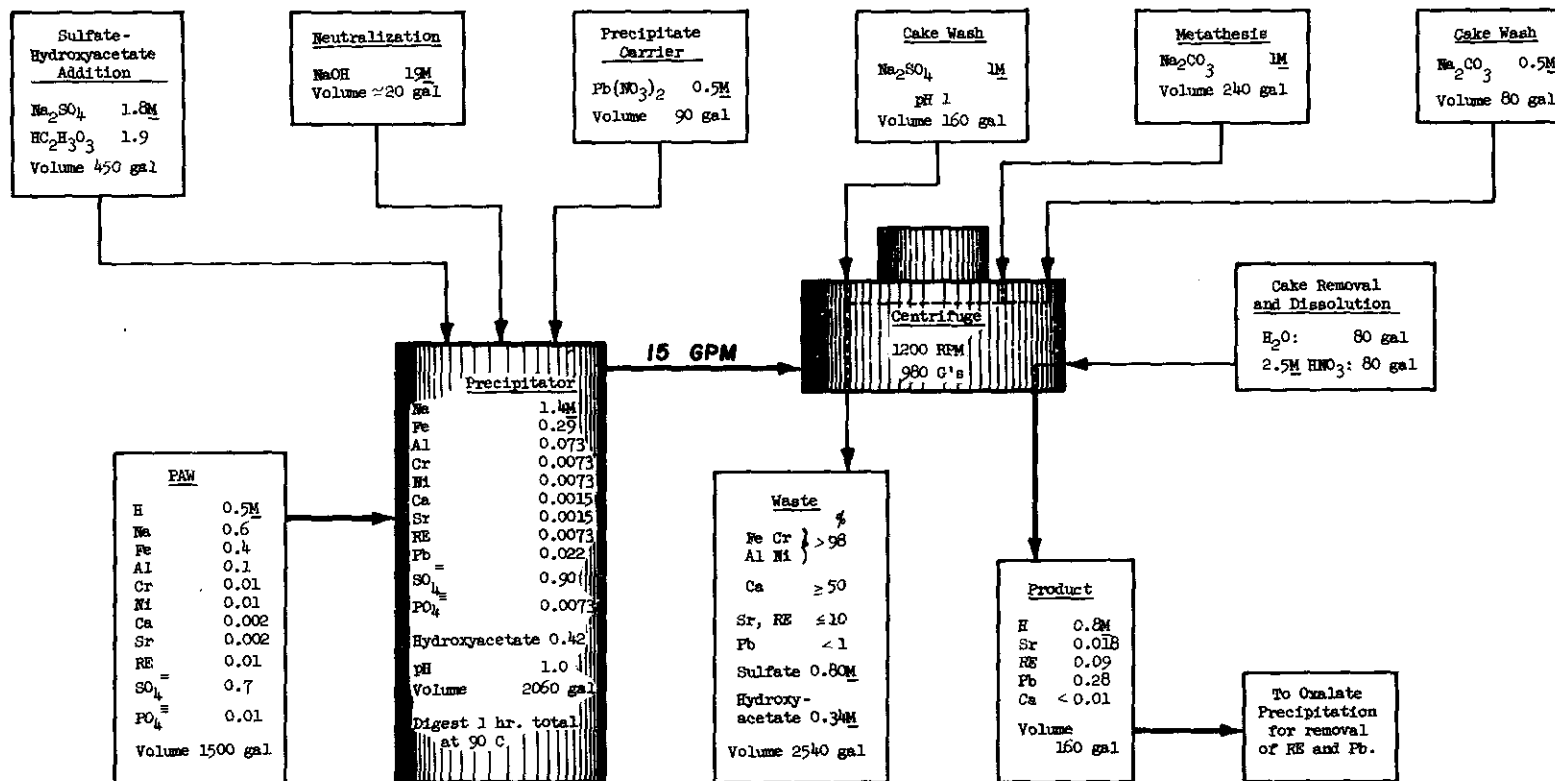


121

DECLASSIFIED

Fig.IV-1 CENTRIFUGATION AND LEACHING OF PUREX ACID WASTE SOLIDS - CONCEPTUAL FLOWSHEET

DECLASSIFIED



1/22

DECLASSIFIED

Fig. IV-2 LEAD-CARRIER SULFATE PRECIPITATION PROCESS  
 PAW FEED

1/50

A modification of this procedure has been developed for removing strontium and rare earths from the stored alkaline waste sludge<sup>(5,14)</sup>. The process is similar to the LW process except that it uses a weaker base,  $\text{Na}_2\text{CO}_3$ , for pH adjustment rather than  $\text{NaOH}$  and thus obviates the need for a complexant to prevent ferric hydroxide precipitation. A flowsheet based on the dissolved Purex sludge, described in Chapter III, is presented in Figure IV-3.

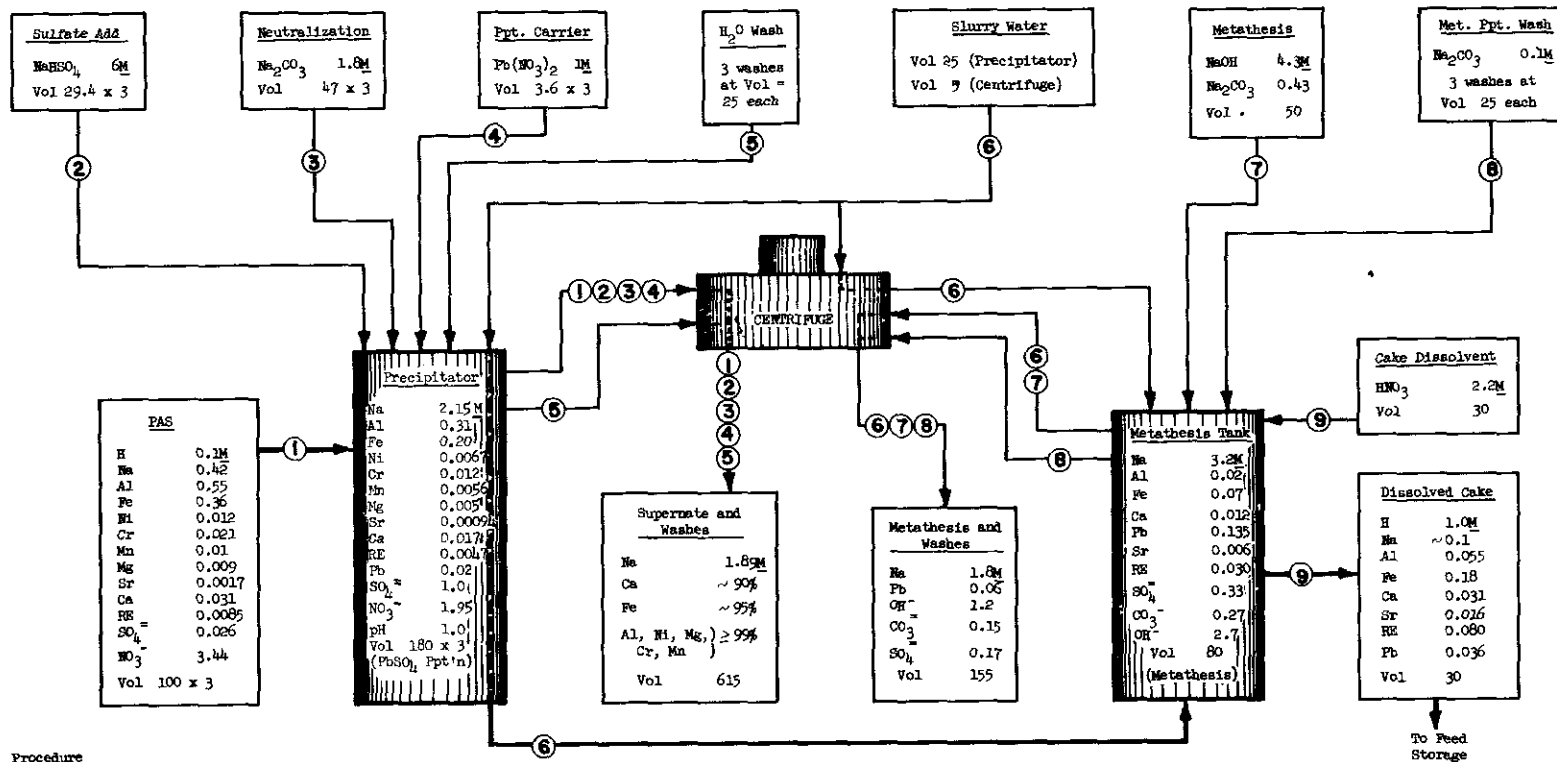
The variables affecting the performance of the two processes are discussed in the following sections. Most of the laboratory studies were made with the Purex LW and dissolved sludge compositions shown in Table IV-1. These solutions were diluted about two-fold, typically, during the precipitation procedure. With the exception of iron, variations in the concentrations of the cationic constituents over the range studied did not appear to affect the performance of the process. Although solutions derived from Redox sludge (RAS) were not tested, the results are expected to be similar.

TABLE IV-1  
TYPICAL PUREX WASTE COMPOSITIONS USED IN LABORATORY  
AND PILOT PLANT STRONTIUM PRECIPITATION STUDIES  
(Source of Data: HW-69534, HW-79286, BNWL-4)

Constituent	Concentration, M <sup>(a)</sup>		
	Purex LW	Purex Dissolved Sludge	
		#1	#2
Na	0.6	0.5	1.4
H	4.0	1.0	0.7
Fe(III)	0.5	0.1	0.3 - 0.7
Al	0.1	0.29	0.20
Cr	0.01	0.02	0.014
Ni	0.01	0.02	0.014
U(VI)	0.01	----	----
Sr	0.002	0.0008	0.0008
RE	0.01	0.004	0.004
Ca	----	0.014	0.01
Mg	----	0.004	0.0028
Mn	----	0.02	0.014
$\text{SO}_4^{=}$	1.0	0.044	1.4
$\text{PO}_4^{=}$	0.01	----	0.02
$\text{NO}_3^-$	4.5	2.8	2.1

(a) Initial composition. Final solution was usually diluted about two-fold by addition of complexant, sulfate, and pH adjustment solutions.

DECLASSIFIED



Procedure

1. Adjust PAS to 1M  $SO_4^{2-}$  and pH 1 with  $H_2SO_4$  and  $Na_2CO_3$ .
2. Heat to 80 C, add  $Pb(NO_3)_2$ , and digest for 30 minutes.
3. Allow slurry to settle and cool ( 1 hr ), then decant through centrifuge.
4. Repeat steps 1, 2, and 3 two more times.
5. Wash accumulated ppt. 3 times with hot water; settle and decant each wash through centrifuge.
6. Slurry precipitates from precipitator and centrifuge to metathesis tank.
7. Add sufficient metathesis solution to give 20 moles  $OH^-$ /mole Pb. Digest 30 min. at 80 C. Decant through centrifuge.
8. Wash ppt. with hot  $Na_2CO_3$  solution; decant through centrifuge.
9. Dissolve ppt. with  $HNO_3$  (routed first through centrifuge).

Fig. IV-3 LEAD-CARRIER SULFATE PRECIPITATION  
 PROCESS - PAS FEED: Conceptual Flowsheet  
 (Based on data from BNWL-4)

L2L

DECLASSIFIED

100

## 2.2 Strontium and Rare Earth Precipitation

### 2.2.1 Effect of Sulfate Concentration

Sulfate alone precipitated much of the strontium from synthetic Purex LW, as shown in Figure IV-4<sup>(7)</sup>. The strontium recovery reached a maximum of 80% at 3M sulfate.

Copious amounts of iron also precipitated when the sulfate concentrations exceeded 1M at pH 1. Iron precipitation could be prevented without affecting strontium recovery by adding about one mole of tartrate per mole of iron, and most of the laboratory and Purex plant data were obtained with tartrate present. More recently, iron precipitation in Purex plant runs has been prevented by the addition of less expensive hydroxyacetic acid at the rate of two moles per mole of iron.

### 2.2.2 Effect of Carriers

The use of carrier precipitates gave improved strontium recovery at relatively low sulfate concentrations. Several carrier ions were tested, with the results shown in Figure IV-5<sup>(7)</sup>. Of the ions tested, lead was chosen for Purex plant use because of ease of subsequent removal.

The precipitation was found to be an adsorption or carrier-type reaction and not simply a solubility-product precipitation of  $\text{SrSO}_4$ . The fraction of strontium precipitated decreased with increasing strontium concentration, implying saturation of specific adsorption sites.

### 2.2.3 Effect of Sulfate and Lead Carrier Concentration

The effect of lead carrier concentration on strontium recovery at various sulfate concentrations is shown in Figure IV-6<sup>(7)</sup>. The results show that near quantitative strontium recovery can be obtained at pH 0.4 upon the addition of 0.02 to 0.03M  $\text{Pb}(\text{NO}_3)_2$  to feed adjusted to  $\geq 1\text{M}$  sulfate.

Cerium losses (not shown) were not affected by the addition of lead. Cerium losses were generally less than 4% except at 0.5M sulfate where the losses increased to 14 to 37%.

### 2.2.4 Effect of pH and Tartrate

The effect of pH on strontium precipitation is shown in Figure IV-7 at several levels of lead and sulfate concentrations<sup>(7)</sup>. Strontium recovery was near optimum at a pH of 1 to 2 (with 1.7 to 2 moles of tartrate present per mole of iron). The losses tended to increase gradually as the pH increased beyond 2, possibly through tartrate complexing. In another series of experiments with about 50% more tartrate present (2.5 moles

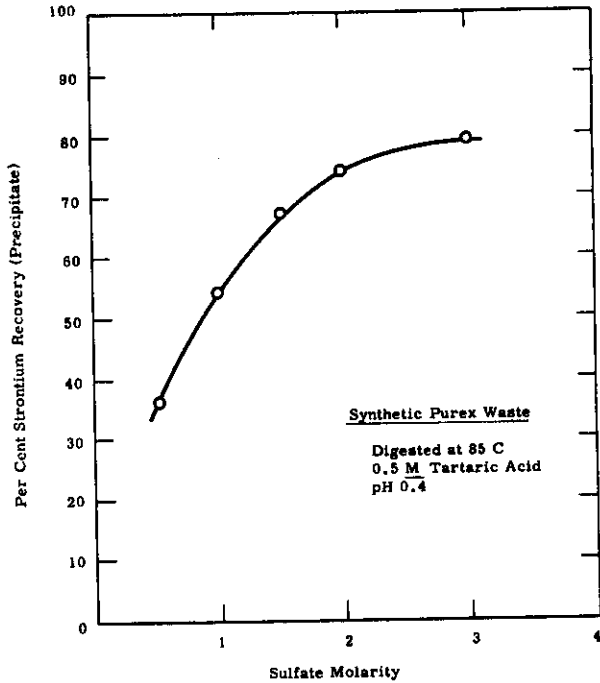


FIGURE IV-4

Recovery of Strontium From Synthetic Purex Waste as a Function of the Sulfate Concentration  
(Source of Data: HW-69534)

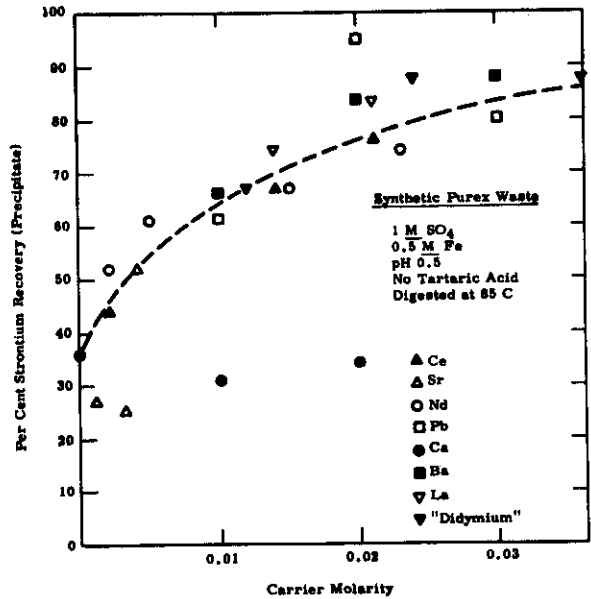


FIGURE IV-5

Recovery of Strontium From Synthetic Purex Waste as a Function of the Carrier Concentration  
(Source of Data: HW-69534)

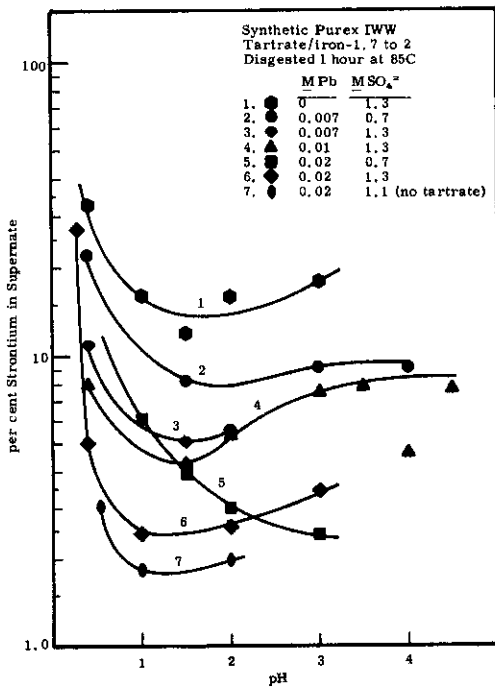


FIGURE IV-6

EFFECT OF LEAD CARRIER AND SULFATE CONCENTRATION ON STRONTIUM RECOVERY  
(Source of Data: HW-69534)

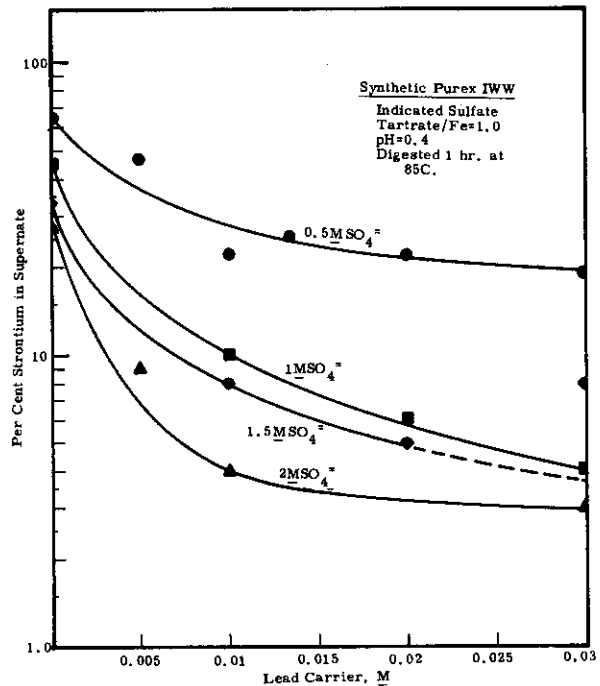


FIGURE IV-7

EFFECT OF pH ON STRONTIUM RECOVERY  
(Source of Data: HW69534, HW79286)

tartrate/mole iron), the strontium losses rose sharply from 6.4% at pH 2.5 to 65% at pH 3.6<sup>(7)</sup>. Cerium losses increased even more sharply with increasing pH and tartrate concentration, and a pH of 2 would be the maximum pH recommended for recovering strontium and rare earths with a tartrate-complexed flowsheet.

### 2.2.5 Effect of Temperature

Both strontium and cerium losses were substantially lowered by digestion at elevated temperatures, as shown in Figure IV-8<sup>(5,7)</sup>. Pilot plant studies indicated that the effect was irreversible; after digestion at 80 C, precipitate slurries were cooled and held overnight without significant increases in the concentrations of either strontium or cerium in the supernate<sup>(12)</sup>.

### 2.2.6 Effect of Digestion Time

Strontium recovery was improved by digesting the feed at 80 C several minutes prior to lead addition, as shown in Table IV-2<sup>(5)</sup>.

TABLE IV-2  
EFFECT OF DIGESTION TIME ON STRONTIUM LOSSES  
(Source of Data: HW-79286)

Synthetic Purex LW

1.1M  $\text{SO}_4^{=}$   
0.02M Pb  
pH 1.0

Digested at 80 C for  
indicated time before lead  
addition and centrifugation

<u>Digestion Time, Min</u>	<u>% Sr Remaining in Supernate</u>
1	19.0
15	4.1
30	5.0
45	2.4
60	4.8

Strontium losses in pilot plant runs were not affected by the rate of lead addition, by the degree of agitation during addition, or by the time of addition after reaching the digestion temperature, provided that at least 15 min of digestion were provided<sup>(12)</sup>. In other experiments, losses increased significantly when the lead was added before the pH adjustment step<sup>(7)</sup>.

The digestion period was not required in the absence of rare earths<sup>(5)</sup>. This suggests that the formation of the sodium-rare earth sulfates, known to be

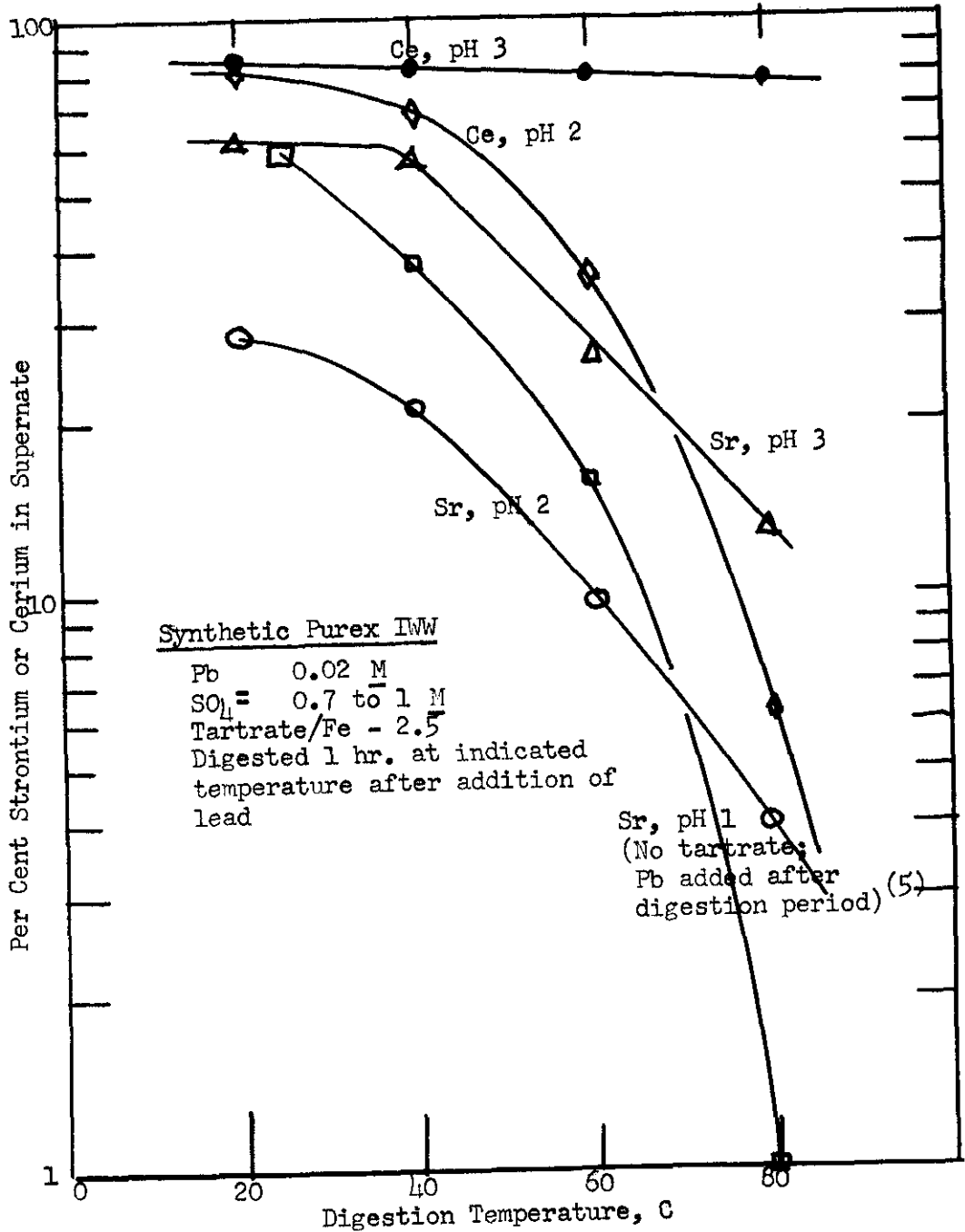


FIGURE IV-8

EFFECT OF DIGESTION TEMPERATURE ON STRONTIUM AND CERIUM RECOVERY

(Source of Data: HW-69534, HW-79286)

DECLASSIFIED

429

temperature dependent and slow<sup>(6,15)</sup>, has an initially adverse effect on strontium recovery.

Lead sulfate precipitate from a previous strontium precipitation strike will scavenge strontium from fresh feed solution (after sulfate addition and pH adjustment). Equilibrium removal in pilot plant runs was reached within about 40 minutes after reaching the 80 C digestion temperature<sup>(12)</sup>.

### 2.2.7 Effect of Iron Concentration

Iron proved to be the most troublesome impurity in the feed. Its presence in Purex feed required the addition of tartaric or hydroxyacetic acid to prevent its precipitation during the NaOH pH adjustment step. In several Purex plant runs, higher-than-normal iron concentrations (ca 0.7M) also limited the maximum pH to about 1.5 through precipitation of an iron-tartrate complex that solubilized the cake during subsequent metathesis operations.

In the absence of complexing agents, the pH can be adjusted to at least pH 2 without precipitating iron by using a weak base such as sodium carbonate to neutralize the excess acid<sup>(5)</sup>. Further safe "neutralization" can be obtained by adding the required sulfate as Na<sub>2</sub>SO<sub>4</sub>, which reduces the free hydrogen ion concentration through formation of the bisulfate ion (HSO<sub>4</sub><sup>-</sup>). Very little foaming was observed during neutralization of sludge feed #1 (Table IV-1) when carbonate was added after the sulfate concentration had been adjusted to 1M by the addition of 2M Na<sub>2</sub>SO<sub>4</sub><sup>(12)</sup>.

Without complexants, the iron solubility in synthetic sludge feeds was limited to about 0.2M at 1M sulfate (pH 1.2)<sup>(12)</sup>. The precipitate obtained with higher iron concentrations was apparently ferric sulfate. High strontium losses (6 to 28%) in several pilot plant runs with 0.35M iron initially present in the adjusted feed were attributed to sulfate depletion due to iron complexing and precipitation<sup>(12)</sup>.

### 2.3 Sulfate Cake Washing

The supernate must be removed from the lead sulfate cake to prevent precipitation of sulfate-soluble impurities (iron, magnesium, manganese, etc.) during the alkaline metathesis step. Commonly, 1M Na<sub>2</sub>SO<sub>4</sub> at pH 1 has been used for this purpose, with the sulfate added to prevent dissolution of the cake. Laboratory and pilot plant studies have since shown that the cake was equally insoluble in water and 0.05M HNO<sub>3</sub> at temperatures ranging from 30 to 80 C<sup>(3,12)</sup>. Cerium and strontium losses, however, were excessive in 0.1M HNO<sub>3</sub> washes<sup>(12)</sup>. Typical solubility losses obtained during pilot plant washing studies are shown in Table IV-3. The use of a dilute acid or salt wash solution may be preferred over water to prevent possible peptization of the precipitate, though this was not observed in laboratory water washing tests.

DECLASSIFIED

DECLASSIFIED

TABLE IV-3  
STRONTIUM AND CERIUM LOSSES  
OBTAINED DURING SULFATE CAKE WASHING STUDIES  
 (Source of Data: BNWL-4)

Conditions: Precipitate stirred with wash solutions for 5 to 20 min. at indicated temperatures.

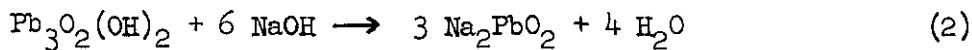
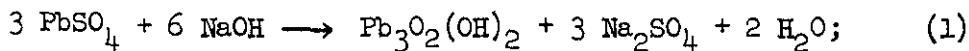
Wash Composition <u>M HNO<sub>3</sub></u>	Vol. per Wash, <u>L./Mole Pb</u>	No. of Washes	Temp <u>°C</u>	Total % Dissolved	
				<u>Sr</u>	<u>Ce</u>
0	3	1	30	<2	--
0.05	1.5	3	40	1.3	--
0.05	{ 2.8 7.3	2	50	2.3	--
		1(a)	80	0.7	--
0.1	2.5	2	80	3.1	--
0.1	8.8	2	80	18 <sup>(b)</sup>	63 <sup>(b)</sup>

- (a) The third of three successive washes.
- (b) Approximately 5% loss in the first wash.

2.4 Metathesis and Cake Dissolution

Although various leaching techniques have been tested for dissolving the lead sulfate cake<sup>(7)</sup>, the most effective cake dissolution method has involved carbonate metathesis: The cake is digested with a sodium carbonate solution to convert the sulfate precipitates to the less soluble carbonates; the sulfate supernate is washed from the converted carbonate cake; and the precipitate is dissolved in nitric acid. Sodium hydroxide is usually added to the metathesis solution to partially or completely dissolve the lead and to accelerate the metathesis reaction.

Lead sulfate forms hydrated lead oxide with NaOH and is soluble in an excess of the reagent, forming the plumbite ion:



Typical data for the solubility of lead in NaOH are shown in Figure IV-9<sup>(1,9,12)</sup>. The data show that the lead solubility in saturated solutions is greatly lowered by aging, attributed to the conversion of the more soluble hydrated lead oxide to the less soluble but more stable yellow and red lead oxides<sup>(1)</sup>.

DECLASSIFIED

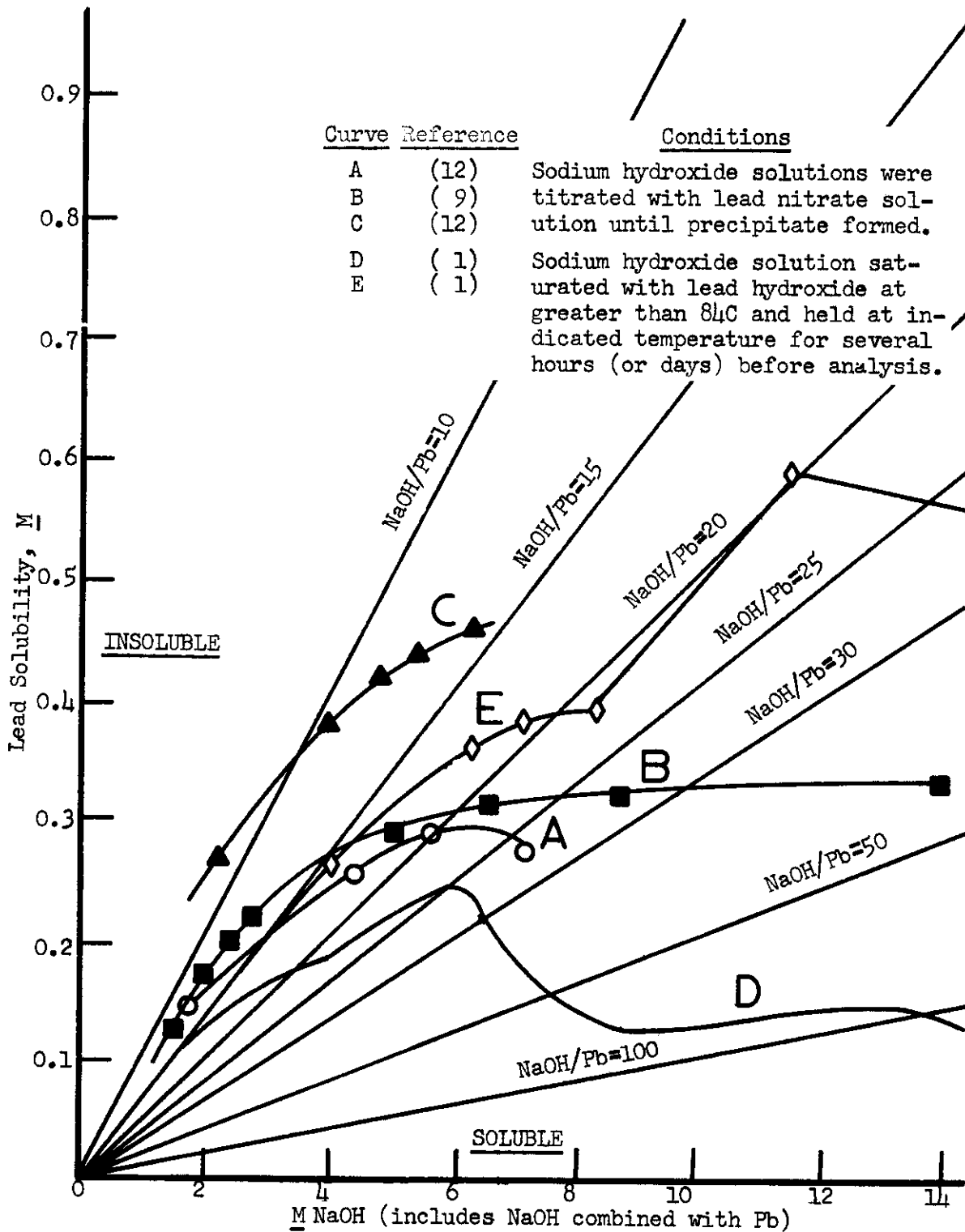


FIGURE IV-9

LEAD SOLUBILITY IN SODIUM HYDROXIDE

Lead, strontium, and cerium losses to some of the carbonate-hydroxide metathesis solutions used in laboratory and pilot plant tests are shown in Table IV-4. Strontium and cerium losses were quite low under all conditions shown. As little as 0.1M carbonate was sufficient to prevent strontium dissolution<sup>(3)</sup>. In the absence of carbonate, however, about 20 to 50% of the strontium was dissolved along with 85% of the lead<sup>(7)</sup>.

TABLE IV-4  
LEAD, STRONTIUM, AND CERIUM DISSOLUTION  
DURING METATHESIS OF LEAD SULFATE CAKE  
WITH CARBONATE-HYDROXIDE MIXTURES

(Source of Data: HW-69534, HW-81201, BNWL-4)

Conditions: Lead sulfate cake from LWV or dissolved sludge precipitations was washed 2 or 3 times to remove supernatant waste, then contacted 10 to 30 min with leach solutions, using the conditions shown.

Leach Composition, M		Vol per Leach L/Mole Pb	Number of Leaches	NaOH/Pb (a)	Temp °C	Total % Dissolved			Ref.
Na <sub>2</sub> CO <sub>3</sub>	NaOH					Pb	Sr	Ce	
1	5	1.3	2	13	60	41	2.2	<0.4	(7)
1	5	1.3	3	20	60	33	1.0	<0.3	(7)
1	5	2.0	3	30	60	70	1.2	---	(7)
1	5	1.3	6	40	60	57	<1.0	<0.5	(7)
1	5	2.7	4	53	60	95	1.3	<1.0	(7)
1	5	8.0	3	120	60	81	0.7	---	(7)
1	1	~2.5	1	~2.5	80	--	±1.2	---	(3)
0.5	2	7.3	1	15	80	66	0.8	---	(12)
0.5	1	3.1	2	6.9	80	--	1.2	---	(12)
0.2	2	8.3	1	17	80	87	1.5	0.4	(12)
0.1	6	~2.5	1	15	80	--	±2.0	---	(3)
0.1	6	~2.5	3	45	80	--	±2.0	---	(3)

(a) Cumulative mole ratio for the complete series of leaches.

Lead solubility increased both with increasing temperature and cumulative NaOH addition. In all cases, however, the total lead dissolved was less than predicted from the solubility data shown in Figure IV-9. This may be partially due to sulfate and carbonate competition, but it may also be caused by the intermediate conversion of the lead sulfate to less soluble lead oxide crystalline forms or inadequate digestion times.

The solubility of the metathesized precipitate in  $\text{HNO}_3$  is dependent on both the completion of the metathesis and the elimination of the displaced sulfate ions. With good agitation, the metathesis reaction was essentially complete within 5 min at 80 C<sup>(3)</sup>; but with inadequate agitation (slow-speed stirring or air sparging), strontium conversion was incomplete even after digesting 40 min at 80 C<sup>(12)</sup>.

The free sulfate can be washed from the cake with water or dilute  $\text{Na}_2\text{CO}_3$ . Product losses in pilot plant wash solutions were low in either case, as shown in Table IV-5. The effectiveness of the wash in removing sulfate is dependent on the wash volume and the degree of agitation and phase separation. These factors have not been extensively investigated, but 6 to 9 liters of wash solution per mole of lead in the initial cake proved adequate in pilot plant runs to permit quantitative strontium dissolution in nitric acid.

TABLE IV-5  
STRONTIUM AND CERIUM LOSSES  
OBTAINED DURING METATHESIZED-CAKE WASHING

(Source of Data: BNWL-4)

Conditions: Metathesized (carbonate) precipitates were stirred with wash solutions for 15 to 40 min at the indicated temperature.

Wash Composition <u>M <math>\text{Na}_2\text{CO}_3</math></u>	Wash Vol L/Mole Pb (a)	Temp., °C	% in Supernate	
			<u>Sr</u>	<u>Ce</u>
0	2.5	50	1.5	--
0.1	2.8	25	0.6	--
0.1	0.8	40	0.2	--
0.1	2.3	40	1.3	--
0.1	2.8	80	0.2	--
0.1	8.3	80	1.5	0.3

(a) Based on lead content of original sulfate cake.

## 2.5 Precipitate - Supernate Separation Methods

### 2.5.1 Centrifugation

Centrifugation has been satisfactorily used as the conventional plant method for removing the supernate from the lead sulfate and metathesized carbonate slurries. Table IV-6 illustrates the effect of centrifuge operating variables on pilot plant strontium losses when removing the supernate

from the lead sulfate cake<sup>(12)</sup>. The results were obtained with a 26-in. solid-bowl centrifuge. The data indicate that adequate separation can be obtained over at least a two-fold range of flow rates and operating speeds. The centrifuge cake volume averaged about 0.5 liter per mole of lead added. The lead sulfate cake had a pasty, clay-like consistency and was very difficult to slurry and wash in the pilot-plant centrifuge.

TABLE IV-6  
EFFECT OF HOLD-UP TIME AND CENTRIFUGAL FORCE  
ON CENTRIFUGATION OF LEAD-SULFATE STRONTIUM-  
SULFATE SLURRIES

(Source of Data: BNWL-4)

Conditions: Strontium precipitated with 0.02M Pb, digested 30 min at 80 C before pumping to centrifuge. (Run 12 had an additional decantation step preceding the centrifuge that removed 80 to 95% of the strontium.)

<u>Run No.</u>	<u>Hold-up Time, Min.</u>	<u>Centrifuge Speed, RPM</u>	<u>Centrifugal Force, Gravities</u>	<u>% Sr in Supernate</u>
10	3.8	1860	1280	5.3
10	5.1	1860	1280	4.7
10	5.7	1860	1280	3.6
10	7.1	1860	1280	3.2
<hr/>				
12	4.6	930	320	2.4
12	4.6	1860	1280	1.9

2.5.2 Settling and Decantation

Settling rates for pilot plant lead sulfate and carbonate precipitates are shown in Table IV-7 as a function of supernatant solutions and temperature<sup>(12)</sup>. In all cases, the settling rate was greatest at elevated temperature and in low-salt wash solutions. The settling studies showed that effective particle sizes were at least 10 microns, much greater than the sub-micron sizes found by microscopic analysis, indicating that coagulation occurred during settling.

DECLASSIFIED

TABLE IV-7  
SETTLING RATES FOR LEAD SULFATE  
AND CARBONATE PRECIPITATES

(Source of Data: BNWL-4)

Conditions: Slurry at indicated temperatures allowed to settle in a tall, graduated cylinder over distances of 4 and 8 inches.

<u>Supernatant Solution</u>	<u>Temp, °C</u>	<u>Settling Rate, in/min</u>	
		<u>4</u>	<u>8</u>
Sulfate waste supernate (a)	30	1.1	---
Sulfate waste supernate (a)	40	0.9	0.7
Sulfate waste supernate (a)	50	1.7	---
Sulfate waste supernate (a)	80	2.2 (b)	2.5 (c)
0.1M HNO <sub>3</sub> (sulfate cake wash)	80	5.3, 6.0	---
2M NaOH, 0.2M Na <sub>2</sub> CO <sub>3</sub>	20	0.5	---
2M NaOH, 0.2M Na <sub>2</sub> CO <sub>3</sub>	50	1.0	1.1
2M NaOH, 0.2M Na <sub>2</sub> CO <sub>3</sub>	80	2.8	2.3
0.1M Na <sub>2</sub> CO <sub>3</sub> (carbonate cake wash)	80	6.0	5.6

(a) Supernate from lead sulfate precipitation of synthetic sludge wastes

(b) Average of 8 determinations, ranging from 1.6 to 3.1 in/min

(c) Average of 5 determinations, ranging from 1.3 to 3.8 in/min

Pilot plant decantation studies, made in a 55 gal drum with a central bottom outlet, demonstrated excellent separation performance<sup>(12)</sup>. The precipitates were allowed to settle 10 to 75 min at 80 C (liquid depths of 15 to 24 in) before the supernate was pumped from the bottom of the first drum to a second drum where the procedure was repeated - this time pumping to waste. The complete process, including dissolution of the metathesized cake, was demonstrated in this fashion. Supernate samples accounted for 98% of the strontium in the system, showing that very little settled precipitate was lost - even without a backup centrifuge.

DECLASSIFIED

Settling and decantation through a backup centrifuge would afford the greatest flexibility for B-Plant. For example, several batches of feed can be precipitated in the precipitation tank without removing the lead sulfate cake. The cake can be washed, metathesized, and dissolved in the same vessel or transferred to a smaller tank for metathesis and dissolution. The centrifuge load should be less than 5% of the precipitate.

Multiple lead sulfate strikes were made in pilot plant precipitators without removing the lead sulfate cake between strikes to demonstrate this concept<sup>(12)</sup>. This method of operation actually reduced lead consumption. Although 0.02M lead was required on the first strike, the remaining strikes required as little as 0.010 to 0.0125M added lead to reduce the strontium losses to 5% or less. As discussed in Section 2.2.6, a 40 min digestion period was required to obtain the optimum benefit with this scavenging technique.

### 3. References

1. M. P. Applebey and H. M. Powell. "The Polymorphism of Lead Monoxide", J. Chem. Soc. London, pp 2821-9. 1931.
2. S. J. Beard. Personal Communication. Isochem Inc.
3. A. L. Boldt. Lead Sulfate - Strontium Sulfate Metathesis Studies, HW-81201. March 5, 1964.
4. L. A. Bray. Denitration of Purex Wastes with Sugar, HW-76973 REV. April, 1963.
5. L. A. Bray. Strontium Recovery from Acidified Hanford Sludge, HW-79286. October 30, 1963.
6. L. A. Bray, R. L. Moore, H. H. Van Tuyl, and E. J. Wheelwright. The Recovery and Individual Isolation of Macroscopic Quantities of Cerium, Strontium, and Trivalent Rare Earths from Purex-Type Fission Product Waste, HW-SA-1939. June 27, 1960.
7. L. A. Bray and H. H. Van Tuyl. Laboratory Development of a Carrier-Precipitation Process for the Recovery of Strontium from Purex Wastes, HW-69534. May 9, 1961.
8. D. A. Bruce. Personal Communication. Isochem Inc. 1966.
9. C. A. Colvin. Solubility of Lead Hydroxide in Sodium Hydroxide - Lead Removal from Cerium Rare-Earth Fraction, RL-SEP-370. March 16, 1965.
10. L. L. Humphreys. Personal Communication. Battelle-Northwest Laboratories. 1966.

# DECLASSIFIED

437

11. H. C. Rathvon and P. W. Smith. Waste Management Program Process Flowsheets, HW-78061. July, 1963.
12. G. L. Richardson. Recovery of Strontium from Stored Purex Waste by Lead Sulfate Carrier Precipitation - Pilot Plant Studies, BNWL-4. January 15, 1965.
13. H. H. Van Tuyl. Composition of Solids from Purex LWV, HW-58970. January, 1959.
14. H. H. Van Tuyl. Improvement of Strontium Sulfate Precipitation Process, HW-74036. June 18, 1962.
15. E. J. Wheelwright and W. H. Swift. The Recovery of Fission Product Rare Earth Sulfates from Purex LWV, HW-63051. April 27, 1961.

# DECLASSIFIED

DECLASSIFIED

438

C. STRONTIUM AND RARE EARTH SOLVENT EXTRACTION PROCESSES:  
PROCESS CHEMISTRY

1. General Principles of Solvent Extraction

If an aqueous solution of  $\text{Sr}(\text{NO}_3)_2$  is placed in a beaker and a layer of di(2-ethylhexyl)phosphoric acid (D2EHPA) diluted with kerosene is added and stirred with the aqueous layer for a few minutes, it may be shown by chemical analysis of the resulting aqueous and organic phases that some of the strontium transferred from the aqueous to the organic phase. The operation is referred to as solvent extraction. Further, if the organic layer is removed from the above-mentioned system and placed in contact with a dilute solution of acid in water, some of the strontium transfers back to the aqueous phase. These two steps, extraction and stripping, operated in sequence and under optimized conditions, are the basic elements of a solvent extraction process for recovering and purifying a desired constituent from an aqueous feed containing one or more impurities.

In either of the above two-phase systems, if mixing is continued long enough, the strontium concentration in each phase becomes constant, although usually not the same in each phase. When constant concentrations have been attained, a dynamic equilibrium has become established, with the amount of strontium leaving the aqueous phase equal to the amount returning in a given time. The process is referred to as equilibration of the phases.

The ratio between the concentrations of a given solute in each of two liquid phases in contact equilibrium is variously referred to as the distribution ratio, distribution coefficient, or partition coefficient. It is designated in this manual by the letter E to which a subscript and superscript are appended to indicate which phase is the reference phase. Thus,  $E_o^a$  indicates the ratio of the solute concentration in the organic phase to the concentration in the aqueous phase. The term "distribution ratio" is used in the sense of this organic-to-aqueous distribution ratio throughout this manual, although  $E_a^o$ , the reciprocal of  $E_o^a$ , is sometimes used elsewhere in project literature. Other symbols (e.g. D,  $K_d$ , etc.) are also employed in solvent extraction literature.

The distribution ratio is the ratio of solute concentrations regardless of the relative volumes of the two liquid phases. It is apparent, however, that the amount of strontium extracted from the aqueous solutions by a D2EHPA solution, for example, is dependent upon the relative volume of D2EHPA phase as well as on the strontium distribution ratio.

The equilibrium distribution of a solute in liquid-liquid extraction systems ordinarily depends on many factors. For instance, in the example cited above, the distribution of strontium between aqueous and D2EHPA phases depends on the aqueous phase acidity, temperature, presence of complexing agents in the aqueous phase, and concentration of D2EHPA in the organic phase, as well as on several other factors. D2EHPA is also

DECLASSIFIED

an excellent solvent for extracting many other metal ions, but it is possible by careful control of these variables to improve greatly the selectivity of the solvent for a desired cation. A comprehensive account of the theory and operation of D2EHPA extraction processes is given in the ensuing parts of this section.

## 2. Theory of D2EHPA Solvent Extraction Systems

### 2.1 Historical Introduction

Active interest in D2EHPA as an extractant in solvent extraction separations began about 10 years ago. In 1955, K. B. Brown and associates at Oak Ridge National Laboratory (ORNL) developed the Dapex process<sup>(7,8,9,34)</sup> for the D2EHPA extraction recovery of uranium from uranium ore sulfate leach liquors. Since that time numerous applications have been made in chemical separations processes, especially in the nuclear field. Processes have been developed both at Hanford and at ORNL for recovering Sr-90<sup>(46,76,81)</sup>, mixed fission product rare earths<sup>(41)</sup>, ZrNb-95<sup>(26)</sup>, and Np-237 from reactor fuel process waste liquors. An important milestone has been operation of a D2EHPA extraction process in the Hanford Strontium Semiworks to recover and purify more than 10 megacuries of Sr-90<sup>(5,33,76)</sup>.

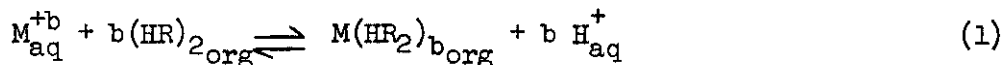
Extensive physicochemical studies of the theory and mechanisms involved in D2EHPA extraction systems have progressed concurrently with the process studies. Especially significant contributions have been made at Argonne National Laboratory by Peppard, et. al.<sup>(15,48-58)</sup>; at ORNL by Baes, McDowell, Coleman et. al.<sup>(1-3,45)</sup>; in Sweden by Dyrssen<sup>(36)</sup>; and in Japan by Sato<sup>(66-69)</sup>. Pertinent aspects of the current (1966) theory of D2EHPA extraction systems are reviewed in the sections immediately following. More detailed reviews are to be found in recent papers by Baes<sup>(2)</sup> and Peppard, et. al.<sup>(58)</sup>.

### 2.2 Reactor Mechanisms

#### 2.2.1 Trace Solvent Loading

D2EHPA exists as a hydrogen-bonded dimer in the non-polar diluents n-hexane, cyclohexane, benzene, and CCl<sub>4</sub><sup>(37)</sup>. Presumably the same is true in the non-polar, commercially available hydrocarbon solutions used as diluents for D2EHPA in B-Plant operations.

The general extraction of tracer-level concentrations of a metal ion M<sup>+b</sup> may be represented as



where R represents the di(2-ethylhexyl)phosphate anion, (HR)<sub>2</sub> represents

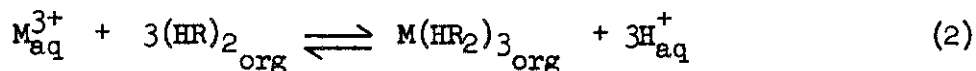
DECLASSIFIED

440

IS

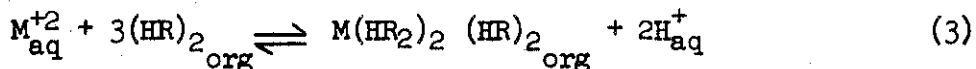
dimerized D2EHPA, and the subscripts aq and org refer to aqueous and organic phases, respectively. In general, extraction of a bth-valent metal ion requires b dimer molecules and releases b hydrogen ions to the aqueous phase.

Expression (1) is applicable, for example, to the D2EHPA extraction of tracer level U(VI) existing as  $UO_2^{++(1)}$ . Further, Peppard and co-workers (48,50,52-56) in a long series of investigations have established that D2EHPA in non-polar diluents extracts tracer-level lanthanide(III) and actinide(III) elements according to the reaction:

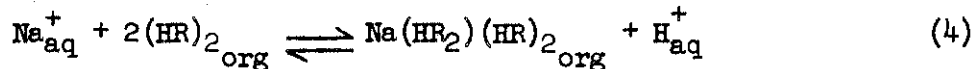


Peppard notes that Reaction (2) is in accord with observed solvent dependencies but that dependency data do not distinguish between  $M(HR_2)_3$ ,  $MR_3(HR)_3$ ,  $MR_2(HR_2)(HR)_2$ , etc. Peppard chooses the  $M(HR_2)_3$  formulation because it represents extraction by a mono-ionized dimer, but no proof that this is correct has been given.

Recent tracer-level studies have indicated D2EHPA extraction mechanisms other than that given in Reaction (1). Cases are now known where the extractant dependency for  $M^{+b}$  is either greater or less than bth power. For example, a third power extractant dependency has been found for Ca(II) [Peppard and Mason(57)] and for Sr(II) [McDowell and Coleman(45)]. Peppard suggests the "third power extractant dependency" systems might be expressed as:



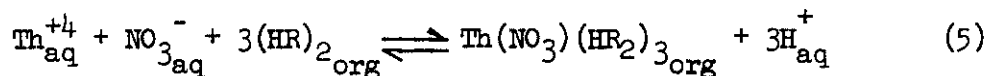
with the reservation that the formulation of the extracted species is consistent with the stoichiometric data but is not necessarily structurally correct. Along these same lines McDowell and Coleman(45) also report that the stoichiometry for tracer sodium extraction by dimerized D2EHPA is:



In contra-distinction to calcium, strontium, and sodium which exhibit an extractant dependency greater than the charge of the cation, thorium exhibits an extractant dependency smaller than the charge of the cation. Thus, third-power dependency was observed when tracer thorium was extracted from a nitrate media into toluene-D2EHPA solutions(56). Also in

DECLASSIFIED

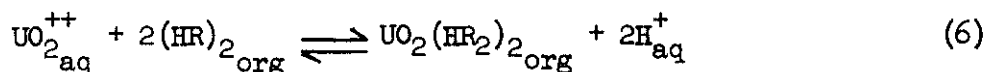
this system, the presence of nitrate in the organic phase was proved. Consequently, Peppard represents the extraction as:



Similarly, in the D2EHPA (toluene) vs. (perchlorate + nitrate) system, the neptunium(IV) extracted species has been shown to contain one nitrate group and the mechanism to correspond to Equation (5) (58). No corresponding study of Pu(IV) is known.

### 2.2.2 High Solvent Loading

Although extraction of tracer-level U(VI) may be represented by the expression:



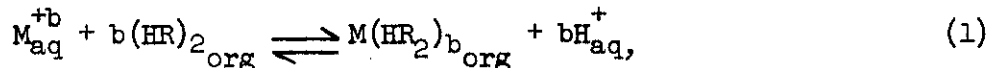
this expression is only valid if a reasonably large portion of the D2EHPA is free, i.e., not found in the extracted species. As the relative  $\text{UO}_2^{++}$  content of the organic is increased (high solvent loading), a point is reached at which the solution becomes quite viscous, and finally a gel-like solid is found. This solid has the empirical composition  $\text{UO}_2\text{R}_2$  and appears to exist in solution as a chain polymer<sup>(1)</sup>.

Similarly, trivalent lanthanides at saturation in D2EHPA form a gel-like solid of empirical composition  $\text{MR}_3$  which is assumed to be formed through three dimensional polymerization<sup>(58)</sup>. The phenomenon appears general. Peppard and co-workers have prepared, for example, solids having the composition  $\text{KR}$ ,  $\text{LiR}$ ,  $\text{NaR}$ ,  $\text{ScR}_3$ ,  $\text{ThR}_4$  and  $\text{HfR}_4$ . McDowell and Coleman<sup>(45)</sup> have also reported that ultimate loading of a D2EHPA solution with sodium or strontium leads to the salts  $\text{NaR}$  and  $\text{SrR}_2$ , respectively.

According to Peppard the simplest interpretation of these observations is as follows: "In the region far below saturation, the  $\text{M}^{+b}$  cation is complexed by a mono-ionized dimer forming  $\text{M}(\text{HR}_2)_b$ , the  $\text{HR}_2^{-}$  being capable of chelation to form an eight-membered ring with the M atom as a member. However, as saturation is approached, the proton of the extracted species may be replaced by an M atom. This replacement results, ultimately, in the formation of a three-dimensional polymer of empirical formula  $\text{MR}_b$ ."

### 2.3 Effects of pH and Ion Charge and Size

For the generalized reaction



the equilibrium constant can be written as

DECLASSIFIED

442

$$k_{eq} = \frac{[M(HR_2)_b] [H^+]^b}{[(HR)_2]^b [N^{+b}]} \quad (7)$$

Defining  $[M(HR_2)_b] / [M^{+b}]$  as the distribution ratio,  $D_M$  (using concentrations rather than activities), Equation (7) can be rearranged to

$$D_M = \frac{k_{eq} [(HR)_2]^b}{[H^+]^b} \quad (8)$$

Equation (8) illustrates a general principle in D2EHPA extraction systems, namely that the distribution ratio for a  $M^{+b}$  metal ion is inversely proportional to the  $b$ th power of the equilibrium aqueous phase hydrogen ion concentration. Proper control of aqueous phase acidity (pH) is thus essential in D2EHPA systems to extract desired metals and to separate them from impurities. To achieve such pH control it is customary, as discussed more fully later, to add organic acids as buffering agents to aqueous streams.

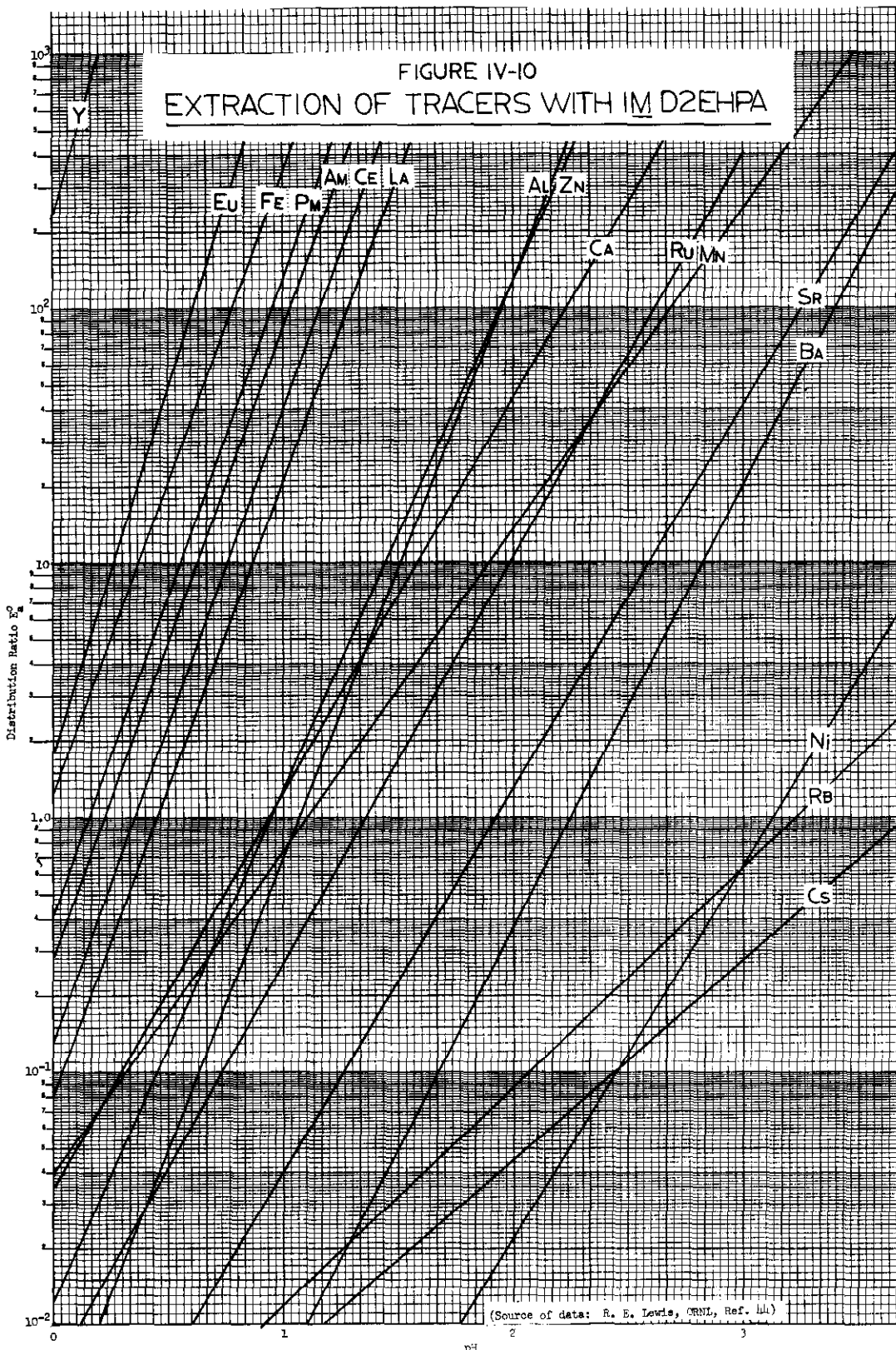
Lewis at ORNL, among others, has made detailed studies of the variation of the distribution ratio of various metal ions (at tracer level concentration) into 1M D2EHPA as a function of aqueous phase pH<sup>(44)</sup>. Selected data from Lewis' work are shown in Figure IV-10.

In general, the larger the charge on the metal cation the greater the magnitude of the equilibrium constant as expressed by Equation (1). That is to say, quadrivalent ions are extracted more strongly than divalent ions, etc. A partial list of the affinity of metal ions for D2EHPA is Zr(IV)  $\approx$  Ce(IV)  $\approx$  Pu(IV) > Np(IV) > Y(III) > Eu(III) > Fe(III) > Pm(III) > Ce(III) > La(III) > Ca(II) > Ru(III) > Sr(II) > Ba(II) > Na(I) > Cs(I) (39).

Dyrssen<sup>(36)</sup> has pointed out that for the trivalent lanthanide and actinide ions  $\log k_{eq}$  appears to vary inversely with ion radius. A similar correlation has been found for the alkali and the alkaline earth ions<sup>(2)</sup>. In all of these groups, the smaller the metal ion the more strongly it is extracted.

The oxocations  $UO_2^{++}$ ,  $PuO_2^{++}$ , and  $NpO_2^{++}$  are by far more strongly extracted than other divalent cations<sup>(2)</sup>. These cations appear to hold a unique position in the affinity series.

DECLASSIFIED



DECLASSIFIED

444

IS

#### 2.4 Effects of Aqueous Phase Complexants

Strontium, fission product rare earths, and americium in PAS and PAW solutions are associated with various inert (e.g., iron, chromium, nickel, etc) and radioactive (e.g., Ru-106, ZrNb-95, etc.) contaminants. Chemical flowsheets used in the B-Plant for D2EHPA extraction recovery of Sr-90, Am-241, and rare earths specify, as discussed more fully later, preparation of extraction column feed solutions having a pH in the range 3 to 5. It is customary to add to these feed solutions water soluble organic reagents to form soluble coordination compounds with many of the polyvalent inert and radioactive contaminants. Addition of these complexing agents serves the primary purpose of preventing or suppressing coextraction of contaminants and of preventing their precipitation as hydroxides or basic salts in feed solutions adjusted to pH's above 3. Added benefits accrue with certain of the complexing agents from the pH control afforded during the D2EHPA extraction step by the formation or dissociation of protonated forms of the complexing agent.

The complexing agents (ligands) most intensively studied in connection with suppressing extraction of undesirable elements in B-Plant D2EHPA processes are HEDTA (N-hydroxyethylethylenediaminetriacetic acid), EDTA (ethylenediaminetetraacetic acid), DTPA (diethylenetriaminepentaacetic acid), citric acid, tartaric acid, and oxalic acid. The reagents acetic acid and hydroxyacetic acid are also used in B-Plant D2EHPA processes. These latter reagents, although added generally for pH control, also form weak complexes with various di- and trivalent metal ions.

The general reaction of a metal ion  $M^{+b}$  and an unprotonated ligand  $L^{-a}$  which react stepwise to form the coordination complex  $ML_n$  can be represented as (omitting charges for simplicity)



The thermodynamic stability constants for each step are given by an expression of the form

$$K_n + \frac{[ML_n]}{[ML_{n-1}][L]} \quad (10)$$

Generally n is greater than 1; in certain important instances, however, (e.g., EDTA, HEDTA, DTPA), 1:1 complexes are the only significant ones found. Extensive tabulations of  $K_n$  values for various metal ions and ligands have been prepared<sup>(6)</sup>;  $K_n$  values of interest to B-Plant separations are listed in Table IV-67.

The complexing agents useful in B-Plant separations are all weak organic acids and thus, depending on aqueous phase acidity (pH), can

DECLASSIFIED

be present as various protonated species. For example, EDTA ( $H_4L$ ) can be present as  $H_4L$ ,  $H_3L^{-1}$ ,  $H_2L^{-2}$ ,  $HL^{-3}$ , and  $L^{-4}$ . The relative proportions of the various protonated forms can be calculated from the appropriate acid dissociation constants tabulated in Table IV-66 and more extensively in Reference 6.

The protonated ligands can also react with metal ions to form complexes. Thus, omitting charges, the general reaction is



with the stability constant defined as

$$K_{MH_pL}^M = \frac{[MH_pL]}{[M][H_pL]} \quad (12)$$

Normally  $K_{MH_pL}^M$  values are considerably less than  $K_n$  values for the same

ligand and can be ignored except at low pH's where the proportion of protonated ligands greatly exceeds the fully dissociated ligands. Selected  $K_{MH_pL}^M$  values are listed in Table IV-67.

Since the relative proportions of free ligand and protonated ligands are a function of the hydrogen ion concentration, a conditional stability constant can be defined at any given pH by

$$K' = \frac{(ML')}{(M^{+b})(L')} \quad (13)$$

where  $(L')$  is the total concentration of uncomplexed ligand species ( $H_nL$ ,  $H_{n-1}L^{-}$ ,  $H_{n-2}L^{-}$  ...  $L^{-n}$ ) and  $(ML')$  is the total concentration of complexed metal species. This equation can be rearranged to

$$(ML') = K'(M^{+b})(L') \quad (14)$$

The distribution ratio for M can be written as

$$E_{aM}^o = \frac{M_{org}}{M_{aq}} = \frac{\text{Concentration of all species of M in organic phase.}}{\text{Concentration of all species of M in aqueous phase}} \quad (15)$$

In the presence of a complexing agent L in the aqueous phase, the metal M exists in the aqueous phase both in complexed and uncomplexed forms. Hence, the distribution ratio can be written as

$$E_{aM}^o = \frac{[M_{org}]}{[M^{+b}] + [ML']} \quad (16)$$

DECLASSIFIED

Substituting (14) into (16) yields

$$E_{aM}^{\circ} = \frac{[M_{org}]}{(M^{+b}) [1 + K'(L')]} \quad (17)$$

If there is only species of M in the organic phase, the previously defined  $D_M$  (the distribution ratio for M in the absence of a complexing agent - see Sect. 2.3) can be substituted for  $\frac{[M]_{org}}{[M^{+b}]_{aq}}$  and (17) can be written as

$$E_{aM}^{\circ} = \frac{D_M}{1 + K'(L')} \quad (18)$$

The importance of selecting and controlling aqueous phase pH in B-Plant D2EHPA processes cannot be over-emphasized. The distribution ratio for an  $M^{+b}$  metal ion, as noted earlier (Sec. 2.3) is inversely proportional to the bth power of the equilibrium aqueous phase hydrogen ion concentration irrespective of the presence or absence of a complexing agent. With a complexing agent present, the aqueous phase pH, as just noted, also determines the relative proportions of protonated ligands and hence the extent of complexing of metal ions. A pH must be specified, therefore, which permits quantitative recovery of desired constituents with maximum complexing of unwanted impurities.

## 2.5 Calculation Procedures for Estimating Strontium Distribution Ratios

In D2EHPA solvent extraction processes for recovering and purifying Sr-90, it is obviously desirable to be able to predict quantitatively the effect of flowsheet variables on strontium distribution ratios. As discussed above, there are three principal factors which affect the strontium  $E_a^{\circ}$ : (a) the pH of the aqueous feed; (b) the presence in the aqueous feed of other extractable metal ions which compete with strontium for the solvent; and (c) the presence in the aqueous phase of ligands such as acetate, EDTA, etc which can form in-extractable complexes with strontium.

A procedure for estimating the strontium  $E_a^{\circ}$  which takes into account the three factors mentioned above is outlined in the following sections (33a). As will become apparent, certain assumptions (particularly about solvent extraction mechanisms) and approximations have been made in developing this calculation procedure. These approximations reflect the present inadequate knowledge of D2EHPA extraction chemistry as applied to other than extraction of metals at tracer concentrations. Nevertheless, the calculation procedure shown is the best currently available and, as will be shown, can be used to predict strontium distribution ratios.

DECLASSIFIED

2.5.1 Estimation of Strontium  $E_a^O$  in Absence of Complexants

A procedure for estimating the Sr  $E_a^O$  will be considered first for a D2EHPA-TBP-hydrocarbon diluent solution in contact with an aqueous solution containing small concentrations of strontium and other divalent and trivalent ions and up to 1.5M  $Na^+$ . Subsequently, the effects of aqueous phase complexing agents which lower the Sr  $E_a^O$  will be considered.

In treating this system, any effects of TBP (Section 2.6.2) and of the hydrocarbon diluent on the extraction reactions are neglected. Further, it is assumed that  $Sr^{++}$ ,  $Ca^{++}$ ,  $Am^{+++}$ , and the trivalent rare earths are extracted according to the mechanism shown in Equation (1), Section 2.2.1, that is, as the species  $M(HR_2)_2$ . Because of its high concentration in extraction feeds of interest,  $Na^+$  may be extracted as  $(NaR)_x$  as well as  $NaHR_2$ . For the purposes of this calculation procedure, it was assumed that  $x = 2$ .

The equilibrium constants for the reactions of interest, expressed in molar concentrations, are

$$Sr\ k_{eq} = \frac{[Sr(HR_2)_2] [H^+]^2}{[Sr^{++}] [(HR)_2]^2}, \quad (19)$$

$$Na\ k_1 = \frac{[NaHR_2] [H^+]}{[Na^+] [(HR)_2]}, \quad (20)$$

and

$$Na\ k_2 = \frac{[(NaR)_2] [H^+]^2}{[Na^+]^2 [(HR)_2]}. \quad (21)$$

Using the definition of  $D_M$  from Section 2.4, Equation (19) can be rearranged to

$$D_{Sr} = \frac{Sr\ k_{eq} [(HR)_2]^2}{[H^+]^2}. \quad (22)$$

The extent to which the solvent is loaded with other extractable ions must be considered in determining the value of  $[(HR)_2]$  to be used in Equation (22). Since extraction of rare earth and alkaline earth ions has been assumed to occur by the mechanism shown in Equation (1), it follows that a suitable solvent loading correction for such ions in the solvent is given by  $M$  "free D2EHP" =  $2 [(HR)_2] + 2 [(NaHR_2)] + 2 [(NaR)_2] =$

$$R-4 (\sum M^{+2})_{org} - 6 (\sum M^{+3})_{org} \quad (23)$$

where R represents the initial D2EHPA molarity (formula weights of D2EHPA/114.1).

Equation (23) defines the free D2EHP as that amount of solvent not associated with multivalent ions. (Iron and aluminum are often present in fission product feeds and can extract under certain conditions but their effect on solvent loading is relatively minor. Data obtained by Bray<sup>(17)</sup> on the inhibiting effect of iron and aluminum on the strontium  $E_a^0$  suggests that only about 1.8 to 2.6 moles of D2EHPA are tied up by the extraction of a mole of combined iron and aluminum.)

To obtain a suitable correction for sodium loading, Equation (20) and (21) are rearranged to give

$$[\text{NaHR}_2] = \frac{\text{Na } k_1 [(\text{HR})_2] [\text{Na}^+]}{[\text{H}^+]} \quad (24)$$

and

$$[(\text{NaR})_2] = \frac{\text{Na } k_2 [(\text{HR})_2] [\text{Na}^+]^2}{[\text{H}^+]^2} \quad (25)$$

Substitution of these values of  $[\text{NaHR}_2]$  and  $[(\text{NaR})_2]$  in Equation (23) and rearranging slightly leads to

$$2 [(\text{HR})_2] \left[ 1 + \text{Na } k_1 \frac{[\text{Na}^+]}{[\text{H}^+]} + \text{Na } k_2 \frac{[\text{Na}^+]^2}{[\text{H}^+]^2} \right] = \underline{M} \text{ free D2EHP.} \quad (26)$$

Hence,

$$[(\text{HR})_2] = \frac{\underline{M} \text{ free D2EHP}}{2 \left[ 1 + \text{Na } k_1 \frac{[\text{Na}^+]}{[\text{H}^+]} + \text{Na } k_2 \frac{[\text{Na}^+]^2}{[\text{H}^+]^2} \right]} \quad (27)$$

Finally, substituting this value of  $[(\text{HR})_2]$  into Equation (22), the expression for  $D_{\text{Sr}}$  is

$$D_{\text{Sr}} = \frac{\text{Sr } k_{\text{eq}}}{[\text{H}^+]^2} \cdot \frac{[\underline{M} \text{ free D2EHP}]^2}{4 \left[ 1 + \text{Na } k_1 \frac{[\text{Na}^+]}{[\text{H}^+]} + \text{Na } k_2 \frac{[\text{Na}^+]^2}{[\text{H}^+]^2} \right]^2} \quad (28)$$

The value of  $D_{\text{Sr}}$  is thus shown to be a function of  $[\text{Na}^+] / [\text{H}^+]$ .

Experimentally obtained values of  $\frac{(D_{\text{Sr}}) [\text{H}^+]^2}{[\underline{M} \text{ free D2EHP}]^2}$  are plotted versus

the ratio  $[Na^+]/[H^+]$  in Figure IV-11. Similarly, experimental values of

$\frac{(D_{Na}) [H^+]}{M \text{ free D2EHP}}$  versus the ratio  $[Na^+]/[H^+]$  are plotted in Figure IV-12.

Until the chemistry of D2EHPA extraction systems is better understood, caution should be exercised in extrapolating the curves in Figures IV-11 and IV-12 to conditions far removed from those used in their derivation.

### 2.5.2 Estimation of $Sr E_a^O$ in Presence of Complexants

As discussed in Section 2.4, ligands such as acetate, HEDTA, EDTA, etc. which are added to the aqueous phase to control pH or to suppress extraction of undesirable inert and fission product ions form complexes with strontium which lower the strontium distribution ratio. A method of correcting the  $Sr E_a^O$  for the effect of such complexing agents is considered below.

The essential points in the derivation of the correction factor are:

- (1) Consider a system which contains the ligands,  $L_a$ ,  $L_b$ , and  $L_c$  in the aqueous phase which form with  $Sr^{++}$  only inextractable 1:1 complexes of the type  $SrL_a'$ ,  $SrL_b'$ , and  $SrL_c'$ . Assume, for the time being, that there are no other metal ions present which will form complexes with these ligands; the effect of the presence of these metal ions will be considered later.
- (2) From Equations (15) and (16)

$Sr E_a^O = \frac{\text{Concentration of all Sr species in organic phase}}{\text{Concentration of all Sr species in aqueous phase}}$

$$= \frac{[Sr]_{org}}{[Sr^{++}] + [SrL_a'] + [SrL_b'] + [SrL_c']}. \quad (29)$$

- (3) At any given pH the conditional stability constant (Equation 13) for ligand  $L_a$  can be written as

$$K_a' = \frac{[SrL_a']}{[Sr^{++}] [L_a']}. \quad (30)$$

Thus,

$$[SrL_a'] = K_a' [Sr^{++}] [L_a']. \quad (31)$$

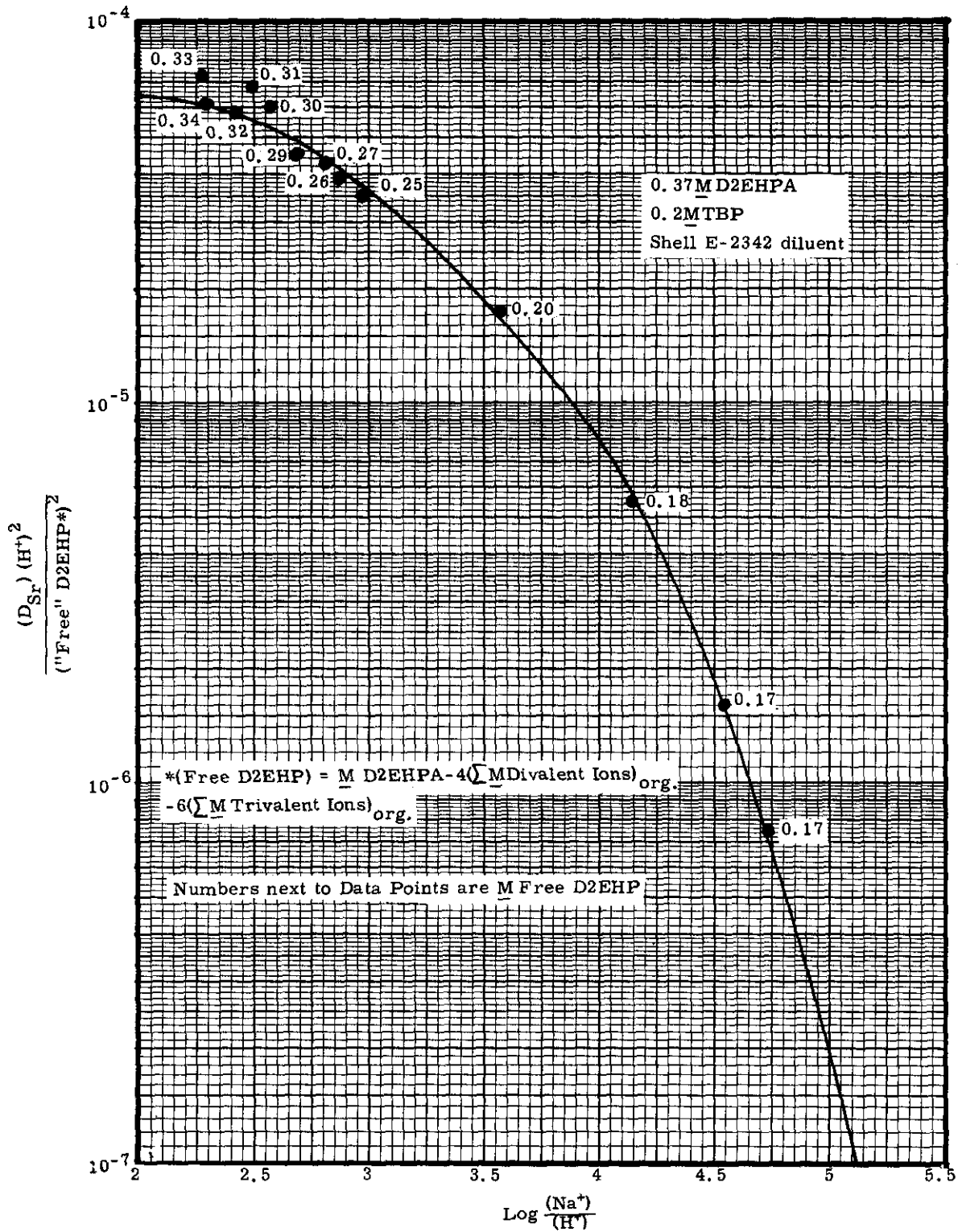


FIGURE IV-11

Preliminary Correlation of D2EHPA-Strontium Extraction Data  
 (Source of Data: HW-72666)

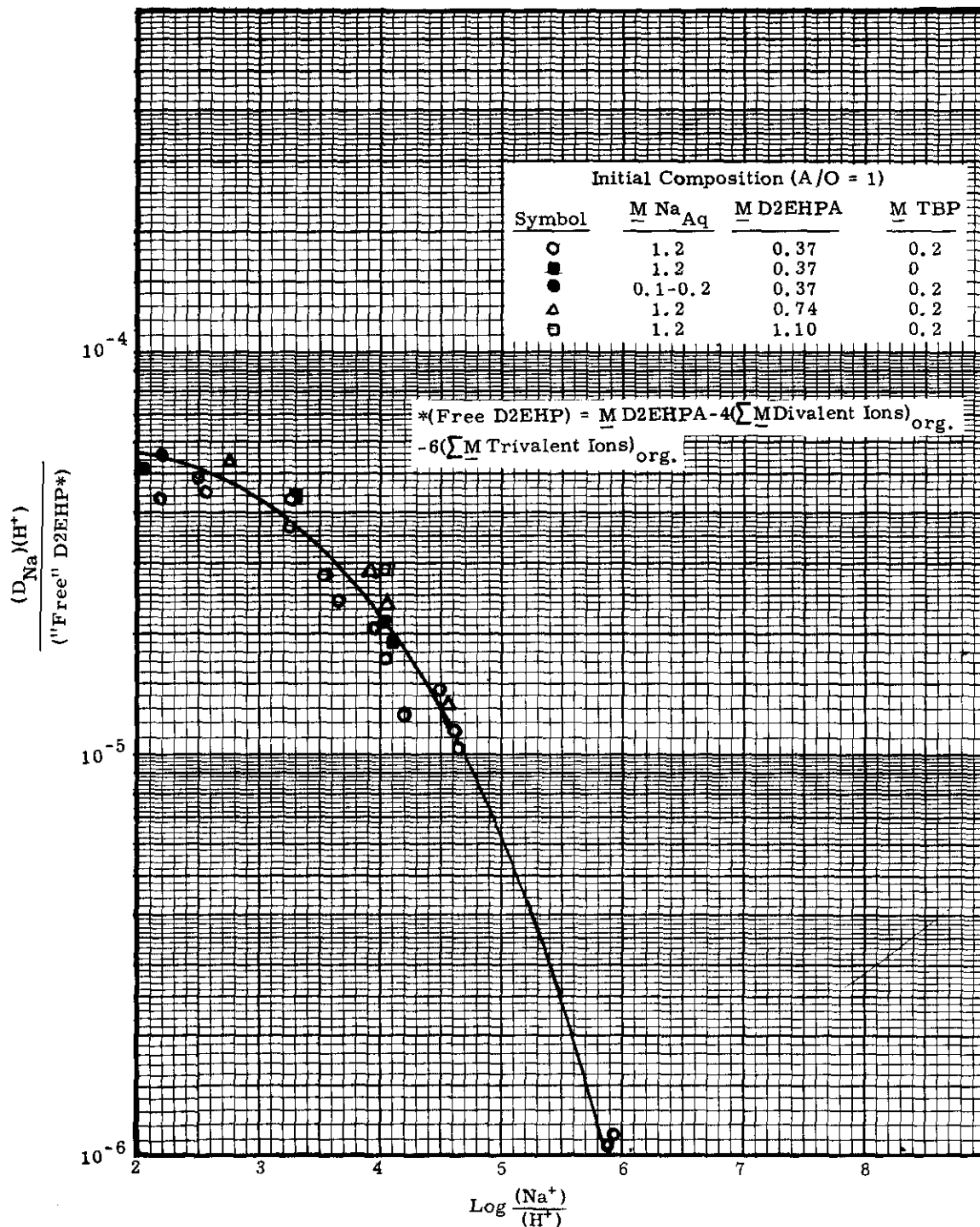


FIGURE IV-12

Preliminary Correlation of D2EHPA - Sodium Extraction Data  
 (Source of Data: HW-72666)

- (4) Substitution of this value of  $[SrL'_a]$  and the analogous values of  $SrL'_b$  and  $SrL'_c$  into Equation (29) gives

$$Sr E_a^O = \frac{[Sr]_{org}}{[Sr^{++}] + K'_a [L'_a] [Sr^{++}] + K'_b [L'_b] [Sr^{++}] + K'_c [L'_c] [Sr^{++}]} \quad (32)$$

- (5) If, as has been assumed earlier, the only species of strontium in the organic phase is the complex  $Sr(HR_2)_2$ , then by Equation (18),

$$Sr E_a^O = \frac{D_{Sr}}{1 + K'_a [L'_a] + K'_b [L'_b] + K'_c [L'_c]} \quad (33)$$

Equation (33) is the relationship desired to permit calculation of the strontium extraction coefficient in the presence of aqueous phase complexing agents. Application requires a knowledge of the values of the various  $K'$  and  $[L']$  terms and the value of  $D_{Sr}$ , which can be obtained from Figure IV-11.

Conditional stability constants for the various ligands studied in this program are presented in Figure IV-13. The values for acetate, hydroxyacetate, and tartrate were calculated from the published dissociation constants of the acids and corresponding strontium complexes (See Tables IV-66 and IV-67). The  $K'$  values for citrate, HEDTA, EDTA, and DTPA were calculated from the experimental effect of these complexants on strontium  $E_a^O$ 's (33a). Experimental values of  $K'$  are preferred when available because of the complexity of systems containing multibasic acids.

Estimation of the  $[L']$  values to use in Equation (33) requires a knowledge of the metal ions other than strontium ion which are present in the aqueous phase and the extent and manner in which these other metal ions react with the various complexing ligands. The sample flowsheet calculation shown below illustrates how  $[L']$  values are calculated.

### 2.5.3 Sample Calculation of Strontium $E_a^O$

With the above correlation for estimating strontium distribution ratios, it is now possible to determine the feasibility of a given flowsheet to quantitatively extract strontium. The following steps can be used for this purpose:

- (1) Determine the feed composition, including the concentration of both the extractable ions (strontium, calcium, sodium, etc) and those ions which will be essentially completely complexed

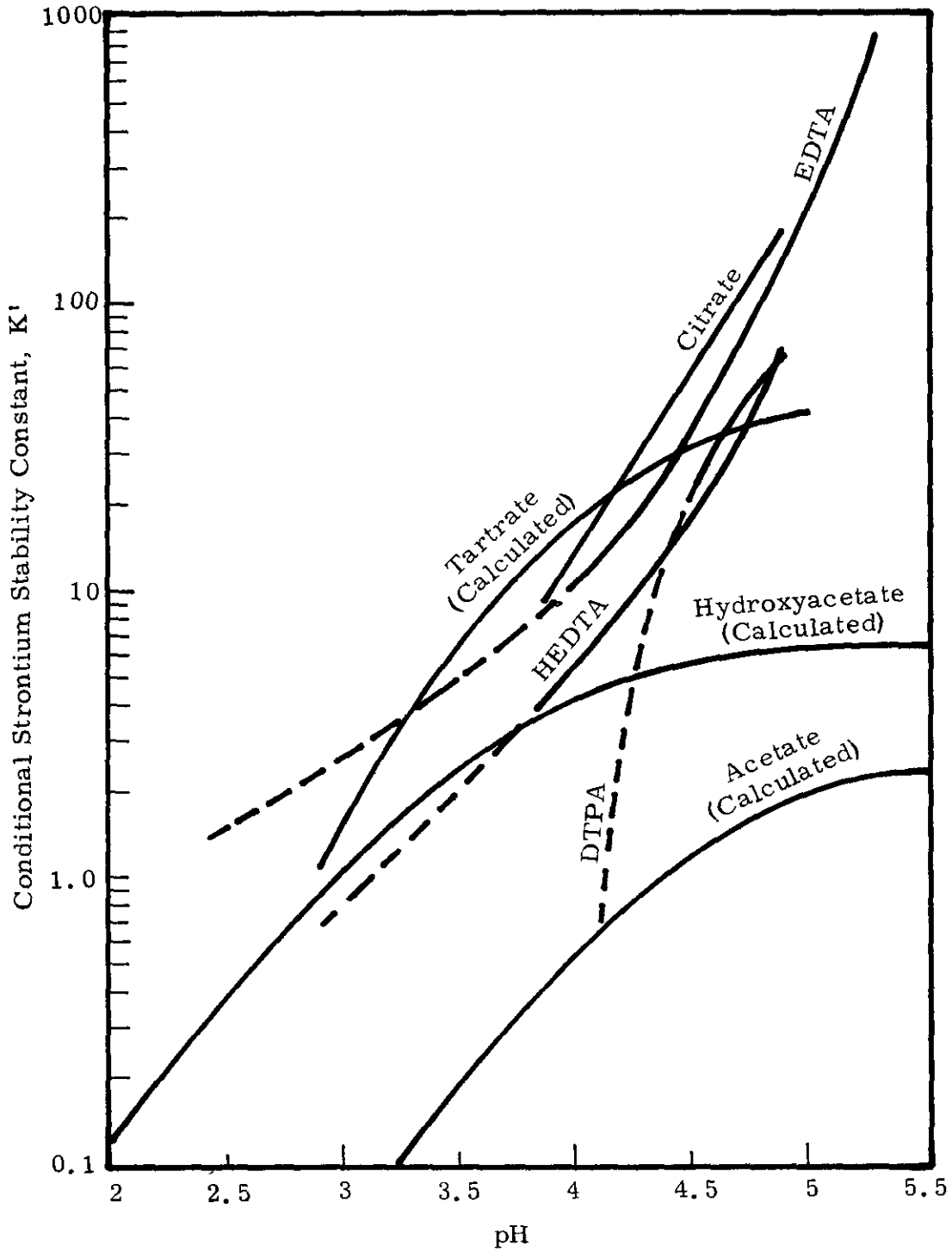


FIGURE IV-13

Effect of pH on Conditional Strontium Stability Constants  
(Source of Data: HW-72666)

DECLASSIFIED

by ligands (iron, lead, etc.). If a scrub stream is used, assume that it is stoichiometrically combined with the feed to establish the total concentration of ligands and metal ions entering the extraction section at the feed point.

- (2) Select a feed pH. This will normally be in the range of pH 3.5 to 5, high enough to prevent extraction of undesired, complexed metals (such as iron) but not high enough for sodium extraction to depress strontium extraction. If the system is adequately buffered, the equilibrium pH will be essentially the same as the feed (or combined feed plus scrub) pH.
- (3) Select a solvent concentration and a solvent-to-feed flow ratio. Assume that the more extractable ions, and only these ions (such as calcium, strontium, and the rare earths), are completely extracted. Calculate their concentrations in the product solvent and use the values to determine the free D2EHP concentration in the product (Equation 23). This will be the minimum value of free D2EHP in the system.
- (4) Assume that the equilibrium sodium concentration in the aqueous phase at the feed point is the same as the stoichiometric sodium concentration in the combined feed plus scrub. This will be approximately true if sodium extraction is minimized by selection of a low feed pH, a low solvent-to-feed flow ratio, or the use of a scrub stream which returns extracted sodium to the extraction section.
- (5) Calculate  $D_{Sr}$  using Figure IV-11 and the values of (free D2EHP), pH, and  $(Na^+)$  determined above.
- (6) Establish the ligand concentrations in the feed and scrub according to the requirements of the process. Calculate the concentrations of uncomplexed ligands in the combined feed-plus-scrub. If only 1:1 complexes are formed, this will be equal to the total ligand concentration minus the total molarity of metal ions complexed by that ligand. (In a mixture of metal ions and ligands, the complexes with the greatest stability constants would preferentially be formed. Thus in a mixture of ferric and lead ions and EDTA and citrate ligands, the ferric-EDTA complex would form first; any excess EDTA would then complex the lead. Citrate would form complexes only if there were insufficient EDTA to complex all of the iron and lead.) Assume that only negligible quantities of the extracting ions (strontium, calcium, etc.) are complexed (this will be true if the concentrations of extractable components are small and if the distribution ratios are relatively high).
- (7) Determine the ligand-complexing correction factor  $[1 + K'_a(L'_a) + K'_b(L'_b) \dots + K'_c(L'_c)]$ , from Figure IV-13, using the above values of free ligand concentrations and the feed pH to determine individual  $K'(L')$  values.

DECLASSIFIED

- (8) Calculate the actual strontium  $E_a$  by dividing the  $D_{Sr}$ , determined in Step 5, by the ligand-complexing correction factor (see Equation (33)).

To insure adequate strontium extraction, the calculated distribution ratio should be at least twice the assumed aqueous-to-organic flow ratio. If not, a new flow ratio or a more favorable pH should be assumed and the calculation repeated. A safety margin of  $\pm 50\%$  should be applied to the results to compensate for the simplifications inherent in the derivation. The use of the procedure is more clearly illustrated in the following example (33a).

1. Initial Aqueous Phase Composition:

	<u>Feed</u>	<u>Scrub</u>	<u>Combined Feed and Scrub</u>
$\underline{M}$ Sr	0.0016	0	0.0015
$\underline{M}$ Ca	0.004	0	0.0038
$\underline{M}$ Na	1.1	0.3	1.06*
$\underline{M}$ Fe + Pb	0.033	0	0.031
$\underline{M}$ Acetate	0.46	0	0.435
$\underline{M}$ EDTA	0.09	0	0.085
$\underline{M}$ Citrate	0	0.6	0.033
pH	4.7	2.9	(4.7)*
Relative Flow	130	7.5	137.5

\*Assumed equilibrium values

2. Solvent Composition: 0.4M D2EHPA; 0.2M TBP; Relative Flow = 30.

3. Free D2EHP: (Assume only strontium and calcium extract and that their extraction is quantitative.)

$$\underline{M} (\text{Sr} + \text{Ca})_{\text{aq}} = 0.0053$$

$$\underline{M} (\text{Sr} + \text{Ca})_{\text{org}} = \frac{(0.0053)(137.5)}{30} = 0.0243$$

$$\underline{M} \text{ free D2EHP} = 0.4 - 4(0.0243) = 0.303$$

4. Strontium Distribution Ratio,  $D_{Sr}$ :

$$\text{For } \text{Na}^+ = 1.06 \text{ and } \text{pH} = 4.7 \log \frac{(\text{Na}^+)}{(\text{H}^+)} = 4.72$$

$$\text{From Figure IV-11, } \frac{D_{Sr} (\text{H}^+)^2}{(\text{free D2EHP})^2} = 8 \times 10^{-7}$$

$$\text{Then } D_{Sr} = \frac{(8 \times 10^{-7})(0.303)^2}{(2 \times 10^{-5})^2} = 184$$

5. "Free" Ligand Concentration, [L] :  
(Assume all iron and lead are complexed by EDTA)

$$\text{Free EDTA} = 0.085 - 0.031 = 0.054\text{M}$$

$$\text{Free Citrate} = 0.033\text{M} = \text{total citrate}$$

$$\text{Free Acetate} = 0.435\text{M} = \text{total acetate}$$

6. Correction Factor for Ligand Complexing:

From Figure IV-13, using the feed pH of 4.7,

$$K'_{\text{EDTA}} = 60 \quad \text{and} \quad (K'L')_{\text{EDTA}} = (60)(0.054) = 3.2$$

$$K'_{\text{Citrate}} = 100 \quad \text{and} \quad (K'L')_{\text{Citrate}} = (100)(0.033) = 3.3$$

$$K'_{\text{Acetate}} = 1.5 \quad \text{and} \quad (K'L')_{\text{Acetate}} = (1.5)(0.435) = 0.7$$

$$\therefore 1 + \Sigma(K'L') = 8.2$$

7. Corrected Strontium  $E_a^0$ :

$$\begin{aligned} \text{Sr } E_a^0 &= \frac{D_{\text{Sr}}}{1 + \Sigma(K'L')} \\ &= \frac{184}{8.2} = 22. \end{aligned}$$

Applying the recommended  $\pm 50\%$  safety margin, the minimum  $E_a^0$  would be about 11.

## 2.6 Diluent and Solvent Modifier Effects

### 2.6.1 Third Phase Formation

Alkaline ( $\text{Na}_2\text{CO}_3$  or  $\text{NaOH}$ ) wash solutions are commonly used to remove yttrium and other contaminants from recycled D2EHPA extractants. Treatment of the extractant with such solutions converts D2EHPA to its sodium salt,  $\text{NaD2EHP}$ . This salt is soluble in water but only sparingly soluble in aqueous solutions which contain sodium ion. The solubility of  $\text{NaD2EHP}$  in  $\text{Na}_2\text{CO}_3$  solutions, for example, decreases from 325 mg/l at  $0.38\text{M Na}^+$  to 7 mg/l at  $2.8\text{M Na}^+$  (23).

The sodium salt also has limited solubility in common kerosene-type diluents (e.g., Soltrol-170 or NPH). Under certain conditions a  $\text{NaD2EHP}$ -rich phase can form when kerosene solutions containing D2EHPA are contacted with alkaline wash solutions. This  $\text{NaD2EHP}$ -rich phase lies between the kerosene diluent and the alkaline aqueous phase. To prevent

formation of this third liquid phase, it is customary to add to the D2EHPA extractant a modifier such as tributylphosphate (TBP). ORNL workers have shown<sup>(8)</sup> that the solubility of NaD2EHP in kerosene diluents is greatly increased by addition of neutral organic phosphorous compounds such as TBP, tributyl phosphine oxide, dibutyl-butylphosphonate, etc. TBP is the preferred modifier at Hanford because of its low cost and availability.

An empirical expression:

$$\underline{M} \text{ TBP} = 0.063 + 0.2 (\underline{M} \text{ D2EHPA}) \quad (34)$$

defining the concentration of TBP necessary to prevent third phase formation was derived at ORNL<sup>(8,9)</sup>. This expression was derived for a specific diluent (Amsco 125-82) from data obtained with an aqueous phase initially 10% Na<sub>2</sub>CO<sub>3</sub> and, according to recent Hanford work<sup>(59)</sup>, is not valid for systems in which the aqueous sodium concentration is less than about 0.6M. TBP requirements at aqueous phase sodium concentrations lower than 0.6M have been determined by Mendel<sup>(72)</sup> for the system NaOH-TBP-D2EHP-Soltrol-170-H<sub>2</sub>O. Mendel's data, plotted in Figure IV-14, have been correlated by the equation:<sup>(59)</sup>

$$\underline{M} \text{ TBP} = 0.156 - 0.093 (\underline{M} \text{ Na}_{\text{aq}}^{+}) + 0.2 (\underline{M} \text{ Na.D2EHP}_{\text{org}}) \quad (35)$$

for (Na<sup>+</sup>)<sub>aq</sub> concentrations above 0.2M.

The nature of the diluent is believed to affect the constants in the above equation, and suitable correction factors should be obtained for other candidate diluents.

### 2.6.2 Synergistic Effects

A strong enhancement of U(VI) extraction was first observed at ORNL<sup>(9)</sup> when mixtures of dialkylphosphoric acids and neutral organophosphorus compounds were used as solvents, the extraction power of the mixture being greater than the sum of the extraction powers of the separate reagents. The term synergistic extraction was applied to the effect by Coleman.

Recent studies at Hanford have also shown that D2EHPA extraction of strontium from various aqueous solutions is slightly enhanced when TBP is present in the extractant<sup>(72)</sup>. McDowell, Coleman, and Case at ORNL<sup>(29)</sup> have confirmed the synergistic effect of TBP on the D2EHPA extraction of strontium when an aliphatic hydrocarbon is used as the diluent (Figure IV 15). Almost complete lack of synergism was noted when benzene was used as a diluent for D2EHPA.

A general review of synergistic effects in extraction systems involving D2EHPA (HR) and neutral organophosphorus reagents (B) has been given by Baes<sup>(3)</sup>. According to Baes the effect may be attributed to the formation of a mixed complex - either a substitution product or an addition product - resulting from the reaction of B with the extraction complex normally formed with HR alone. Available extraction data appear more consistent with the addition product model.

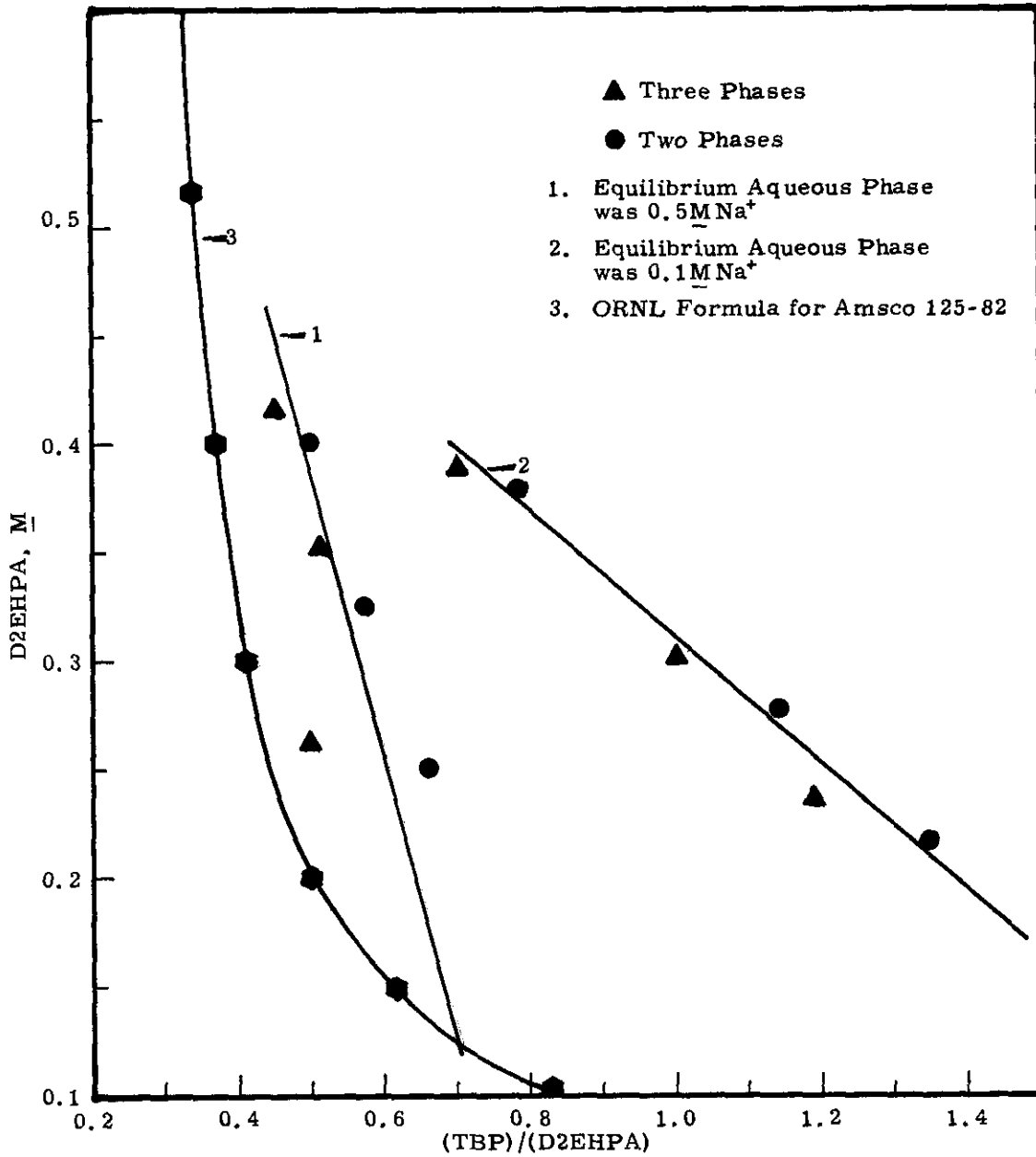


**FIGURE IV-14**  
 Third Phase Formation in System:  
 NaOH-H<sub>2</sub>O-TBP-D2EHPA-Soltrol-170  
 (Source of Data: HW-79762PT1)

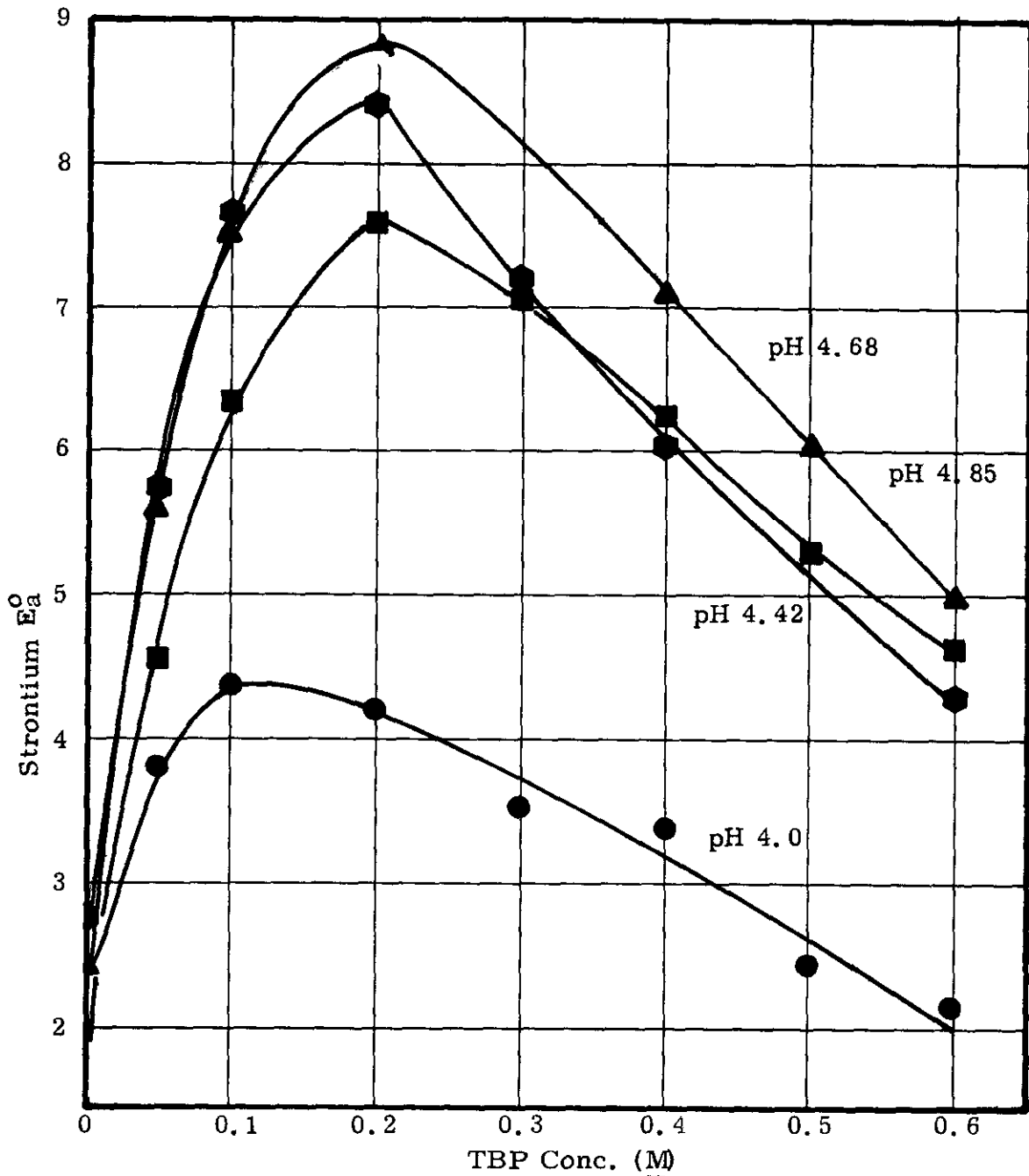


FIGURE IV-15

Strontium Extraction by 0.10M D2EHPA in *n*-Nonane as a Function of Added Tri-*n*-butyl Phosphate Molarity  
(Source of Data: ORNL 3492)

### 2.6.3 CSREX Process

A most unusual synergistic effect, discovered by L. A. Bray<sup>(10)</sup>, occurs when 4-sec-butyl-2( $\alpha$ -methylbenzyl)phenol (BAMBP) is added to D2EHPA in a kerosene carrier solvent. In the pH range 4 to 5, as noted above, D2EHPA extracts strontium and rare earths very efficiently but cesium hardly at all. Conversely, BAMBP is a highly specific solvent for cesium at pH's above 12<sup>(15)</sup> and does not extract strontium and rare earths. However when BAMBP is added to D2EHPA, the combined solvent exhibits maximum cesium extraction at a pH of 4 to 5, the aforementioned optimum pH range for extraction of strontium and rare earths.

From this unusual phenomenon evolved the CSREX process for co-extraction of cesium, strontium and rare earths from various waste solutions. (The name CSREX is an acronym for Cesium, Strontium, and Rare Earth Extraction.) The CSREX process has been thoroughly explored on both laboratory and pilot plant scale<sup>(12,60)</sup>. In many ways it parallels the D2EHPA process for extraction of strontium and rare earths described later (Section C-3) in this chapter. Thus, strontium, cesium, and rare earths are coextracted from a tartrate-complexed feed in the extraction column, along with calcium and about 10 to 20% of the sodium. The sodium is removed from the solvent in the scrub column and the strontium and cesium, along with calcium and residual sodium, are stripped in the partition column with very dilute acid. Finally, cerium and other rare earths are stripped from the solvent with stronger acid in the strip column.

The major limitation to the use of the CSREX process at the present time is the unusually high susceptibility of the solvent to radiation and nitrous acid degradation<sup>(47,65)</sup>. Sulfamic acid and hydrazine have been successfully used in nonradioactive solutions to inhibit nitrous acid formation and solvent degradation, but their performance in preventing degradation in a radiation field has not yet been satisfactorily demonstrated.

### 2.7 Kinetic Effects

No systematic study of the rate of extraction of metal ions from aqueous phases into D2EHPA-containing organic solutions has been made. Results obtained at both Hanford and ORNL indicate the reaction between strontium and D2EHPA is complete within about a minute at either 25 or 60 C. Recent work at Hanford and ORNL also has shown that rare earth (III) ions extract considerably more slowly than strontium ions at 25 C and that an increase of temperature to 50 or 60 C markedly increases the rate of extraction of the rare earth ions. Kinetics of extraction of strontium and rare earth ions are more fully discussed later (Section 3.2.3).

Extraction of Fe(III), Zr(IV), and Al(III) is especially slow at 25 C, requiring up to several hours to attain equilibrium<sup>(7,24,25,26)</sup>. The back-extraction of these ions with HNO<sub>3</sub> is also slow. Effective re-  
[redacted] of iron and aluminum from a D2EHPA extractant within a practical time at 25 C requires the use of alkaline wash solutions or aqueous solutions containing complexing agents.

### 3. Extraction of Strontium, Rare Earths, and Americium

#### 3.1 Process Concept

The D2EHPA continuous countercurrent extraction process for recovery of strontium, americium, and fission product rare earths from clarified PAW and PAS solutions can be readily visualized with the aid of the accompanying schematic (Figure IV-16). The processing sequence for PAS solution also includes  $PbSO_4$  carrier precipitation of strontium, americium, and rare earths (Section B-2) prior to the D2EHPA extraction process discussed in this section.

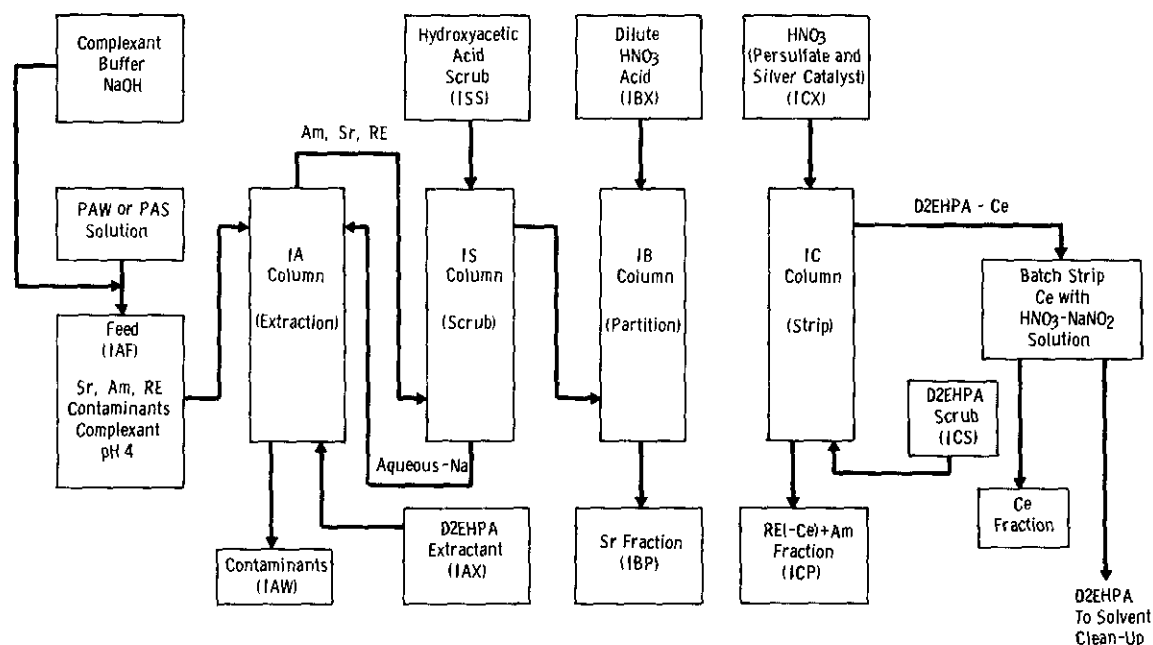


FIGURE IV-16

#### Schematic of D2EHPA Extraction Process

Extraction column feedstock is prepared from the PAW or PAS solution by addition of a suitable complexant, a buffer reagent (hydroxyacetic acid is currently favored) for pH control, and NaOH to adjust the pH to 4. This feed solution is contacted countercurrently with a D2EHPA-TBP diluent extractant in the IA Column to extract strontium, americium, and rare earths. The bulk of the contaminants, both inert and radioactive, including Cs-137 from the PAW solution, are rejected to the aqueous raffinate; however, essentially all of the calcium and magnesium in the feed solutions are also extracted.

DECLASSIFIED

462

Further purification of the extracted strontium, americium, and rare earths is achieved in the 1S Column. Here a small flow of hydroxyacetic acid solution partially neutralized with NaOH is used to scrub out sodium and other weakly coextracted impurities. The pH is carefully controlled to retain most of the strontium, americium, and rare earths in the organic phase. The aqueous stream from the scrub column is routed back to the extraction column to re-extract the small amounts of strontium, americium, and rare earths present.

In the 1B Column, strontium is partitioned from americium, rare earths, and from most of the calcium by stripping with a dilute HNO<sub>3</sub> solution. The pH of the aqueous phase in the column is controlled at approximately 2 to allow stripping of strontium but to retain americium, rare earths, and calcium in the organic phase. Sodium, magnesium, nickel, and some manganese - if present - follow the strontium.

Cerium is separated from the other rare earths, americium, and calcium in the 1C Column. This is done by oxidizing Ce(III) to the much more extractable Ce(IV) with a HNO<sub>3</sub> solution containing peroxydisulfate (persulfate) and silver ions. The other rare earths, including Pm-147, are not oxidized and they, along with americium and residual calcium, transfer to the aqueous phase. A D2EHPA scrub stream is employed to assure maximum decontamination from cerium.

Finally cerium is batch stripped with a HNO<sub>3</sub> solution containing NaNO<sub>2</sub> to reduce Ce(IV) to Ce(III). The D2EHPA extractant is then washed with various reagents to remove impurities and recycled to the extraction column. With PAW feeds where the Ce-144 content is negligible, the silver peroxydisulfate are omitted, and the cerium is stripped along with the other rare earths.

The remaining parts of this section discuss this process in detail.

### 3.2 1A Column

#### 3.2.1 Function

The function of the 1A Column is to provide for essentially complete extraction of strontium, americium, and rare earths, including Pm-147, while rejecting the bulk of the inert and radioactive contaminants to the aqueous raffinate. This is accomplished by proper choice of complexant and control of aqueous phase pH, temperature, D2EHPA, concentration, and flowrates.

#### 3.2.2 Complexant - Choice and Effects

Proper selection of the complexant(s) to add to the extraction column feed to prevent extraction of unwanted impurities and yet permit extraction of strontium, americium, and rare earths is critical to

DECLASSIFIED

DECLASSIFIED

463

satisfactory operation of the 1A Column. Choice of this complexant is influenced by economic as well as chemical factors. Among the latter are the nature and concentration of the contaminants to be complexed in the various waste solutions, and the relative strengths (stability constants) of the complexes formed at a particular pH with these contaminants and with strontium, rare earths, and americium.

A large amount of laboratory work with synthetic waste solutions has been done to furnish an empirical basis for selecting complexants for PAW and ZAW feeds<sup>(17,18,72)</sup>. The most promising candidates as this manual was written were HEDTA, citric acid, and tartaric acid. Gluconic acid has been eliminated from consideration because of the weak complexes it forms with iron and aluminum<sup>(17)</sup>. EDTA and DTPA are unacceptable in this application because of the strong complexes they form with rare earths and americium (Figure IV-17 and Section C-4). Laboratory tests of nitrilotriacetic acid were in progress as this manual was written; published formation constants (Table IV-67) indicate this complexant may compare favorably to HEDTA and citric and tartaric acids.

As this manual was written, the final choice of complexant for PAW and ZAW feeds had not been made. Tests in the Semiworks with radioactive feeds were being made to evaluate the performance of the various complexants under B-Plant Flowsheet conditions. Only HEDTA of the complexants studied adequately prevented lead extraction (see below), and it is specified as the complexant for lead-containing PAS solutions.

Compositions of synthetic wastes used in the laboratory studies are presented in Table IV-8. The PAW compositions are representative of Purex acid waste derived from processing of aluminum-clad uranium fuels. The ZAW (Zirflex Acid Waste) is that expected from Purex Plant processing of zircaloy-clad N-reactor fuel. It contains a relatively large amount of aluminum added to complex fluoride carried over into the waste from the Zirflex decladding process.

Feeds were normally aged several hours to assure chromium complexing. Digestion for 3 to 5 hours at room temperature or 30 min at 60 C resulted in a 10-fold decrease in the chromium distribution ratio compared with that after aging only one hour<sup>(72)</sup>. The distribution ratios of other components were unaffected by digestion. As discussed in Section D, feed aging or digestion generally improved the stability of the 1A Column. Solvents used in most of the studies were either 0.37 - 0.4M D2EHPA - 0.2M TBP in Shell Spray Base, Soltrol-170, or NPH diluents or 0.2M D2EHPA - 0.1M TBP in Soltrol-170. Feed solutions were contacted 10 min at room temperature with an equal volume of extractant unless otherwise noted.

DECLASSIFIED

DECLASSIFIED

464

00

TABLE IV-8  
APPROXIMATE SYNTHETIC WASTE COMPOSITIONS USED IN LABORATORY STUDIES

Source of Data: ORNL-3204 (ORNL PAW)  
 HW-79762 PT1 (PAW-A and B)  
 BNWL-CC-595 (PAW-C, ZAW)

Constituent	PAW				ZAW
	ORNL	A	B	C	
Na	2.7	0.8	1.2	1.5	1.5
Fe	0.15	0.037	0.075	0.068	0.17
Al	0.033	0.0185	0.0375	0.034	0.34
Cr	0.0033	0.0074	0.015	0.013	0.007
Ni	0.0033	0.0037	0.0075	0.007	0.004
Sr	0.00065	0.00033	0.00068	0.00056	0.00056
RE	0.0030	0.0020	0.0041	0.0028	0.0028
F <sup>-</sup>	0	0.0007	0.0015	0	0.15
SO <sub>4</sub> <sup>=</sup>	0.33	0.019	0.038	0.104	0.052
PO <sub>4</sub> <sup>=</sup>	0.003	0.0019	0.0038	0	0
HEDTA	0	(a)	(b)	(d)	(e)
Citrate	0	(a)	(b)	(d)	0
Tartrate	0.33	(a)	(b)	(d)	(e)
Acetate	0	0.35	0 (c)	0	0
Hydroxy-acetate	0	0	0	0.25	0.25

- (a) 0.12M complexant; either HEDTA, citrate, or tartrate.
- (b) Either 0.19M HEDTA, 0.19M citrate or 0.25M tartrate.
- (c) The HEDTA feed also contained 0.35M acetate.
- (d) 0.17M complexant (HEDTA, citrate, or tartrate) plus an additional 0.0125M tartrate.
- (e) Either 0.5M HEDTA plus 0.0125M tartrate or 0.6125M tartrate.

DECLASSIFIED

Effect of Complexant Type and pH

Data obtained to compare the effects of the complexants on distribution ratios of various constituents of PAW and ZAW at several pH's are presented in Tables IV-9(17) and IV-10(72). The data in Table IV-10 are also presented graphically in Figures IV-17 through IV-23. Data for tracer americium extraction from a 1M NaNO<sub>3</sub> solution is presented in Figure IV-24(18). With the exception of the ZAW data in Table IV-9, all systems contained 0.05M free complexant (above that required to form 1:1 complexes).

TABLE IV-9  
DISTRIBUTION RATIOS AS A FUNCTION OF COMPLEXING AGENTS

(Data from BNWL-CC-595)

Contact Time: 2 minutes

Temperature: 35 C

O/A: 1

Extractant: 0.4M D2EHPA-0.2M TBP-NPH

Feed: (see Table IV-8)

	Distribution Ratio, E <sub>a</sub> <sup>o</sup>					
	HEDTA		Tartaric Acid		Citric Acid	
	pH3	pH4	pH3	pH4	pH3	pH4
<u>PAW-C</u>						
Strontium	2	17	0.85	10	1.4	13
Cerium	460	48	800	200	700	40
Promethium	32	3.6	700	150	370	16
Lead	0.006	0.0009	4.5	9	4.5	2
Iron	0.0006	0.0006	0.45	0.75	0.08	0.016
Aluminum	0.07	0.07	0.15	0.28	0.52	0.026
<u>ZAW</u>						
Strontium	0.8	7	0.65	6		
Cerium	1000	600	170	160		
Promethium	440	210	70	63		
Lead	0.007	0.002	2.7	4.5		
Iron	0.0003	0.0003	0.1	0.025		
Aluminum	0.12	0.09	0.03	0.13		

Significant conclusions derived from these data are:

- Iron, aluminum, and lead are complexed much more effectively by HEDTA than by either citrate or tartrate. In turn citrate is more effective than tartrate in complexing iron, and tartrate is more effective than citrate in complexing aluminum. (The apparent superiority of tartrate over HEDTA for complexing aluminum in ZAW feed is probably due to the greater excess of complexant with the tartrate feed.)

DECLASSIFIED

466

100

TABLE IV-10  
EFFECT OF COMPLEXANT TYPE AND pH ON DISTRIBUTION RATIOS, 25 C

Data from: HW-79762PT1

Conditions: PAW-A feed solutions (Table IV-8) were spiked with various radioisotopes and allowed to stand at least 16 hr at 25 C. Solutions then contacted 10 min at 25 C with an equal volume of 0.37M D2EHPA-0.2MTBP - SSB.

Final Aqueous pH	Distribution Ratios							
	Sr-85	Ce-144	Fe-59	Cr-51	Eu-152	ZrNb-95	Ru-106	Pm-147
<u>0.12 M Citrate</u>								
3.1	3.1	77.8	0.22		30.0	0.021	0.0046	34.7
3.6	26.1	35.7	0.050		20.4	0.0086	0.0032	21.4
4.15	78.8	55.4	0.017		20.1	0.0093	0.0036	20.9
4.5	76.7	23.2	0.013		3.34	0.0086	0.0045	3.71
4.85	29.2	7.22	0.032		4.92	0.017	0.020	3.98
<u>0.12M Tartrate</u>								
3.65	19.8	81.6	0.29		30.0	0.20	0.0035	20.8
4.2	50.8	35.5	0.19		17.5	0.13	0.0045	16.9
4.6	59.6	18.2	0.29		8.22	0.13	0.0074	9.37
4.85	41.6	8.99	0.71		2.63	0.17	0.023	4.07
<u>0.12M HEDTA</u>								
3.5	20.8	509	0.0017	0.0018	10.3			15.6
4.0	62.8	867	0.0010	0.0029	7.0			4.48
4.5	88.6	137	0.00024	0.0006	1.9			3.1

- Tartrate and citrate are about equally effective in suppressing ruthenium extraction; however citrate is more effective than tartrate in suppressing ZrNb-95 extraction.
- Citrate and HEDTA have about the same effect on strontium extraction. Below pH 4.7, strontium extracts better from citrate or HEDTA-complexed feeds than from tartrate complexed feeds.
- The relative effects of the complexants on rare earth extraction in the two studies are anomalous. Apparently extraction kinetics, discussed in Section C 3.2.3, were overriding factors.
- An aqueous phase pH of about 4 appears optimum for satisfactory extraction of strontium, rare earths, and americium. Strontium extraction is depressed at lower pH's, and rare earth extraction (and extraction kinetics) are decreased at higher pH's. A pH of 4 also provides near minimum distribution ratios for many of the impurities, including iron and aluminum.

DECLASSIFIED

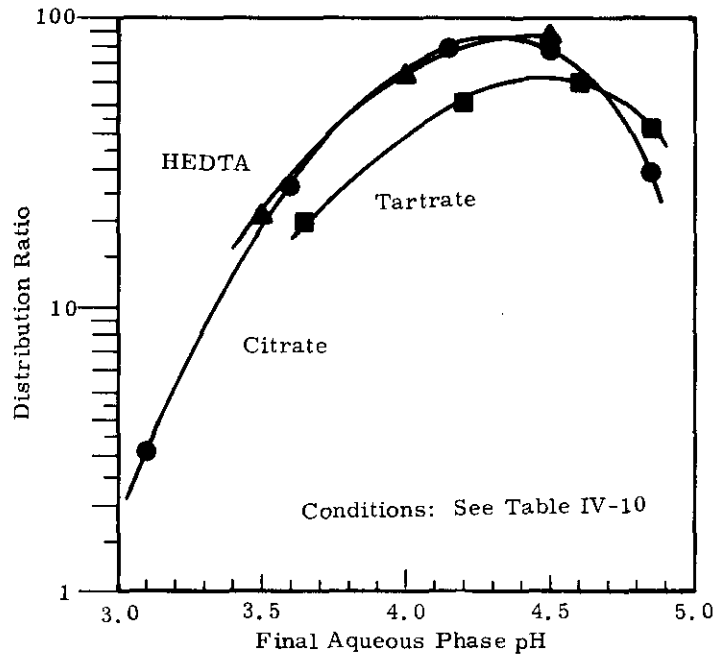


FIGURE IV-17

Variation of Strontium Extraction with Complexant Type and pH at 25 C  
(Source of Data: HW-79762PT1)

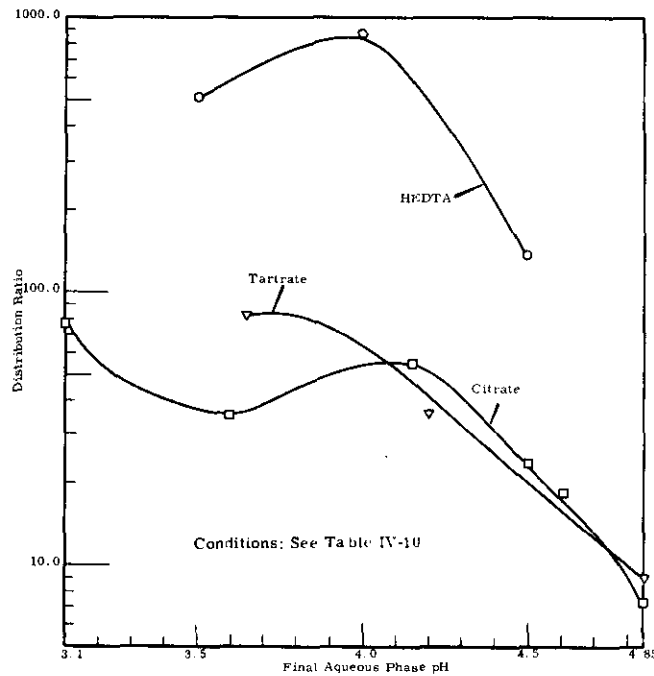


FIGURE IV-18

Variation of Cerium Extraction with Complexant Type and pH at 25 C  
(Source of Data: HW-79762PT1)

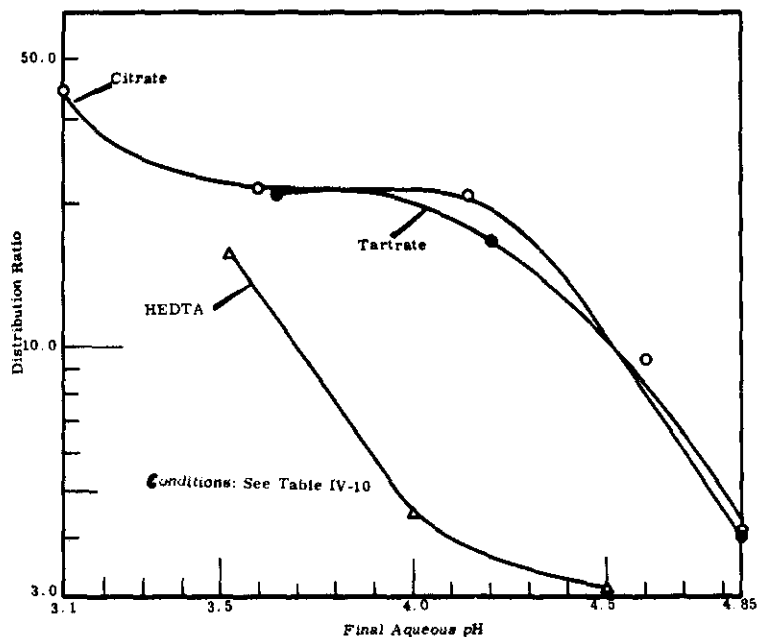


FIGURE IV -19

Variation of Promethium Extraction with Complexant Type and pH at 25 C  
(Source of Data: HW-79672PT1)

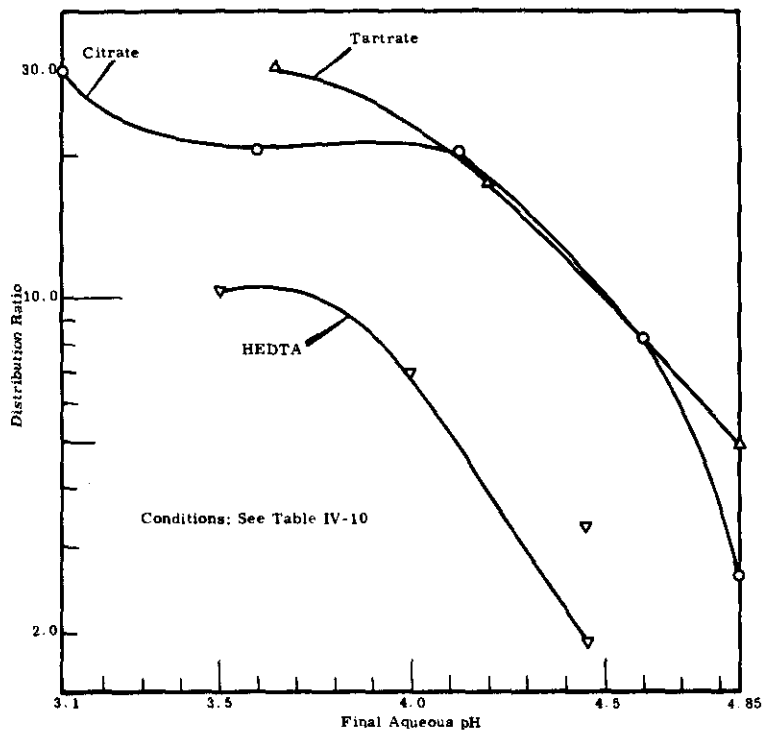


FIGURE IV -20

Variation of Europium Extraction with Complexant Type and pH at 25 C  
(Source of Data: HW-79672PT1)

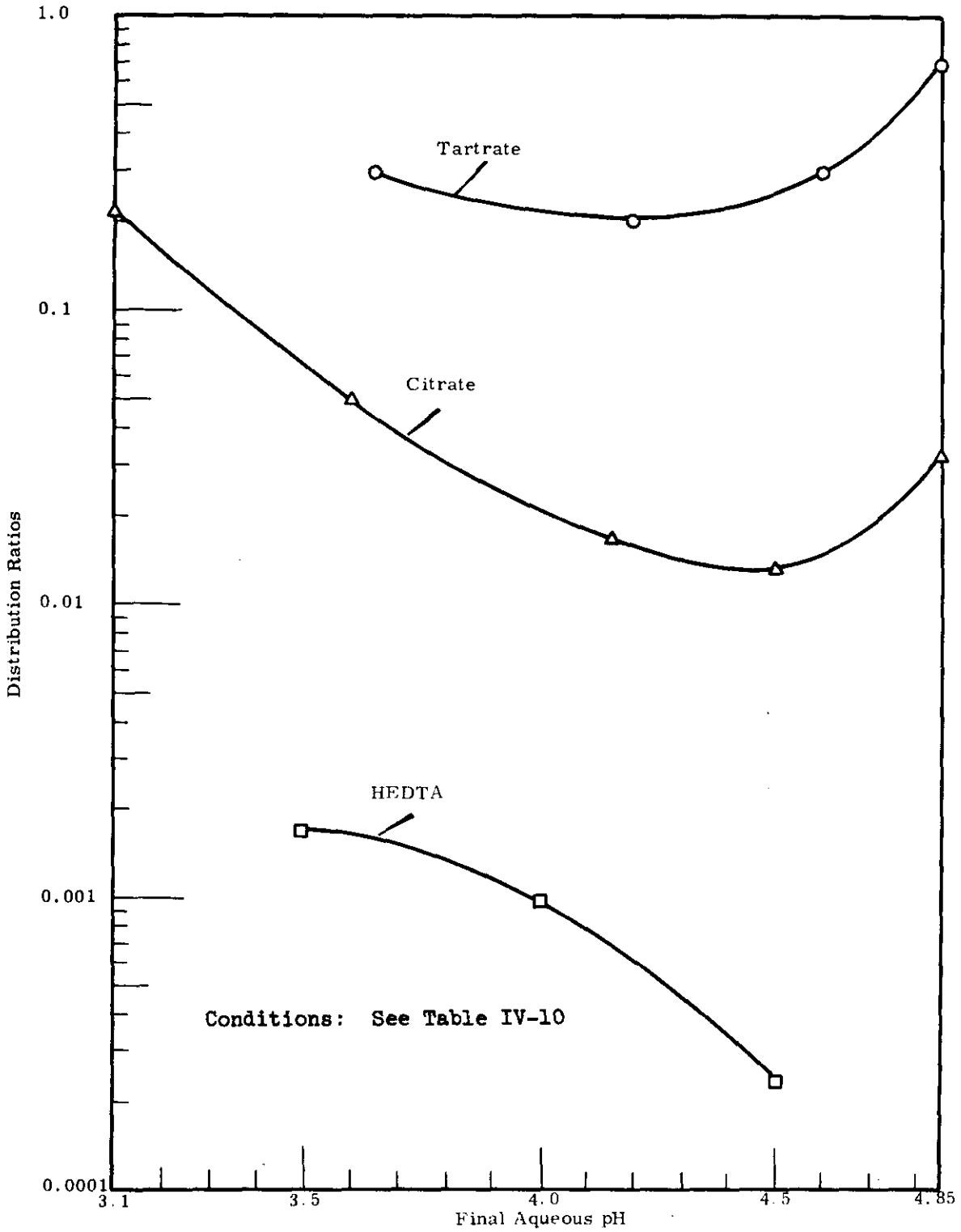


FIGURE IV-21

Variation of Iron Extraction with Complexant Type and pH at 25 C  
(Source of Data: HW-79726PT1)

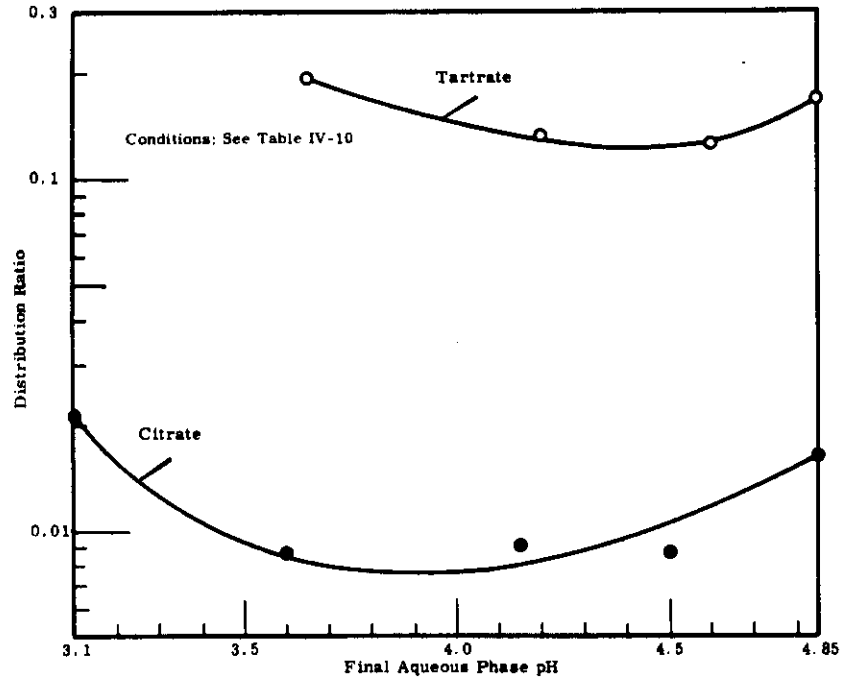


FIGURE IV-22

Variation of Zr-Nb Extraction with Complexant Type and pH at 25 C  
(Source of Data: HW-79762PT1)

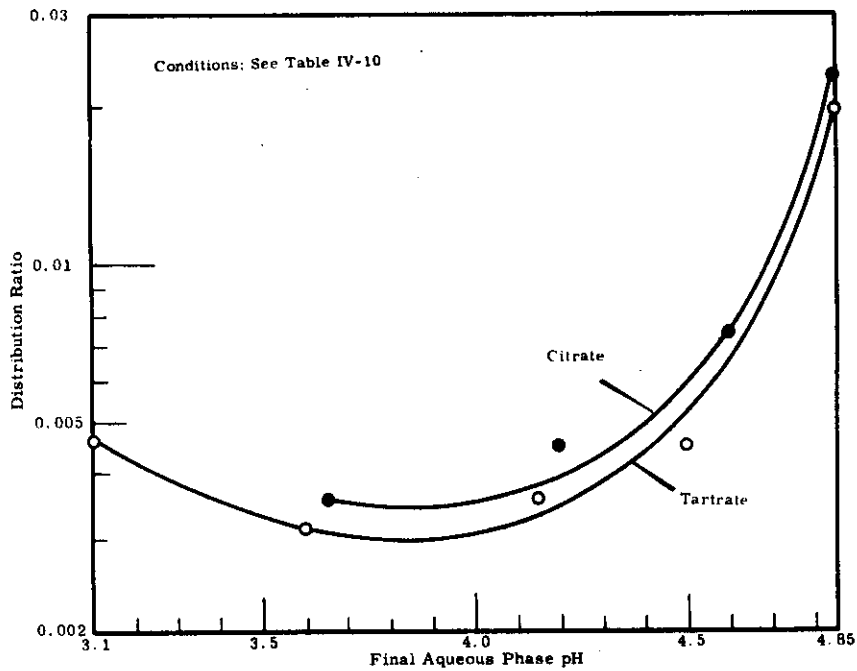


FIGURE IV-23

Variation of Ruthenium Extraction with Complexant Type and pH at 25 C  
(Source of Data: HW-79762PT1)

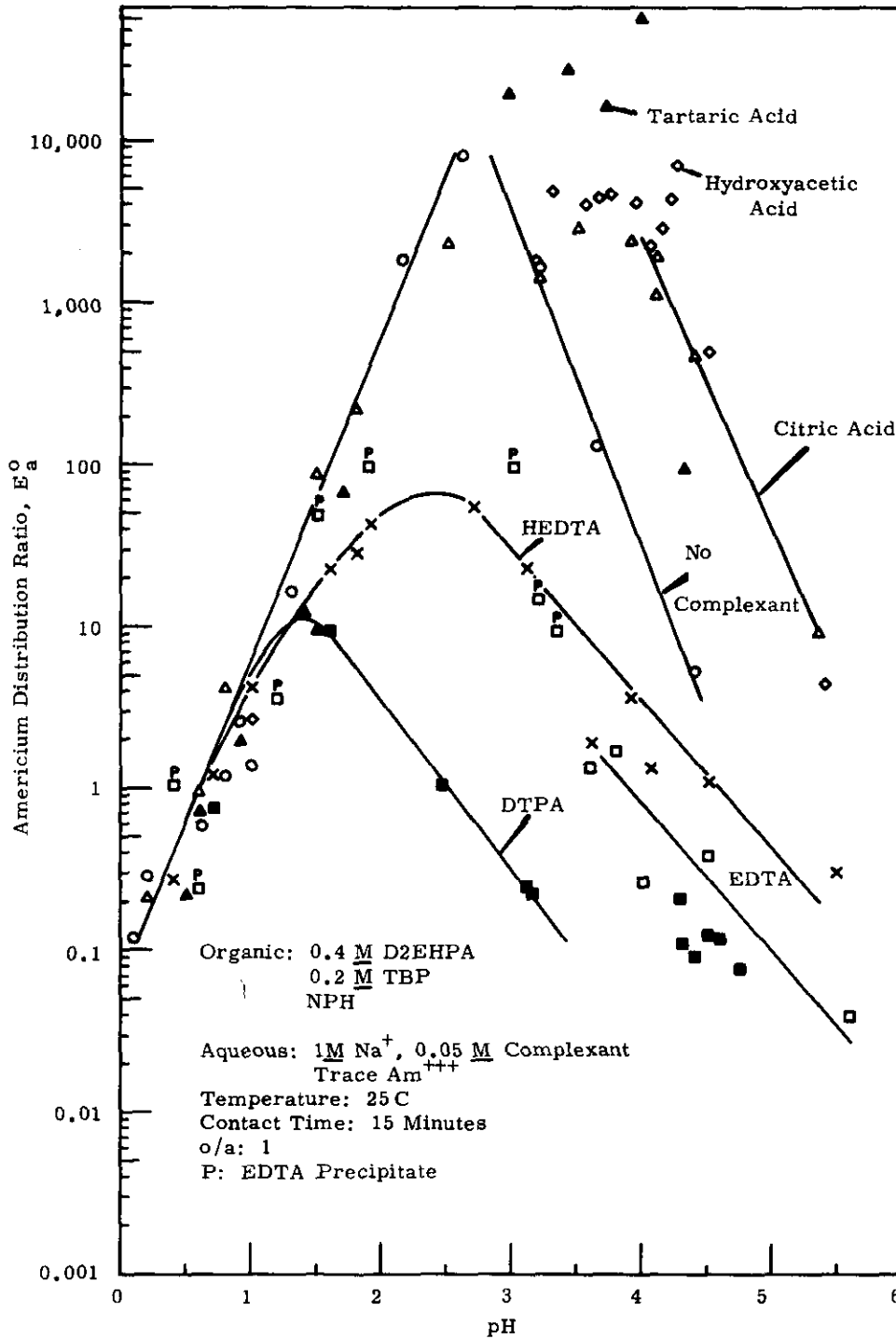


FIGURE IV-24

Effect of Complexants on Extraction of Americium  
(Source of Data: ISO-95)

DECLASSIFIED

472

Effect of Temperature and D2EHPA Concentration

Additional data to compare the tartrate and citrate systems at 25 and 60 C are presented in Table IV-11 and Figure IV-25 (72). The extractant for these tests contained 50% less D2EHPA and TBP than the solvent in the preceding studies. The data show the expected 4-fold decrease in strontium distribution ratios because of the lower solvent concentration. Kinetic effects evidently obscured the solvent dependency effect for other constituents.

TABLE IV-11  
EFFECT OF COMPLEXANT TYPE AND pH ON DISTRIBUTION RATIOS  
(Data from HW-79762PT1)

Element	0.25M Tartrate System				0.19M Citrate System			
	25 C		60 C		25 C		60 C	
	pH	$E_a^0$	pH	$E_a^0$	pH	$E_a^0$	pH	$E_a^0$
Strontium	3.3	1.3	3.3	0.071	3.1	0.845	3.2	0.0971
	3.9	2.3	3.7	0.19	3.5	6.43	3.7	1.29
	4.0	3.5	4.0	0.40	4.0	24.2	4.1	12.1
	4.4	8.0	4.4	2.6	4.4	28.2	4.6	16.9
	4.9	10	4.9	12	5.0	16.2	5.1	13.6
Iron	3.3	0.34	3.3	0.96	3.05	0.085	3.18	0.27
	3.85	0.27	3.7	0.65	3.5	0.031	3.65	0.16
	4.0	0.37	4.0	0.95	4.0	0.012	4.10	0.066
	4.3	0.40	4.3	0.86	4.42	0.008	4.55	0.035
	4.9	0.29	4.9	1.47	5.0	0.010	5.05	0.027
Chromium	3.3	0.0037	3.3	0.0080	3.05	0.0070	3.18	0.0012
	3.85	0.0034	3.7	0.0072	3.50	0.00030	3.65	0.0026
	4.0	0.0027	4.0	0.0079	4.0	0.00093	4.10	0.00013
	4.4	0.0020	4.4	0.0025	4.42	0.00082	4.55	0.00017
	4.9	0.013	4.9	0.019	5.0	0.0067	5.05	0.0071
Aluminum	3.3	0.26	3.3	0.39				
	3.85	0.29	3.7	0.39				
	4.0	-	4.0	0.53				
	4.9	0.40	4.9	0.77				
Europium	3.3	2.51	3.3	33.6				
	3.85	8.19	3.7	155				
	4.0	9.11	4.0	85.9				
	4.4	4.75	4.3	64.1				
	4.9	2.41	4.9	40.1				

In both systems, an increase in temperature decreased the strontium distribution ratios while extraction of all other major constituents, including rare earths, increased with temperature. The adverse effect of increased temperature on strontium extraction may be attributed to the greater loading of the solvent with trivalent ions, although there may also be an enthalpy effect.

DECLASSIFIED

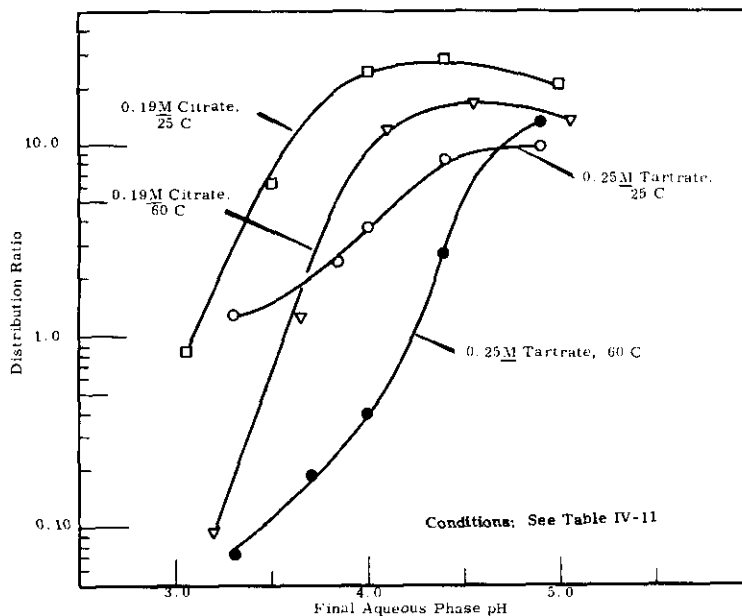


FIGURE IV-25

Variation of Sr Extraction with Complexant Type and pH at 25 and 60 C  
(Source of Data: HW-79762PT1)

#### Effect of Complexant Concentration

The complexant concentration used in most laboratory studies and specified in chemical flowsheets was based on the assumption of the formation of 1:1 complexes with iron, aluminum, chromium, nickel, and other polyvalent impurities. An excess of 0.05M complexant was usually supplied to simulate an assumed 20 to 30% Plant safety margin. Higher concentrations are uneconomical and, in HEDTA systems, lead to decreased distribution ratios for strontium and rare earths as shown in Table IV-12<sup>(72)</sup>. In citric-acid complexed feeds, however, an increase in unused complexant concentration of 0.05 to 0.1M resulted in improved rare earth extraction, as shown in Table IV-13<sup>(72)</sup>. This unusual effect was less pronounced at elevated temperatures and may reflect a change in extraction kinetics.

#### Effect of Radiolysis

B-Plant complexants, particularly in PAW and ZAW solutions, are subject to radiolytic destruction. Calculations based on data published by Van Tuyl<sup>(78)</sup> indicate the exposure level in feed solutions prepared from PAW will be about  $2 \times 10^6$  rad/hr. At this exposure level, about 10 hours will be required to attain a total exposure of  $2 \times 10^7$  rad. Limited results indicate that both HEDTA and citrate are sufficiently stable at this exposure to permit their use as complexants<sup>(72)</sup>.

DECLASSIFIED

474

00

TABLE IV-12  
EFFECT OF FEED HEDTA CONCENTRATION  
ON DISTRIBUTION RATIOS  
 (Data from HW-79762PT1)

Contact Time: 10 min.  
 Temperature: 25 C  
 O/A: 1  
 Extractant: 0.37M D2EHPA, 0.2MTBP, SSB  
 Feed: PAW-A (Table IV-8) except variable HEDTA concentration.

HEDTA M	Distribution Ratios			
	Sr	Ce	Pm	Eu
0.10	67.9	-	18.0	-
0.12	63.3	572	19.0	4.22
0.20	38.7	303	-	4.22
0.30	22.9	179	9.0	1.49

(a) Final aqueous pH was 4.0

TABLE IV-13  
EFFECT OF FEED CITRATE CONCENTRATION ON DISTRIBUTION RATIOS  
 (Data from HW-79762PT1)

Contact Time: 10 min.  
 Temperature: 25 C  
 O/A: 1  
 Extractant: 0.2M D2EHPA, 0.1M TBP, Soltrol-170  
 Feed: PAW-B (Table IV-8) except variable citrate concentration.

Citrate M	Temperature C	Aqueous pH	Distribution Ratios				
			Ce	Eu	Sr	Fe	Cr
0.19	25	4.0	14.7	1.72	20.3	0.013	0.00058
0.25	25	4.0	35.3	16.7	18.4	0.013	0.00017
0.30	25	4.1	29.3	20.6	8.77	0.017	0.00015
0.35	25	4.1	15.7	18.6	7.36	0.017	0.000011
0.19	60	4.2	89.1	107.0	7.10	0.057	0.00094
0.25	60	4.2	104.0	145.0	-	0.059	0.00011
0.30	60	4.0	86.2	131.0	3.74	0.11	0.00020
0.35	60	3.9	47.0	133.0	2.55	0.11	0.000064

DECLASSIFIED

### 3.2.3 Extraction Kinetics

Kinetics of D2EHPA extraction of various elements from complexed feed solutions have been studied at Hanford<sup>(17,72)</sup> and ORNL<sup>(27)</sup>. Data illustrating the variation of distribution ratios with contact time at both 25 and 60 C for PAW feeds containing either citrate or tartrate are presented in Table IV-14 and Figures IV-26 through 29<sup>(72)</sup>. The results of studies at 35 C with HEDTA, citrate, and/or tartrate-complexed PAW and ZAW feeds are presented in Figures IV-30 through 34<sup>(17)</sup>.

TABLE IV-14  
EXTRACTION KINETICS: CITRATE AND TARTRATE FEEDS  
(Data from HW-79762PT1)

Contact Time min.	Distribution Ratios			
	0.25M Tartrate System			0.19M Citrate System
	Cr	Ru	ZrNb	Cr
25 C <sup>(a)</sup>				
1	0.00054	0.0012	0.017	0.00088
3	0.0018	0.0019	0.035	0.00079
5	0.0020	0.0015	0.028	0.00067
10	0.0020	0.0017	0.039	0.00058
30	0.0021	0.0024	0.066	0.00044
60	0.0015	0.0018	0.075	0.00085
60 C <sup>(b)</sup>				
1	0.00063	--	0.018	0.00071
3	--	0.0017	0.050	0.00061
5	--	0.0015	0.069	0.00049
10	0.0025	0.0028	0.067	0.00094
30	0.0029	0.0028	0.11	0.00049
60	0.0049	0.0028	0.098	0.0014

(a) Final aqueous pH was 4.0 for citrate feeds and 4.2 to 4.4 for tartrate feeds.

(b) Final aqueous pH was 4.15 for citrate feeds and 4.1 to 4.5 for tartrate feeds.

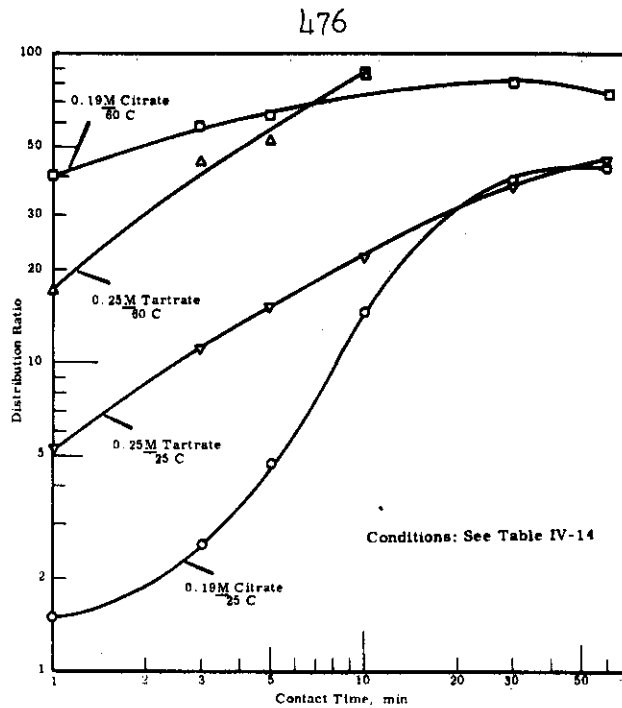


FIGURE IV-26

Kinetics of Extraction of Cerium  
(Source of Data: HW-79762PT1)

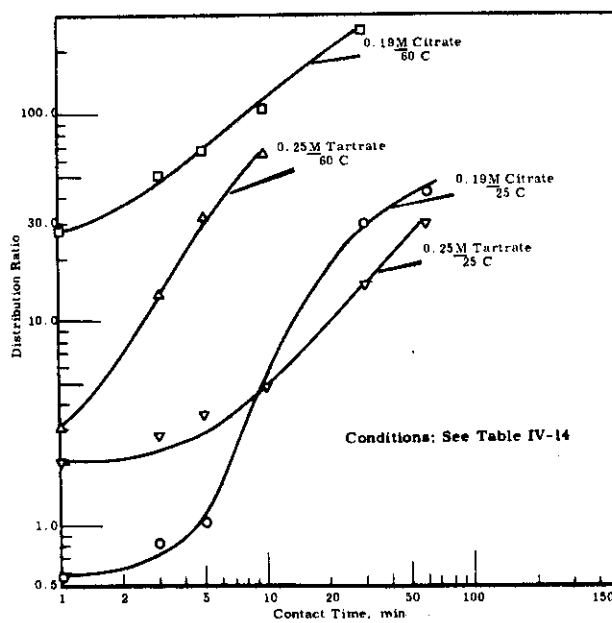


FIGURE IV-27

Kinetics of Extraction of Europium  
(Source of Data: HW-79762PT1)

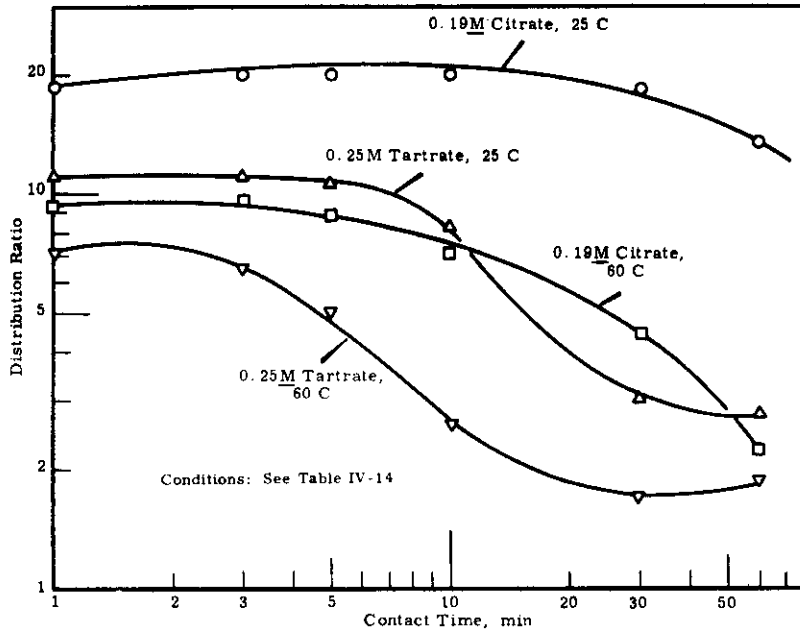


FIGURE IV-28

Kinetics of Extraction of Strontium  
(Source of Data: HW-79762PT1)

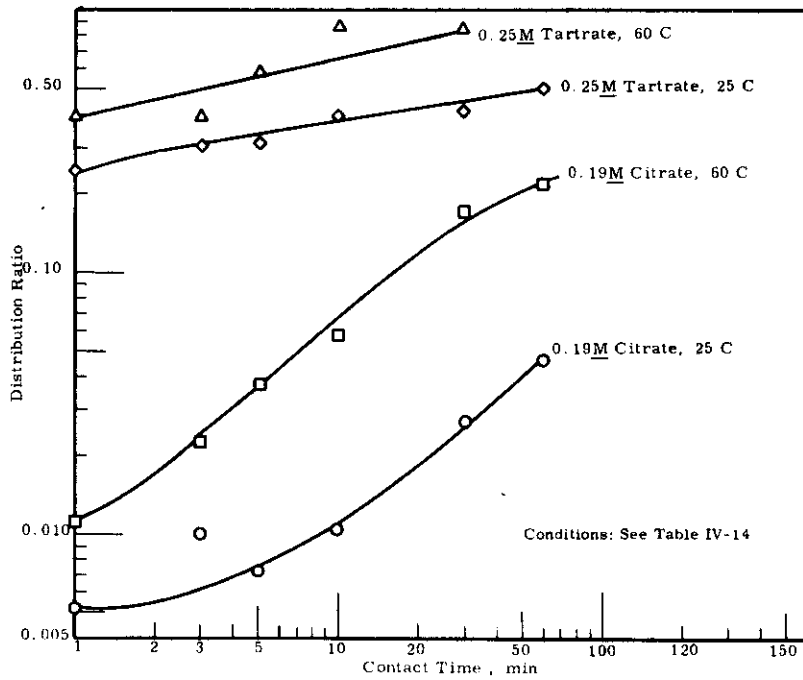


FIGURE IV-29

Kinetics of Extraction of Iron  
(Source of Data: HW-79762PT1)

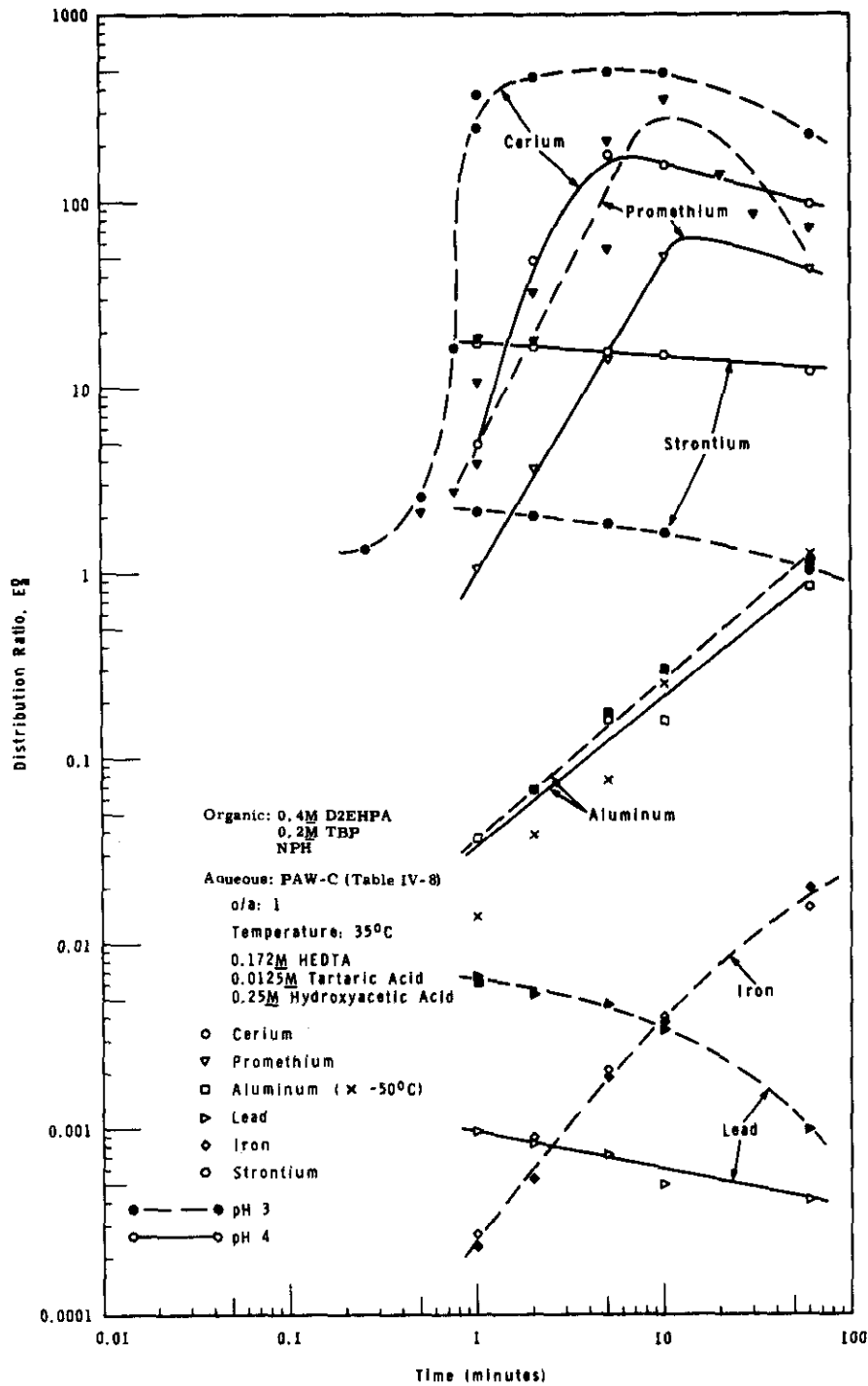


FIGURE IV-30

Distribution Ratio as a Function of Contact Time-PAW  
(HEDTA Complexed)  
(Source of Data: BNWL-CC-595)

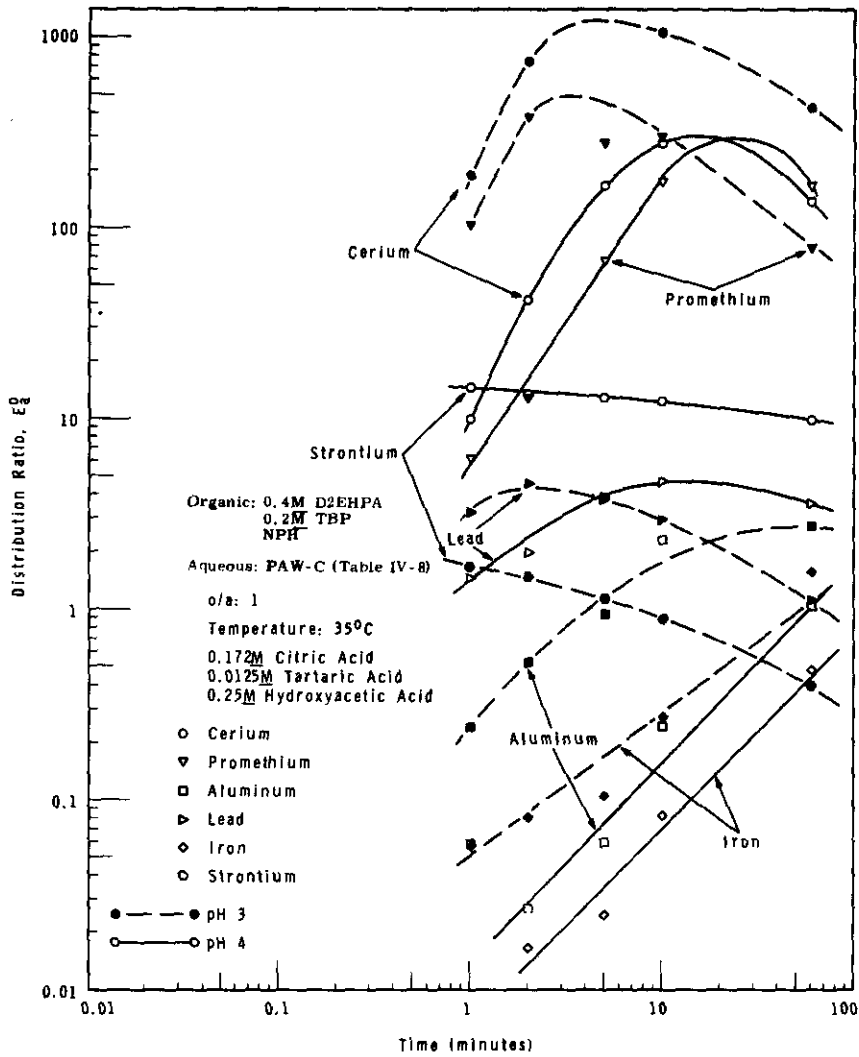


FIGURE IV-31

Distribution Ratio as a Function of Contact Time-PAW  
(Citric Acid Complexed)  
(Source of Data: BNWL-CC-595)

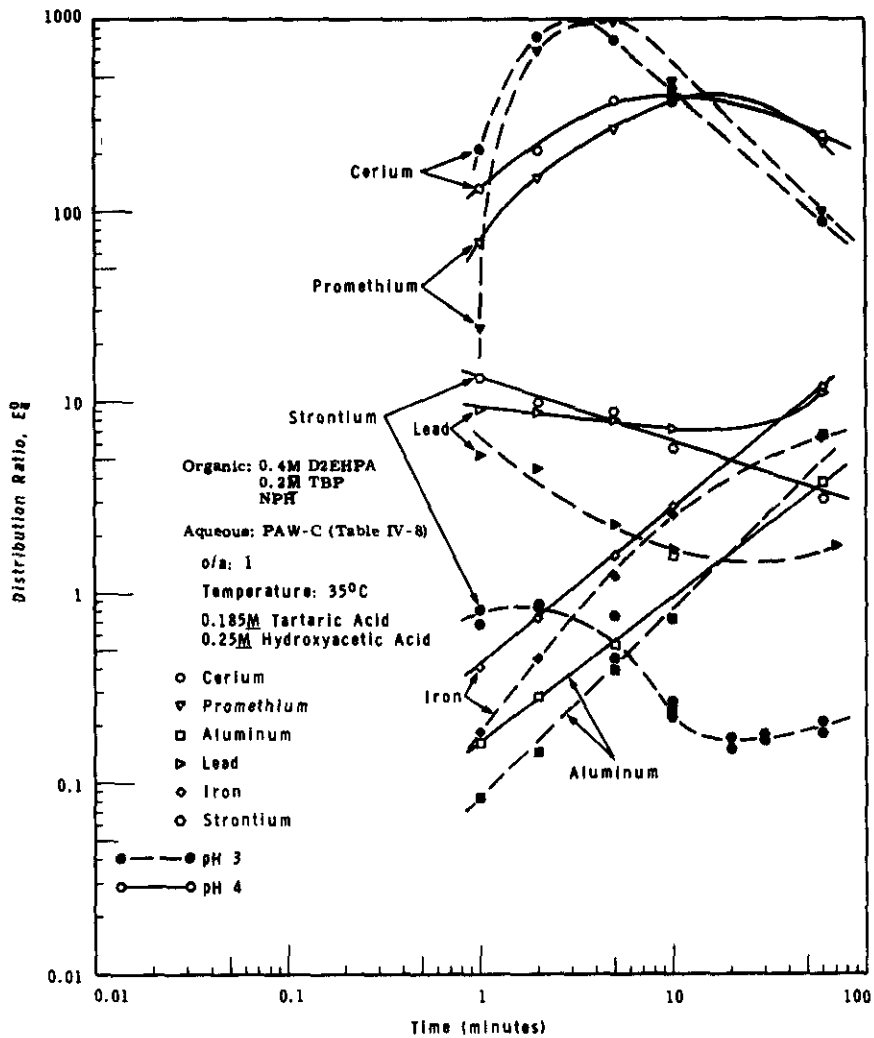


FIGURE IV-32

Distribution Ratio as a Function of Contact Time-PAW  
 (Tartrate Complexed)  
 (Source of Data: BNWL-CC-595)

481

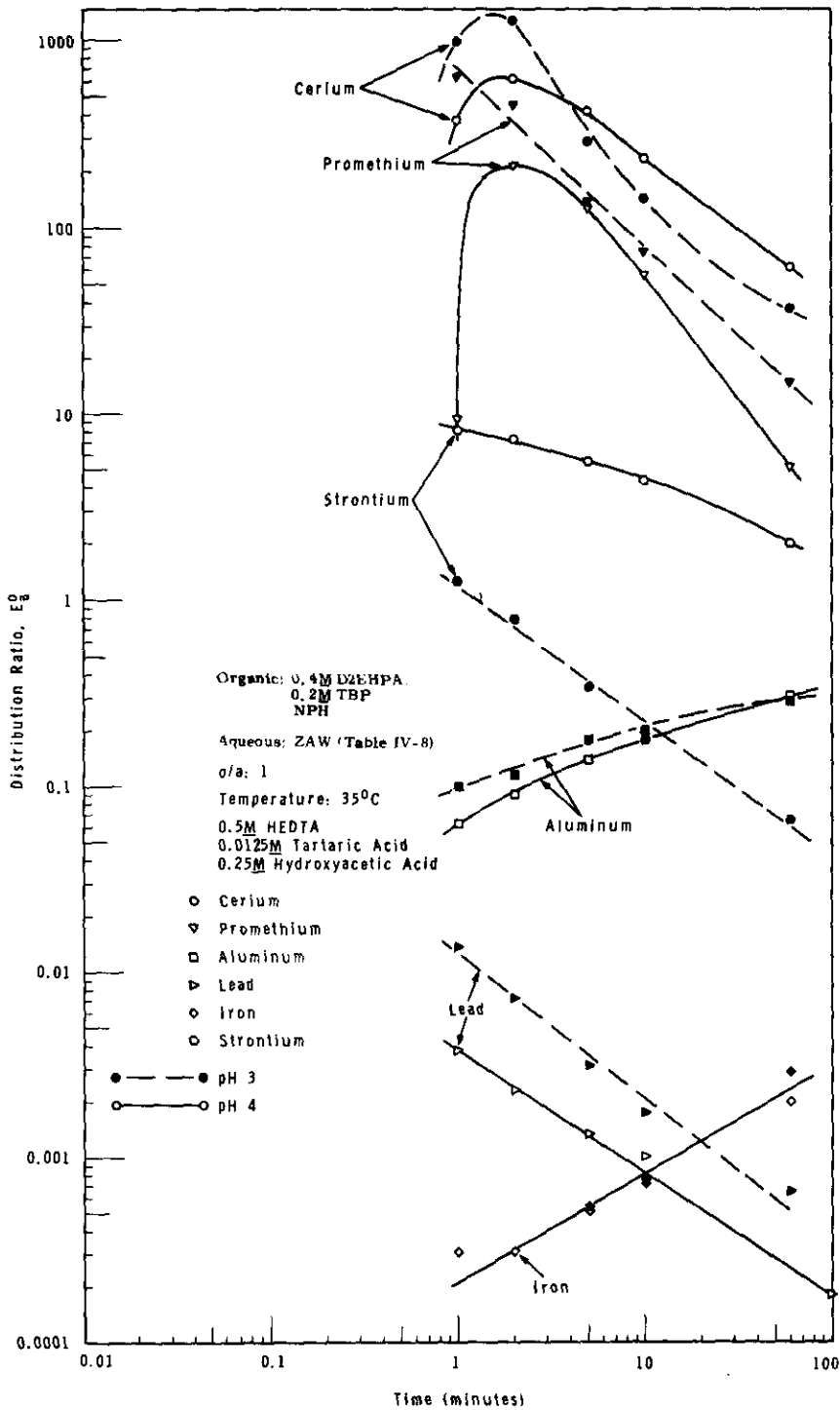


FIGURE IV-33

Distribution Ratio as a Function of Contact Time - ZAW  
(HEDTA Complexed)  
(Source of Data: BNWL-CC-595)

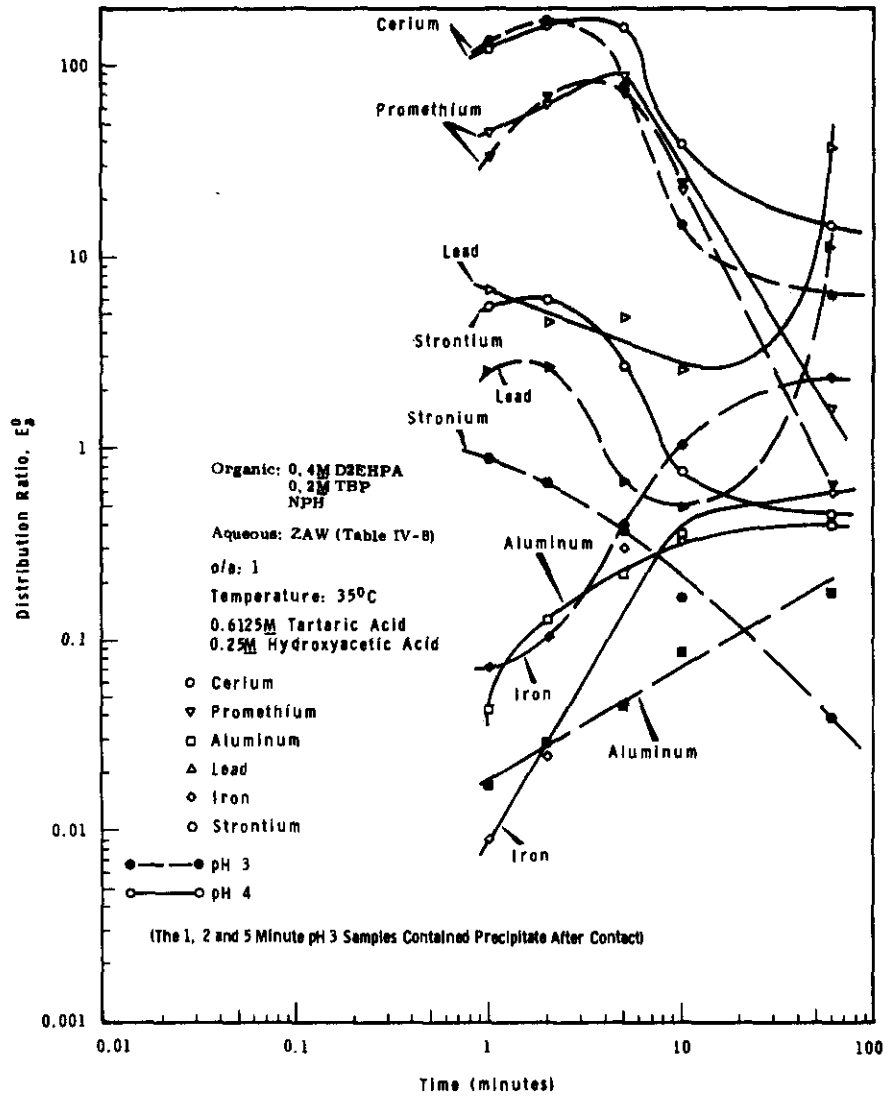


FIGURE IV-34

Distribution Ratio as a Function of Contact Time - ZAW  
(Tartrate Complexed)  
(Source of Data: BNWL-CC-595)

DECLASSIFIED

483

Generally, four classes of extraction performance were observed, irrespective of either the feed type or complexant. Strontium and lead were representative of the first class: Equilibrium was reached within one minute, and the distribution ratios began to fall with increased contact time as the solvent became loaded with the slower extracting components. The rare earths represented the second class: Extraction was appreciably slower than with strontium, and several minutes were usually required for the distribution ratio to reach a maximum before decreasing from increased solvent loading. In the third class were iron, aluminum, and ZrNb-95 which extracted very slowly and continued to extract throughout the 60 min equilibrations. Finally, ruthenium and chromium extraction appeared to be unaffected by contact time.

The decrease in strontium extraction can be accounted for by the continually increasing concentrations of iron and aluminum in the solvent. For example, the observed decrease in strontium  $E_g^0$  from 14 to 3.1 (pH 4) over the 60 min experiment shown in Figure IV-32 was accompanied by an increase from 0.025M to 0.090M (Fe + Al) in the solvent. If the strontium extraction obeyed a squared free solvent concentration dependency as expected (Section C.2), the change in the strontium  $E_g^0$  implies that 2.5 to 2.6 moles of D2EHPA were tied up for each mole of iron plus aluminum extracting. For comparison, trivalent lanthanides are reported to complex six moles (formula weights) of D2EHPA per mole of lanthanide at low solvent loading<sup>(48)</sup>.

Increased temperature greatly speeds up the rate of extraction of rare earths from citrate and tartrate-complexed feeds (and presumably also from HEDTA-complexed feeds), as shown in Figures IV-26 and IV-27. For example, in a 3-minute contact with a citrate-complexed feed, distribution ratios at 60 C for cerium and europium were 22 and 81 times higher, respectively, than they were at 25 C. A disadvantage of increased temperature, however, is that strontium extraction decreases while extraction of iron increases, (Figures IV-28 and IV-29).

The extent of complexing by ligands is less at lower pH's, and the rates of rare earth extraction are markedly improved by reducing the pH, as shown in Figures IV-30 through 34.

Almost without exception, the rates of rare earth extraction decreased with increasing atomic number (Ce Pm Eu). The effect was less pronounced with tartrate feeds (Figures IV-32 and IV-34); and in an ORNL study, the cerium-promethium order was reversed<sup>(27)</sup>.

Evidence has been obtained which suggests the kinetics of rare earth extraction from HEDTA-complexed PAW are noticeably improved when the feed also contains 0.01 to 0.03M tartrate<sup>(18)</sup>. For example, the cerium and promethium  $E_g^0$ 's were 7 and 0.6, respectively, when PAW containing 0.17M HEDTA at pH was contacted 3 min with an equal volume of 0.4M D2EHPA-0.2M TBP-NPH. The distribution ratios were about 10-fold higher

DECLASSIFIED

DECLASSIFIED

for the same extraction conditions when the feed also contained 0.125M tartrate (Figure IV-30). By comparison of these data and those in Table IV-9, the relative promethium extraction rates at 35 C are seen to decrease with complexants in the order tartrate citrate (+0.0125M tartrate) HEDTA (+0.0125M tartrate) HEDTA.

Detailed studies with citrate-complexed feeds have shown that the presence of several of the major cations in the feed have a pronounced inhibiting effect on the rate of cerium extraction(59,72). The largest effect was found with chromium ion and attributed to the formation of a stable complex, identified as CeCr(citrate)<sub>2</sub>, (75) which dissociates very slowly under extraction conditions. The results of a series of 10 min equilibrations, in which several PAW components were added separately to simplified feeds containing 0.05M excess citrate, are shown in Table IV-15(72). Data from pilot plant runs with similar feeds(59) indicated that the equilibrium cerium E<sub>a</sub><sup>o</sup> exceeds 100 in all cases. Similar kinetic effects have been noted at ORNL with tartrate-complexed feeds(35).

TABLE IV-15  
EFFECT OF FEED IMPURITIES ON THE EXTRACTION OF STRONTIUM  
AND CERIUM FROM CITRATE-COMPLEXED FEEDS

(Data from HW-79762PT1)

Conditions: Feed solutions containing 1.4M NaNO<sub>3</sub>, 0.001M Sr, 0.038M rare earths and indicated impurity and citrate concentrations contacted 10 min. at 25 C with an equal volume of 0.2M D2EHPA, 0.2M TBP, Soltrol-170.

<u>M Fe</u>	<u>M Cr</u>	<u>M Ni</u>	<u>M Al</u>	<u>M Citrate</u>	Equil. pH	E <sub>a</sub> <sup>o</sup>	
						Ce	Sr
0	0	0	0	0.05	4.05	2740.	28
0.075	0	0	0	0.125	4.2	54.	24
0	0.015	0	0	0.065	4.1	1.9	27
0	0	0.0075	0	0.0575	4.05	384.	29
0	0	0	0.0375	0.0875	4.0	95.	28
0.075	0.015	0.0075	0.0375	0.185	4.1	3.4	21

Laboratory kinetic data can be used to estimate (very approximately) the extraction performance of a pulse column when the extraction rate is limited by reaction kinetics in the raffinate (feed) phase. Under these conditions, particularly when the time required for the desired solute in the feed to reach equilibrium with the solvent exceeds the feed residence time in the column, the performance of the column will approach that of a single stage batch contactor. The percent of the solute extracted will be given approximately by the material balance equation.

$$\% \text{ extracted} = \frac{100 E_a^o}{E_a^o + (A/O)}, \quad (36)$$

DECLASSIFIED

where  $E_a^0$  is the laboratory distribution ratio for a contact time corresponding to the feed residence time in the column and A/O is the aqueous to organic volumetric flow ratio. From this equation and the data in Figure IV-30, 31 and 32, the estimated residence times to achieve 95% promethium extraction from HEDTA, citrate, and tartrate-complexed PAW feeds (pH 4) are 6, 2, and 1 min, respectively, at an A/O of 1.

### 3.2.4 Extraction of Miscellaneous Feed Impurities

The extraction of major inert and radioactive impurities has been extensively covered in preceding sections. Considerably less work has been done to determine the extraction behavior of minor inert impurities such as nickel, calcium, barium, etc, under B-Plant flowsheet conditions. Highlights of some of the most applicable data are presented below.

Uranium. Uranium will quantitatively extract from a tartrate-complexed feed. A distribution ratio of 150 was measured at pH 4.5 with the ORNL PAW recipe shown in Table IV-8 and a solvent containing 0.3M D2EHPA - 0.15M TBP-Amsco 125-82 diluent<sup>(28)</sup>.

Calcium. Calcium distribution ratios are generally about 30 to 50-fold higher than strontium distribution ratios under all flowsheet conditions. A calcium distribution ratio of 490 was measured under the tartrate flowsheet conditions described above<sup>(81)</sup>.

Barium. Barium distribution ratios of 0.03 and 0.1 were measured in batch counter-current contacts with the ORNL tartrate-complexed PAW (pH 4 to 5)<sup>(81)</sup>. Barium distribution ratios as high as 3 (compared with 19 for strontium) have been measured under somewhat similar conditions but with sulfate absent<sup>(30)</sup>. Sulfate addition to a simplified strontium-sodium nitrate system has essentially no effect on strontium extraction<sup>(81)</sup>, and deliberate sulfate addition to sulfate-deficient feeds would appear warranted to improve the barium decontamination.

Molybdenum. Molybdenum  $E_a^0$ 's into 0.4M D2EHPA - 0.2M TBP - NPH were less than 0.01 at pH's from 4 to 5. The aqueous phase contained 1M  $\text{NaNO}_3$ , 0.01M Mo, and 0.05M of either citrate, tartrate, or HEDTA<sup>(18)</sup>.

Nickel. The nickel distribution ratio from the ORNL tartrate-complexed PAW was about 0.7 at pH 4.6<sup>(28)</sup>. The addition of 0.02M EDTA to a feed containing 0.017M Ni, 0.001M Sr, 1.7M  $\text{NaNO}_3$  and 0.004M tartrate decreased the nickel  $E_a^0$  from 8.4 to 0.006 at pH 4.2<sup>(28)</sup>. From the stability constants (Table IV-67), HEDTA should be just about as effective as EDTA in suppressing nickel extraction.

DECLASSIFIED

486

Magnesium. Magnesium and strontium distribution ratios were found to be identical for 0.4M D2EHPA-0.2M TBP-Soltrol-170 and were unaffected by the addition of complexing agents<sup>(16)</sup>.

Manganese. Manganese distribution ratios of 0.8 to 1.2 have been measured between a rare earth crude feed complexed with 0.15M HEDTA and 0.4M D2EHPA-0.2M TBP-NPH over the pH range 2.2 to 3.8<sup>(22)</sup>. In the absence of complexants, manganese distribution ratios fall midway between those of calcium and strontium (Figure IV-10).

Cesium. Cesium distribution ratios were 0.0068, 0.038, 0.054 and 0.067 at equilibrium pH's of 3.2, 4.1, 4.4, and 4.7, respectively, between 0.37M D2EHPA-0.2M TBP-Shell Spray Base and PAW-B (See Table IV-8 for composition)<sup>(70)</sup>.

### 3.2.5 pH Control

As discussed earlier, an aqueous phase pH of about 4 is optimum of coextraction of strontium and rare earths. The complexant and the hydrolytic impurities iron and aluminum provide some hydrogen ion buffer capacity, but additional buffering is usually required to assure a smooth titration to the desired feed pH and to prevent an excessive pH change during extraction. Reagents satisfactory for this purpose are acetic and hydroxyacetic acids. The latter is preferred since its dissociation constant (Table IV-66) provides more buffer capacity at pH 4 than that of acetic acid. The curve shown in Figure IV-116 can be used to estimate feed neutralization requirements. Unfortunately, at this time there is no good procedure to compensate for the base used up in titrating iron and aluminum and their respective complexes. Additional pH control can be provided in batch and column extractions by partially pre-neutralizing the solvent with NaOH. In this way, sodium ions rather than hydrogen ions are exchanged for part of the extracted strontium, americium, and rare earths.

## 3.3 1S Column

### 3.3.1 Function

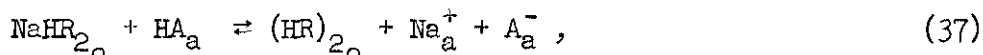
The 1S Column is used primarily to reduce the concentration of sodium in the solvent to a level that will not interfere with the performance of the 1B Column. Secondary benefits will be gained by elimination of feed entrainment from the 1A Column and from scrubbing the more weakly extracted cations from the 1A product stream. Hydrogen-ion control is achieved at the desired pH range of 2.4 to 4 by buffering the scrub stream with any of several suitable organic acids. Hydroxyacetic is the current choice but formic acid and citric acid have also been used successfully.

DECLASSIFIED

DECLASSIFIED

3.3.2 Calculated Sodium Equilibrium

The sodium distribution between the solvent and scrub solutions is highly dependent on the buffer used and its concentration. The overall reaction for sodium exchange between the solvent and a weak buffer acid, HA, can be expressed by



which is equivalent to the neutralization reaction for the weak acid:



The pH varies during the exchange reaction because of the dissociation of the buffer acid. For a monobasic acid, the dissociation constant is given by

$$K_{\text{dis}} = \frac{(\text{H}^+) (\text{A}^-)}{(\text{HA})} . \quad (39)$$

Since  $(\text{Na}^+) = (\text{A}^-)$  and  $(\text{HA}) + (\text{A}^-) = (\text{total A})$ , Equation (39) can be rearranged to give

$$(\text{H}^+) = \frac{K_{\text{dis}} [(\text{total A}) - (\text{Na}^+)]}{(\text{Na}^+)} \quad (40)$$

Values of  $(\text{H}^+)$  determined in this way were used in the empirical sodium equilibrium correlation presented in Figure IV-14 Section 2.5.1 to calculate the sodium equilibrium curves shown in Figure IV-35. These curves were developed specifically for hydroxyacetate buffer solutions but should be valid, within the accuracy of the correlation, for formic acid buffer solutions also. (The dissociation constants for hydroxyacetic acid and formic acid are  $1.52 \times 10^{-4}$  and  $1.77 \times 10^{-4}$  respectively.)

The amount of sodium in the solvent entering the 1S Column can be estimated from Figure IV-36. The equilibrium data shown in this figure was calculated in the same method as the scrub data with the exception that sufficient buffering is usually provided in the 1A Column so that the pH is essentially constant throughout the column.

DECLASSIFIED

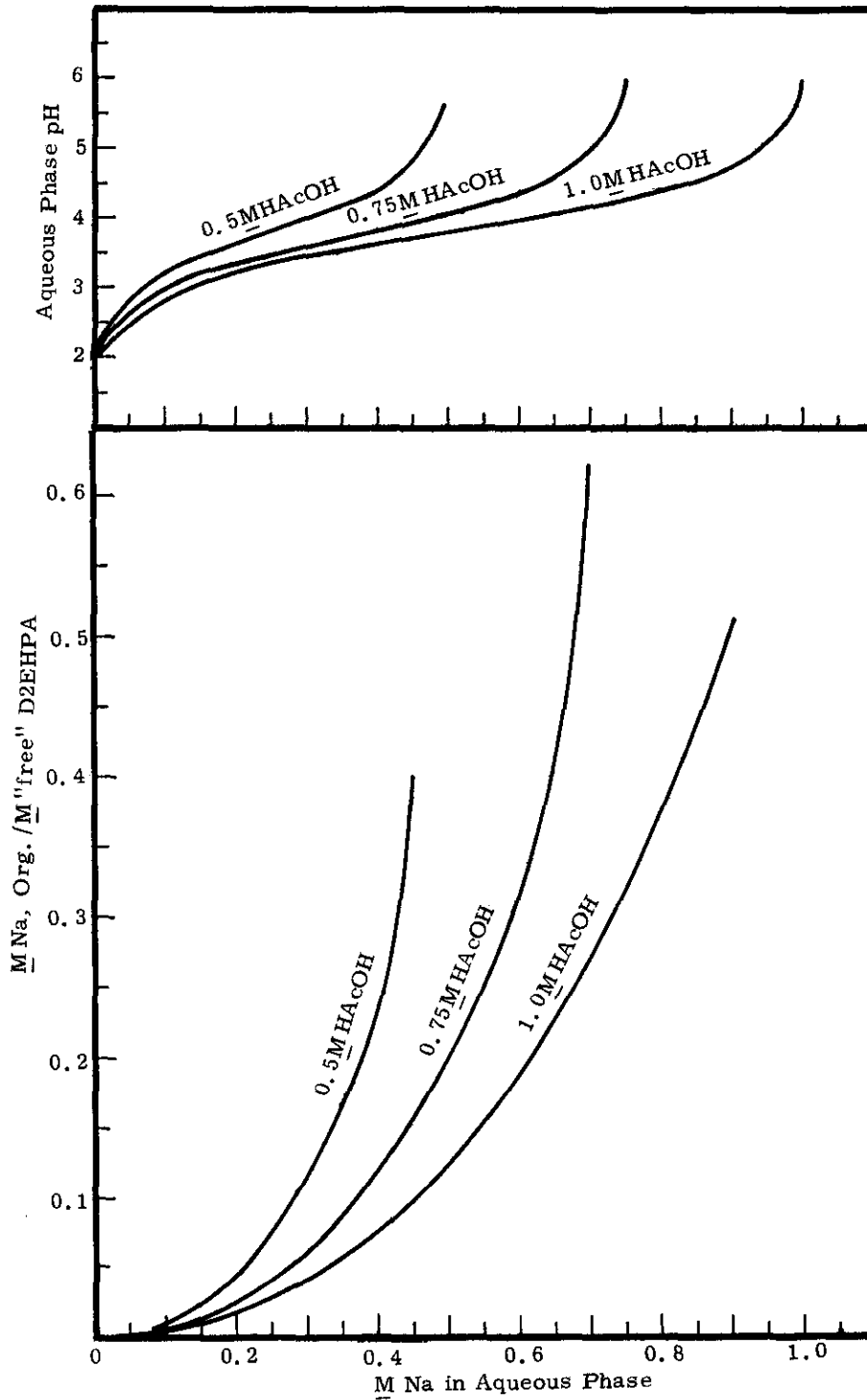


FIGURE IV-35

1S Column Sodium Equilibrium Data  
(Calculated from data given in Figure IV-10)

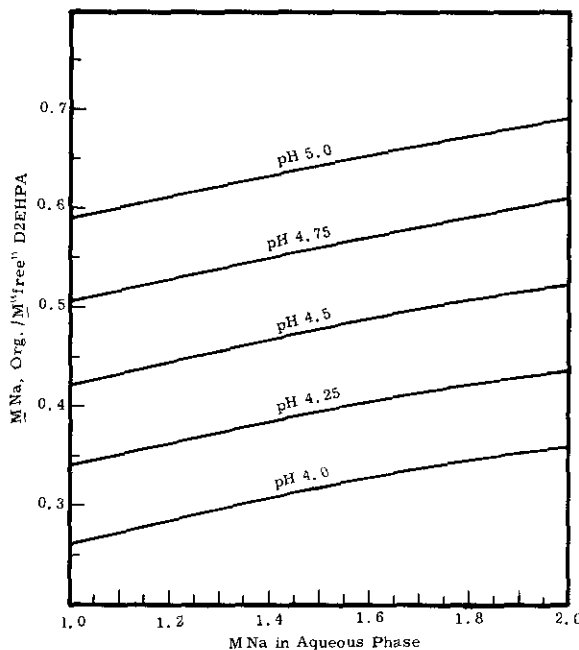


FIGURE IV-36

1A Column Sodium Equilibrium Data  
(Calculated from data given in Figure IV-10)

### 3.3.3 Selection of Scrub Compositions

The optimum scrub composition for a given aqueous/organic flow ratio (ISS/ISF) is one that will provide a sodium distribution ratio less than the flow ratio over the entire range of sodium concentrations in the aqueous phase. This can most conveniently be determined by constructing a sodium operating diagram as described in Section D. The minimum allowable pH of the scrub will be about 2.4. Below this pH, the strontium distribution ratio becomes low enough for significant strontium reflux to occur.

### 3.4 1B Column

#### 3.4.1 Function

The purpose of the 1B (partition column) is to remove strontium to an aqueous phase while retaining, as completely as possible, americium, fission product rare earths, and calcium in the organic phase. Successful partitioning depends on maintaining the aqueous phase pH in the range 1.5 to 2.2. The pH is dependent on the quantity of ions exchanged between the solvent and strip solution. In the chemical flow-sheets specified for B-Plant use (Section C 3.6), the hydrogen ion exchange is minimized by removing sodium, the macro exchangeable cation,

DECLASSIFIED

490

ISO 100

from the organic phase in the scrub column, and by extracting strontium to a low concentration in the solvent. These provisions make it relatively easy to control pH in the partition column, even when a small flow of dilute  $\text{HNO}_3$  is used as the partitioning agent.

#### 3.4.2 Partitioning of Strontium with Dilute Nitric Acid

The efficiency of dilute (0.02 to 0.03M  $\text{HNO}_3$ ) in partition column operations has been amply demonstrated in cold pilot plant pulse column studies. Results of these studies are discussed in detail elsewhere in this manual (Section D). They show that, when the sodium concentration in the D2EHPA phase is controlled by proper scrub column operation, a small flow of 0.02 to 0.03M  $\text{HNO}_3$  strips over 99% of the strontium with minimal contamination from rare earths and calcium.

The effect of pH on strontium and cerium distribution ratios under conditions approximating those of the 1B Column is shown in Figure IV-37<sup>(13)</sup>. Complexant concentrations up to 0.05M had little or no effect on strontium and cerium  $E_D$  below pH's of 3 and 2, respectively. Calcium distribution ratios have not been determined for this system but should be about 30 to 50-fold greater than corresponding strontium distribution ratios. These data indicate that the optimum decontamination performance will be obtained by operating the 1B Column at the highest pH compatible with strontium recovery. The maximum allowable pH for quantitative strontium recovery, using the data shown in Figure IV-37, is about 2.1 at an A/O of 0.2. Higher pH's are allowable at lower solvent concentrations or at higher A/O ratios.

Results plotted in Figure IV-38 demonstrate that 0.03M  $\text{HNO}_3$  strips strontium from a 0.2M D2EHPA solution very rapidly at both 25 and 60 C. The equilibrium distribution ratio, although lower at 60 C than at 25 C, was attained at both temperatures in about three minutes.

#### 3.4.3 Partitioning of Strontium with Organic Acids

Aqueous solutions of di- and tricarboxylic acids, such as tartaric and citric acids, can also be used as strontium partitioning agents in 1B Column operation. Such solutions have the advantage over  $\text{HNO}_3$  solutions of providing more hydrogen ion buffer capacity to offset possible off-standard extraction or scrub column operation.

Dilute citric acid solutions, in particular, have been examined as candidate partitioning agents. Such solutions readily strip strontium from the organic D2EHPA phase, as is evident from the data in Table IV-16 but at the expense, compared to  $\text{HNO}_3$  solutions, of decreased decontamination from cerium. The higher cost of citric acid over  $\text{HNO}_3$  is also a disadvantage. Problems arising from the radiolytic decomposition of

DECLASSIFIED

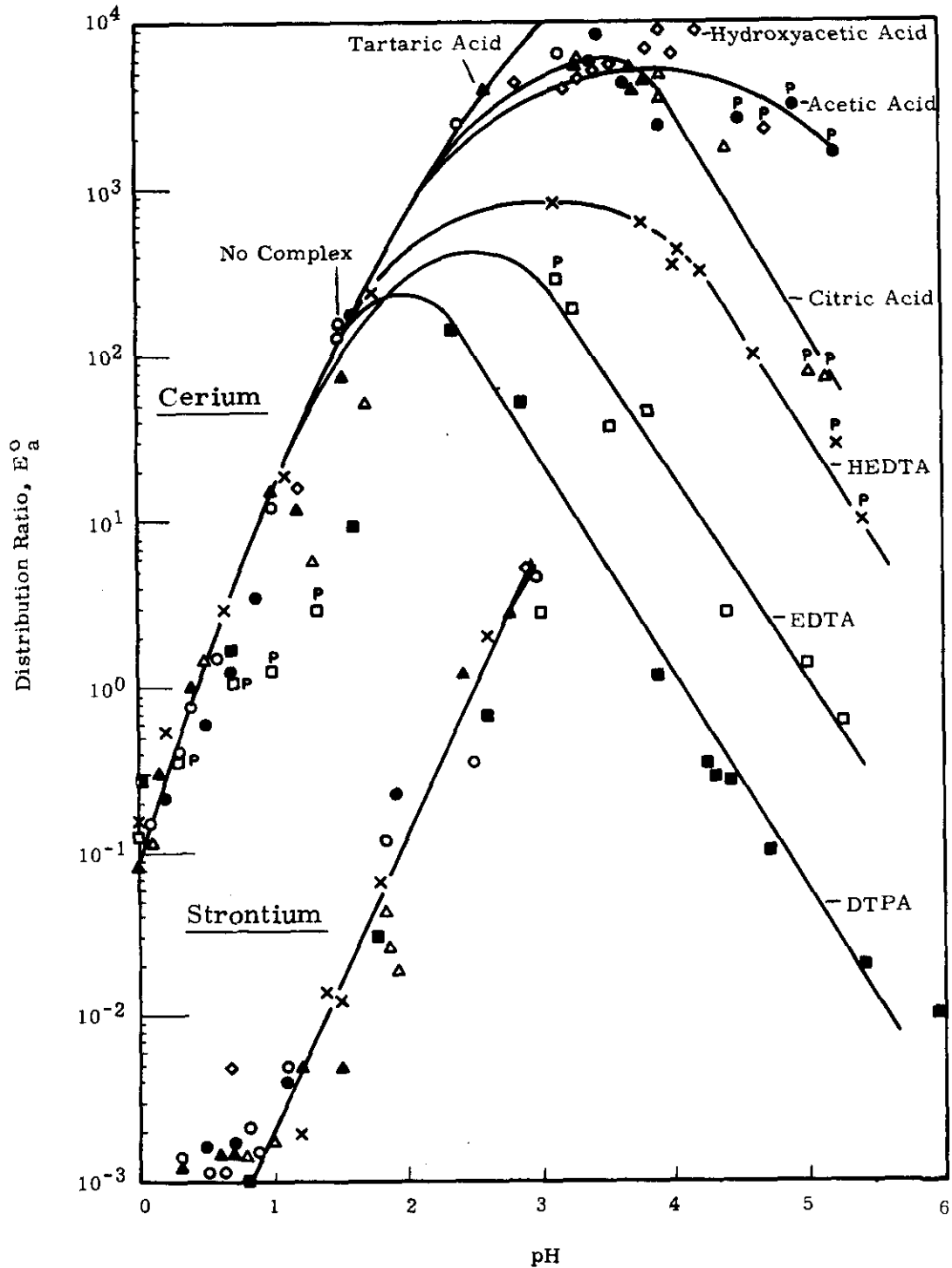


FIGURE IV-37

Strontium and Cerium Distribution as a Function of pH and Complexing Ion (Source of Data: HW-80595)

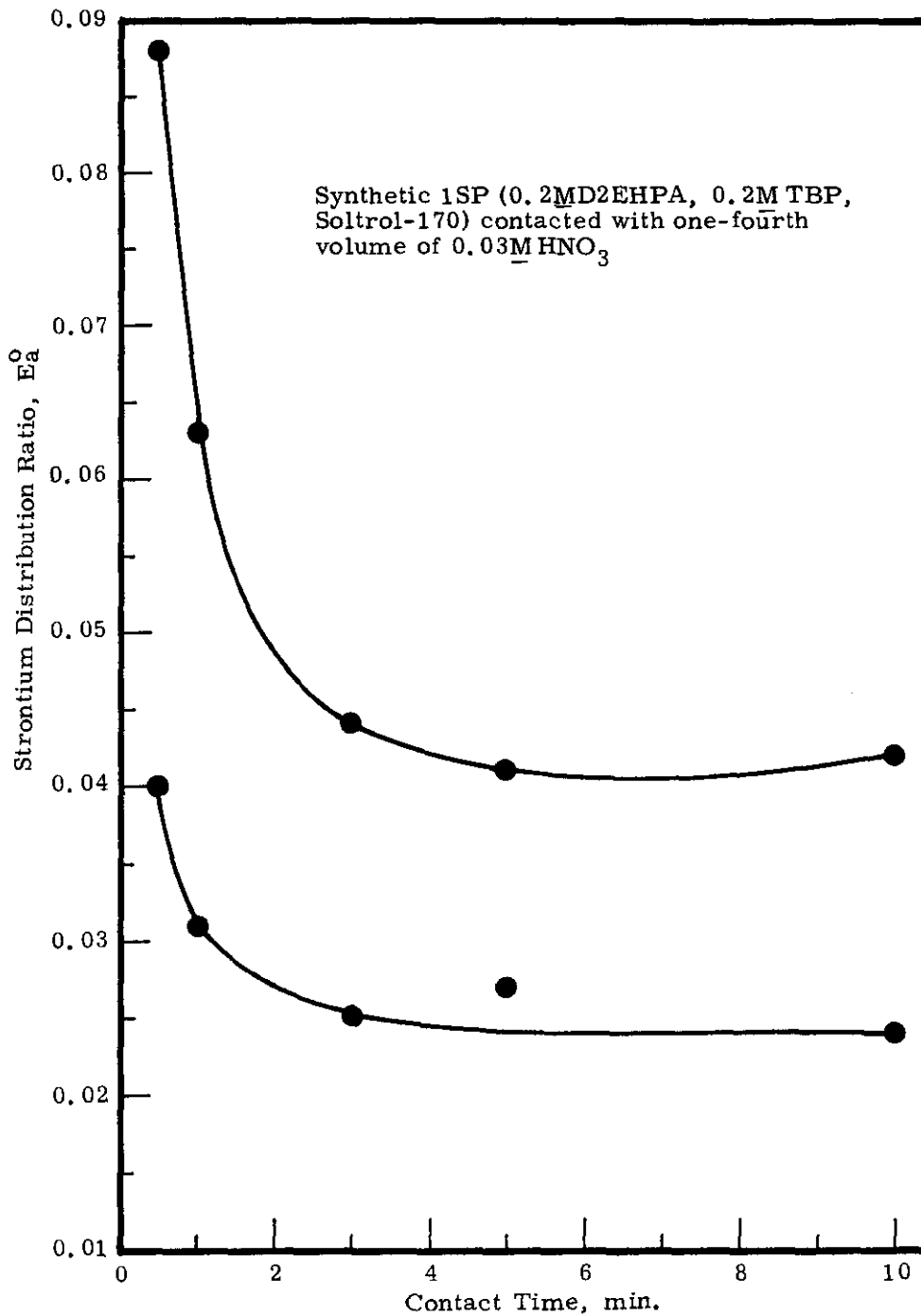


FIGURE IV-38

Kinetics of Strontium Stripping  
(Source of Data: HW-79762PT1)

citrate solutions containing high concentrations of Sr-90 (see Section 4.3.5) constitute, perhaps, the greatest objection to partitioning with citric acid solutions.

TABLE IV-16  
EFFECT OF CITRATE CONCENTRATION ON  
PARTITION COLUMN DISTRIBUTION RATIOS

(Source of Data: HW-79762PT1)

Conditions: Synthetic 1SP (0.2M D2EHPA, 0.2M TBP, Soltrol-170) contacted 10 min. at 25 C with one-fourth volume of aqueous phase.

Citric Acid, M	Cerium Final Aqueous		Strontium Final Aqueous	
	pH	$E_a^0$	pH	$E_a^0$
0.0*	1.70	48.3	--	--
0.1	1.70	28.5	1.78	0.0133
0.2	1.76	18.1	1.72	0.0124
0.3	1.70	10.6	1.72	0.0127
0.4	1.72	8.1	1.72	0.0127
0.5	1.75	6.5	1.80	0.0145

\*Initially 0.035M  $HNO_3$

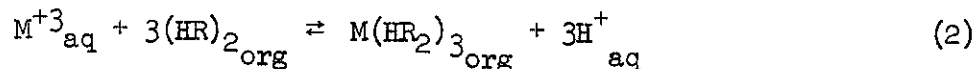
### 3.5 1C Column

#### 3.5.1 Function

When processing feeds prepared from PAW solution the 1C Column has two functions: to provide for oxidation of Ce(III) to Ce(IV) so so that Ce-144 is retained in the D2EHPA phase and to strip americium and trivalent lanthanides, including Pm-147, to an aqueous  $HNO_3$  solution. Both purposes are accomplished in a single step by using, as aqueous phase in the 1C Column, a  $HNO_3$  solution containing the strong oxidant, peroxydisulfate (persulfate), plus silver ion as a catalyst. Retention of cerium in the organic phase is neither desirable nor necessary when processing feeds derived from PAS, and in this case peroxydisulfate and silver are not added to the  $HNO_3$  solution.

3.5.2 Nitric Acid Stripping of Americium and Trivalent Rare Earths

As noted earlier, the extraction of trivalent rare earths, and presumably americium as well, into D2EHPA solutions can be represented by the reaction



By Le Chatelier's principle, increase of aqueous phase acidity shifts this equilibrium to the left; thus HNO<sub>3</sub> solutions can be used to strip americium and trivalent rare earths from D2EHPA extractants. Typical distribution coefficient data for rare earths under strip column conditions are shown in Figure IV-39<sup>(20,27)</sup>. The distribution ratios obey the expected  $(M \text{ HNO}_3)^{-3}$  dependency at low acidities, but above 1M HNO<sub>3</sub> the acid dependency falls off to about the -1.4 power. Comparable data for americium are not available, but an americium distribution ratio of about 0.1 has been reported at 1M HNO<sub>3</sub> for a system containing 0.3M D2EHPA in N-dodecane<sup>(79)</sup>. Also, comparison of the americium and cerium distribution ratio data in Figures IV-24 and IV-37 indicates that americium behaves much like cerium at low pH's; thus americium should follow the trivalent rare earths in the LC Column.

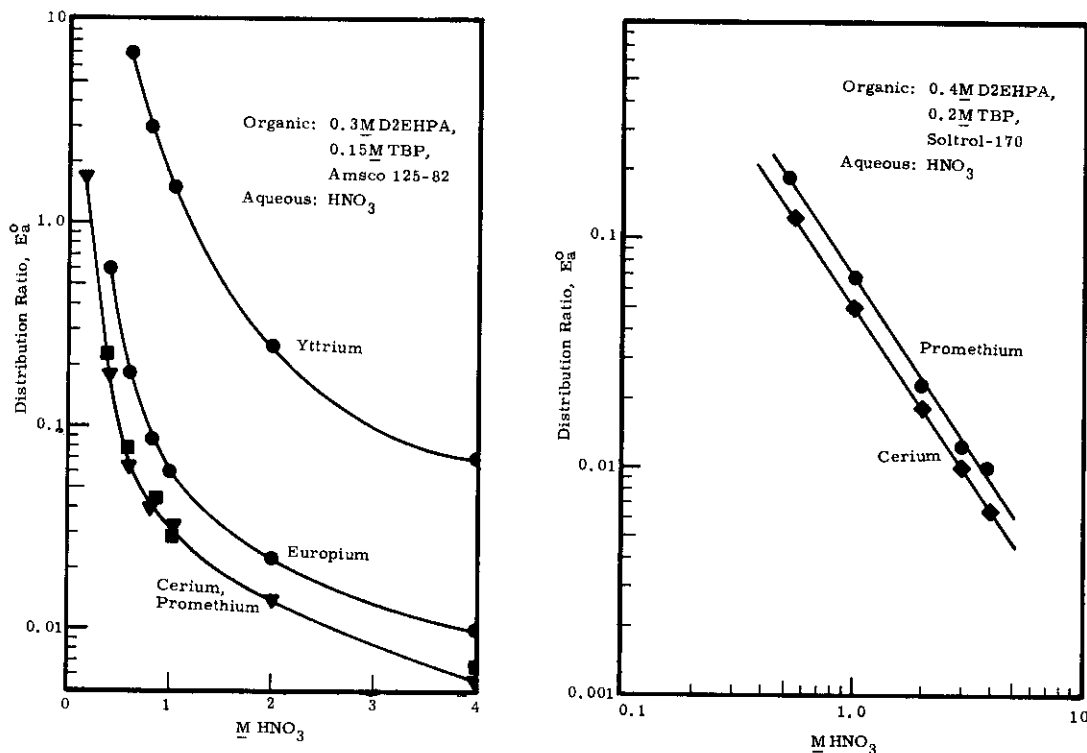


FIGURE IV-39

Distribution of Rare Earths as a Function of Acid Concentration  
(Source of Data: ORNL-TM-265 and HW-78987REV)

Nitric acid stripping of cerium is only slightly faster at 60 C than at 25 C as shown in Figure IV-40<sup>(72)</sup>. Kinetics of cerium stripping thus parallel those of strontium shown in Figure IV-38.

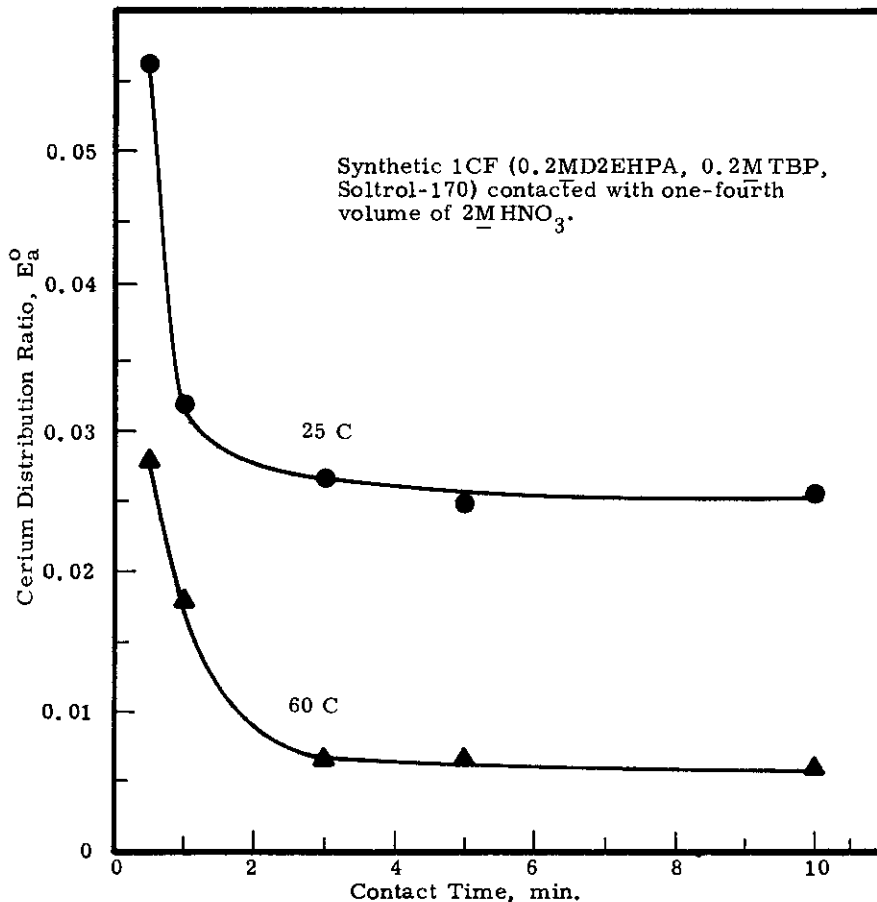


FIGURE IV-40

Kinetics of Cerium Stripping  
(Source of Data: HW-79762PT1)

Calcium, iron, and aluminum will be major impurities in the LCF. Calcium will quantitatively be stripped with the rare earths, iron will remain in the solvent, and aluminum will tend to follow the rare earths.

Iron distribution ratios of 21 to 28 have been obtained when a synthetic LCF (obtained during the demonstration of a citrate-complexed PAW flow-sheet) was stripped with one-tenth volumes of 1 to 3M HNO<sub>3</sub><sup>(72)</sup>. The solvent was 0.2M D2EHPA-0.2M TBP-Soltrol-170.

Aluminum distribution ratios under stripping conditions have been obtained for a solvent system containing about 0.23M aluminum in 0.55M D2EHPA-0.25M TBP-Soltrol-170<sup>(71)</sup>. Distribution ratios measured after 30 min equal-volume equilibrations at 60 C were 0.06, 0.04, and 0.01 at equilibrium nitric acid concentrations of 1.4, 2.1, and 4.2M, respectively. Aluminum stripping was quite slow, even at 60 C; and the distribution ratios (obtained in a similar system but at double the solvent concentration) continued to decrease after 30 min of contact. Except for the kinetic factor, aluminum should strip as readily as the rare earths.

DECLASSIFIED

496

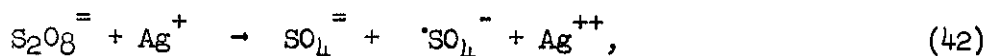
IS 100

3.5.3 Silver-Catalyzed Persulfate Oxidation of Cerium(III)

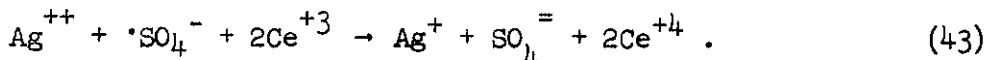
Factors affecting the oxidation of Ce(III) to Ce(IV) by silver-catalyzed persulfate have been extensively investigated by Bray and Roberts (20,21,22) and Richardson (61). Persulfate has a sufficiently high oxidation potential to oxidize cerium quantitatively, but the reaction rate at room temperature is so slow that oxidation does not occur. The addition of silver ion markedly increases the rate. The rates of reaction catalyzed by silver are, without exception, independent of the reductant concentration but depend on the first power of the persulfate and catalyst concentrations<sup>(42)</sup>; that is,

$$\frac{-d(S_2O_8^{=})}{dt} = k(S_2O_8^{=}) (Ag^+) \quad (41)$$

The following rate controlling reaction has been proposed by several investigators<sup>(42)</sup>:



where the sulfate radical ion,  $\cdot SO_4^-$ , and the  $Ag^{++}$  are the active oxidants:



Since the silver ion concentration for a given composition remains constant while the persulfate is used up, the rate law in effect corresponds to a first order reaction in which the half-life of the persulfate is inversely proportional to the silver ion concentration:

$$t_{1/2} = \frac{0.693}{k(Ag^+)} \quad (44)$$

When used to oxidize cerium in a solvent extraction process, much of the persulfate will be destroyed by radiolysis and in side reactions with water and solvent. Hence it is important to use low silver concentrations to increase the persulfate life and to maintain the desired reaction rate by starting with high persulfate concentrations.

Hot cell batch contacts were made to demonstrate the effects of composition variables on the rate of extraction and the life of the persulfate<sup>(20)</sup>. The solvent feed for these tests was prepared by quantitative extraction of rare earths from one liter of Purex Plant rare earth concentrate containing 800 Ci Ce-144/1 and 100 Ci Pm-147/1 into 2.2 liters of 0.4M D2EHPA-0.2M TBP-Soltrol-170 diluent.

DECLASSIFIED

DECLASSIFIED

497

Portions of the loaded solvent were then contacted with equal volumes of aqueous solutions containing  $\text{Ag}^+$ ,  $\text{S}_2\text{O}_8^{=}$ , and  $\text{HNO}_3$ . Samples were taken at intervals and analyzed to determine the cerium distribution ratio. Results of the tests, all carried out at about 35 C, are shown in Figures IV-41, IV-42 and IV-43. The following observations can be made from these results:

1. Cerium initially transfers to the aqueous phase, and five minutes or more are required to quantitatively oxidize it to solvent-favoring Ce(IV).
2. The initial rates of oxidation are improved by increasing either the silver or persulfate ion concentrations.
3. The life of the persulfate is greatly reduced by silver concentrations above 0.02M and  $\text{HNO}_3$  concentrations above 2M.
4. The persulfate concentrations should be greater than 0.1M to assure quantitative cerium extraction.

The adverse effect of high radiation fields on cerium separation is shown in Figure IV-44 where the results of tracer experiments are compared with those of full-level runs<sup>(20)</sup>.

The effect of temperature in a tracer system is shown in Figure IV-45<sup>(20)</sup>. The initial rate of oxidation is greatly accelerated at elevated temperature, but the effect is balanced by the reduced life of the persulfate. Comparable data with full level cerium are not available.

The effect of solvent radiolysis on cerium separation was determined by measuring the cerium behavior in the persulfate system with fresh solvent and with solvent that had been in contact with an aqueous phase containing 300 curies Ce-144/l in 2M  $\text{HNO}_3$  for over 100 hours<sup>(21,22)</sup>. Two diluents were used: Soltrol-170 and South Hampton NPH (Normal Paraffin Hydrocarbon). The results, presented in Figure IV-46, show that prolonged radiation seriously affects the Ce(IV) distribution ratio and that the NPH diluent is definitely superior to Soltrol-170 in resisting the adverse effect of radiation.

#### 3.5.4 Alternate Oxidants for Cerium(III)

Potassium permanganate has been used satisfactorily to oxidize cerium in batch D2EHFA extraction processes<sup>(32,33)</sup>. Cerium distribution ratios in excess of 100 have been measured when feeds containing 0.05M  $\text{KMnO}_4$  and 0.033M Ce in 1M  $\text{HNO}_3$  were contacted with an equal quantity of 0.4M D2EHFA-0.2M TBP-Shell Spray Base<sup>(33b)</sup>. The permanganate life is quite short in radiation fields, and permanganate must continually be

DECLASSIFIED

DECLASSIFIED

498

added to maintain the oxidation potential<sup>(32)</sup>. Phase separation is complicated by the formation of interface-seeking  $MnO_2$  precipitate. The  $MnO_2$  can be further reduced to  $Mn^{++}$ , however, by adding citric acid before allowing the phases to settle. Although used routinely at ORNL to extract Ce-144, the process has been tested with only mixed success at the Semiworks<sup>(33,43)</sup>.

An electrolytic oxidation procedure for oxidizing cerium has also been developed at ORNL<sup>(40)</sup>. The aqueous feed is adjusted to  $2M HNO_3 - 2M H_2SO_4$  and pumped through an electrolytic cell where a portion of the cerium is oxidized to Ce(IV). The feed then overflows into a vessel where it is intimately contacted with a continuously introduced stream of  $0.5M D_2EHPA$ . The two phases are pumped together to a settling chamber where the solvent containing the Ce(IV) is withdrawn and the aqueous phase is returned to the electrolytic cell. The process proceeds until the cerium content of the feed is reduced to the desired level. Under optimum conditions, about 12% of the cerium was removed per cycle through the laboratory apparatus.

### 3.5.5 Stripping of Cerium(IV)

Extracted Ce(IV) is slowly reduced to Ce(III) by the solvent. In one experiment, over 95% of the Ce(IV) in a solvent loaded to about 300 Ci Ce-144/1 was reduced and transferred to an aqueous phase containing  $2M HNO_3$  after 4 hours of contact (Figure IV-47)<sup>(45)</sup>.

Rapid, quantitative reduction of Ce(IV) can be obtained by adding  $H_2O_2$  or  $NaNO_2$  to the  $HNO_3$  strip. The effect of  $NaNO_2$  concentration is shown in Figure IV-47. The reaction is complete within 25 minutes with  $0.005M NaNO_2$  and within 5 minutes with  $0.05M NaNO_2$ <sup>(22)</sup>. The reaction with  $0.3M H_2O_2$  in 1 to 5  $M HNO_3$  was complete within 10 minutes<sup>(33b)</sup>.

### 3.5.6 Disposition of Cerium Product

Cerium-144 production is expected to exceed the market requirements. The excess cerium product will be neutralized and sent to a single underground storage tank for aging<sup>(4)</sup>. Eventually the aged cerium product will be combined with other high-level wastes for in-tank solidification.

DECLASSIFIED

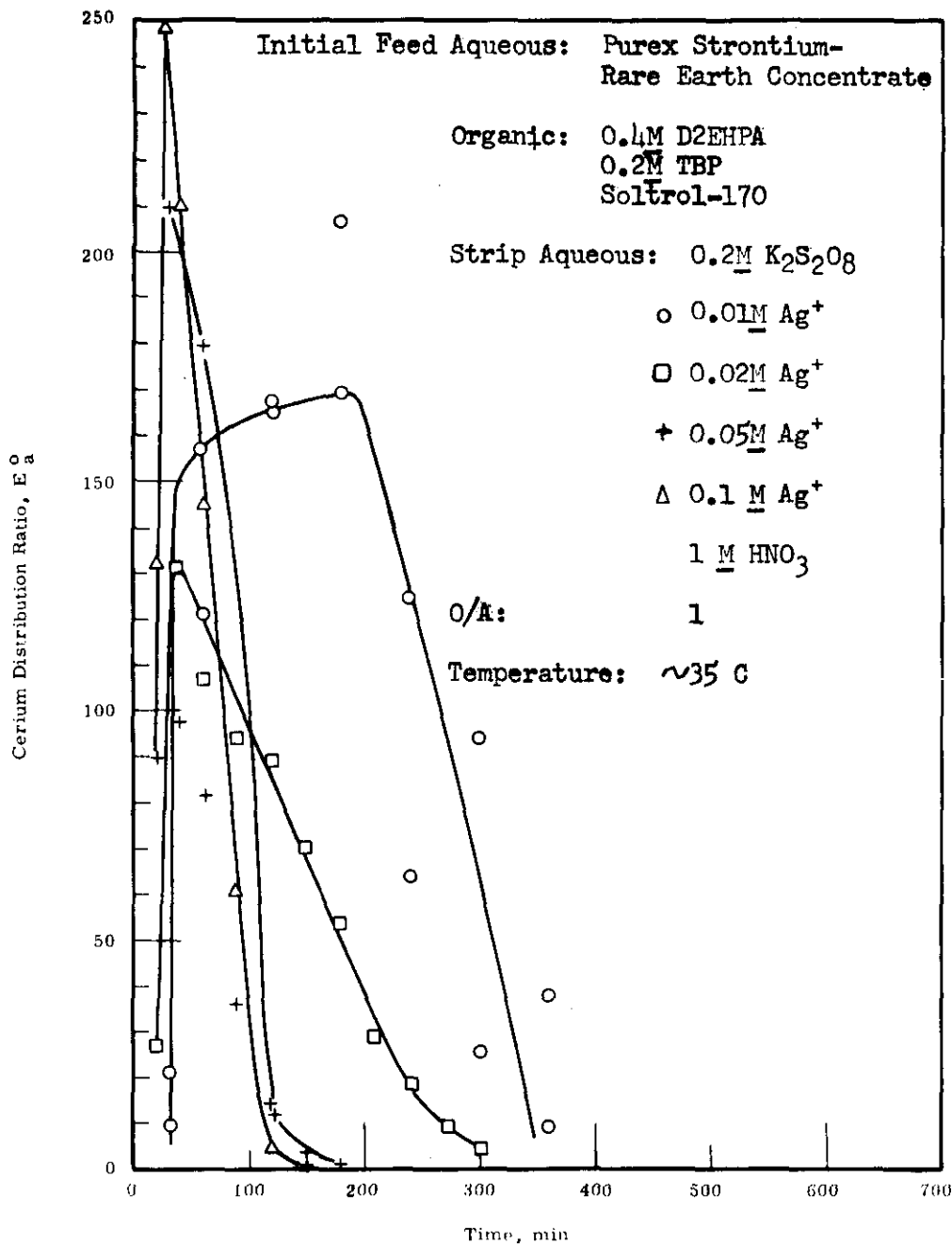


FIGURE IV-41

Cerium Distribution as a Function of Time and Silver Concentration (Source of Data: HW-78987)

DECLASSIFIED

L100

IN 100

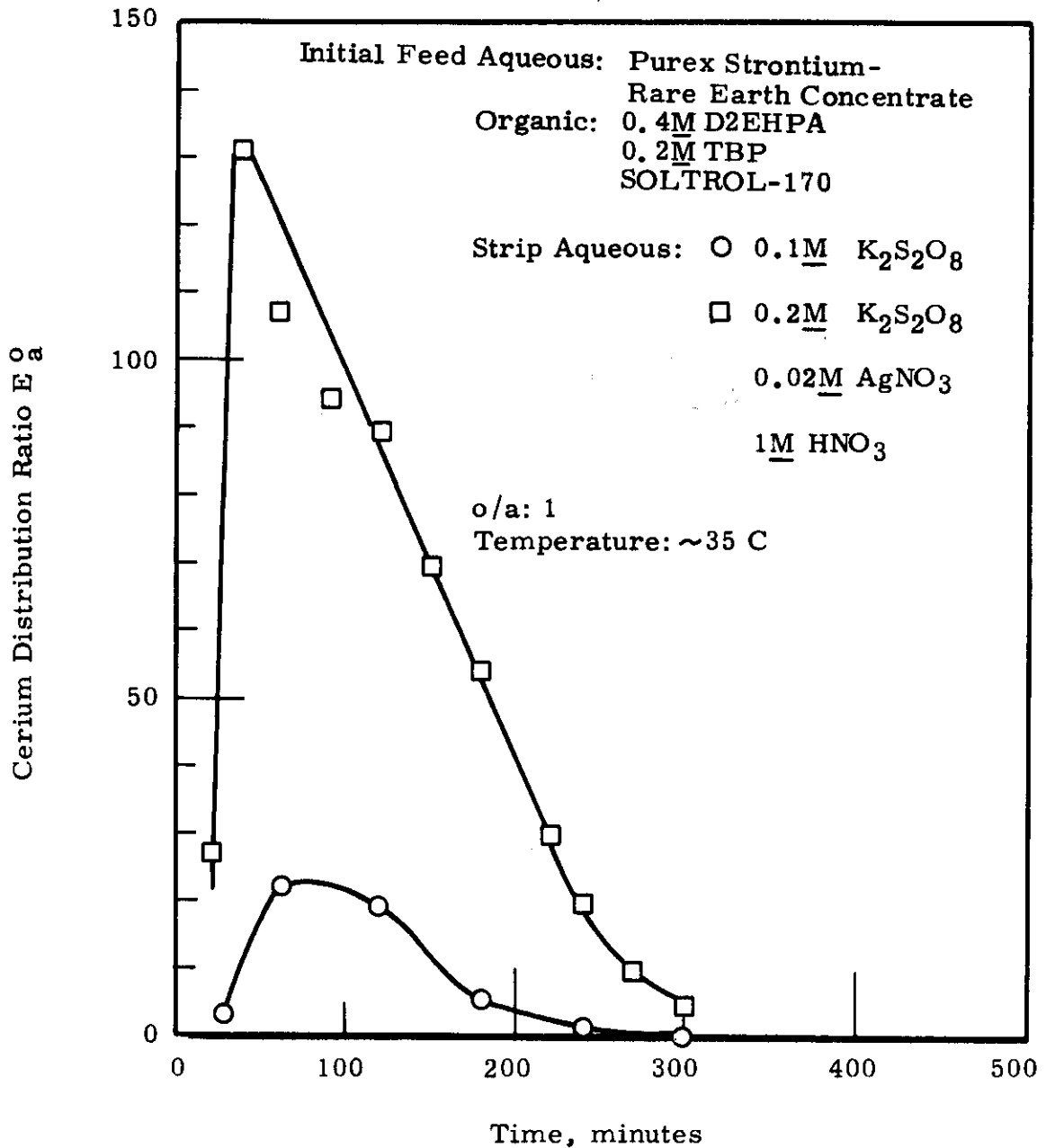


FIGURE IV-42

Cerium Distribution as a Function  
of Time and Persulfate Concentration  
(Source of Data: HW-78987)

DECLASSIFIED

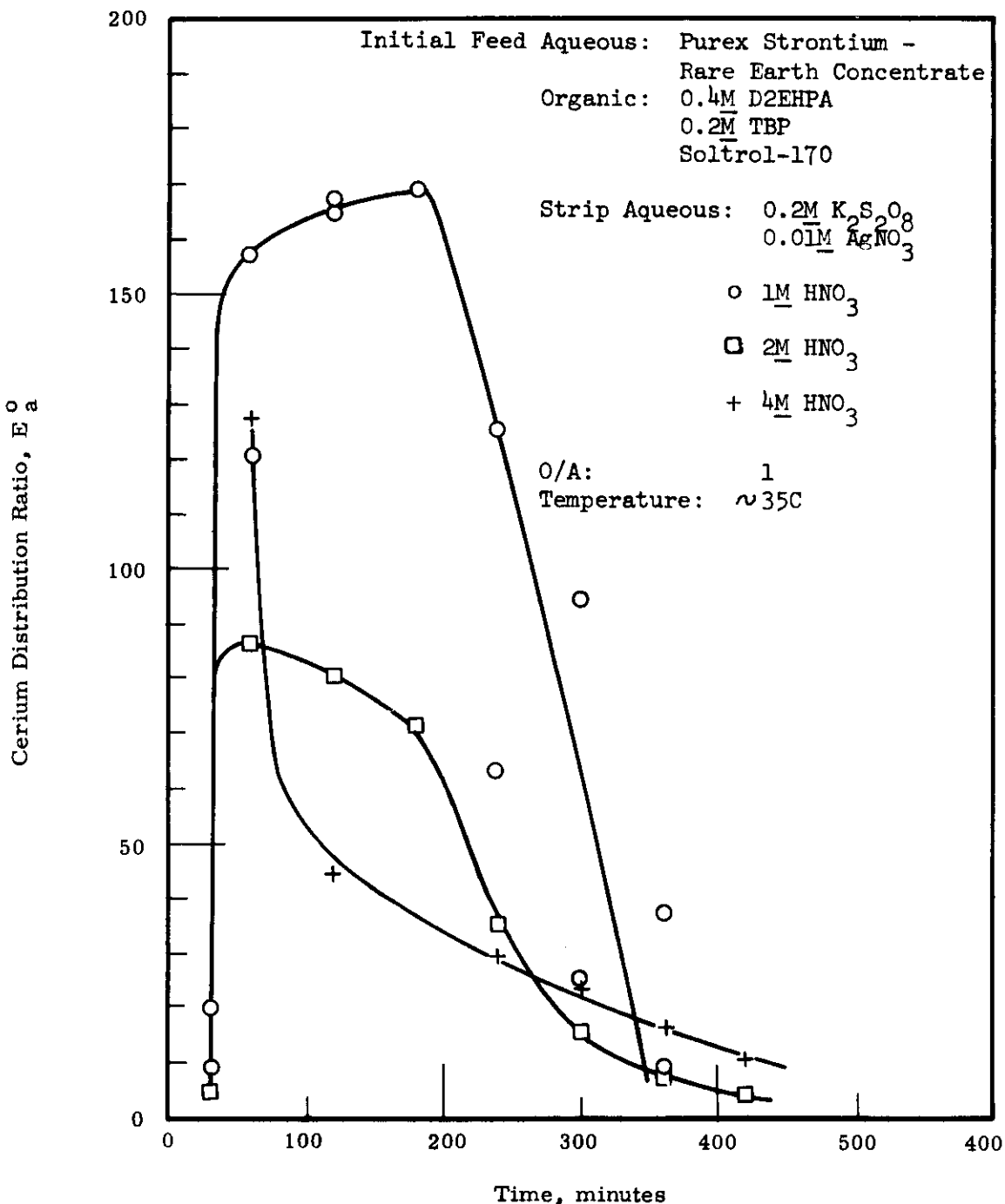


FIGURE IV-43

Cerium Distribution as a Function  
of Time and Acid Concentration  
(Source of Data: HW-78987)

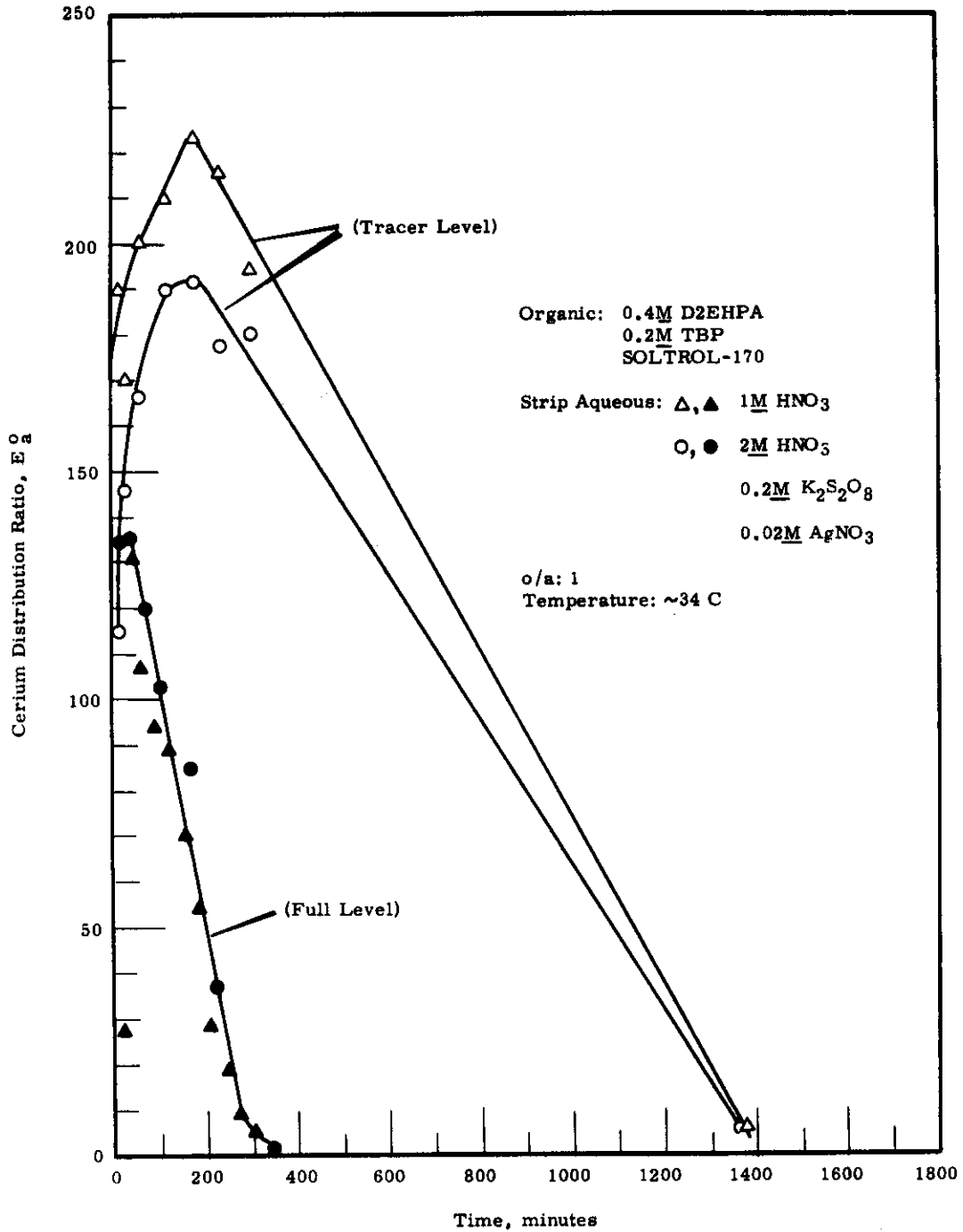


FIGURE IV-44

Cerium Distribution as a Function  
of Time and Radiation Field  
(Source of Data: HW-78987)

DECLASSIFIED

4103

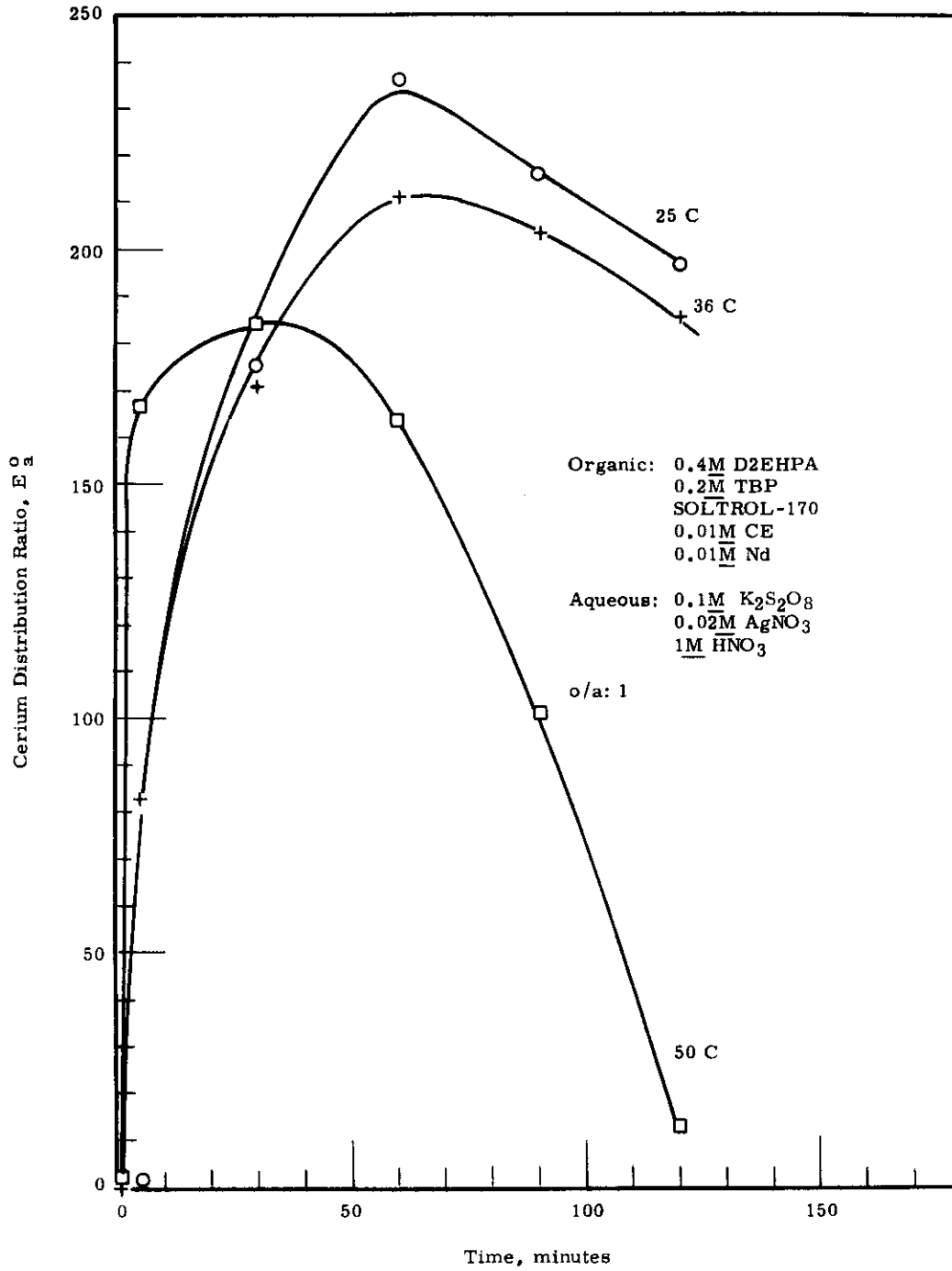


FIGURE IV-45

Cerium Distribution as a Function  
of Time and Temperature  
(Tracer Level)  
(Source of Data: HW-78987)

DECLASSIFIED

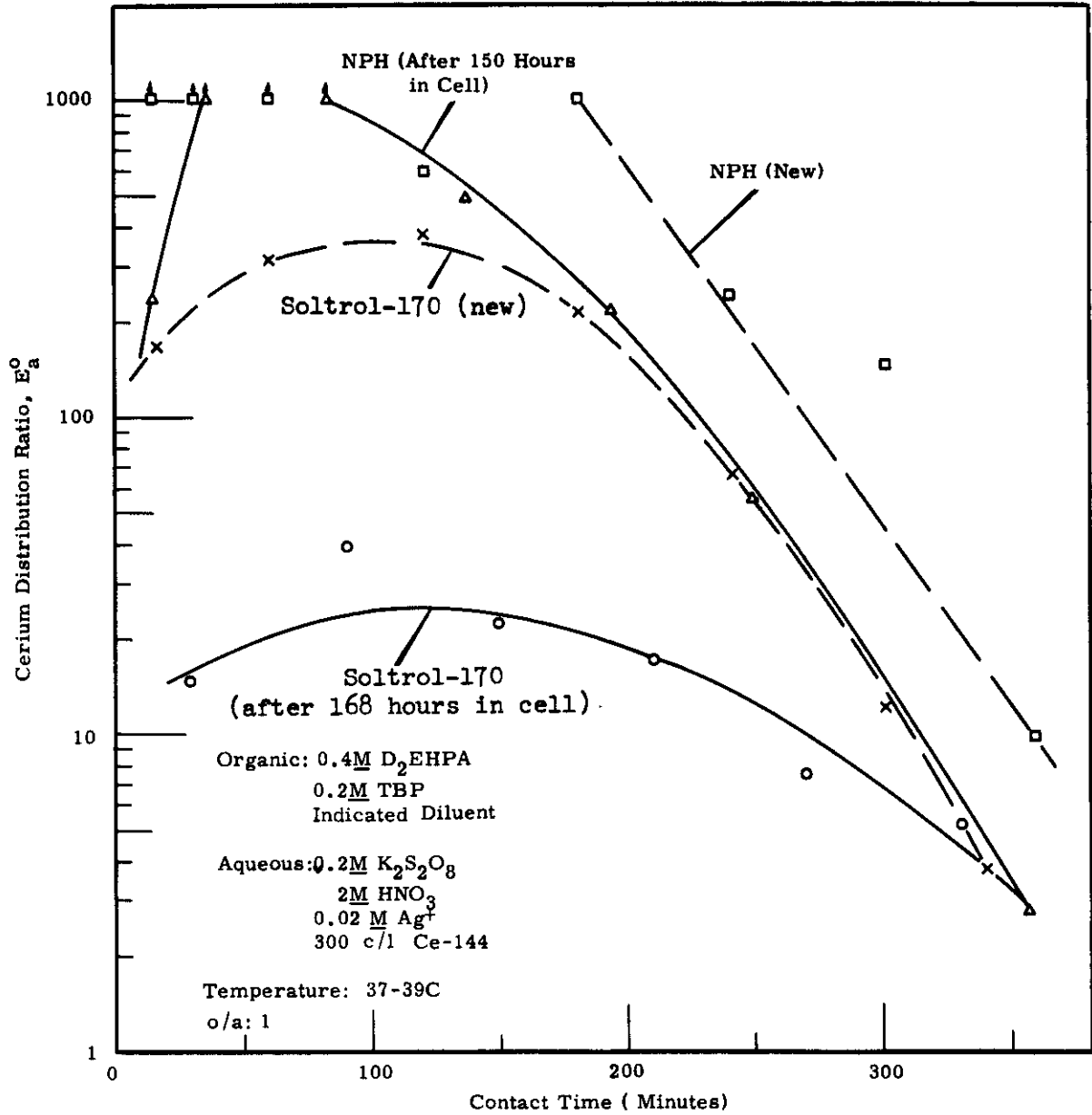


FIGURE IV-46

Cerium Distribution as a Function of Contact Time  
(Comparison of NPH and SOLTROL-170 as Diluents)  
(Source of Data: HW-84101)

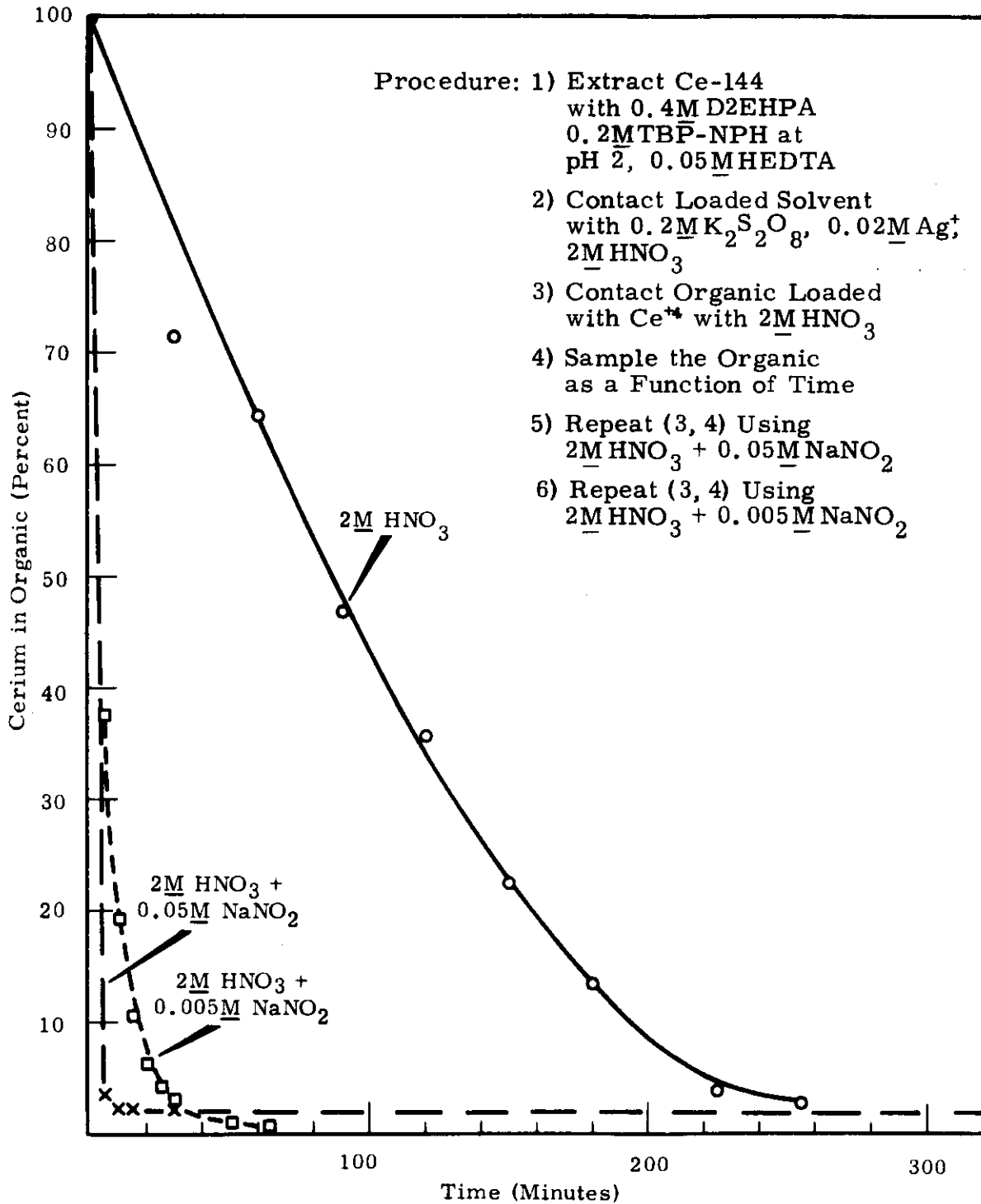


FIGURE IV-47

Stripping Studies for Ce(IV)  
 (Hot Cell)  
 (Source of Data: BNWL-187)

DECLASSIFIED

4106

### 3.6 Chemical Flowsheets

Detailed chemical flowsheets are presented in Figures IV-48, IV-49 and IV-50 for the primary extraction of strontium, rare earths, and americium from the three major Purex waste streams: PAW, ZAW (current waste derived from zirconium-clad fuels), and PAS (acidified stored sludge). Feeds for the processes are prepared in head-end steps involving centrifugation and leaching of the PAW and ZAW and  $PbSO_4$  scavenging of the PAS.

The feeds are first adjusted with hydroxyacetic acid for pH control and HEDTA and tartaric acid to complex unwanted fission products and inert impurities. Approximately 10 to 20% excess HEDTA is added over that required to form 1 to 1 complexes with iron, aluminum, chromium, nickel, and lead. The tartaric acid addition is based on the apparent improvement in rare earth extraction kinetics described in Section 3.2.3. Tartaric acid alone is a reasonably effective complexant for most of the impurities (with the notable exception of lead) and it, citric acid, or other as yet unspecified complexants, may be substituted for HEDTA for certain applications.

The feed is adjusted to  $pH\ 4.0 \pm 0.1$  by the addition of NaOH and digested at cell temperature for several hours or at 60 to 90 C for about 30 min to assure complete complexing of the impurities. Digestion may not be required with all feeds, but pilot plant experience has shown that more reproducible performance and less trouble with solids and solid-induced instability are obtained with digested feeds.

A solvent composition of 0.3M D2EHPA was chosen as a compromise to provide adequate strontium extraction in the 1A Column while allowing strontium and rare earths to be stripped with a minimum amount of dilute acid in the 1B Column and 1C Column, respectively. The solvent is partially neutralized to minimize sodium transfer in the 1A Column and thus to improve pH control. The addition of 0.2M TBP prevents "third phase" formation in the solvent washing procedure and also improves the strontium distribution ratio as discussed in Section C 2.5.2).

The LSS contains sufficient hydroxyacetic acid to be capable of quantitatively removing extracted sodium from the LAP, according to the criteria discussed in Section C 3.3. The LSS optionally contains a small amount of HEDTA to improve decontamination from nickel and other strongly complexed impurities which may have extracted in minor quantities in the 1A Column. Finally, the LSS pH is adjusted to 2.4 to avoid scrubbing significant quantities of strontium from the solvent.

The LEX stream is supplied with about a 2-fold excess of  $HNO_3$  over that required to stoichiometrically exchange with the strontium and sodium entering the 1B Column. Insufficient  $HNO_3$  will result in exceeding the desired maximum pH of 2.2 and may lead to excessive strontium losses and

DECLASSIFIED

DECLASSIFIED

4107

column instability while excessive  $\text{HNO}_3$  will lower the decontamination from calcium and rare earths. The LBP is routed to the LBP concentrator and interim crude strontium storage.

The LCX stream composition will vary depending on whether or not cerium is to be separated from the other rare earths. When cerium separation is desired, the LCX must be supplied as two separate streams -- one containing the persulfate and the other the silver catalyst. Premature mixing can result in destruction of the persulfate by silver-catalyzed reactions with water and  $\text{HNO}_3$ . The proposed concentrations of  $0.4\text{M}$   $\text{Na}_2\text{S}_2\text{O}_8$  and  $0.005\text{M}$   $\text{AgNO}_3$  were chosen from the results of pilot plant tests designed to minimize reagent costs. The combined LCX in all three flowsheets contains  $2\text{M}$   $\text{HNO}_3$ , sufficient to quantitatively strip the promethium and other rare earths while leaving most of the yttrium in the solvent. A LCS stream is specified for the PAW and ZAW flowsheets. This stream can either be fully acid-form solvent or, for simplicity, the same as the LAX. The flow ratio in the scrub section is not critical but was chosen at a relatively high O/A ratio for improved dispersion characteristics.

The LCP stream from current wastes will be routed to a batch contactor for re-extraction of the rare earths away from silver and the sulfate formed by reduction of the persulfate. A description of this process is presented in Section C 5.

The LCW from the PAW and ZAW flowsheet contains the Ce(IV) extracted in the LC Column and most of the yttrium entering the process. The cerium is removed in a batch contactor with  $2\text{M}$   $\text{HNO}_3$  containing  $0.05\text{M}$   $\text{NaNO}_2$ . Again, most of the yttrium will remain in the solvent. The cerium product is routed to a concentrator (not shown) where the volume is reduced about ten-fold and the excess  $\text{HNO}_3$  is destroyed by sugar treatment. The concentrated cerium is then routed to FPCE or to underground storage. The stripped solvent is sent to a batch solvent wash, described in Section C 6.

All solvent extraction operations should be carried out at elevated temperature for optimum extraction efficiency and improved column stability. The expected cell ambient temperature of  $35\text{ C}$  should be adequate for all columns with the possible exception of the LA Column which may require operation at higher temperatures to obtain the required extraction of Pm-147.

DECLASSIFIED

DECLASSIFIED

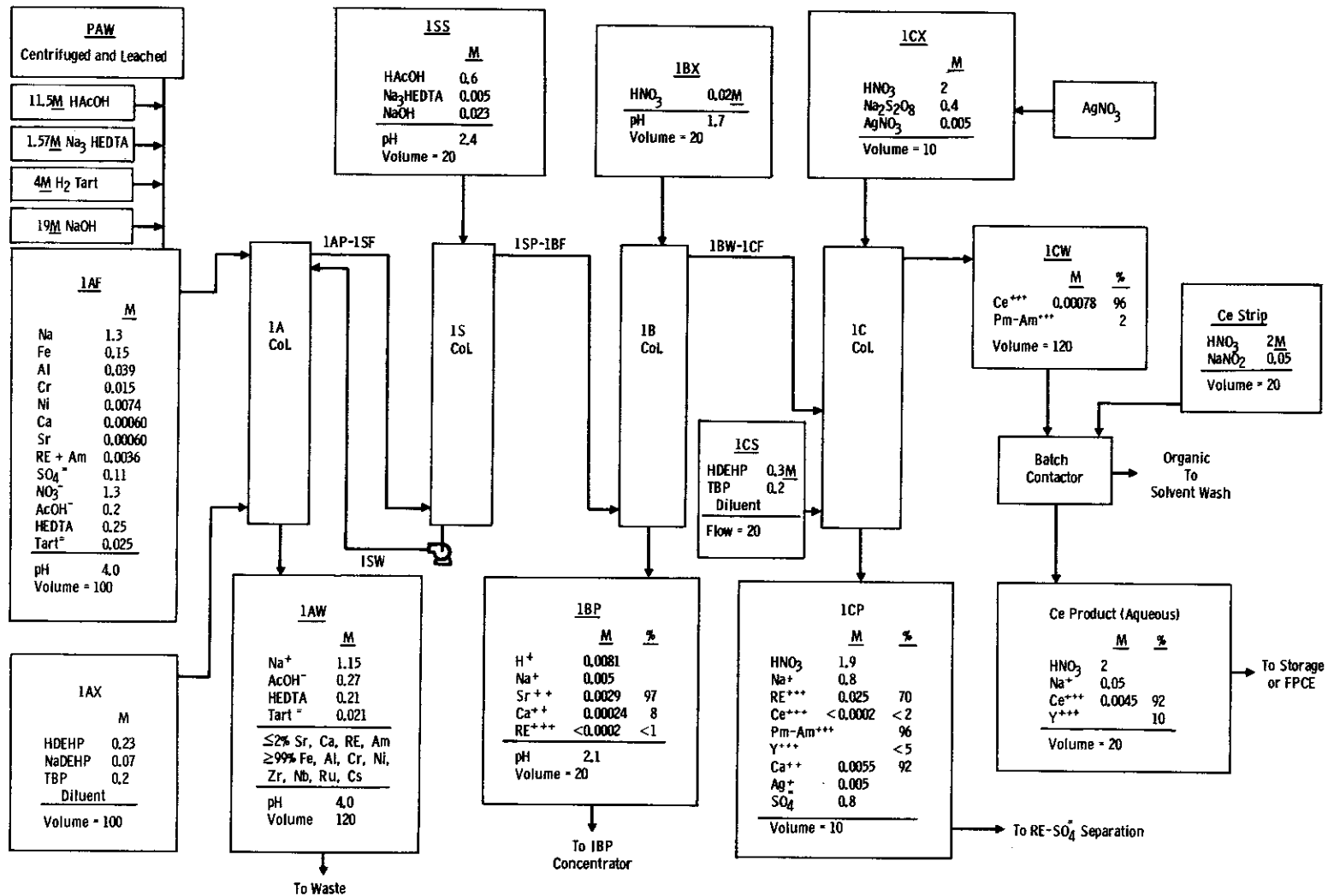


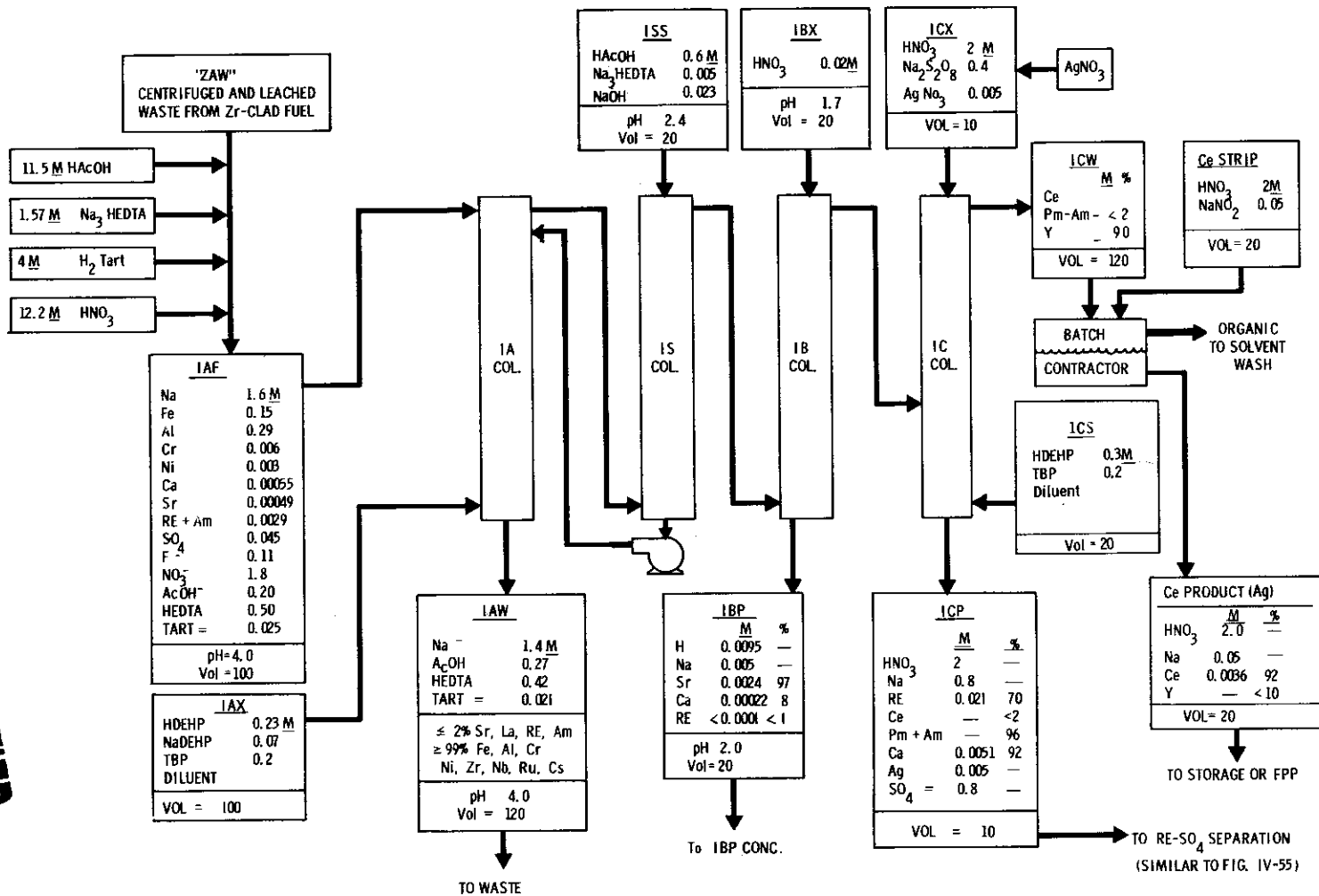
FIGURE IV-48

D2EHPA Extraction of Current Acid Waste (PAW) - Conceptual Flowsheet

DECLASSIFIED

ISG

DECLASSIFIED



1109

DECLASSIFIED

FIGURE IV-49

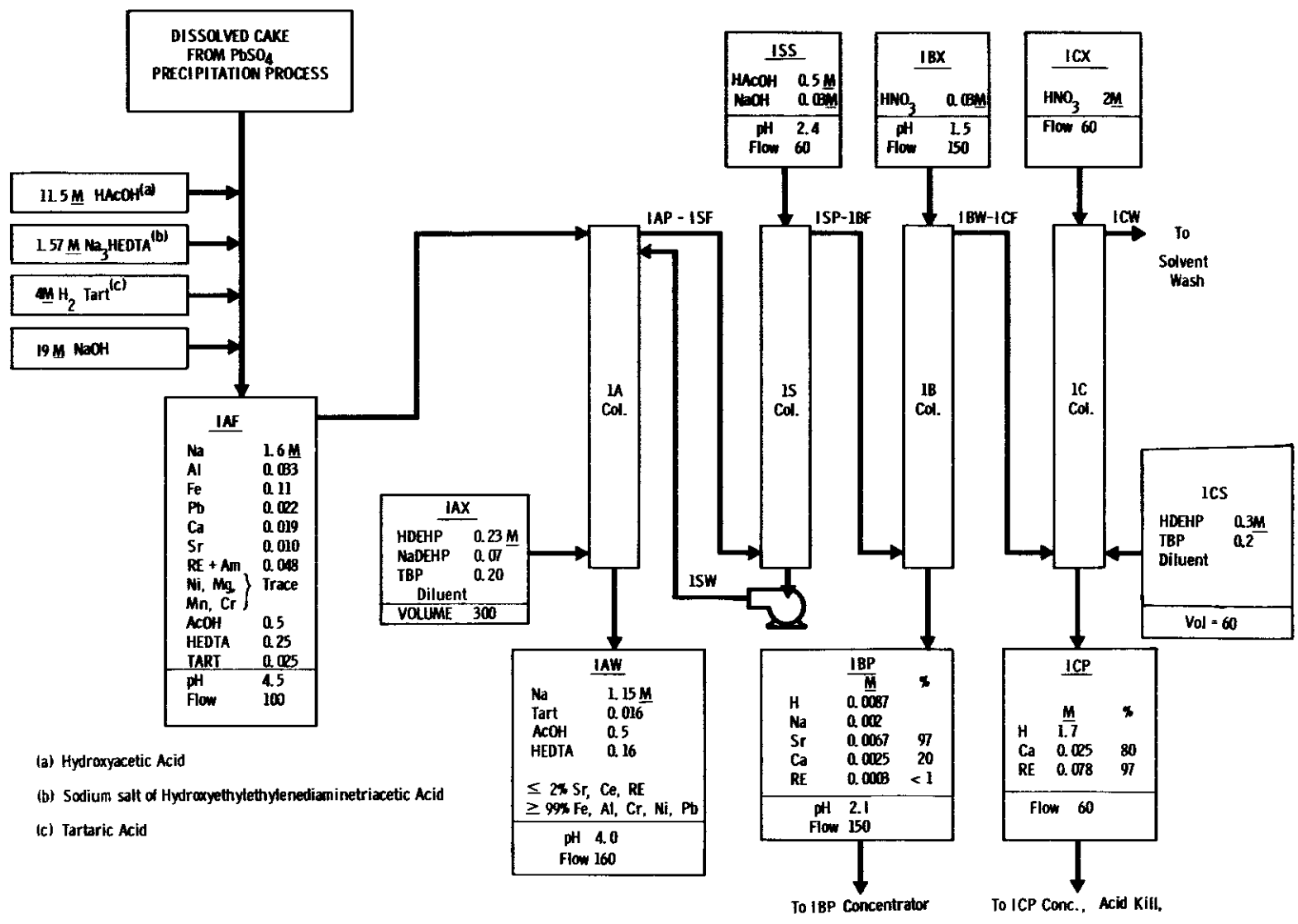
D2EHPA Extraction of Zirflex Acid Waste - Conceptual Flowsheet

11

UNCLASSIFIED

1110

ISO-100



- (a) Hydroxyacetic Acid
- (b) Sodium salt of Hydroxyethylethylenediaminetriacetic Acid
- (c) Tartaric Acid

UNCLASSIFIED

FIGURE IV-50  
 D2EHPA Extraction of Acid Sludge Waste - Conceptual Flowsheet

#### 4. Solvent Extraction Purification of Strontium Fraction

##### 4.1 Introduction

The strontium fraction obtained from current acid waste by the mainline D2EHPA extraction process described in Section C 3 is scheduled to be sent to the privately-owned Fission Products Containment and Encapsulation (FPCE) plant at Hanford for fabrication into strontium titanate sources. However, before fabrication into such sources can be undertaken, the strontium fraction must be purified further from inert and radioactive contaminants. This is accomplished by the D2EHPA solvent extraction process described in this section.

This D2EHPA extraction process can also be used to purify the strontium fraction obtained from sludge wastes. However, because of the low Sr-90 isotopic content of the Redox sludges and a portion of the Purex sludges, it is anticipated that only about 30% of the sludge strontium product would be purified by further D2EHPA extraction. The remainder will be packaged in Waste Management containers for storage according to the scheme discussed in Section F of this chapter and in Chapter VII.

##### 4.2 Feed Material and Impurities

Feed stock for the D2EHPA purification cycle will be prepared from the crude-strontium fractions obtained from processing PAW and stored sludge. These crude strontium fractions are estimated (from Figures IV-48 and 50) to have the composition shown in Table IV-17.

TABLE IV-17  
COMPOSITION OF IMPURE STRONTIUM FRACTIONS

<u>Component</u>	<u>Composition (M) of</u> <u>Strontium Fraction From</u>	
	<u>PAW</u>	<u>Stored Sludge</u>
Na	0.10	0.04
Ca	0.0048	0.05
Sr	0.058	0.13
Rare Earths	<0.004	<0.006
HNO <sub>3</sub>	0.16	0.17

As this manual was written there was still some uncertainty about the expected calcium concentration of the strontium fraction recovered from stored sludge. Actual operating experience will resolve this difficulty. Trace quantities of lead, aluminum, nickel, iron, and chromium are also expected to be present in the crude strontium fractions.

### 4.3 Purification Process

#### 4.3.1 Process Concept

The accompanying schematic (Figure IV-51) illustrates the D2EHPA extraction process for purification of the Sr-90 fraction:

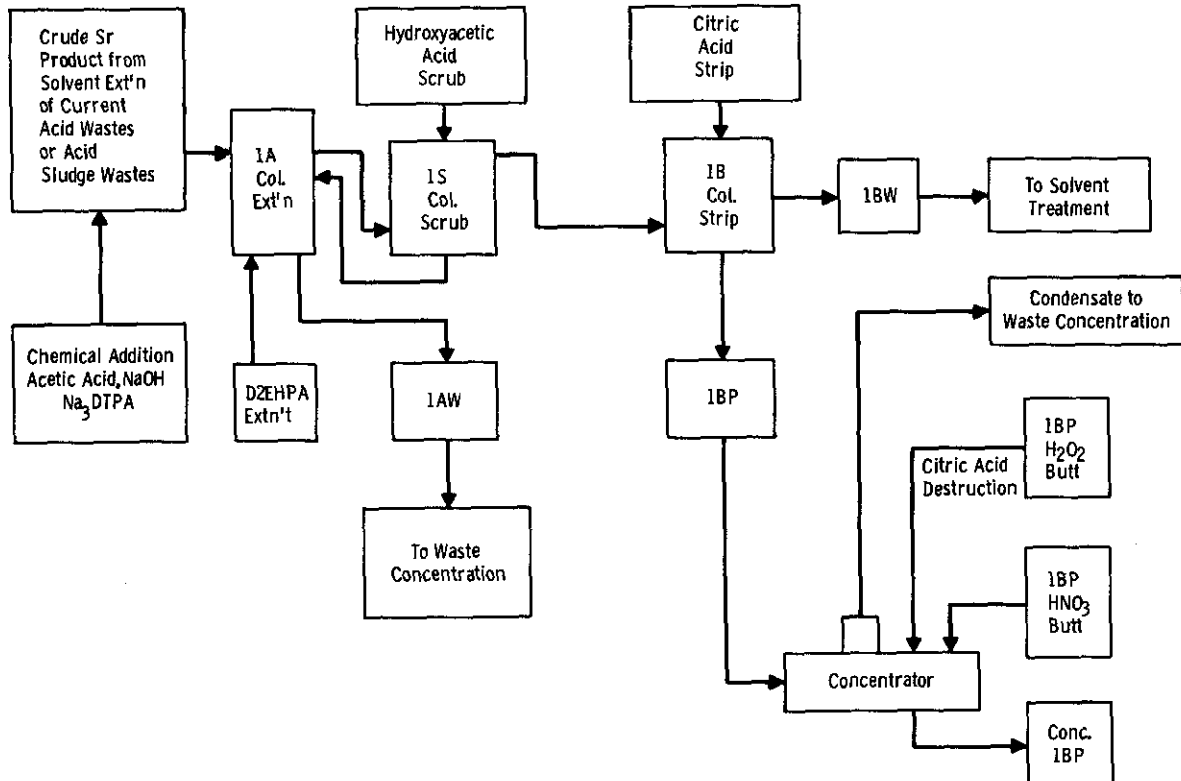


FIGURE IV-51

#### D2EHPA Purification of the Sr-90 Fraction

Crude strontium feed is butted with DTPA (diethylenetriaminepentaacetic acid), acetic acid, and caustic prior to introduction to the 1A Column. DTPA is used to complex most metal ions present, including the rare earths, to prevent their extraction by the solvent. Strontium and calcium are extracted by the D2EHPA extractant in the 1A Column. A highly buffered feed to the 1A Column is necessary to provide the pH control necessary for proper extraction of strontium. Hence, acetate is used as a buffer with caustic providing the pH adjustment necessary to maintain a feed pH of 4.9. A hydroxyacetic acid scrub is used in the 1S Column to strip sodium from the solvent. The reduction in sodium content in the solvent from the 1S Column facilitates pH control and improves the decontamination from calcium and cerium that can be achieved in the 1B Column by minimizing hydrogen ion exchange there.

Strontium and sodium are stripped from the solvent with 1M citric acid in the 1B Column. Conditions are adjusted so that nearly all of the calcium present remains in the organic phase. The strontium product from the 1B Column is concentrated while  $H_2O_2$  and  $HNO_3$  are added to destroy citric acid. Finally, the concentrated and purified strontium product is sent to storage for eventual use in a Fission Product Program or to storage on zeolite.

The waste from the 1A Column is sent to waste concentration while the solvent from the 1B Column is routed to solvent treatment facilities for removal of cations present (principally calcium).

The D2EHPA extraction process was originally developed<sup>(33)</sup> for use in the Hanford Strontium Semiworks to recover and purify Sr-90 from Purex Plant crude Sr-90 concentrate as produced by  $PbSO_4$  carrier precipitation from Purex Plant LWW solution. The process has been used very extensively since the original development; this Strontium Semiworks experience is reviewed in Section D 7.

#### 4.3.2 1A Column

The function of the 1A Column in the strontium purification process is to provide for essentially complete extraction of strontium while rejecting, as completely as possible, Ce-144, other rare earths, and inert contaminants to the aqueous waste. This is accomplished by control of feed pH and by selection of a suitable complexing agent (DTPA) to add to the extraction column feed.

Data which illustrate the effectiveness of DTPA over several other complexants in suppressing extraction of Ce-144 are presented in Table IV-18 and Figure IV-52<sup>(33b)</sup>. At approximately equal concentrations, EDTA and DTPA have about the same effect on the strontium  $E_a^0$ , but DTPA complexes cerium more strongly than EDTA, in agreement with the stability constants presented in Table IV-67. Data in Table IV-18 also predict that DTPA would strongly suppress extraction of iron, lead, etc.; this expectation is borne out by Strontium Semiworks experience.

TABLE IV-18  
COMPARISON OF COMPLEXING AGENTS

(Source of Data: HW-72666, Section 3)

Conditions: Purex plant crude concentrate<sup>(a)</sup> made 0.45M sodium acetate and 0.15 to 0.20M complexant, adjusted to pH 4.7 with NaOH, and contacted 10 min. at 25 C with one-fifth volume of 0.37M D2EHPA, 0.2M TBP, diluent.

Complexing Agent			Equil. Aq. pH	$E_a^0$				
Type	M	Free M <sup>(b)</sup>		Fe	Sr	Ca	Ce	Eu
DTPA	0.15	0.07	4.6	--	15	--	0.07	--
EDTA	0.19	0.11	4.4	0.0002	10	100	0.70	0.15
HEDTA	0.20	0.12	4.6	0.005	23	1500	12	1.1
Citric Acid	0.20	0.12	4.6	0.043	14	1900	280	400
Tartaric Acid	0.20	0.12	4.6	1.3	13	2600	120	110

(a) 1.0M  $HNO_3$ , 0.0025M  $Sr(NO_3)_2$ , 0.003M  $Ca(NO_3)_2$ , 0.0035M RE, and 0.001 to 0.1M Pb, Zr, and Fe.

(b) M "Free" complexant = total M complexant - (M Fe + M Pb + M Zr + M RE)

DECLASSIFIED

4111

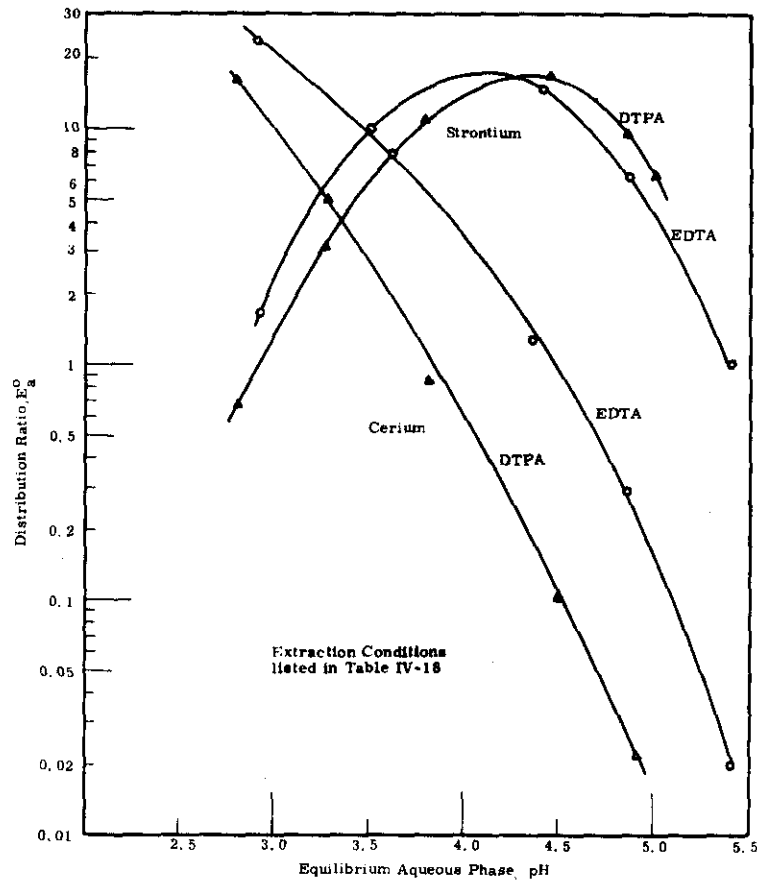


FIGURE IV-52

Comparison of DTPA and EDTA as Complexing Agents  
for Cerium and Strontium  
(Source of Data: HW-72666)

Data in Figure IV-52 indicate that operation of the extraction column with high pH (pH 4.5) feeds is desirable to minimize contamination of the Sr-90 product with Ce-144. However, complexing of strontium by either EDTA or DTPA begins to occur at about pH 4 and increases at higher pH's. The choice of a suitable feed pH must thus be a compromise between the need for satisfactory extraction of strontium and maximum decontamination from Ce-144. A feed pH of 4.9 is considered optimum.

Neither DTPA nor EDTA complexes calcium efficiently in the pH range of interest. Hence, essentially all of the inert calcium in the strontium fraction is extracted with the strontium.

DECLASSIFIED

DECLASSIFIED

4115

DTPA forms 1:1 complexes with most metal ions. Hence, the amount of DTPA added to the impure Sr-90 fraction is calculated to be sufficient to form 1:1 complexes with the rare earths and to make the final feed about 0.07M "free" (uncomplexed) DTPA. Higher concentrations of complexant are uneconomical and result in decreased distribution ratios for all feed components (33b).

Complexing of cerium by DTPA is adversely affected by radiolysis. Laboratory studies (33b) indicate cerium decontamination in the extraction column would be completely lost after feeds containing DTPA had been irradiated to a total exposure of about  $8 \times 10^7$  rad (about 2 days standing).

#### 4.3.3 1S Column

In the extraction column, because of the high pH and the concentration of sodium ions in the 1AF stream, considerable sodium extracts even though the sodium  $E_a^0$  is smaller than either the strontium or calcium  $E_a^0$ . The primary function of the 1S Column in the Sr-90 purification process is the same, therefore, as in the mainline D2EHPA process (Section C. 3.3.1), namely, to remove the bulk of the coextracted sodium prior to stripping of strontium. Removal of most of the sodium at this point not only gives a purer strontium product but makes control of pH in the 1B Column much easier.

Proper scrub column operation requires adequate pH control to ensure maximum scrubbing of sodium without excessive losses of strontium. A small flow of hydroxyacetic acid adjusted to pH 2.6 provides the required buffer capacity. Citric acid should be a suitable alternate. A small amount of DTPA is added to the scrub to provide additional decontamination from Ce-144 and other trivalent contaminants. Sodium equilibrium data for hydroxyacetate scrub systems are presented in Section C. 3.3.2.

Sodium scrubbing has not been studied in detail on a laboratory scale. It has, however, been extensively tested and satisfactorily demonstrated on a plant scale, both in the Strontium Semiworks and in cold pilot plant studies (33c,59).

#### 4.3.4 1B Column

Strontium and sodium not removed in the scrub column are stripped from the organic phase into an aqueous 1M citric acid solution in the 1B Column while calcium and rare earths are left in the organic phase. Precise control of pH is required to obtain good calcium and rare earth decontamination factors. Because of their lack of buffer capacity, dilute  $HNO_3$  solutions cannot be used to obtain this control within desired strontium solvent loadings and flow rates; however, satisfactory buffer capacity is provided by several organic polycarboxylic acids.

DECLASSIFIED

DECLASSIFIED

4116

100

Distribution ratios of strontium, calcium, and cerium between 0.37M D2EHPA-0.2M TBP-Shell Spray Base and aqueous solutions of citric and tartaric acids as a function of equilibrium aqueous phase pH are given in Table IV-19(33b).

TABLE IV-19  
1B COLUMN DISTRIBUTION RATIOS  
(Source of Data: HW-72666, Section 3)

Conditions: Citric or tartaric acid solutions containing either 0.01M Sr(NO<sub>3</sub>)<sub>2</sub>, 0.0005M Ce(NO<sub>3</sub>)<sub>3</sub>, or 0.05M Ca(NO<sub>3</sub>)<sub>2</sub> were adjusted to the desired pH with NaOH and contacted 10 min. at 25 C with an equal volume of 0.37M D2EHPA, 0.2M TBP, Shell Spray Base.

A. Citric Acid

Initial Aqueous Phase Composition		Strontium		Cerium		Calcium	
Citrate, M	Na <sup>+</sup> , M	Equil. pH	E <sub>a</sub> <sup>o</sup>	Equil. pH	E <sub>a</sub> <sup>o</sup>	Equil. pH	E <sub>a</sub> <sup>o</sup>
0.833	0.588	3.2	2.3	2.9	57	2.8	29
0.870	0.460	2.9	1.1	2.7	53	2.7	15
0.909	0.321	2.6	0.48	2.4	46	2.3	6.6
0.952	0.168	2.1	0.15	2.0	33	1.9	2.5
0.976	0.086	1.8	0.034	1.7	15	1.6	1.2
0.988	0.044	1.7	0.030	--	--	1.5	0.67
1.00	0.00	--	--	1.2	4.4	1.0	0.2
1.88	0.963	2.5	0.28	2.5	8.7	--	--
1.92	0.456	2.0	0.083	2.0	7.4	--	--
1.94	0.148	1.6	0.02	1.4	4.4	--	--
2.48	1.62	2.6	0.22	2.6	4.4	--	--
2.71	0.939	2.0	0.07	2.1	3.2	--	--
2.74	0.41	1.6	0.02	1.5	2.4	--	--

B. Tartaric Acid

Tartrate, M	Na <sup>+</sup> , M	Equil. pH	E <sub>a</sub> <sup>o</sup>	Equil. pH	E <sub>a</sub> <sup>o</sup>	Equil. pH	E <sub>a</sub> <sup>o</sup>
0.833	0.588	2.9	0.7	2.8	32	2.8	21
0.870	0.460	2.7	0.38	2.6	42	2.6	9.6
0.909	0.321	2.4	0.17	2.3	23	2.3	4.5
0.952	0.168	2.0	0.055	1.9	12	1.9	1.6
0.976	0.086	1.7	0.022	1.7	6.6	1.6	0.79
0.988	0.044	1.6	0.011	--	--	1.4	0.45
1.00	0.00	--	--	1.2	2.0	--	--

Cerium distribution ratios decrease as citrate concentration increases because of formation of cerium citrate complexes in the aqueous phase. Strontium distribution ratios also decrease as citrate concentration increases but to a lesser extent. One molar citric acid was chosen for use in the 1B Column since this concentration supplies sufficient buffer capacity and provides adequate separation of strontium from calcium and cerium.

DECLASSIFIED

Tartaric and maleic acids were also considered as alternate stripping agents. In the final evaluation these reagents showed no promise over citric acid. Maleic acid formed an insoluble strontium salt, and tartaric acid, during radiolytic decomposition, formed porous solid compounds of about the same volume as the starting solution<sup>(77)</sup>.

Titration curves for 1M tartaric acids are shown in Figure IV-53<sup>(33b)</sup>. These can be used to estimate the effect of hydrogen-cation exchange in the 1B Column on the equilibrium aqueous phase pH.

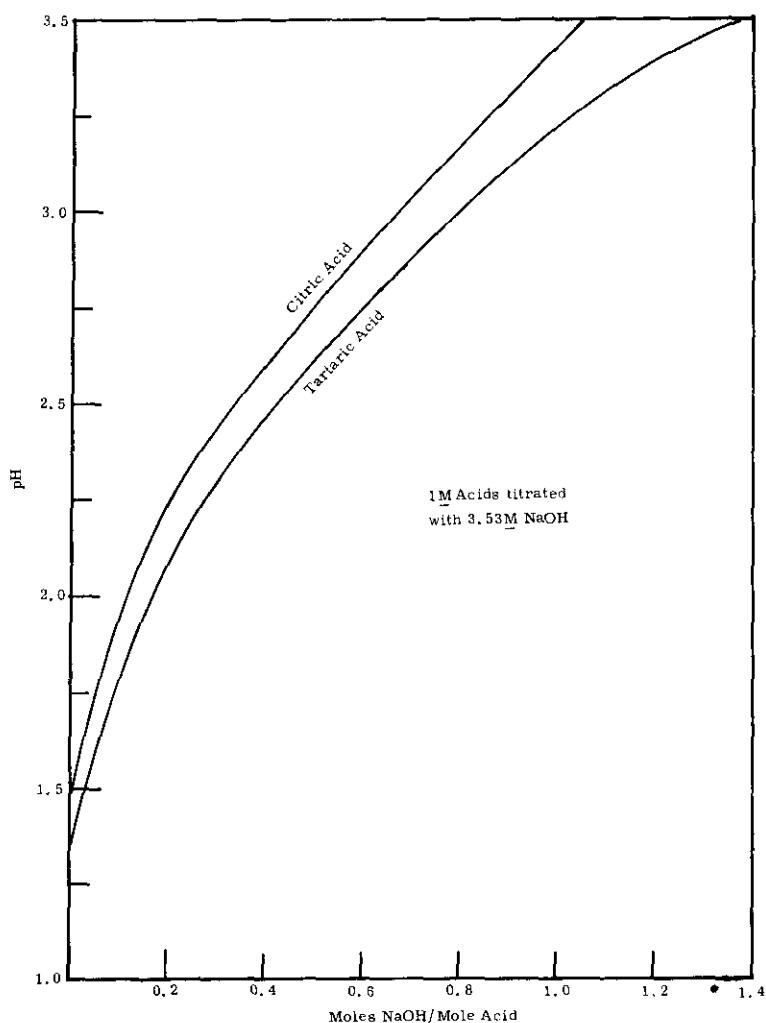


**FIGURE IV-53**

Variation in pH as a Function of Neutralization  
of Citric and Tartaric Acids

(Source of Data: HW-72666, Section 3)

DECLASSIFIED

4118

#### 4.3.5 Concentration of Strontium Product

The purified strontium product (LBP) solution obtained from the D2EHPA purification process is too dilute for storage and must be concentrated. To avoid process problems caused by citric acid radiolytic degradation products, it is necessary to destroy citric acid in the LBP solution and convert to a nitrate media prior to storage. These radiolytic products have not been identified but include tars as well as other objectionable solids when radiolysis proceeds far enough. Furthermore, in one Strontium Semiworks run, addition of  $\text{HNO}_3$  to a strontium-citric acid solution which had undergone extensive radiolysis resulted in formation of unmanageable foams and gels<sup>(77)</sup>.

Citric acid in  $\text{HNO}_3$  solutions can be readily and rapidly destroyed by reaction with  $\text{H}_2\text{O}_2$ . This was first demonstrated on a laboratory scale by Buckingham<sup>(31)</sup> and subsequently on a plant scale in the Strontium Semiworks. The end products of the reaction between citric acid and  $\text{H}_2\text{O}_2$  are undoubtedly water and carbon dioxide, but neither the reaction mechanism nor the reaction stoichiometry have been defined rigorously. Buckingham's experiments indicated that destruction of a mole of citric acid in 1 to 2M  $\text{HNO}_3$  required from 5 to 10 moles of  $\text{H}_2\text{O}_2$ . In the Strontium Semiworks, the combination of radiolysis and  $\text{H}_2\text{O}_2$  addition has provided adequate destruction of citrate with as little as 4 moles of  $\text{H}_2\text{O}_2$  added per mole of citrate<sup>(38)</sup>.

Nitric acid is also used up during the radiolytic-peroxide reaction, and recent Strontium Semiworks experience demonstrates that very careful control of the  $\text{HNO}_3$  concentration is necessary to avoid operational problems during citrate destruction. If  $\text{HNO}_3$  is not added as fast as it is destroyed by radiolysis, the product concentrator solution can become acid deficient. Severe foaming occurred when this happened in one Semiworks run; the foaming was stopped by cooling the concentrator and acidifying the solution with  $\text{HNO}_3$ . Also, when the  $\text{HNO}_3$  concentration becomes too high ( $< 7\text{M}$ ) a fast denitration reaction can occur. Such reactions can occur also at lower  $\text{HNO}_3$  concentrations ( $\leq 3\text{M}$ ) when peroxide addition is stopped. Laboratory investigations indicate that the fast denitration is a formic acid- $\text{HNO}_3$  reaction and that it is initiated by the presence of nitrite ion. Nitrite is known to be a product from the radiolysis of nitrate, and formic acid is thought to be one of the intermediate degradation products of citric acid. Hydrogen peroxide is a nitrite suppressant, and the reaction has not occurred while peroxide was being added under conditions where the  $\text{HNO}_3$  concentration was less than 3M and the organic acid concentration (calculated as "equivalent" citric acid) was less than 2M except during periods when the peroxide flow was stopped.

The denitration reaction that occurs under high acid conditions is quite violent compared to the foaming that occurs when the product solution becomes acid deficient. Process control of the citrate destruction re-

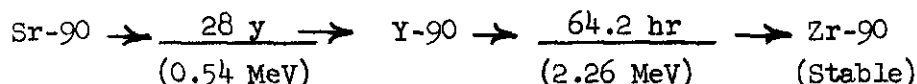
DECLASSIFIED

action is thus pointed toward low acid operations. At the time this manual was written, tests were in progress in the Semiworks to define optimum reaction conditions. It is anticipated that results of these tests will be applicable to destruction of citric acid in the B-Plant.

#### 4.3.6 Disposition of Strontium Product

The concentrated strontium product solution obtained after destruction of citrate and peroxide will be stored pending transfer to a Fission Product Program. Alternatively, the strontium can be adsorbed on zeolite for long-term storage (see Section F of this chapter).

Strontium-90 decays by the scheme:



Consequently, significant quantities of zirconium grow into the purified strontium as it is allowed to stand. A precipitation process for separating the zirconium from strontium has been developed<sup>(14)</sup>; present B-Plant plans, however, do not call for purification of the stored strontium from zirconium.

#### 4.4 Chemical Flowsheet

A detailed chemical flowsheet for purification of the strontium fraction from current acid waste is given in Figure IV-54. A similar flowsheet would be used for purification of the strontium fraction from stored sludge with the feed flow adjusted to provide about the same strontium and calcium loading in the solvent.

#### 4.5 Alternate Precipitation Purification Process

Precipitation of insoluble hydroxides has been studied by Bray<sup>(16)</sup> as a means of purifying the strontium fraction obtained from current acid waste. Bray's work was performed with a synthetic crude strontium feed containing 0.058M Sr, 0.017M Mg, 0.012M Ca, 0.01M Fe, 0.001M Cr, 0.002M RE, 0.2M Na, and 0.12M HNO<sub>3</sub>. Neutralization of this feed to pH 10 (by addition of NaOH to a warm (80-90 C solution) precipitated wssentially all the cerium and iron and over 95% of the magnesium. Approximately 98, 51, and 8% of the calcium remained in solution at the respective pH values of 11, 12.4, and 13. Less than 2% of the initial strontium was lost below a pH of 11, but the loss increased to 15% at a

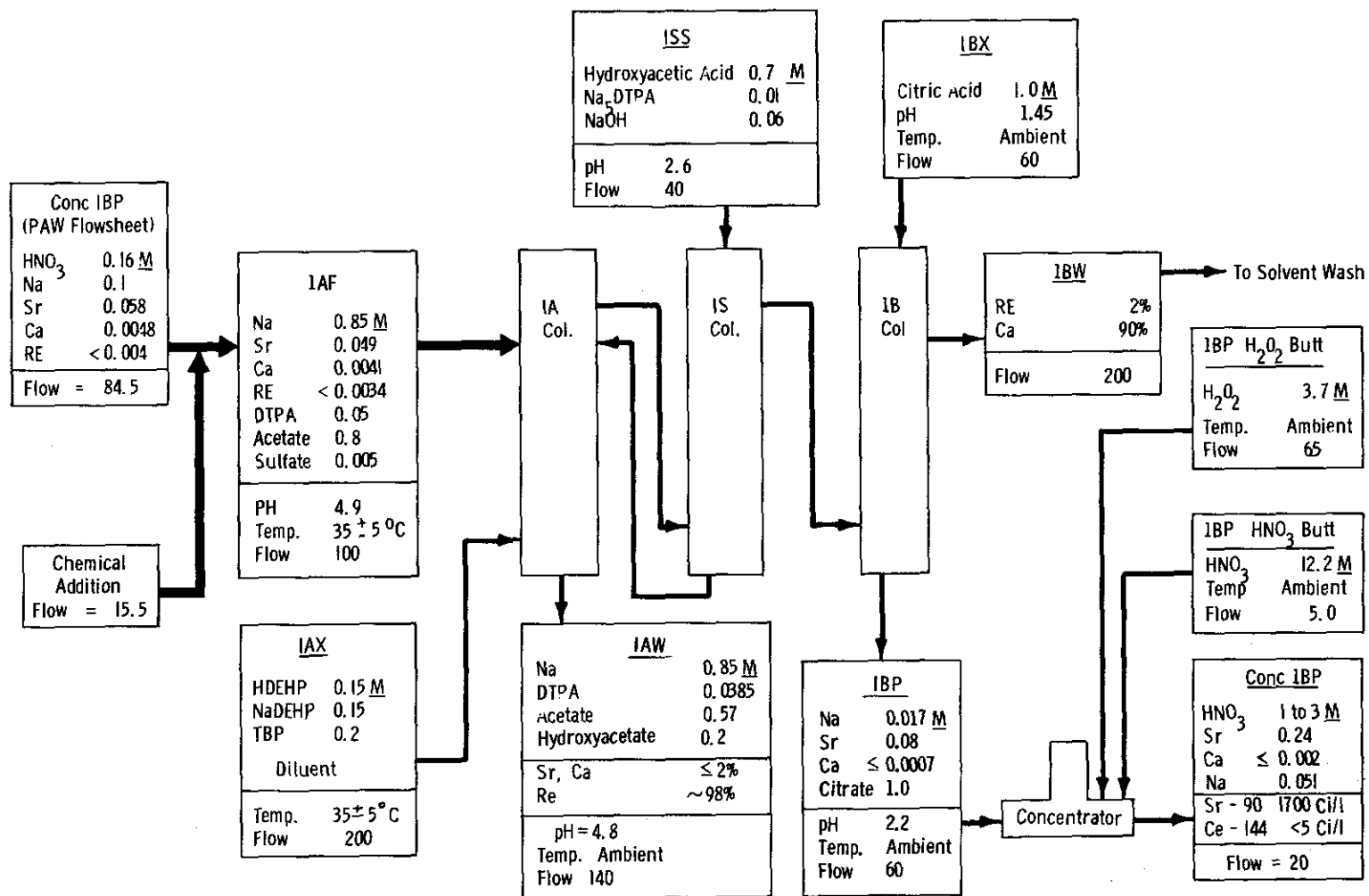


FIGURE IV-54

Chemical Flowsheet for Purification of Strontium Fraction Derived from Current Acid Waste

pH of 13. According to Bray, the final precipitate occupied a volume less than 8% that of the original solution and was somewhat gelatinous but centrifuged well.

This precipitation process is particularly suited for purification of strontium from magnesium if such purification might be required. Currently, there is very little magnesium in the uranium metal or other essential materials used in the Hanford Purex Plant, but suggested alterations in the metallurgical processes used by uranium suppliers may result in the introduction of significant quantities of magnesium. Bray reports the D2EHPA solvent extraction of magnesium is identical to that of strontium even in the presence of DTPA; thus magnesium will quantitatively follow strontium through the D2EHPA extraction process.

## 5. Semi-Purification of Rare Earth - Americium Fraction

### 5.1 Introduction

When operated with feeds prepared from current waste (PAW and ZAW solutions) the LC Column in the mainline D2EHPA extraction process will be used to separate cerium from the other rare earths and americium (see Section C 3.5.3). The aqueous rare earth - americium fraction from the LC Column will be contaminated with sulfate, silver, and sodium ions, all resulting from the silver-catalyzed persulfate oxidation of Ce(III) to Ce(IV). Sulfate is also derived from the decomposition of persulfate by radiation and reaction with water. Its removal is necessary to prevent precipitation of double rare earth sulfates and to allow concentration of the rare earth - americium fraction to volumes small enough for storage and/or eventual transfer to a Fission Product Program. Purification is achieved by the batch D2EHPA extraction process described in this section.

### 5.2 Feed Material and Impurities

The estimated composition of the rare earth - americium fraction from the LC Column when processing current acid waste is listed in Table IV-20.

TABLE IV-20

ESTIMATED COMPOSITION OF RARE EARTH - AMERICIUM FRACTION

(Source of Data: Figure IV-48)

<u>Component</u>	<u>% of Total in PAW</u>	<u>Concentration, M</u>
H	--	2.7
Na	--	0.8
Ag	--	0.005
Ca	92	0.0055
Sr (a)	1	--
RE (a)	70	0.025
Pm	96	--
Ce	<2	--
Y	<5	--
NO <sub>3</sub> <sup>-</sup>	--	2.0
SO <sub>4</sub> <sup>=</sup>	--	0.8

(a) Total rare earths, including cerium and promethium.

5.3 Purification Process5.3.1 Process Concept - Chemical Flowsheet

A batch D2EHPA extraction process for purifying the rare earth - americium fraction from sulfate ion and other impurities<sup>(62)</sup> is illustrated by the flowsheet shown in Figure IV-55.

Extraction feed for the process is prepared by adding NaOH and HEDTA or citric acid to the aqueous promethium-americium solution from the IC Column. The HEDTA (or citrate) prevents precipitation of rare earth sulfates when NaOH is added to adjust the solution to the extraction pH of 3.5. Trivalent rare earths and americium are coextracted into the D2EHPA phase leaving the sulfate and most other impurities in the aqueous raffinate. After decanting the aqueous waste, the solvent is washed with 1M HNO<sub>3</sub> to recover americium, promethium, and other rare earths. Finally, the promethium-americium product solution is continuously concentrated, and denitrated (by addition of sucrose), and then stored for aging of the promethium. The solvent will normally be recycled without further washing to eliminate any promethium stripping losses.

5.3.2 Batch Extraction Step

Bray and Roberts have investigated the D2EHPA solvent extraction behavior of rare earths complexed with HEDTA in the presence of sulfate<sup>(22)</sup>. Their results are shown in Figure IV-56 and indicate that a pH of 2.5 to 3.5 is optimum for nearly quantitative extraction of the

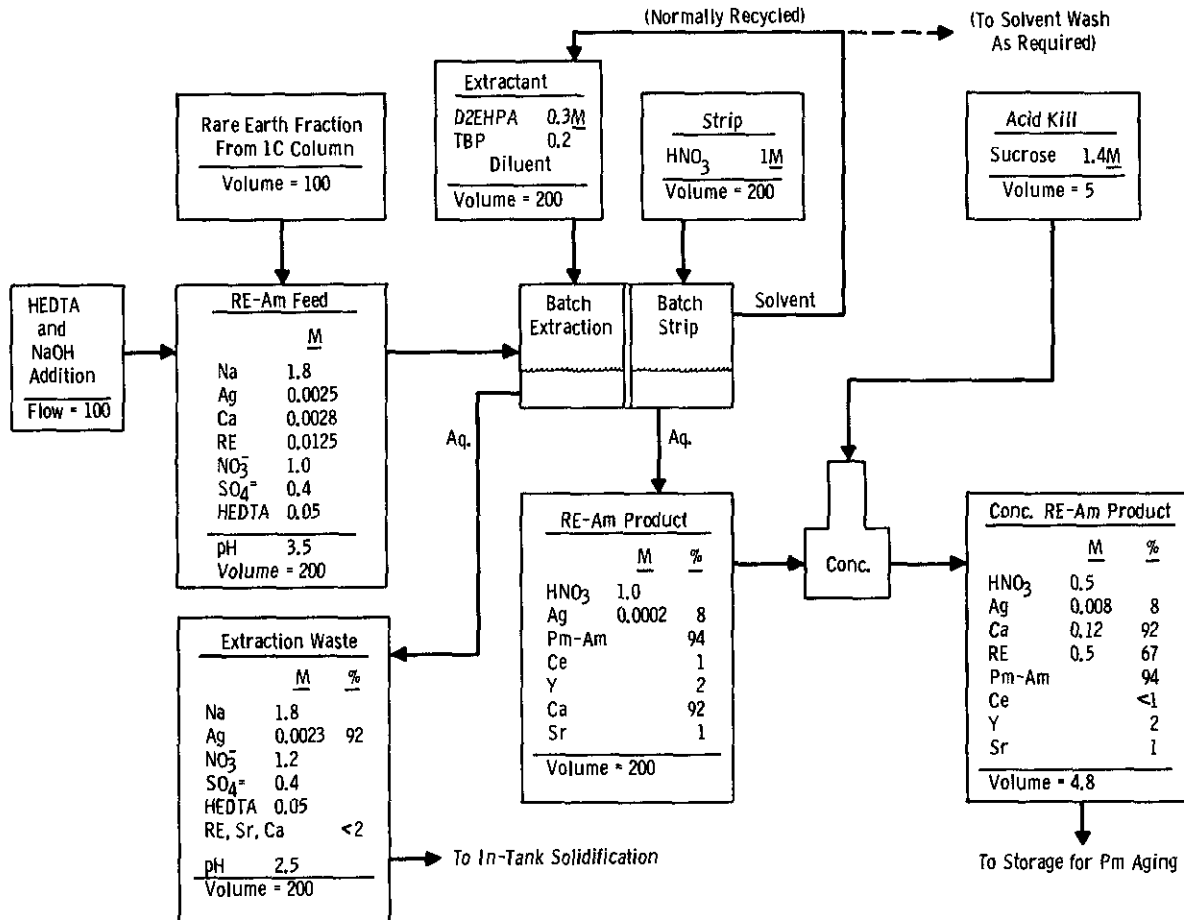


FIGURE IV-55

Chemical Flowsheet for Semi-Purification of Rare Earth - Americium Fraction

(Based on the flowsheet presented in ISO-42)

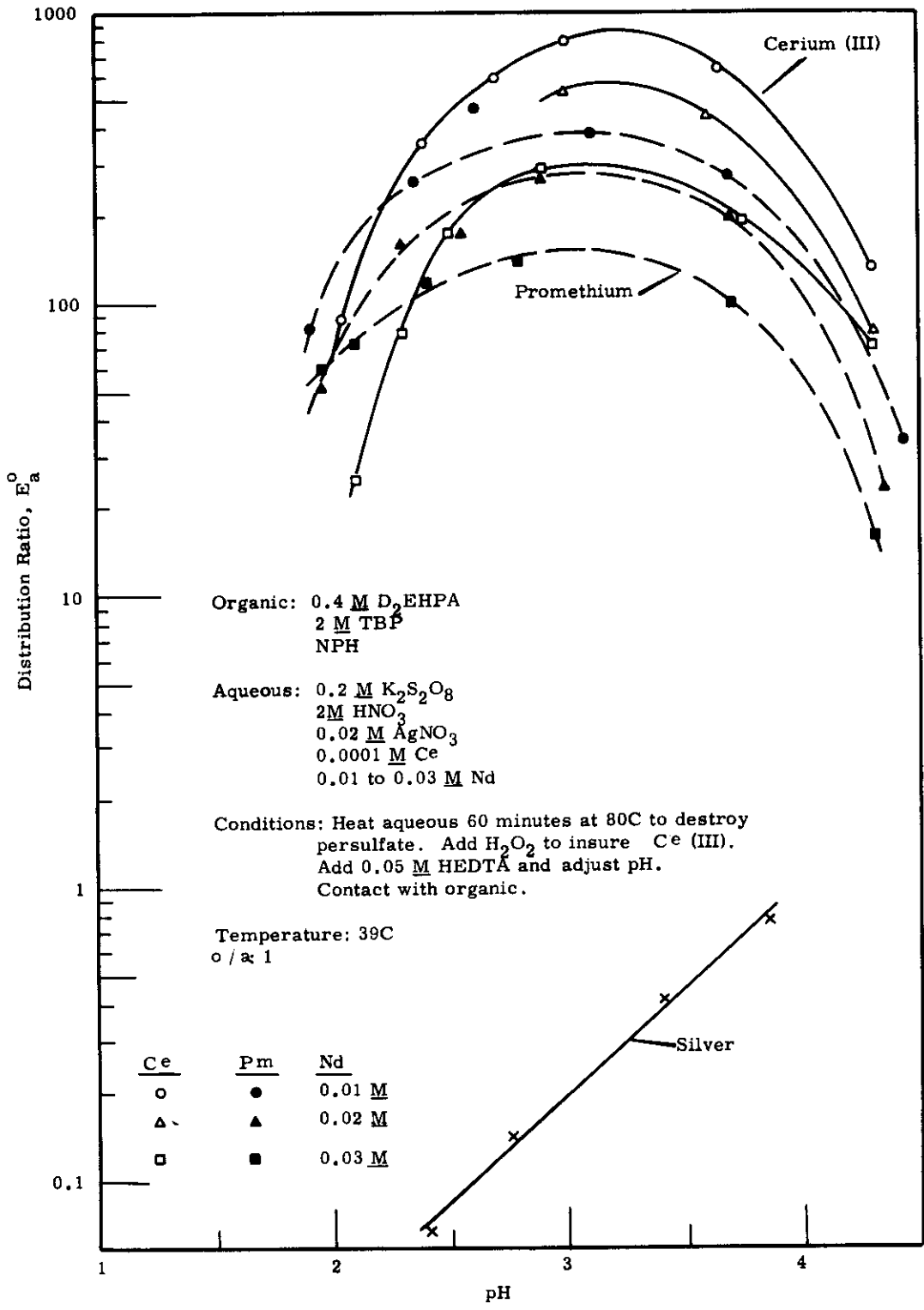


FIGURE IV-56

Extraction of Rare Earths and Silver from Sulfate Solutions Containing HEDTA as a Function of pH (Source of Data: BNWL-187)

DECLASSIFIED

4125

ISO-100

rare earths. The extraction behavior of americium was not studied in these particular experiments, but americium is expected to follow promethium and the other rare earths into the organic phase. Some silver is also extracted but not enough to interfere with subsequent ion exchange separation of the individual rare earths.

The purpose of the HEDTA in the extraction feed is, as mentioned earlier, to prevent precipitation of rare earth sulfates. Bray and Roberts report that either 0.05M citrate or 0.05M HEDTA prevents precipitation of rare earths at pH's above 3 if the sulfate concentration is 0.4M or less<sup>(22)</sup>. Conditions were not found which would prevent rare earth precipitation when the feed solution contained more than 0.4M sulfate. A summary of the results of their solubility studies is presented in Figure IV-57.

### 5.3.3 Batch Strip Step

Contact of the pregnant D2EHPA phase with 1.0M HNO<sub>3</sub> readily strips rare earths and americium as discussed earlier in Section C 3.5.2. Stripping is not quantitative at 1M HNO<sub>3</sub>, and the solvent is normally recycled without washing to prevent promethium loss.

### 5.3.4 Concentration - Denitration of Product

The HNO<sub>3</sub> solution from the strip contact constitutes the feed for further separation and purification of Pm-147 by chromatographic ion exchange techniques. Concentration and HNO<sub>3</sub> destruction are required to meet the storage volume and ion exchange requirements. A final product containing about 0.5M rare earths and 0.1 to 1M HNO<sub>3</sub> is desired<sup>(80)</sup>. To meet this requirement denitration by sucrose addition during thermal concentration will be employed.

Sucrose denitration is a well-demonstrated process and is used routinely in the Hanford Purex Plant to prepare PAW solution from LWV solution<sup>(11,19)</sup>. Laboratory scale concentration and sucrose denitration of the HNO<sub>3</sub> strip solution have been tested successfully with both synthetic and Strontium-Semiworks solutions<sup>(22)</sup>.

### 5.3.5 Disposition of Rare Earth - Americium Product

The concentrated, denitrated rare earth - americium product solution will be stored pending transfer to a Fission Product Program for recovery and purification of the Pm-147 content.

DECLASSIFIED

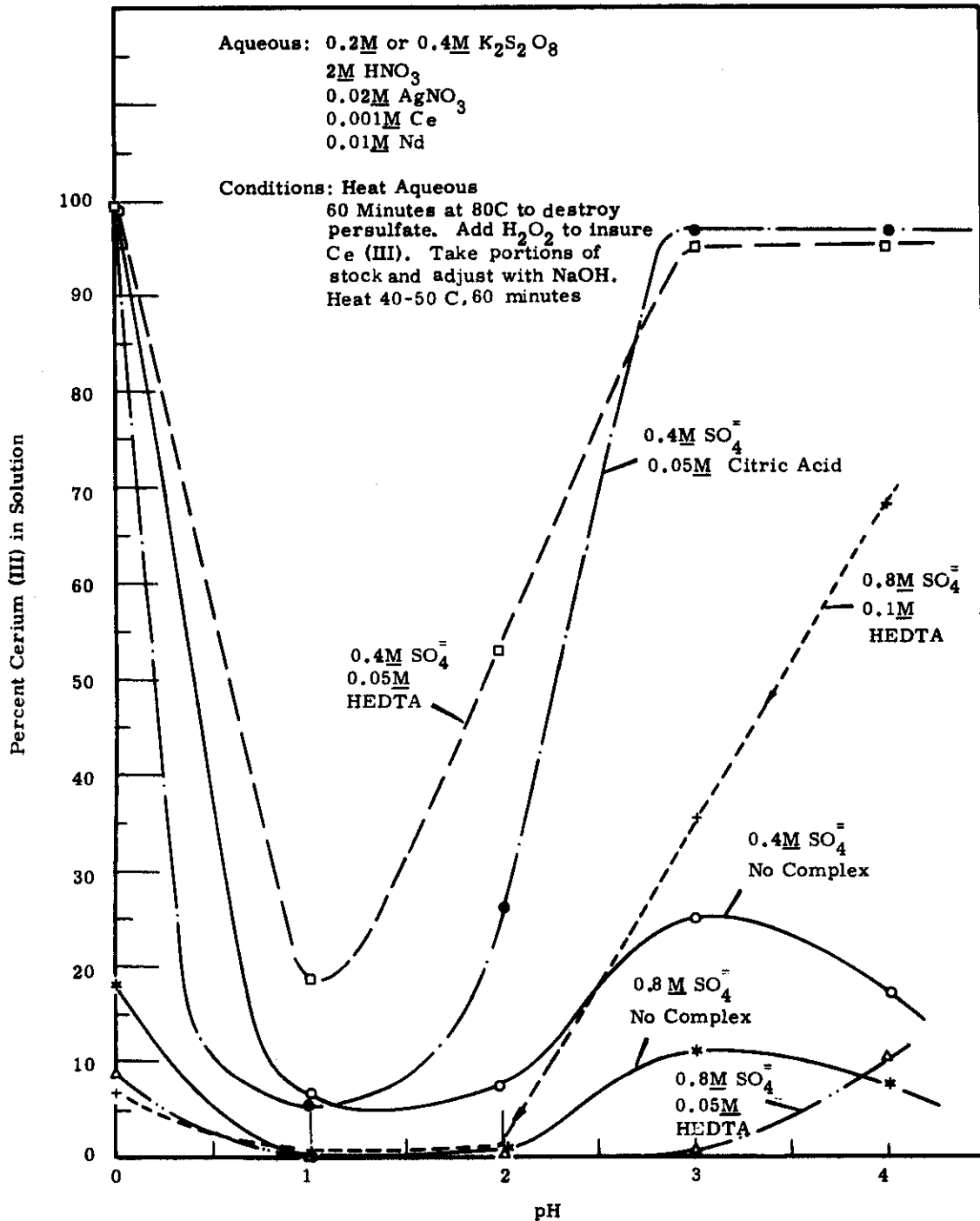


FIGURE IV-57

Rare Earth Solubility in the Presence of Varying Concentrations of Sulfate and Complexant as a Function of pH  
 (Source of Data: BNWL-187)

DECLASSIFIED

4127

ISO-100

#### 5.4 Strontium Semiworks Process Demonstration

A chemical flowsheet similar to that shown in Figure IV-55 was used in the Strontium Semiworks to purify four batches of Pm-147 (plus associated Am-241 and other trivalent rare earths) from sulfate. Each batch comprised 50 to 100 kilocuries of Pm-147 in about 1000 liters; the composition of these feed solutions was essentially that listed in Section C 5.2 except that the sulfate concentration was 0.4M and the silver concentration was 0.02M. Extraction-strip performance was excellent; typically, 2-3% of the Pm-147 was not extracted from the feed, and about 2% of the Pm-147 was left in the solvent after stripping with 2M  $\text{HNO}_3$  (63).

Continuous concentration and sucrose destruction of nitrate in the  $\text{HNO}_3$  strip solution was also accomplished very satisfactorily in the Strontium Semiworks runs. The final concentrates approximated the composition indicated in the chemical flowsheet shown in Figure IV-55.

In the concentration - denitration runs, temperature and specific gravity measurements were used to control rates of addition of sucrose solution and of the dilute rare earth feed. These runs demonstrated the desirability of maintaining a steady state  $\text{HNO}_3$  concentration greater than 3 or 4M in the concentrator to maintain rapid kinetics of nitrate destruction and to prevent precipitation of rare earth oxalates. (Oxalic acid is an intermediate in the conversion of sucrose to  $\text{CO}_2$ .) Typically, one mole of sucrose destroyed 30 to 40 moles of  $\text{HNO}_3$ . The steady state concentration of carbon compounds (calculated as sucrose) was about 0.05M. Normally, continuous concentration and denitration of a batch of Pm-147 strip solution was halted when the  $\text{HNO}_3$  concentration fell to 1M. The residual carbon compounds were then sufficient to reduce the  $\text{HNO}_3$  concentration to about 0.5M in a 72-hour digestion period.

#### 6. Solvent Treatment

##### 6.1 Introduction

The D2EHPA extractant used to recover strontium, rare earths, and americium from current acid waste and stored sludge waste will become contaminated with various inert and radioactive inorganic contaminants. Periodic removal of these contaminants and adjustment of the sodium to hydrogen ratio in the extractant is required. The chemical wash treatments designed to accomplish these objectives are discussed in this section.

DECLASSIFIED

DECLASSIFIED

4128

130

The same extractant used in the mainline recovery process (Section C 3) will also be used, as required, to purify the strontium and rare earth fractions (Sections C 4 and C 5). The chemical wash procedures discussed in this section will also apply for removing inorganic contaminants introduced into the solvent during these operations.

## 6.2 Solvent Contaminants

Solvent from the mainline D2EHPA processes for treating current acid waste and stored sludge waste will contain nearly all of the yttrium entering the process together with small amounts of "irreversibly" extracted iron, chromium, and zirconium. Yttrium follows the rare earths through the 1A, 1S, and 1B Columns but is not stripped into 2M HNO<sub>3</sub> in the 1C Column. The solvent leaving the 1C Column (when processing current acid waste) will contain about 0.00028 mole/liter of yttrium<sup>(62)</sup>. Inert impurities will range, typically, within a factor of ten of this value.

On the basis of Strontium Semiworks experience, small amounts of uranium and fission products (principally Ce-144, ZrNb-95, Ru-103, and Ru-106) are also expected to be present in used mainline process solvent. The oxo cation UO<sub>2</sub><sup>++</sup>, as noted earlier, is extracted more strongly than other divalent cations such as Ca<sup>++</sup> and Sr<sup>++</sup> and is not stripped in either the 1B or 1C Column.

In the mainline process, cerium is removed from the D2EHPA solvent leaving the 1C Column by batch stripping with a HNO<sub>3</sub>-NaNO<sub>2</sub> solution. The unused nitrite ion extracts nearly quantitatively into the solvent as nitrous acid and must be removed by an appropriate chemical wash treatment before reuse of the solvent.

The D2EHPA extractant used in auxiliary purification processes will contain about the same cation impurities as the used mainline solvent except, of course, to a lesser extent.

## 6.3 Washing Procedures

### 6.3.1 Sodium Hydroxide-Complexant

Treatment of used D2EHPA extractants with NaOH solutions containing either citrate or tartrate is a highly efficient way to remove metal contaminants from such solutions. This has been demonstrated in both laboratory experiments<sup>(74)</sup> and in Strontium Semiworks operation (Section C 6.5.1). Most effective removal of contaminants is realized when sufficient NaOH is used to convert all the extractant to the sodium salt form and to make the equilibrium wash solution 0.5 to 1.0M NaOH. Complexants such as citrate or tartrate in the alkaline wash aid in removal of contaminants and prevent precipitation of metals such as iron and yttrium

DECLASSIFIED

by forming soluble complexes; uranium, if present, precipitates as the diuranate even in the presence of citrate or tartrate. Laboratory results presented in Table IV-21 show that slightly better decontamination performance is obtained with citrate than with tartrate<sup>(74)</sup>. In laboratory studies, gravity phase separation was faster at 50 C than at 25 C.

TABLE IV-21  
NaOH - COMPLEXANT SOLVENT WASHES  
 (Source of Data: HW-84592)

Conditions: Unwashed Strontium Semiworks solvent<sup>(a)</sup> contacted 15 min. with one-fifth volume of indicated aqueous wash.

Wash Composition	Temp. C	Decontamination Factor <sup>(b)</sup>				
		Y-91	Ce-144	ZrNb-95	Ru-103	Gross Gamma
2.5M NaOH	50	37	43	32	3	31
2.5M NaOH	25	15	24	26	4	22
2.5M NaOH - 0.1M Na <sub>2</sub> Tar.	50	15	57	33	4	27
2.5M NaOH - 0.1M Na <sub>3</sub> Cit.	50	240	220	87	4	75

(a) 0.35 M D2EHPA, 0.22M TBP, Soltrol-170 containing 0.164 Ci/l Y-91, 0.0745 Ci/l Ce-144, 0.08 Ci/l ZrNb-95, and 0.0045 Ci/l Ru-106.

(b) Ratio of concentration in unwashed and washed solvents.

### 6.3.2 Nitric-Oxalic Acid Washes

Nitric acid washes alone are not effective in removing tightly bound impurities, and laboratory washing studies<sup>(74)</sup> have demonstrated that very little additional fission product activity is removed by a HNO<sub>3</sub> wash following sodium hydroxide washes. Addition of oxalic acid to the HNO<sub>3</sub> wash gives slightly increased decontamination from ZrNb-95 and Ce-144 activity as illustrated by the results in Table IV-22.

TABLE IV-22  
MULTIPLE BATCH WASHING OF STRONTIUM SEMIWORKS SOLVENT  
 (Source of Data: HW-84592)

Conditions: Portions of unwashed Strontium Semiworks solvent<sup>(a)</sup> washed (15 min. at 50C) consecutively with equal volume portions of following washes:

Wash 1 - 2.0M sodium tartrate or 0.1M sodium citrate

Wash 2 - Same as Wash 1

Wash 3 - 2.0M HNO<sub>3</sub>, 0.1M oxalic acid

Contaminant	Decontamination Factor					
	Sodium Tartrate			Sodium Citrate		
	Wash 1	Wash 2	Wash 3	Wash 1	Wash 2	Wash 3
Y-91	73	(b)	(b)	150	(b)	(b)
Ce-144	19	34	5	240	6	2.5
ZrNb-95	55	13	1.6	78	6.6	2
Ru-106	2	1	1	7	1	1

(a) 0.35M D2EHPA, 0.22M TBP, Soltrol-170 containing 0.0164 Ci/l Y-91, 0.0745 Ci/l Ce-144, 0.08 Ci/l ZrNb-95, and 0.0045 Ci/l Ru-106.

(b) Y-91 not detected in organic phase after second wash.

DECLASSIFIED

4130

100

### 6.3.3 Nitric Acid-Permanganate Washes

Both laboratory<sup>(74)</sup> and Strontium Semiworks experience<sup>(63)</sup> indicate that the Ce(IV) extraction capacity of a D2EHPA-TBP-diluent solvent deteriorates on repeated solvent use. A large fraction of this decreased capacity appears to be caused by the generation, either chemically or radiolytically or both, of reducing impurities in the extractant. These impurities appear to arise from attack of the hydrocarbon diluent, and, in this connection, NPH is more stable to generation of such impurities than is Soltrol-170<sup>(21,22)</sup>.

Results obtained by Schulz and Beard<sup>(73)</sup> demonstrate that  $\text{HNO}_3$ - $\text{KMnO}_4$  washes are very effective in restoring Ce(IV) extraction capacity of degraded D2EHPA solvents. In contrast, Ce(IV) extraction capacity is little, if any, affected by normal NaOH-complexant or  $\text{HNO}_3$ -oxalic acid washing. The effectiveness of  $\text{KMnO}_4$  washing appears to be connected in some way with the production of  $\text{MnO}_4^-$  when the solvent contacts the aqueous  $\text{KMnO}_4$  solution. The  $\text{MnO}_4^-$  which collects at the organic-aqueous interface at the conclusion of the wash can be destroyed by reaction with either  $\text{H}_2\text{O}_2$  or oxalic acid without impairing the improved Ce(IV) extraction capacity. Some typical data illustrating the effectiveness of  $\text{HNO}_3$ - $\text{KMnO}_4$  washing are listed in Table IV-23.

TABLE IV-23

#### $\text{HNO}_3$ - $\text{KMnO}_4$ WASHING OF D2EHPA SOLVENTS

(Source of Data: HWIR-1836)

Conditions: 0.37M D2EHPA, 0.2M TBP solvents of various histories washed one hour at 25C with an equal volume of 2M  $\text{HNO}_3$ , 0.05 to 0.25M  $\text{KMnO}_4$ . Ce(IV) extraction capacity measured by contacting washed solvent with an equal volume of 2M  $\text{HNO}_3$ , 0.2M  $(\text{NH}_4)_2\text{S}_2\text{O}_8$ , 0.02M  $\text{AgNO}_3$ , 0.007M  $\text{Ce}(\text{NO}_3)_3$  for one hour at 25C.

Diluent	M $\text{KMnO}_4$ in Wash	Cerium $E_a^0$	
		Unwashed	Washed
Soltrol-170 <sup>(a)</sup>	0.25	27.8	360
Soltrol-170 <sup>(b)</sup>	0.05	0.17	21.4
Soltrol-170 <sup>(b)</sup>	0.10	--	360
Soltrol-170 <sup>(b)</sup>	0.25	--	1320
Soltrol-170 <sup>(c)</sup>	0.10	5.7	620
NPH <sup>(c)</sup>	0.10	19.3	980

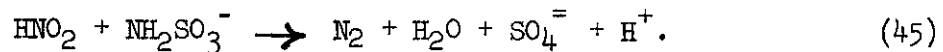
- (a) Strontium Semiworks solvent washed previously with NaOH and  $\text{HNO}_3$ -oxalic acid.  
 (b) Laboratory solvent prepared with chemically degraded ( $\text{HNO}_3$ - $\text{NaNO}_3$ ) Soltrol-170.  
 (c) Laboratory solvent irradiated to about 400 watt-hrs/liter.

DECLASSIFIED

As this manual was written there were no plans for routine washing of B-Plant D2EHPA solvents with  $\text{HNO}_3$ - $\text{KMnO}_4$  solutions. The present choice of a hydrocarbon diluent for B-Plant use is NPH. On the basis of Strontium Semiworks experience, this diluent should not degrade sufficiently to impair Ce(IV) oxidation and extraction under countercurrent flow conditions in the mainline process 1C Column.

#### 6.3.4 Nitrous Acid Removal

Sulfamate ion reacts rapidly and completely with nitrous acid in acid systems according to the reaction<sup>(82)</sup>



Sulfamic acid and sulfamic-nitric acid washes have been successfully used in pilot plant studies<sup>(61)</sup> and Strontium Semiworks campaigns<sup>(63)</sup> to remove nitrous acid from solvent after Ce(IV) stripping. The reaction rate is too slow in alkaline systems (above pH 5) to be of value.

Caustic washing should also effectively remove nitrous acid by converting it to the inextractable nitrite. A small sulfamic acid addition during solvent acidification should provide additional assurance of nitrite removal.

#### 6.4 Chemical Flowsheet

A tentative chemical flowsheet for batch washing of the used D2EHPA extractant from the processing of current acid waste is presented in Figure IV-58. It is anticipated that this flowsheet will also be followed in washing solvent from the processing of stored sludge waste and from the auxiliary strontium and rare earth purification processes. In these latter processes, nitrite will not be introduced into the extractant and addition of sulfamic acid to the 100 stream will not be necessary. Also, during D2EHPA purification of the strontium fraction from both current and stored waste (Section C 4) only three of the four available pulse columns will be used; thus if desirable, the fourth column can be used to perform the solvent washing step on a continuous rather than a batch basis.

The chemical flowsheet specified in Figure IV-58 involves only a NaOH-complexant wash and a  $\text{HNO}_3$  butt to the desired Na/H mole ratio. If necessary or desirable, additional washes ( $\text{HNO}_3$ -oxalic or  $\text{HNO}_3$ - $\text{KMnO}_4$ ) can be made.

#### 6.5 Strontium Semiworks Process Demonstration

Chemical washing of the D2EHPA extractant used in Strontium Semiworks operation for Sr-90 recovery has been performed routinely for more

than two years with satisfactory results<sup>(63)</sup>. Equally successful performance was obtained in either batch or continuous countercurrent column washing, both at about 50 C. In batch washing, the solvent was first washed with a double volume of 2M NaOH-0.2M citrate (or tartrate). This was followed by washing with an equal volume of 2M HNO<sub>3</sub>-0.2M oxalic acid. Typical over-all decontamination factors were about 70 for Ce-144 and ZrNb-95, about 10 for Ru-106, and about 70 to 200 for Y-91. Hydraulic and chemical performance of the washed solvent in Sr-90 recovery operations were excellent throughout.

The procedure used for column washing was similar to the batch wash procedure except that the A/O ratios were 1 and 5 for the caustic and acid washes, respectively. The pulse columns were operated at volume velocities of 360 (caustic washing) and 1100 gph/ft<sup>2</sup> (acid washing). The cartridge geometries were comparable with those used in the B-Plant 1A and 1B Columns, respectively.

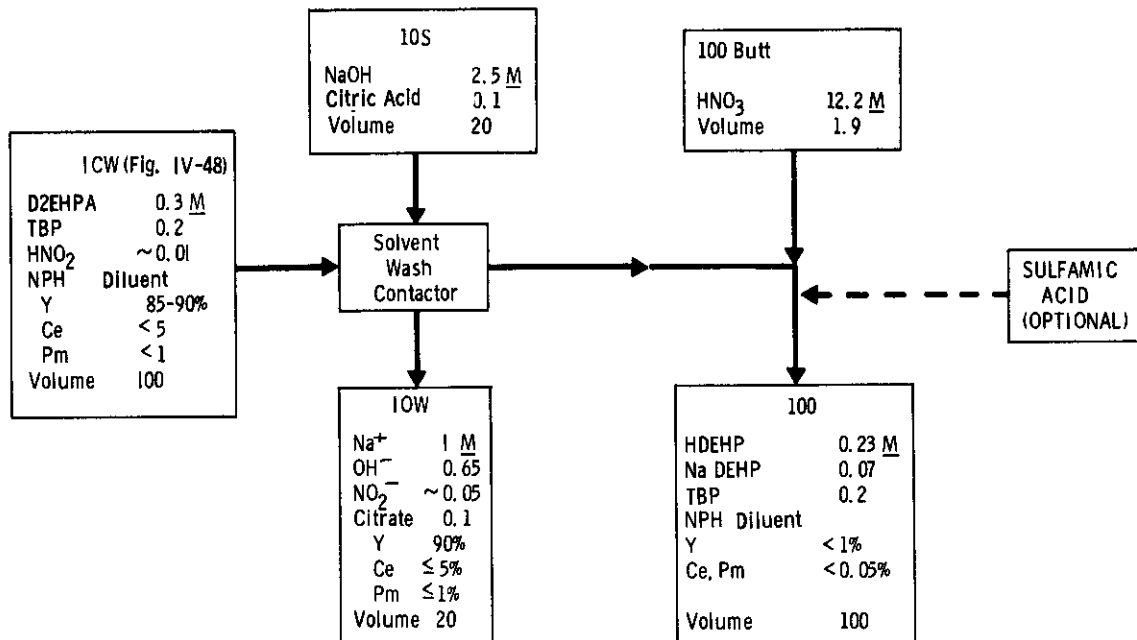


FIGURE IV-58

Chemical Flowsheet for Washing D2EHPA Extractant

7. References

1. C. F. Baes, Jr., R. A. Zingaro, and C. F. Coleman. "The Extraction of Uranium(VI) from Acid Perchlorate Solutions by Di-(2-ethylhexyl)-Phosphoric Acid in N-Hexane", J. Phys. Chem., vol. 62, pp. 129-136. 1958.
2. C. F. Baes, Jr. "The Extraction of Metallic Species by Dialkylphosphoric Acids", J. Inorg. Nucl. Chem., vol. 24, pp. 707-720. 1962.
3. C. F. Baes, Jr. "The Synergistic Effects in Organophosphate Extraction Systems", Nucl. Sci. & Eng., vol. 16, pp. 405-412. 1963.
4. S. J. Beard, R. J. Kofoed, J. J. Shefcik, and P. W. Smith. Waste Management Program, Chemical Processing Department, HW-81481. May 24, 1964.
5. S. J. Beard, P. W. Smith, and J. S. Cochran. Large Scale Processing and Source Preparation of Separated Fission Products, RL-SA-59. December 6, 1965.
6. J. Bjerrum, G. Schwarzenbach, and L. Sillen. Stability Constants, Part I: Organic Ligands, London: The Chemical Society, Burlington House, W.1, 1957.
7. C. A. Blake, K. B. Brown, and C. F. Coleman. The Extraction and Recovery of Uranium (and Vanadium) from Acidic Liquors with Di(2-ethylhexyl)Phosphoric Acid and Some Other Organophosphorous Acids, ORNL-1903. May 13, 1955.
8. C.A. Blake, D.J. Crouse, C.F. Coleman, K.B. Brown, and A.D. Kelmers. Further Studies of the Dialkylphosphoric Acid Extraction (Dapex) Process for Uranium, Progress Report, ORNL-2172. January 23, 1957.
9. C. A. Blake, D. E. Horner, and J. M. Schmitt. Synergistic Uranium Extractants: Combination of Neutral Organophosphorous Compounds with Dialkylphosphoric Acids, ORNL-2259. February 25, 1959.
10. L. A. Bray. Invention Report. Solvent Extraction Process for Recovery of Strontium, Cerium, Rare Earths, and Cesium from Radioactive Waste Solutions, HW-75537. November 5, 1962.
11. L. A. Bray. Denitration of Purex Waste with Sugar, HW-76973 REV. April, 1963.
12. L. A. Bray. Solvent Extraction Process for the Recovery of Strontium, Rare Earths, and Cesium from Radioactive Waste Solutions, HW-SA-2982. June 17, 1963.
13. L. A. Bray. D2EHPA Extraction of Bi, Ce, Fe, Pb, and Sr as a Function of Acidity and Complexant, HW-80595. February 15, 1964.

DECLASSIFIED

4134

ISO-100

14. L. A. Bray. Zirconium Removal from Purified Strontium-90, BNWC-24. February 5, 1965.
15. L. A. Bray. Solvent Extraction of Cesium from Hanford Alkaline Supernate by 4-Sec-Butyl-2 ( -Methylbenzyl)Phenol-Laboratory Studies, BNWL-68. March 1, 1965.
16. L. A. Bray. Purification of Strontium-90 from Magnesium, BNWL-26. March 15, 1965.
17. L. A. Bray. D2EHPA Solvent Extraction of Zirflex and Purex Acid Wastes, BNWL-CC-595. April 8, 1966.
18. L. A. Bray. Unpublished Data, Battelle-Northwest Laboratories, 1966.
19. L. A. Bray and E. C. Martin. Method of Treating Radioactive Waste, U. S. Patent 3158577. June 20, 1963.
20. L. A. Bray and F. P. Roberts. Separation of Trivalent Rare Earths from Cerium, HW-78987 REV. October, 1963.
21. L. A. Bray and F. P. Roberts. Supplemental Studies on the Separation of Cerium(IV) from the Trivalent Rare Earths, HW-84101. October 1, 1964.
22. L. A. Bray and F. P. Roberts. Purification of Rare Earths from Hanford Wastes by Solvent Extraction, BNWL-187. February, 1966.
23. K. B. Brown, C. F. Coleman, D. J. Crouse, and A. D. Ryan. Progress Report on Raw Materials, Chemical Development Section C, November, 1957, ORNL-2466. March 11, 1958.
24. K. B. Brown et. al. Chemical Technology Division, Chemical Development Section C, Progress Report for September, 1959, CF-59-9-85. October 20, 1959.
25. K. B. Brown. Chemical Technology Division, Chemical Development Section C, Progress Report for Feb.-Mar., 1960, CF-60-3-136. April 27, 1960.
26. K. B. Brown. Chemical Technology Division, Chemical Development Section C, Progress Report April, 1961-July, 1961, CF-61-7-76. September 26, 1961.
27. K. B. Brown. Chemical Technology Division, Chemical Development Section C, Progress Report for April-June, 1962, ORNL-TM-265. August 10, 1962.
28. K. B. Brown. Chemical Technology Division, Chemical Development Section C, Progress Report for July-Dec. 1962, ORNL-TM-449. [REDACTED] 11 22, 1963.

DECLASSIFIED

DECLASSIFIED

4135

ISO-100

29. K. B. Brown. Chemical Technology Division, Chemical Development Section C, Progress Report on Separations Process Research for Jan-June, 1963, ORNL-3496. October 25, 1963.
30. K. B. Brown and R. P. Wischow, ORNL, Personal Communication, 1961.
31. J. S. Buckingham. The Destruction of Citric Acid with Peroxide, HW-80992. February 25, 1964.
32. T. A. Butler and E. E. Ketchen. "Solvent Extraction Separation of Cerium and Yttrium from Other Rare Earth Fission Products," Ind. & Eng. Chem. vol. 53, pp. 651-654. 1961.
33. Chemical Development Operation. Hot Semiworks Strontium-90 Recovery Program, HW-72666. July 17, 1963.
- 33a. G. L. Richardson and W. W. Schulz. Ibid, Section 2: Technical Bases.
- 33b. W. W. Schulz, R. E. Burns, J. E. Mendel, and P. R. Rushbrook. Ibid, Section 3: Laboratory Studies.
- 33c. M. D. Alford and G. L. Richardson. Ibid, Section 4: Cold Semiworks D2EHPA Solvent Extraction Studies.
34. D. J. Crouse and K. B. Brown. Solvent Extraction Recovery of Vanadium (and Uranium) from Acid Liquors with Di(2-ethylhexyl) - Phosphoric Acid, ORNL-2820. November 25, 1959.
35. D. J. Crouse and D. E. Horner. "Unexpected Rate Effects in the Extraction of Rare Earths by Di(2-ethylhexyl)Phosphoric Acid," ORNL, Paper presented at Int'l. Conf. on Chem. of Solvent Ext'n. of Metals, Harwell, England. September 27-29, 1965.
36. D. Dyrssen and L. D. Hay. "Solvent Extraction of Eu-152, 154 and Am-241 by Di-N-Butyl Phosphate (DBP) in Different Organic Solvents", Acta. Chem. Scand. vol. 14, pp. 1100-1111. 1960.
37. J. R. Ferraro and D. F. Peppard. "Structural Aspects of Organo-Phosphorous Extractants and their Metallic Complexes as Deduced from Spectral and Molecular Weight Studies," Nucl. Sci. & Eng., vol. 16, pp. 389-400. 1963.
38. Fission Products Process Engineering. Specifications and Standards: Strontium Purification at the Strontium Semiworks, RL-SEP-20, February 15, 1965.
39. J. H. Gillette. Isotopes Division Quarterly Report, Jan-Mar., 1961, CF-61-3-143. September 28, 1961.

DECLASSIFIED

DECLASSIFIED

40. J. H. Gillette. Isotopes Division Research and Development Report, May, 1962, ORNL-TM-415. December 18, 1962.
41. D. E. Horner, D. J. Crouse, K. B. Brown, and B. Weaver. "Fission Product Recovery from Waste Solutions by Solvent Extraction," Nucl. Sci. & Eng. vol. 17, pp. 234-246. 1963.
42. D. A. House. "Kinetics and Mechanism of Oxidations by Peroxydisulfate", Chemical Reviews, vol. 62, pp. 185-201. 1962.
43. B. F. Judson. Purex Process Performance Summary, January, 1963, through December, 1963. HW-76912. 1963 (Secret)
44. R. E. Lewis. Unpublished Data, Oak Ridge National Laboratory. 1960.
45. W. J. McDowell and C. F. Coleman. "Sodium and Strontium Extraction by Di(2-Ethylhexyl)Phosphate: Mechanisms and Equilibria," J. Inorg. & Nucl. Chem., vol. 27, pp. 1117-1139. 1965.
46. R. E. McHenry, J. C. Posey. "Separation of Strontium-90 from Calcium by Solvent Extraction", Ind. Eng. Chem., vol. 53, pp. 647-650. 1961.
47. R. L. Moore, L. A. Bray, and F. P. Roberts. "Applications of Solvent Extraction Techniques to the Large-Scale Recovery and Purification of Fission Product Elements", BNWL-SA-259. July 16, 1965. Paper presented at Int'l Conf. on the Chemistry of the Solvent Extraction of Metals, Harwell, England. September 27-29, 1965.
48. D. F. Peppard, G. W. Mason, J. L. Maier, and W. J. Driscoll. "Fractional Extraction of the Lanthanides as their Di-Alkyl Orthophosphates," J. Inorg. Nucl. Chem., vol 4, pp. 334-343. 1957.
49. D. F. Peppard, J. F. Ferraro, and G. W. Mason. "Possible Hydrogen Bonding in Certain Interactions of Organic Phosphorus Compounds," J. Inorg. Nucl. Chem., vol. 4, pp. 371-372. 1957.
50. D. F. Peppard, G. W. Mason and S. W. Moline. "The Use of Dioctyl Phosphoric Acid Extraction in the Isolation of Carrier-Free Y-90, La-140, Ce-144, Pr-143, and Pr-144," J. Inorg. Nucl. Chem., vol 5, pp. 141-146. 1957.
51. D. F. Peppard, J. R. Ferraro and G. W. Mason. "Hydrogen Bonding in Organophosphoric Acids," J. Inorg. Nucl. Chem., vol. 7, pp. 231-244. 1958.
52. D. F. Peppard, G. W. Mason, W. J. Driscoll and R. J. Sironen. "Acidic Esters of Orthophosphoric Acid as Selective Extractants for Metallic Cations-Tracer Studies," J. Inorg. Nucl. Chem., vol. 7, pp. 276-285. 1958.

DECLASSIFIED

DECLASSIFIED

4137

53. D. F. Peppard, and J. R. Ferraro. "The Preparation and Infra-Red Absorption Spectra of Several Complexes of Bis-(2-Ethylhexyl)-Phosphoric Acid," J. Inorg. Nucl. Chem., vol.10, pp. 275-288. 1959.
54. D. F. Peppard, J. R. Ferraro and G. W. Mason. "The Preparation, Physical Properties and Infra-Red Spectra of Several New Organophosphonates," J. Inorg. Nucl. Chem., vol. 12, pp. 60-70. 1959.
55. D. F. Peppard, G. W. Mason, W. J. Driscoll and S. McCarty. "Application of Phosphoric Acid Esters to the Isolation of Certain Trans-Plutonides by Liquid-Liquid Extraction," J. Inorg. Nucl. Chem., vol. 12, pp. 141-148. 1959.
56. D. F. Peppard, G. W. Mason and S. McCarty. "Extraction of Thorium(IV) by Di Esters of Orthophosphoric Acid,  $(\text{GO})_2\text{PO}(\text{OH})$ ," J. Inorg. Nucl. Chem., vol 13, pp. 138-150. 1960.
57. D. F. Peppard, G. W. Mason, S. McCarty, and F. D. Johnson. "Extraction of Ca(II), Sr(II), and Ba(II) by Acidic Esters of Phosphorous Oxy Acids," J. Inorg. Nucl. Chem., vol. 24, pp. 321-332. 1962.
58. D. F. Peppard and G. W. Mason. "Some Mechanisms of Extraction of M(II), (III), (IV), and (VI) Metals by Acidic Organo-Phosphorous Extractants," Nucl. Sci. & Eng., vol. 16, pp. 382-388. 1963.
59. G. L. Richardson. Solvent Extraction of Strontium, Cerium, and Rare Earths with D2EHPA, Part 2: Pilot Plant Studies, HW-79762 PT2. February 1964.
60. G. L. Richardson. The CSREX Process for Co-Extraction of Cesium, Strontium, and Rare Earths: Pilot Plant Studies, HW-81091. March 2, 1964.
61. G. L. Richardson. Continuous Separation of Cerium from Trivalent Rare Earths by Persulfate Oxidation and D2EHPA Solvent Extraction: Pilot Plant Studies, HW-81173. November, 1965.
62. G. L. Ritter. Process Flowsheet for Continuous Separation of Cerium from Promethium at B-Plant, ISO-42. January 13, 1966. (Secret)
63. G. L. Ritter. Personal Communication. Isochem Inc., 1966.
64. G. L. Ritter and P. W. Smith. Waste Management Program, Integration with Fission Product Purification, HW-83058, PT1, June 30, 1964.
65. P. R. Rushbrook. Unpublished Data, Hanford Atomic Products Operation.

DECLASSIFIED

DECLASSIFIED

4138

66. T. Sato. "The Extraction of Uranium(VI) from Sulfuric Acid Solutions by Di-(2-ethylhexyl)-Phosphoric Acid," J. Inorg. Nucl. Chem., vol. 24, pp. 699-706. 1962.
67. T. Sato. "The Extraction of Uranium(VI) from Nitric Acid Solutions by Di(2-ethylhexyl)-Phosphoric Acid," J. Inorg. Nucl. Chem., vol. 25, pp. 109-155. 1963.
68. T. Sato. "The Synergic Effect of Tri-n-Butyl Phosphate in the Extraction of Uranium(VI) from Sulfuric Acid Solutions by D2EHPA", J. Inorg. Nucl. Chem., vol. 26, pp. 311-319. 1964.
69. T. Sato. "The Extraction of Uranium(VI) from Hydrochloric Acid Solutions by D2EHPA." J. Inorg. Nucl. Chem., vol. 27 pp. 1853-1860. 1965.
70. W. W. Schulz, BNW, Unpublished Data. 1962.
71. W. W. Schulz. Report of Invention: A Solvent Extraction Process for the Separation and Recovery of Aluminum from Redox Process-Type Aqueous and Waste Solutions, HW-79634. November 27, 1963.
72. W. W. Schulz. Solvent Extraction of Strontium, Cerium, and Rare Earths with D2EHPA Part 1: Laboratory Studies, HW-79762 PT1. February 1964.
73. W. W. Schulz and S. J. Beard. Report of Invention: A Wash Treatment to Restore the Quality of Degraded D2EHPA-TBP Fission Product Extractants, HWIR-1836. December, 1964.
74. W. W. Schulz, D. G. Bouse, and L. C. Neil. Some Recent Observations of Strontium Semiworks Solvent Quality, HW-84592. December 28, 1964.
75. W. W. Schulz, J. E. Mendel, and J. F. Phillips, Jr. "Evidence for a Chromium(III)-Cerium(III)-Citrate Complex," accepted for publication in J. Inorg. Nucl. Chem. 1966.
76. W. W. Schulz, J. E. Mendel, and G. L. Richardson. "Solvent Extraction Recovery and Purification of Strontium-90", I&EC Process Design and Development, vol. 2, pp. 134-140. 1963.
77. P. W. Smith. Letter to O. V. Smiset, Isochem Inc.: Process Test - Hydrogen Peroxide Destruction of Citric Acid. January 13, 1966.
78. H. H. Van Tuyl. Fission Product Generation and Decay Calculations, HW-75978. December 12, 1962.

DECLASSIFIED

DECLASSIFIED

4139

79. B. Weaver and F. A. Kappelmann. Talspeak: A New Method of Separating Americium and Cerium from the Lanthanides by Extraction from an Aqueous Solution of an Aminopolyacetic Acid Complex with a Mono-acidic Organophosphate or Phosphonate, ORNL-3559. August, 1964.
80. E. J. Wheelwright and F. P. Roberts. Development and Demonstration of an Ion Exchange Process for Kilogram Scale Production of High Purity Promethium, HW-78651 REV. October, 1963.
81. R. P. Wischow and D. E. Horner. Recovery of Strontium and Rare Earths from Purex Wastes by Solvent Extraction, ORNL-3204. January 15, 1962.
82. E. L. Zebroski and R. C. Feber. Sulfamic Acid in the Redox Process. KAPL-89. July 15, 1948.
83. L. A. Bray and G. L. Ritter. Solvent Extraction Purification of Americium with Di-(2-ethylhexyl)Phosphoric Acid (PAMEX Process), ISO-95. September 1, 1966.

DECLASSIFIED

DECLASSIFIED

D. STRONTIUM AND RARE EARTH SOLVENT EXTRACTION PROCESSES:  
PROCESS ENGINEERING

1. Types of Contactors

Solvent extraction processes can be performed in a variety of equipment, depending on the objectives, available space, economics, etc. The simplest type of contactor consists of a batch mixing tank in which the two phases are stirred together, allowed to settle, and decanted. Continuous operation can be achieved by providing a separate settling vessel or by incorporating a settling zone in the mixing tank. The Turbo mixers provided in the Purex Plant are examples of this type<sup>(17)</sup>. For any given ratio of solvent to feed, the maximum amount of solute which may be extracted is fixed solely by equilibrium considerations. Because of this, simple batch extraction is economically justified only when the distribution ratio of the transferring component is high enough to permit quantitative extraction with only one stage of contact.

Several types of continuous mixer-settlers are available. These are usually composed of a series of mixing chambers or stages separated by settling chambers, all enclosed in the same shell. The most familiar type in radioactive service is the "Pump-Mix" mixer-settler used in the Savannah River Plant and, in miniature form, in many laboratories<sup>(7)</sup>. In this contactor, the stages are arranged horizontally, and flow from stage to stage is promoted by pump-type impellers used as agitators. Mixer-settlers and other multistage contactors are operated most efficiently with countercurrent flow of feed and solvent phases. Fresh extractant first contacts low-solute-concentration raffinate and then contacts more concentrated raffinate as its own solute concentration increases. If a sufficient number of contacts are made and a sufficiently large volume of solvent is used, the concentration of the extracted component in the final raffinate may be reduced to almost any desired low value. Mixer-settler equipment can frequently be operated at high stage efficiencies (80% of theoretical or better), thus indicating with a fairly high degree of certainty the number of stages to provide for the desired separation.

Columns are used to accomplish solvent extraction by a countercurrent differential contact method wherein a very large number of infinitesimally small contacts are achieved by subdividing (dispersing) one phase and passing it countercurrently through the other (continuous) phase. Either of the phases may be continuous or dispersed. For example, if the lighter phase is to be continuous, the dispersed heavy phase is introduced at the top and allowed to fall by gravity through the continuous phase, and conversely. The simplest type of column is the spray column, which is simply a vertical pipe with an appropriate nozzle for introducing the dispersed phase. The packed column contains a packing material, such as Raschig rings or Berl saddles, to break up the dispersed phase and force it to follow a tortuous path. Although packing improves the extraction efficiency of the column, still more effective contacting can be obtained by adding mechanical energy to

DECLASSIFIED

DECLASSIFIED

4441

IS

the contents. Prominent examples of this type of column are the rotating-disk contactor, the Scheibel column, and the pulse column. The latter has been the most widely used column in radioactive service<sup>(9)</sup> and will be used in the B-Plant.

Pulse columns impose a reciprocating pulsing movement to the column contents by means of a piston or bellows connected hydraulically to the bottom of the column. The contacting section of the column usually contains closely-spaced horizontal, perforated plates. The up-and-down motion of the liquid phases through the perforations provides agitation resulting in more or less intimate mixing of the two countercurrently flowing phases. The resulting dispersion permits an important, often more than two-fold, reduction in column height from the heights needed with conventional packed columns. Additional advantages of pulse columns are a less pronounced dependence of extraction effectiveness (HTU values) on throughput rate and the greater ease of a temporary shutdown and start-up with the property of very little flow through the plates in the absence of pulsing. The need of a pulse generator, with its first cost and maintenance requirements, is a disadvantage. The performance characteristics of pulse columns as a function of design and operating conditions are discussed in Section D. 4.

## 2. Special Terms

The terms defined in this subsection are those used frequently in discussing the operation or evaluating the performance of solvent extraction columns. Convenient colloquial terms which have come into use at Hanford are included in the following discussion:

Extraction is used at Hanford to describe mass transfer from the aqueous to the organic phase as, for example, extracting strontium in the 1A Column.

Stripping is used to describe mass transfer of product ions from the organic to the aqueous phase; thus, strontium is stripped from the organic feed to the aqueous effluent stream in the 1B Column.

The removal of weakly-held impurities in the organic product stream by contacting it with an aqueous stream is referred to as scrubbing. For example, sodium is scrubbed from the 1A Column product stream by contacting it with a buffered scrub stream in the 1S Column. Analogously, an organic scrub can be used to re-extract solvent-favoring impurities from an aqueous product stream, as in the persulfate-oxidized 1C Column.

A simple column is one designed to perform only one solvent extraction function (extraction, scrubbing, stripping). A dual-purpose column combines two separate functions, such as extraction and scrubbing. The 1C Column can be operated as a dual-purpose column with the upper half used to strip rare earths from the solvent feed and the lower half used to re-extract tetravalent cerium.

DECLASSIFIED

DECLASSIFIED

4742

00

Flooding in a pulse column occurs when flow rates are so high that the two phases cannot pass countercurrently through the column, with the result that one of the phases leaves the column at the same end at which it enters. Local flooding in the column consists in an unusually large accumulation of dispersed phase at some location in the two-phase zone. It may occur as an accumulation of closely packed dispersed-phase droplets or, more frequently, as a series of large, coalesced globules channeling through a tightly packed dispersion. When this occurs on a cyclic basis, as it often does, it is termed cyclic local flooding. As long as local flooding does not propagate into complete flooding, the column may be operated indefinitely and give satisfactory extraction performance.

In some of the columns, a portion of one or more of the solutes may be extracted in one part of the column and stripped in the other. This phenomenon is referred to as internal reflux. For example, if the 1A and 1S Columns are considered as one column, strontium is quantitatively extracted in the 1A portion, partially stripped back into the aqueous phase in the 1S portion, and returned to the 1A Column where it is again extracted.

The pulse amplitude is the magnitude of the up-and-down motion of the pulse-column liquid contents, as measured between the extreme positions. The pulse frequency is the time rate of pulsing, expressed in cycles per minute. The amplitude-frequency product is frequently used as a simple means of correlating the pulsing conditions with column performance. It is equal to the pulse amplitude times the frequency and is conveniently expressed in inches per minute.

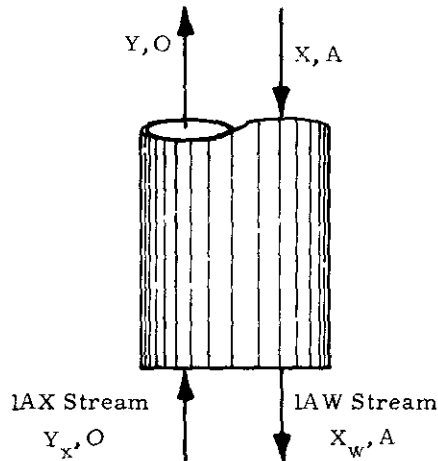
The superficial volume velocity is defined as the sum of the net volumetric flow rates of the two phases in the column divided by the total cross-sectional area of the column, neglecting the cross-section of the column occupied by packing or plates. The volume velocity for comparable performance in columns with like plates or packing but with different diameters is essentially constant. The pulsed volume velocity is simply the amplitude-frequency product expressed in volume-velocity units and, in gal/hr-ft<sup>2</sup>, is equal to  $74.81(\text{amplitude})(\text{frequency})$ , where the amplitude is given in inches and the frequency in cycles per minute. The pulsed volume velocity represents the pumping capacity of the pulse and is the upper capacity limit for sieve plate columns.

The decontamination factor (DF) for a feed contaminant is defined as the weight ratio of contaminant to the desired component in the feed divided by the same ratio found in the product. For convenience, it is frequently calculated as the reciprocal of the fraction of feed component found in the product, ignoring the efficiency of product recovery.

An equilibrium line is a graphical representation of the equilibrium solute distribution between the phases for the chemical conditions existing in the countercurrent solvent-extraction contactors.

DECLASSIFIED

An operating line is a locus of points depicting the actual solute concentrations of the aqueous and organic phases at various heights within the column. The operating-line equation is developed from a solute material balance made around either end of a column section. The schematic diagram below represents the bottom of the 1A Column.



Values of X and Y indicate the solute concentrations in the aqueous and organic phases, respectively; values of A and O indicate the volume flow rates of the aqueous and organic phases, respectively. At steady-state operating conditions, the weight of diffusing solute entering the above section of column over a given time period via the aqueous and organic streams must equal the weight of solute leaving via the effluent streams. The weight of solute carried by each of the four flowing streams in unit time is the product of the flow rate times the solute concentration:  $Y_x O$ ,  $X_w A$ ,  $Y O$  and  $X A$ , respectively. Equating the influent flow of solute to the effluent flow gives

$$X A + Y_x O = Y O + X_w A, \quad (1)$$

which on rearrangement gives the operating line equation:

$$Y = (A/O)X + Y_x - (A/O)X_w. \quad (2)$$

(Recent investigations have shown that this equation is valid only in the absence of longitudinal or back mixing, and that the true operating line in column contactors may have considerable curvature<sup>(16)</sup>. The effect of back mixing is usually ignored in column performance calculations because of the difficulty of determining its magnitude.)

Together, the operating and equilibrium lines make up the operating diagram from which the number of stages required to make a desired separation or the efficiency of a column can be calculated. An operating diagram for the removal of sodium from the solvent in the 1S Column is illustrated in Fig. IV-59 in Section D.3.2. Calculation techniques are summarized below.

### 3. HTU and HETA Calculations

The mass transfer effectiveness of solvent-extraction columns may be evaluated in terms of the height of contactor which is required to perform the same extraction as a single theoretical stage. A theoretical stage is achieved in a column when two influent streams (not at equilibrium) entering a section of the column mix and produce effluent streams which are in equilibrium with one another. For solvent-extraction columns containing several theoretical stages, the HETS (height equivalent to a theoretical stage) may be obtained by dividing the height of the contacting section by the number of theoretical stages required to accomplish the same extraction being carried out by the column. The number of stages can be stepped off graphically on a McCabe-Thiele-type operating diagram, such as that shown in Fig. IV-59. When the operating and equilibrium lines are straight, or nearly so, it is more convenient to calculate the number of stages by Colburn's equation<sup>(6)</sup>:

$$N_s = \frac{\ln [M(1-P) + P]}{\ln (1/P)} \quad (3)$$

where  $P$  = the extraction factor, the ratio of the slopes of the operating and equilibrium lines ( $P = A/mO$  for extraction and  $mO/A$  for stripping).

$$M = \frac{X_1 - Y_2/m}{X_2 - Y_2/m} \quad \text{for extraction and} \quad \frac{Y_1 - X_2m}{Y_2 - X_2m} \quad \text{for stripping.}$$

$A/O$  = slope of the operating line, (volume of aqueous phase per unit time)/(volume of organic phase per unit time).

$m$  = slope of the equilibrium line, (concentration in the organic phase)/(concentration in the aqueous phase in equilibrium with the organic phase). For straight equilibrium lines,  $m$  is equivalent to the  $E_{EQ}$ .

$X$  = the solute concentration in the aqueous phase.

$Y$  = the solute concentration in the organic phase.

Subscripts 1 and 2 refer to concentrated-end and dilute-end concentrations, respectively.

The HTU (height of a transfer unit) is also a measure of mass-transfer effectiveness. It is less sensitive than the HETS to variations in the value of the extraction factor and has been widely used at Hanford for design and development of solvent extraction columns. For most purposes, the number of transfer units can be expressed by the following integrals:

$$N_t = \int_{X_2}^{X_1} \frac{dX}{X - X^*} \text{ for extraction and } \int_{Y_2}^{Y_1} \frac{dY}{Y - Y^*} \text{ for stripping, } \quad (4)$$

where  $N_t$  = the number of transfer units, over-all raffinate-film basis, for transfer from the raffinate to the extract phase.

$X$  = the concentration of the diffusing component in the aqueous phase.

$X^*$  = the concentration of the diffusing component in the aqueous phase in equilibrium with an organic phase of composition  $Y$ .

$Y$  = the concentration of the diffusing component in the organic phase.

$Y^*$  = the concentration of the diffusing component in the organic phase in equilibrium with an aqueous phase of composition  $X$ .

Thus, the number of transfer units is an integrated ratio of the change in diffusing component concentration to the concentration driving force which causes transfer between phases. When the equilibrium and operating lines are straight, as they frequently are at the dilute end of the column, the number of transfer units may be calculated from Colburn's equation<sup>(6)</sup>:

$$N_t = \frac{\ln [M(1-P) + P]}{1 - P} \quad (5)$$

where  $M$  and  $P$  were previously defined. The over-all HTU is then calculated by dividing the height of the contacting section by the number of transfer units.

Colburn's equation has been used extensively for calculating HTU's for strontium and rare earth extraction processes. Conservative HTU values were obtained by selecting those equilibrium data which yielded a minimum value of the extraction factor. Internal reflux (between the 1A and 1S Columns) was generally ignored in HTU calculations; it normally amounted to less than 10% of the material in the feed, and its effect was within the experimental error of the calculation method.

3.1 Example HTU Calculations

3.1.1 1A Column, Strontium Extraction

Assume that the following data were taken during the steady-state period of a typical 1A Column run using a 12-ft-tall perforated plate cartridge:

<u>Stream(a)</u>	<u>Flow Rate, L/Min.</u>	<u>Sr-90, Ci/l</u>	<u>% of Sr-90 in Feed</u>
LAF	1.0	5.0	100
LSW	0.2	2.0	8.0
LAX	1.0	0.005	0.1
LAP	1.0	5.4	108
LAW	1.2	0.020	0.48

(a) See Fig. IV-48 for identification of streams.

Assume further that the strontium  $E_a^0$  decreased from 20 at the waste end of the column to 10 at the feed point under the operating conditions of the column.

Using Colburn's equation, let  $m = 10$  (the minimum  $E_a^0$ ) and the feed point Sr-90 concentration = 4.5 Ci/l (by material balance adding together the LAF and LSW streams). Then

$$M = \frac{X_1 - Y_2/m}{X_2 - Y_2/m} = \frac{4.5 - 0.005/10}{0.020 - 0.005/10} = 231,$$

$$P = \frac{A}{mO} = \frac{1.2}{(10)(1.0)} = 0.12, \text{ and}$$

$$N_t = \frac{\ln [M(1-P) + P]}{1-P} = \frac{\ln 203}{0.88} = \frac{5.32}{0.88} = 6.05$$

$$\text{The strontium HTU} = \frac{12}{6.05} = 2.0 \text{ ft.}$$

The strontium reflux in the example above amounted to 8% of the feed strontium. If reflux were ignored in the calculation, the feed point concentration,  $X_1$ , would have been 4.17 and the resulting HTU would have been  $\frac{12}{5.95} = 2.0$  ft.

The use of an average or weighted  $E_a^0$  also has little effect on the calculation. For example, if the raffinate  $E_a^0$  of 20 were used as  $m$ , the HTU would have been  $\frac{12}{5.70} = 2.1$  ft.

DECLASSIFIED

1117

150-100

### 3.1.2 1B Column, Strontium Stripping

Again, assume that the following typical data were obtained from a 1B Column run using a 12-ft-tall cartridge:

<u>Stream</u>	<u>Flow Rate, L/Min.</u>	<u>Sr-90, Ci/l</u>	<u>% of Sr-90 in Feed</u>
LSP-LBF	1.0	5.0	100
LFX	0.2	0.0	0
LBP	0.2	24.8	99.2
LW	1.0	0.04	0.8

$$\text{Feed point Sr-90 } E_a^0 = 0.04$$

$$\text{Waste (raffinate) Sr-90 } E_a^0 = 0.013$$

The feed point  $E_a^0$  in this example reflects the increased pH at the feed end of the column due to sodium and strontium stripping (see Section C 3.4). The lower  $E_a^0$  more nearly reflects the distribution ratio in the major portion of the column and will be used in Colburn's equation:

$$M = \frac{Y_1 - X_{2m}}{Y_2 - X_{2m}} = \frac{5.0 - 0.0}{0.04 - 0.0} = 125$$

$$P = \frac{m^0}{A} = \frac{(0.013)(1.0)}{0.2} = 0.065$$

$$N_t = \frac{\ln [M(1-p) + P]}{1-P} = \frac{\ln(117)}{0.935} = \frac{4.76}{0.935} = 5.09$$

$$\text{Strontium HTU} = \frac{12}{5.09} = 2.4 \text{ ft.}$$

Had the feed point  $E_a^0$  of 0.04 been used, the strontium HTU would have been  $\frac{12}{5.76} = 2.1 \text{ ft.}$ , a relatively minor difference.

### 3.2 Example Calculation of a 1S Column Sodium Operating Diagram

The conceptual PAW flowsheet (Fig. IV-48) will be used to illustrate the calculation of a sodium operating diagram for the 1S Column. This calculation also illustrates the steps involved in designing the chemical flowsheet for this column.

DECLASSIFIED

DECLASSIFIED

ISO-100

4148

First, estimate the concentration of free D2EHPA in the LAP. Assume that all of the strontium, calcium, and rare earths extract, along with about 0.7% of the iron and aluminum. By material balance the concentrations of these elements in the LAP and the amount of solvent complexed are:

	<u>M in LAP</u>	<u>Moles D2EHPA Complexed Per Mole of Cation<sup>(a)</sup></u>	<u>M D2EHPA Complexed</u>
Sr	0.0006	4	0.0024
Ca	0.006	4	0.0024
RE	0.0036	6	0.0216
Fe + Al	0.0013	2.5	0.0033
		Total	0.0297

(a) See Section C 2.5.1

Thus the "free" D2EHPA will be  $0.3 - 0.03 = 0.27M$ .

The aqueous phase sodium concentration and pH remain relatively constant throughout the LA Column and can be assumed equal to the LAW values. Hence the sodium concentration in the LAP can be calculated from Fig. IV-36 as that in equilibrium with  $1.15M Na^+$ , pH 4.0:

$$\frac{M Na, org}{M free D2EHPA} = 0.278,$$

or

$$Na = (0.278)(0.27) = 0.075M \text{ in the LAP.}$$

The required hydroxyacetate concentration was set by inspection at  $0.6M$  for the trial calculation. This was assumed to be sufficient to assure that the operating line would fall above the equilibrium line over its entire length. The equilibrium data for this calculation were interpolated from Fig. IV-35, using  $0.27M$  "free" D2EHPA, and plotted in Fig. IV-59 on logarithmic coordinates.

A sodium concentration in the LSS of  $0.038M$  was defined by the minimum pH allowed by strontium reflux considerations (pH 2.4) and the hydroxyacetate concentration. The sodium concentration in the LSP was set at  $0.001M$  by LB Column requirements. The operating line can then be calculated by the equation:

$$Y = \frac{A}{0} (X - X_B) + Y_p = 0.2 (X - 0.038) + 0.001.$$

DECLASSIFIED

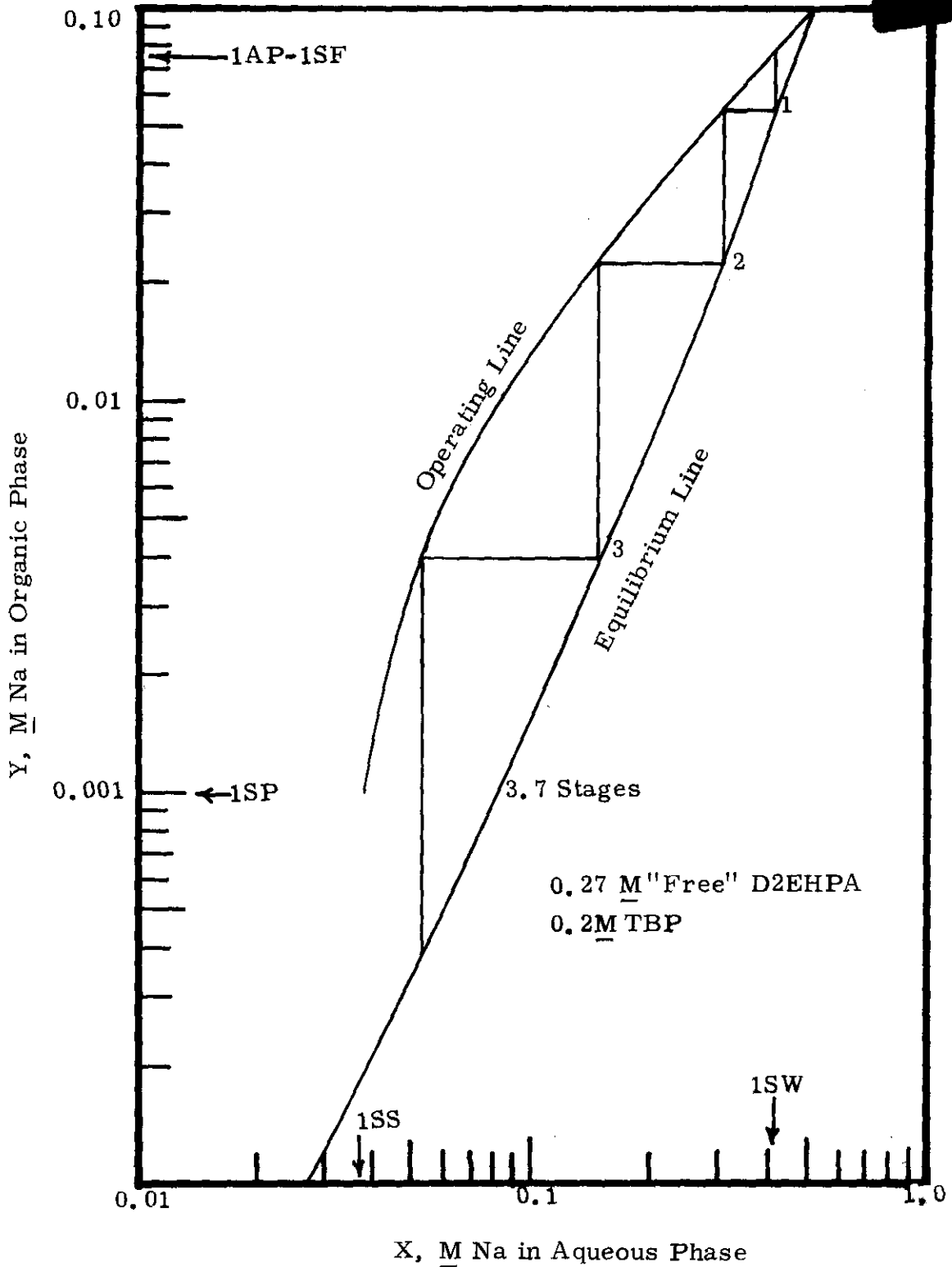


FIGURE IV-59

Sodium Operating Diagram - 1S Column  
PAW Flowsheet Conditions  
(From Figure IV-48)

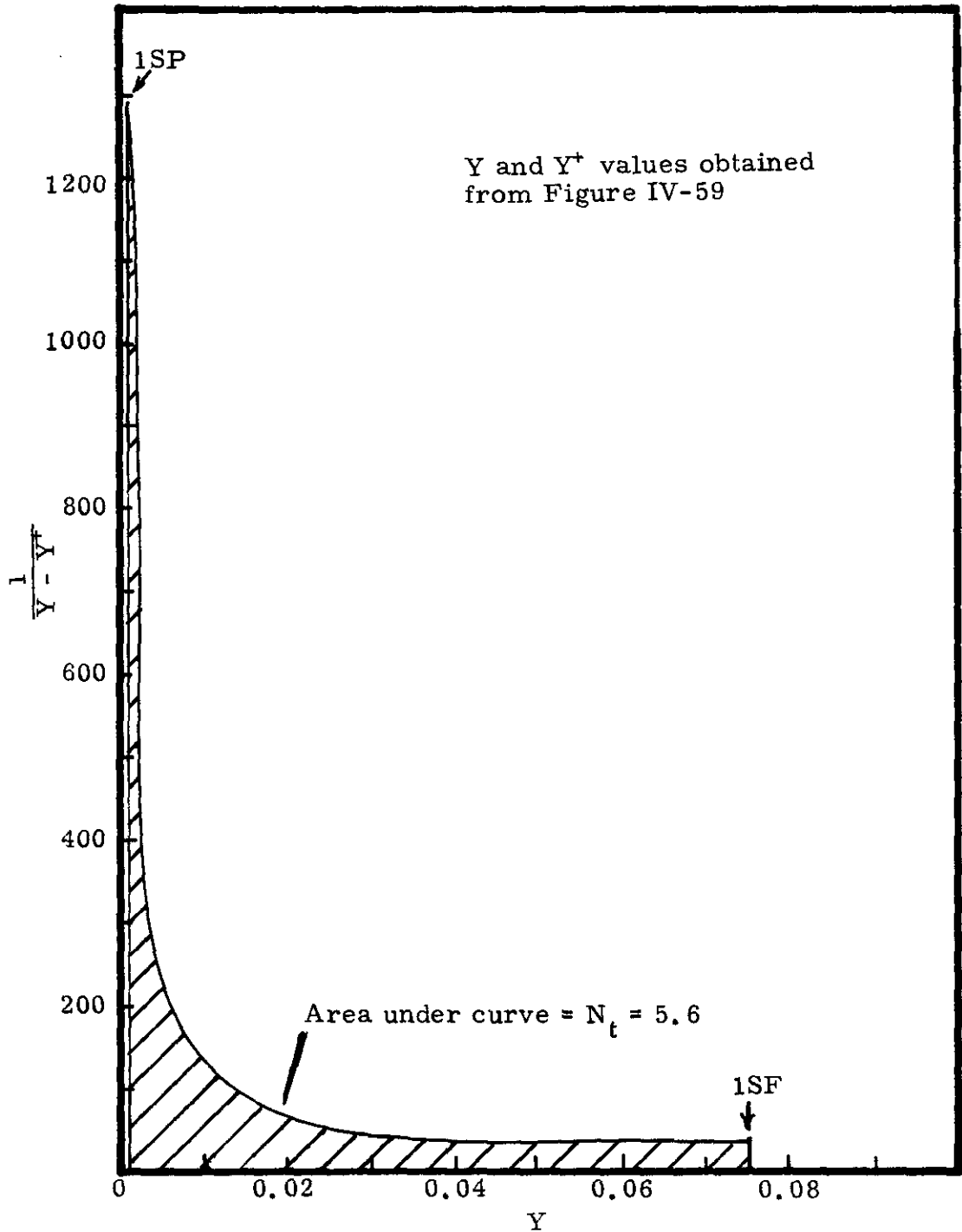


FIGURE IV-60

Calculation of the Number of Transfer Units ( $N_t$ )  
by Graphical Integration

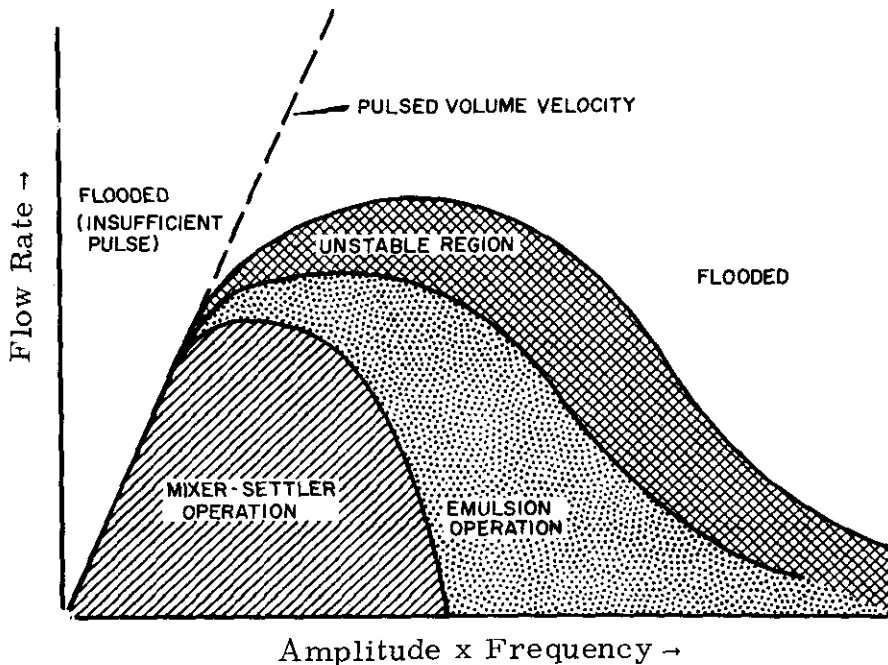
Starting at the "feed" end of the operating diagram, stages are stepped off. As shown in Fig. IV-59, 3.7 stages are required to obtain the desired separation. This is within the range of stages available in conventional extraction equipment, including the B-Plant columns, and the assumed scrub composition is satisfactory.

Extraction efficiency is more often correlated by HTU's. The number of transfer units required in the above example was 5.6, calculated by graphical integration of the area under the curve shown in Fig. IV-60. Here, values of  $Y$  and the corresponding equilibrium  $Y^*$  were taken from Fig. IV-59 and plotted as  $1/(Y-Y^*)$  versus  $Y$  in accordance with Equation (4).

4. Pulse Column Variables

4.1 General Performance Characteristics

Five distinct types of behavior have been observed in conventional perforated plate pulse columns as a function of the throughput rate and the pulsing conditions. These are shown in the sketch below, a typical plot of the total volumetric flow rate versus the product of the pulse amplitude and frequency.



The first zone is flooding due to insufficient pulsing (without down-comers, there is essentially no countercurrent flow in sieve plate columns without the pumping action of the pulser). A mixer-settler type of operation occurs as the frequency is increased beyond this pulsed volume velocity threshold. This is characterized by coarse drops of the dispersed phase and pronounced settling of the two phases into discrete layers in the quiescent portions of the pulse cycle. Although very stable, this type of operation is relatively inefficient. Emulsion-type operation occurs at still higher energy input. This highly efficient type of operation is characterized by small drop size and fairly uniform dispersion throughout the pulse cycle. As the throughput rate or frequency is increased still further, complete flooding eventually results. This is defined as the exit of one of the entering streams through the effluent line intended for the other phase.

Frequently, but not always, an unstable region of operation occurs as the flow rate or frequency is increased to values just less than flooding. This is usually characterized by periodic coalescence of the dispersed phase in a zone of high dispersed-phase holdup and subsequent channeling of these large drops through the column. This type of instability is typical of coalescing systems. In such systems, the ease of dispersion and coalescence appears to be related to the rate of mass transfer favoring coalescence and a low rate favoring dispersion. Generally the extraction efficiency is impaired in the unstable region and often fluctuates widely.

The factors affecting pulse column performance can be divided into two broad groups: those which are fixed by design of the column or of the associated pulse generator and those which may be varied in the course of operating a column of fixed design. Only the general direction and order of magnitude of the effects will be presented.

#### 4.2 Design Variables

The major design variables influencing pulsing column efficiency and capacity are:

- (a) pulse amplitude and wave shape,
- (b) wetting characteristics and choice of continuous phase,
- (c) sieve plate geometry,
- (d) plate section height, and
- (e) column diameter.

DECLASSIFIED

4153

IS

#### 4.2.1 Pulse Amplitude and Wave Shape

The pulse amplitude affects column performance primarily as a contributory component to energy input, that is, as a function of the arithmetic product of amplitude and frequency. This product represents a useful, simple means of correlating the pulsing conditions with column performance. In many systems, the flooding capacity in the high pulse energy region can be correlated by an equation of the form

$$\log (\text{volume velocity}) = C_1 - C_2 (\text{amplitude} \times \text{frequency}), \quad (6)$$

where  $C_1$  and  $C_2$  are constants for a given system.

With appropriate adjustment of the frequency, the pulse amplitude may usually be varied within a 1.5 to 2-fold range without capacity and HTU effects significantly in excess of normal experimental error. This fact enables selection of a minimum number of pulse generator sizes for a plant using columns of different diameters. Generally the pulse amplitudes are about 50% of the plate spacing, a factor believed important for optimum performance and minimization of excessive backmixing (or recycle) of the dispersed phase by the pulse.

A near-sinusoidal pulse wave shape is used in Hanford columns. Limited experience has shown that pulse wave shapes substantially deviating from sinusoidal often give optimum HTU's comparable with a sine wave.

#### 4.2.2 Wetting Characteristics and Choice of Continuous Phase

It is generally considered advantageous from the standpoint of extraction effectiveness to establish the continuous phase with the liquid having the smaller flow rate and to disperse the phase with the larger flow. In nuclear separations processing, however, this advantage is outweighed by the benefits to be gained by maintaining the interface at the "waste" end of the column. Interface-seeking impurities are continually carried to the interface by the films surrounding the dispersed phase droplets and, after building up to a stable depth at the interface, tend to leave the column by the nearby effluent line. These inter-facial films and solids, consisting of substances such as silica or solvent degradation products, usually become extremely contaminated with adsorbed fission products, and their entrainment in the product stream may severely limit fission product decontamination.

For satisfactory operation it is essential that the dispersed phase not wet the sieve plates. When the sieve plates are wet by the dispersed phase, the droplets coalesce on the plates as a film which tends to

DECLASSIFIED

DECLASSIFIED

4154

ISO

leave reluctantly in streamers or as "balloons" enclosing droplets of the continuous phase. This type of performance usually is less efficient and provides lower capacity than the normal emulsion-type operation.

Stainless steel nozzle plates, a recent Hanford development for pulse columns, are a special class of sieve plates. They are characterized by the indentation of the holes to form many tiny jetting nozzles usually oriented toward the dispersed-phase exit of the column, although satisfactory operation can be obtained with the nozzles pointing the other way. Stainless steel nozzle plates can be used with either phase continuous. Their action differs from that of the sieve plates in that the dispersed phase, when it wets the plate, cannot cling to the nozzle tip and is readily redispersed with the pulse. The nozzle depth must be at least 0.035 inch from the base of the nozzle to the tip for optimum performance. Well designed nozzle plates have given capacities about 50% higher and HTU's up to 30% lower than equivalent-geometry flat sieve plates.

The excellent performance obtained with nozzle plates may be related to improved separation of dispersed and continuous phase (the jet produced by the pulse propels droplets up to three or four times the length of the pulse, a distance adequate to reduce the number of drops pulled back with the reverse cycle of the pulse) and to the smoother flow characteristics of nozzles as contrasted to sharp-edged orifices.

#### 4.2.3 Sieve Plate Geometry

Both the capacity and HTU attainable in a pulse column increase with increasing hole size, plate spacing, and percentage of free area of the sieve plates. A cartridge consisting of two-inch-spaced stainless steel plate with 1/8-inch-diameter holes and 23 percent free area has generally proved to be a desirable compromise between high capacity and efficiency and has been designated as the "standard cartridge". In the neighborhood of standard cartridge geometry, up to two-fold variations in capacity and HTU are encountered as hole size, plate spacing, or free area are varied three- to four-fold. Diametric clearances up to 1/8 inch between the plates and the wall of a three-inch diameter column have been noted to have little or no effect on HTU values. Three-eighths inch diametric clearances are used in large columns to permit remote installation of the plate cartridges.

#### 4.2.4 Height of Plate Cartridge

HTU values generally increase with increasing column height. This is believed due to a general trend toward higher HTU values with decreasing diffusing-component concentration. Usually the heights of the plant

DECLASSIFIED

DECLASSIFIED

4155

IS

cartridges are chosen to equal the product of the number of transfer units required times the maximum HTU obtained in pilot plant studies under near optimum conditions - plus a 25 to 100 percent safety margin (the value added depending on whether the pilot plant cartridge height was near or appreciably less than the calculated height). Column height usually has a negligible effect on the flooding capacity; however cases have been noted where the stable capacity was decreased 15 to 30 percent with 50 to 100 percent increases. Possibly some minimum height is required to establish the ultimate dispersion profile.

#### 4.2.5 Column Diameter

As the column diameter increases, the counter flowing liquid phases display an increasing tendency to channel in portions of the cross section rather than to distribute evenly across. Such channeling markedly decreases efficiency. Columns in which channeling is most likely to occur are those in which the continuous phase density is appreciably greater at the top than at the bottom. Louver plate redistributors are often added to counteract potential channeling.

#### 4.3 Operating Variables

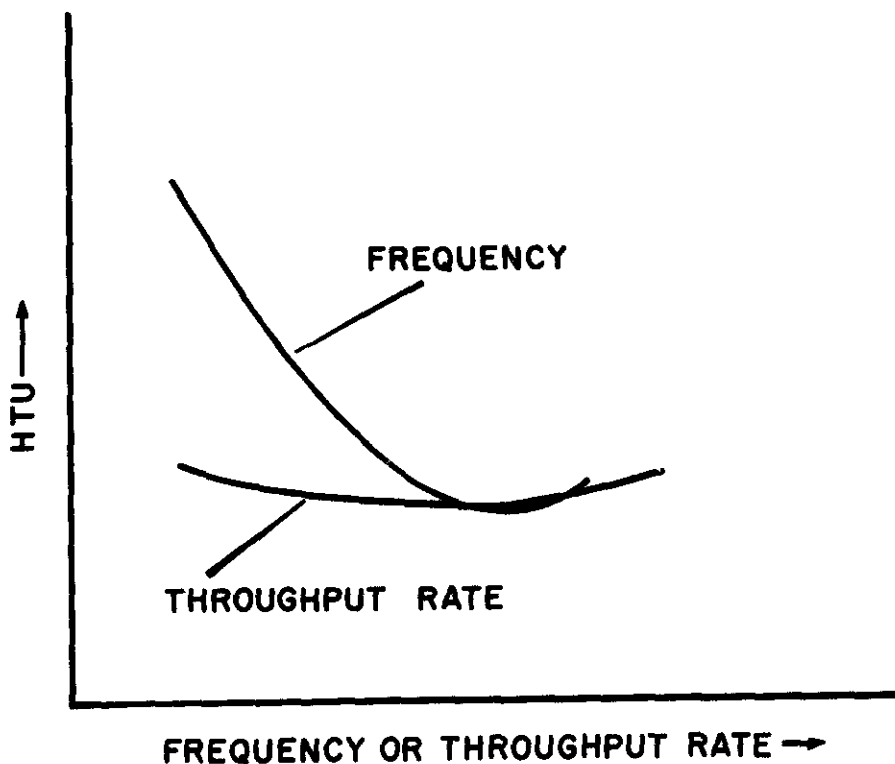
The important operating variables are:

- (a) pulse frequency,
- (b) volume velocity,
- (c) flow ratio,
- (d) solute concentration,
- (e) physical properties of liquids, and
- (f) temperature.

##### 4.3.1 Pulse Frequency

The effect of pulse frequency and the correlation of amplitude-frequency product have already been discussed. As shown in the sketch on the opposite page, HTU values generally decrease sharply with increasing frequency within the region of stable operation. On the threshold of instability there may be a slight reversal of the trend. Experience indicates that minimum HTU values generally lie in a zone between 75 and 95 percent of the flooding frequency.

DECLASSIFIED



#### 4.3.2 Volume Velocity

Pulse column HTU values are relatively insensitive to variations in throughput rate. At constant pulsing conditions, plots of HTU values against volume velocity are usually convex downward and shallow, as shown above. Nearly constant HTU's over a wide range of throughput rates may be obtained by appropriately adjusting the frequency.

#### 4.3.3 Flow Ratio

Although not of practical importance, both HTU values and capacity generally increase slightly with increasing continuous-to-dispersed phase flow ratio. Because of channeling or backmixing tendencies, the extract-to-raffinate flow ratio is usually maintained at least 15 to 20 percent above the minimum value theoretically required to provide the desired extraction service.

#### 4.3.4 Solute Concentration

HTU values are generally higher at the dilute end of a column than at the concentrated end. This results from the trend for HTU values to increase with decreasing solute concentration.

DECLASSIFIED

4157

#### 4.3.5 Physical Properties of Liquids

The flooding capacity of a pulse column using non-coalescing systems has been shown to be approximately proportional to the 0.7 power of the density difference between the phases, the 0.4 power of the interfacial tension, and the 0.3 power of the continuous phase viscosity. Recent studies using three- and four-inch diameter columns have shown that the flooding capacity can be increased in many instances by adding about 50 ppm Mistron\* (a finely-divided talc) or bentonite to the dispersed phase. Addition of either material greatly increases the coalescing tendency of the dispersed phase, typically reducing the disengaging time of an equal-volume emulsion of 30% TBP and water from 60 to 15 seconds. Other additives or impurities, such as colloidal silica or ferric hydroxide, have been observed to decrease the capacity by increasing the emulsification tendency. The inter-action of such trace impurities greatly increases the difficulty of predicting flooding capacities from fundamental relationships.

Since individual film HTU values are believed to vary with the dimensionless Schmidt number (viscosity divided by density and diffusivity of diffusing component) raised to about 0.6 the power, low viscosity and high diffusivity should favor low HTU values.

#### 4.3.6 Temperature

An increase in temperature increases the flooding capacity and decreases the HTU, presumably because the higher temperature reduces the viscosities and increases the diffusivities involved. An increase in temperature also decreases strontium distribution coefficients. Pulse columns are usually operated at temperatures up to 50 C; much higher temperatures run the risk of accelerated solvent degradation and the possibility of approaching or exceeding the solvent flash point.

### 5. B-Plant Pulse Column Specifications

Specifications for the B-Plant pulse columns are presented in Table IV-24 on page 4158.(14)

The 1A and 1C Columns were designed to operate at nominal volume velocities of 300 to 400 gal/hr-ft<sup>2</sup>. The over-all design recoveries were 95% for strontium and 90% for cerium and the promethium-rare earth - americium fractions.

\*Trademark, Sierra Talc Co., South Pasadena, California

DECLASSIFIED

DECLASSIFIED

4158

00

TABLE IV-24  
B-PLANT PULSE COLUMN SPECIFICATIONS

Column	Overall Height, ft.	ID in.	Cartridge Specifications <sup>(a)</sup>				Pulse		Interface Position
			Height feet	Plate Spacing, inches	Hole Diam. inches	% Free Area	Ampl. inches	Freq. Range Cycles/min.	
1A	18.5	20	14	2	3/16	23	1.3	35-90	Bottom
1S	14.5	20	11	2	1/8	10	1.3	35-90	Bottom
1B	18.5	20	14	2	1/8	10	1.3	35-90	Bottom
1C	18.5	15	10(strip) 4(scrub)	4 2	1/8	10	(b)	(b)	Top

- a. Cartridges are made of stainless steel nozzle plates with the nozzle indented about 0.04 in. beyond the adjacent plate face. The 1A, 1S, and 1B columns each contain a louver plate re-distributor in the middle of the cartridge with 6 inches of free space on each side.
- b. Not determined at time of writing.

The specifications were derived from pulse column studies made in 3-inch-diameter glass pulse columns containing 6 to 12-ft tall nozzle-plate cartridges. Highlights of these studies and corroborative data obtained from full-level runs in the Strontium Semiworks with similar cartridges are discussed in the following sections.

#### 6. Cold Semiworks Pulse Column Studies

"Cold" pulse column development runs were made in 3-in.-diameter columns containing 6 to 12-ft tall cartridges of 2 to 4-in. spaced stainless steel nozzle plates. Cartridges used in work applicable to B-Plant are described in Table IV-25.

TABLE IV-25  
NOZZLE PLATE CARTRIDGE USED IN CSW RUNS

(Source of Data: HW-72866, Section 4; HW-79762PT2; BNWL-173)

	Column			
	1A	1S	1B	1C <sup>(a)</sup>
Height, feet	6 to 13	6 to 10	9 to 10	9 to 10 <sup>(a)</sup>
Plate spacing, inches	2 to 4	2 to 4	2 to 4	2 to 4
Hole diameter, inches	3/16	1/8	1/8	1/8
Percent free area	23	10	10	10

(a) A dual-purpose 1C column with a 4 foot tall scrub section added to the bottom was also investigated.

Feed streams simulated the compositions of PAW, ZAW, and several potential Strontium Semiworks crude strontium feeds. Typical feed compositions are presented in Table IV-26. In many runs, feeds were traced with Sr-85, Ce-144, and/or Eu-152-154 to improve analytical precision.

The solvents normally contained 0.2 to 0.4M D2EHPA, 0.12 to 0.2M TBP in various hydrocarbon diluents. Flowsheet conditions were similar to those presented in Figures IV-48, IV-49 and IV-62.

DECLASSIFIED

TABLE IV-26  
TYPICAL "COLD" SEMIWORKS 1AF COMPOSITIONS  
(Nitrate System)

Constituents	M Adjusted 1AF				
	PAW <sup>(10, 11)</sup>	ZAW <sup>(13)</sup>	Sr Crude #1 <sup>(5a)</sup>	Sr Crude #2 <sup>(5a)</sup>	Sr Crude #3 <sup>(12)</sup>
Na	1.8	2.0	1.0	1.6	1.5
Fe	0.075	0.165	0.06	0.02-0.10	0.0088
Al	0.038	0.323	0	0	0
Cr	0.015	0.0068	0	0	0
Ni	0.0075	0.0034	0	0	0
Pb	0	0	0.001	0.003-0.04	0.0336
Zr	0	0	0-0.005	0-0.002	0
Ca	0.00068	0.00062	0.09	0.002-0.026	0
Sr	0.00068	0.00055	0.02	0.002	0.0012
Rare Earths	0.0041	0.0027	0.003	0.002	0.0064
SO <sub>4</sub> <sup>=</sup>	0.11	0.051	0	0-0.012	0.080
F <sup>-</sup>	0	0.13	0	0	0
Buffer <sup>(a)</sup>	0-0.3	0	0.8	0.5	0.26
Complexant <sup>(b)</sup>	0.185-0.27	0.56-0.6	0-0.16	0.15	0.11
"Free" Complexant <sup>(c)</sup>	0.05-0.1	0.06-0.1	0-0.09	0.05-0.1	0.07
pH	3.6-5.5	4.0-4.7	1.9-5.4	3.8-4.9	1.8-3.8

(a) Acetate or hydroxyacetate

(b) Complexants included EDTA, HEDTA, tartaric acid, citric acid and mixtures of HEDTA or citric acid with tartaric acid.

(c) Defined as the total complexant molarity minus the molarities of iron, aluminum, chromium, nickel, lead, and zirconium.

## 6.1 1A Column Performance

### 6.1.1 Capacity Studies - PAW Feeds<sup>(10)</sup>

The maximum demonstrated capacity of the 1A Column was 1070 gph/ft<sup>2</sup>, using a 9-ft-tall cartridge with 2-in. plate spacing. A rather wide range of flooding frequencies was observed at any given flow rate. This variation was attributed to feed impurities, possibly colloidal ferric hydroxide. The choice of interface position had little effect on the flooding capacity, but increasing the temperature from 25 to ca. 50 C usually increased the flooding threshold frequency by 10 to 20 cycles/minute.

A summary of the capacity studies is presented in Table IV-27. The maximum demonstrated frequency shown in this table is presented as an indication of the frequencies obtainable at operating conditions where no flooding determinations were made.

Several solid impurities in the PAW are known to be emulsion stabilizers. These include such compounds as silica and zirconium phosphate (from TBP decomposition). The effects of these two additives on capacity were relatively minor, lowering the flooding frequency about 10 to 15 cycles per minute. The adverse effect could be countered by adding about 60 ppm Mistron to the feed.

TABLE IV-27

1A COLUMN CAPACITY SUMMARY

(Source of Data: HW-79762PT2)

Pulse amp. = 1 in.; cartridge ht. = 9 ft.

Volume Velocity, gph/ft <sup>2</sup>	Temperature, Centigrade	Frequency, Cycles/min.	
		Max. Demonstrated	Flooding
<u>Bottom Interface</u>			
180	25	--	120
360	25	--	68 to 70
360	45	70	--
550	25	--	66 to 83
550	50	--	85
710	25	--	39 to 70
710	50	--	48 to >84
1070	25	--	42
1070	50	44	--
<u>Top Interface</u>			
270	25	--	69
360	25	60	--
550	25	--	53 to 58
710	25	--	53 to 69
710	50	70	--

The stability of the 1A Column when processing citrate-complexed PAW was greatly improved when the pH adjustment was made at 50 C and the adjusted feed was digested for about an hour at 70 to 90 C. This procedure evidently prevented the formation of emulsion-stabilizing hydroxides by increasing the rate of complexing.

#### 6.1.2 Extraction Efficiency - PAW Feeds<sup>(10)</sup>

Optimum strontium HTU's were about 1.5 ft for citrate and tartrate complexed feeds and were fairly insensitive to operating conditions. Cerium HTU's were much more dependent on feed compositions and operating conditions and ranged from 3.2 to greater than 9 ft. The effects of some of the major variables on the HTU's are discussed below.

#### Effect of Solvent Composition

Variations in the D2EHPA composition from 0.16 to 0.48M appeared to have no effect on extraction performance other than that caused by the effect on the strontium distribution ratio. Addition of 0.04 to 0.1M NaOH to the solvent minimized pH changes at the bottom of the column (caused by sodium extraction) and may have contributed to a slight

DECLASSIFIED

4161

ISC 100

improvement in performance. The addition of BAMBP to the solvent in Csrex process demonstration runs (see Section C 2.6.3) had little or no effect on cerium and strontium HTU's(11).

#### Effect of Feed Composition

Strontium HTU's were virtually unaffected by feed composition over the range tested. Cerium HTU's, however, were extremely sensitive to the nature of the feed. Cerium HTU's as low as 1.4 ft were measured at 25 C in an organic-continuous column using a simple, citrate-complexed  $\text{NaNO}_3$  feed. Under comparable operating conditions, the cerium HTU's ranged from 8 to 10 ft with citrate-complexed PAW and, in a limited number of runs, with tartrate-complexed PAW(10). In more extensive tests with Csrex process solvent, however, cerium HTU's of 5 to 10 ft with citrate and HEDTA-complexed PAW's were lowered to 3 to 6 ft with tartrate-complexed PAW(11).

The poor performance with PAW feed has been traced to the presence of chromium and the formation of cerium-chromium complexes which greatly reduce the rate of cerium extraction, as discussed in Section C 3.2.3.

Of the complexants studied, only citrate, tartrate, and HEDTA permit simultaneous recovery of strontium and the rare earths while suppressing the extraction of bulk inert and radioactive impurities. Laboratory tests described in Section 3.2.2 indicate that the effectiveness of complexing increases in the order tartrate-citrate-HEDTA. Thus, the use of tartrate to improve rare earth recovery will be dependent on whether the increased extraction of impurities can be tolerated.

#### Effect of pH

No effect of pH on extraction was observed with citrate and tartrate complexed feeds over the range studied (4.0-5.5)(10). Laboratory work described in Section C 3.2, however, indicates that high pH's decrease the rare earth extraction kinetics. It is also essential that the feed pH may be properly adjusted so that the pH of the combined feed and scrub streams is high enough to permit strontium extraction.

#### Effect of Temperature

Increasing the temperature greatly improved the rate of cerium extraction. Cerium losses in an organic-continuous column with citrate-complexed PAW decreased from 50% to 7% (3.5 ft HTU) when the temperature was increased from 25 to 50 C(10). Temperature had no significant effect on strontium losses provided that the flow ratio was adequate to counter the adverse effect of increased temperature on the strontium distribution ratio.

DECLASSIFIED

DECLASSIFIED

Effect of Interface Position

The preferred interface location in an extraction column is at the bottom to aid in flushing interface-seeking solids from the system; however, putting the interface at the top in the 1A Column increases the aqueous holdup time three-to four-fold and should thereby decrease the cerium loss. This effect was observed in several runs, as shown in Table IV-28<sup>(10)</sup>. A two-fold reduction in cerium HTU's was also observed in Csrex process runs with aqueous-continuous operation<sup>(11)</sup>.

TABLE IV-28  
EFFECT OF TEMPERATURE AND INTERFACE POSITION  
ON CERIUM EXTRACTION

(Source of Data: HW-79762PT2)

1AF = Citrate complexed PAW. Cartridge ht. = 9 ft.

<u>Temp. C</u>	<u>Interface Position</u>	<u>% Ce Loss</u>	<u>Ce HTU, ft.</u>
25	Top	18-35	5 - 9
	Bottom	32-50	8 - 10
45-50	Top	1.4-6.2	2 - 3.2
	Bottom	5-8	3 - 3.5

Effect of Flow Rate

Decreasing the total flow rate also tended to decrease the cerium losses. The effect was relatively minor and was not always observed. Strontium losses were unaffected by flow rates up to a volume velocity of 1060 gal/hr-ft<sup>2</sup>, the maximum rate tested<sup>(10)</sup>.

Effect of Pulse Frequency

Generally, frequencies had to be within 20% of the flooding frequency for optimum performance; the frequency goal was usually within 10% of flooding for most of the runs. Frequency sensitivity was not as pronounced in the 1A Column as it was in the stripping studies reported in following sections. Typical results of frequency variation studies are shown in Table IV-29<sup>(10)</sup>.

Cyclic flooding was rare in these runs; usually local flooding or phase inversion, if it occurred, would build up until a meta-stable condition was reached. This might progress to the extent of having an interface at both ends of the column. Local flooding or instability, such as that occurring in the last run above, did not appear to increase the losses.

DECLASSIFIED

DECLASSIFIED

4163

TABLE IV-29  
EFFECT OF FREQUENCY ON 1A COLUMN PERFORMANCE

(Source of Data: HW-79762PT2)

Citrate complexed PAW, Cartridge ht. = 9 ft.

Temp. °C	Frequency		% Loss		Estimated HTU, Ft.	
	Cycles/Min.	% of Flood	Sr	Ce	Sr	Ce
50	60	ca. 85	--	15	--	4.7
50	69	ca. 95	--	7.5	--	3.5
35	50	ca. 78(a)	0.62	12	1.7	4.1
35	64	ca. 100	0.09	7.5	1.2	3.5

(a) Local flooding observed during the run.

6.1.3 ZAW Flowsheet Demonstration<sup>(13)</sup>

Purex wastes derived from zirconium-clad fuels will contain considerable amounts of aluminum added to complex residual fluoride from the Zirflex decladding process. Laboratory studies<sup>(4)</sup> have shown that aluminum extraction by D2EHPA from complexed feeds is time dependent and can be appreciable after several minutes of contact. A special series of pilot plant runs was made to determine the path of aluminum in the D2EHPA process as a function of complexing agent, pH, and temperature. The feed, shown in Table IV-26, also contained about two-fold more iron than the earlier PAW feeds, and the effect of both iron and aluminum loading in the solvent on strontium and rare earth extraction was of interest. The flowsheet was similar to that shown in Fig. IV-49 except that two complexants were tested. The first was 0.55M HEDTA with 0.0125M tartrate added, as discussed in Section C 3.2.3, to improve rare earth extraction kinetics; the other was 0.6M tartaric acid.

The amount of iron and aluminum extracted from the HEDTA-complexed ZAW was 5 to 10-fold less than that extracted from the tartrate feed. The lower solvent loading with HEDTA feeds also contributed to about 10-fold lower strontium losses. Optimum cerium losses with both complexants ranged from 1 to 4% with the lower loss obtained at elevated temperatures. Cerium losses were highly dependent on the HEDTA feed pH, increasing to 40% as the pH was increased from 4.0 to 4.7. A summary of the extraction performance is presented in Table IV-30. The pilot plant runs were made in a 13-ft-tall column, simulating the B-Plant 1A Column geometry. It was operated at a volume velocity of 360 gal/hr-ft<sup>2</sup> with a 1-in. pulse amplitude and frequencies of 70 to 90 cycles/min. The organic phase was continuous.

DECLASSIFIED

DECLASSIFIED

4164

100

TABLE IV-30  
1A COLUMN PERFORMANCE WITH ZAW FEED

(Source of Data: Ref. 13)

A/O = 1.2, Bottom interface, Cartridge ht. = 13 ft.

Complexant	Feed pH	Temp. °C	% in 1AP <sup>(c)</sup>		% in 1AW <sup>(c)</sup>		Approx. HTU, ft.	
			Fe	Al	Sr	Ce	Sr	Ce
HEDTA <sup>(b)</sup>	4.0	40	0.4	0.7	0.3	≤3.9	1.9	≤4.0
HEDTA <sup>(a)</sup>	4.0	50	0.6	1.1	0.1	0.2	1.6	2.0
HEDTA <sup>(a)</sup>	4.7	25	--	--	<0.1	44	<1.6	>10
HEDTA <sup>(a)</sup>	4.7	50	--	--	<0.1	79	<1.6	>10
Tartrate <sup>(a)</sup>	4.0	25	2.5-7.5	~5.0	1.4	2.0	2.4	3.3
Tartrate <sup>(b)</sup>	4.0	25	2.0	2.3	1.0	3.7	2.0	4.0
Tartrate <sup>(a)</sup>	4.0	45	5.6	5.5	1.8	1.4	2.3	3.1
Tartrate <sup>(b)</sup>	4.5	25	--	--	1.7	7.9	2.2	5.2
Tartrate <sup>(b)</sup>	4.5	35	2.0	5.7	0.4	6.7	1.8	4.9
Tartrate <sup>(b)</sup>	4.5	40	5.2	4.6	2.6	3.1	2.4	3.8

(a) Feed used with no elevated temperature digestion.

(b) Feed digested at 90C for one hour.

(c) Percent of the indicated component entering in the 1AF.

A comparison of the data in this table with data obtained with PAW feeds shows that optimum strontium HTU's were 10 to 50% higher with ZAW feeds, probably because of less favorable strontium distribution ratios and taller column height. Cerium HTU's were essentially unchanged.

Unstable column operation, accompanied by a flocculent precipitate, was observed in one run with freshly prepared tartrate feed. The phenomena was not observed after the feed was aged for one day or after it was digested 1 hour at 90 C. Feed digestion may have increased the cerium losses about 2-fold or more.

6.1.4 Strontium Crude Purification Flowsheet Demonstration<sup>(5)</sup>

The original strontium extraction process was developed to recover and purify strontium-90 from crude fractions prepared in the Purex Plant by lead sulfate precipitation (see Section B 2). The process developed in these early studies has since been refined and used to recover over 10 megacuries of purified Sr-90 in the Strontium Semiworks (SSW).

DECLASSIFIED

DECLASSIFIED

4165

00

Compositions of feeds used in pilot plant runs are included in Table IV-26. The composition of Strontium Crude #2 most nearly resembled the typical SSW feed; Strontium Crude #1 represents an earlier processing concept with a more concentrated feed. The solvent in all of the purification runs contained 0.4M D2EHPA, 0.2M TBP in various saturated hydrocarbon diluents. After the initial scouting efforts, flowsheet development was concentrated on minimizing the extraction of impurities, including cerium and rare earths.

Capacities as high as 1000 and 1300 gal/hr-ft<sup>2</sup> were demonstrated in the pilot plant column with bottom and top interface positions, respectively (5a). Stable operating capacities as high as 1170 gal/hr-ft<sup>2</sup> have been obtained in the SSW 1A Column with its 10-ft cartridge of 4-in.-spaced nozzle plates (5b). A wide range of flooding frequencies was observed in these studies, as well as in the PAW studies described in Section D 6.1.1; and, within experimental precision, the results of the PAW capacity studies should apply also for the strontium purification flowsheets.

Strontium HTU's were estimated at 1 to 2 ft at volume velocities of 700 to 900 gal/hr-ft<sup>2</sup> in both the presence and absence of complexing agents and with strontium feed concentrations from 0.004 to 0.04M (5a). The effects of major flowsheet variables on strontium and impurity extraction are discussed below.

Effect of Complexant - Three complexants were extensively tested: HEDTA, EDTA, and DTPA. All three were quite effective in suppressing the extraction of iron, lead, and zirconium. In "cold" studies (5a), less than 1% of the iron, 3% of the lead, and 6% of the zirconium were extracted with excess HEDTA present. The amount of lead and zirconium extracted was apparently lowered several fold by using EDTA. In the absence of any complexant, essentially all of the zirconium and lead extracted at pH 4 to 5, along with about 70% of the iron.

The effectiveness of the complexants in preventing cerium extraction decreased in the order DTPA EDTA HEDTA. Strontium Semiworks runs at pH 4.3 to 4.7 (5b) demonstrated that 20 to 30% of the cerium extracted from EDTA-complexed feeds but only 4% or less extracted from DTPA feeds. In runs described in Section D 6.1.3, about 26 to 56% of the cerium extracted from an HEDTA-complexed feed at pH 4.7.

Complexant concentrations as high as 0.12M in excess of that required to complex the impurities had, at most, only a minor effect on strontium waste losses.

Effect of Buffer Composition - Acetic acid has been used exclusively to buffer the feed pH in strontium purification runs. Its pK value (the pH at which 50% of the acid is neutralized) is 4.76, the optimum pH for obtaining high cerium decontamination without excessively decreasing the strontium distribution ratio. Concentrations of 0.4 to

DECLASSIFIED

1.0 have proved satisfactory for maintaining the aqueous phase pH, with the higher value being desirable for feeds containing over 0.05M calcium plus strontium. Some improvement in pH control can be achieved by partially neutralizing the solvent with NaOH, but no attempt was made in either pilot plant or SSW runs to use solvent buffering with strontium crude feeds.

Effect of Strontium and Calcium Concentration - Calcium quantitatively extracted under all conditions favoring strontium extraction. Adequate strontium extraction was achieved with strontium plus calcium feed molarities ranging from 0.002 to 0.14 by using sufficient solvent to maintain at least 0.2M free D2EHPA in the solvent. Higher solvent loadings can be used with high feed concentrations because the increased solvent requirement lowers the A/O flow ratio and tends to counter the adverse effect on the extraction factor of lower strontium distribution ratios.

#### 6.1.5 Kinetics of Europium Extraction from HEDTA-Complexed Feed

Laboratory studies, summarized in Section C 3.2, have shown that HEDTA complexing decreases the rate of rare earth extraction as well as the magnitude of the distribution ratios. The rate of extraction decreased with increasing pH and increasing atomic number (i.e., Ce Pm Eu). A series of pilot plant runs, using Strontium Crude #3 (Table IV-26) was made to study in detail the effect of operating variables on rare earth extraction from an HEDTA-complexed SSW feed<sup>(12)</sup>. The feed was traced with Eu-152-154 to ensure the applicability of the results to promethium extraction. All runs were made at a volume velocity of 680 gal/hr-ft<sup>2</sup> and an A/O of 1 in a 10-ft-tall pulse column containing 10% (rather than 23%) free area nozzle plates.

Effect of Feed pH - The europium loss was highly dependent on the feed pH, increasing by a factor of 17 as the pH was increased from 1.8 to 3.8. A summary of the results of room temperature, bottom interface runs is shown in Table IV-31.

TABLE IV-31

#### EFFECT OF FEED pH ON EUROPIUM EXTRACTION

(Source of Data: BNWL-173)

Bottom interface; 25C; A/O = 1; Cartridge ht. = 10 ft.

<u>pH</u>	<u>Aqueous Residence Time, Min.</u>	<u>Europium in 1AW, percent</u>
1.8	2.7	≤2.1
2.4	2.6	3.7
3.8	2.5	36

Laboratory kinetic studies made with the same feeds gave comparable extraction results<sup>(3)</sup>. For example, within 2 min 99% of the europium was extracted at pH 2.3 while only 63% was extracted at pH 3.8. In the latter case, the europium extraction was increased to 96% with a 5 min contact.

The stability of the column was also affected by the pH, with lower pH's favoring increased stability; however a white precipitate, presumably lead sulfate, formed slowly in the column with the pH 1.8 feed.

Effect of Temperature and Interface Position - The increased aqueous-phase residence time obtained by moving the interface from the bottom of the column to the top lowered the europium loss by three-fold at pH 3.8 and 25 C. A still greater factor of improvement was obtained by heating the column to 50 C, as shown in Table IV-32. The europium loss of 0.39% at optimum operating conditions indicated an HTU of 1.8 ft, about as low as that reported for the D2EHPA extraction of strontium and cerium under less severe complexing conditions<sup>(10)</sup> and approaching the 1.2 to 1.4 ft cerium HTU's observed with uncomplexed feeds.

TABLE IV-32

EFFECT OF TEMPERATURE AND INTERFACE POSITION ON EUROPIUM EXTRACTION

(Source of Data: BNWL-173)

Feed pH = 3.8; A/O = 1; Cartridge ht. = 10 ft.

<u>Column Temperature, °C</u>	<u>Interface Position</u>	<u>Aqueous Residence Time, Min.</u>	<u>Europium in 1AW, %</u>	<u>Europium HTU, feet</u>
25	Bottom	2.5	36	10
25	Top	10	12	4.7
50	Bottom	2.5	13	4.9
45-50	Top	12	0.39-0.94	1.8-2.2

The 4.9 ft europium HTU obtained at 50 C with the organic phase continuous was about 2-fold higher than the cerium HTU obtained under similar conditions with HEDTA-complexed ZAW feed (Section D 6.1.3). The slower kinetics of europium extraction may account for the difference, but the ZAW feed also contained a small amount of tartrate which has been shown to improve the rate of rare earth extraction (Section C 3.2.3).

6.2 1S Column Performance6.2.1 Capacity Studies<sup>(5)</sup>

Most of the 1S runs were made in a dual-purpose 1A Column with the scrub section (1S Column) mounted above the 1AF feed point. Since the scrub section was generally more stable than the extraction section, very few flooding runs as a function of flow rates were made. Table IV-33, however, is representative of operating conditions that can be achieved in the 1S Column.

DECLASSIFIED

4168

TABLE IV-33  
1S COLUMN CAPACITY SUMMARY

(Source of Data: HW-79762PT2)

Amplitude = 1 in; Cartridge ht. = 6 to 10 ft.

Plate Spacing inches	Volume Velocity gph/ft <sup>3</sup>	Temperature, Centigrade	Frequency, Cycle/min.	
			Max. Demon.	Flooding
Bottom Interface				
2	200	25	--	70 to 86
2	390	25	--	62 to 72
2	590	25	42	--
4	200	25	61	--
4	200	ca. 40	70	--
4	390	25	--	62 to 74
4	390	ca. 40	70	--
4	550	25	40	--
4	550	ca. 40	44	--
Top Interface				
4	200	25	60	--
4	200	ca. 40	58	--
4	390	25	69	--
4	390	ca. 40	70	--

6.2.2 Sodium (and Cesium) Scrubbing Results

Citric, hydroxyacetic, and formic acids have been extensively studied as sodium reagents<sup>(5a,10,13)</sup>. All three buffer well in the desired pH range of 2.4 to 4 and were about equally effective in removing sodium from the LAP. Mole-for-mole, citric acid supplies about 60% more buffer capacity than either of the other two reagents over the desired pH range, but relative costs per mole of buffer capacity favor the use of formic acid and hydroxyacetic acid, in that order. Other factors affecting the choice of reagent composition are discussed in Sections C 3.3 and D 3.2.

Residual sodium concentrations in solvent scrubbed in pilot plant 1S Columns containing cartridges similar to that in the B-Plant 1S Column are shown in Table IV-34. Many of the runs were made in dual purpose columns under relatively inefficient pulsing conditions, and these results are not necessarily indicative of the optimum performance that can be achieved.

The results illustrate the importance of using a low pH in the 1SS; however, in one series of runs at pH 1.7, excessive strontium reflux resulted in gross strontium loss in the 1A Column. Strontium reflux

DECLASSIFIED

DECLASSIFIED

4169

TABLE IV-34  
1S COLUMN SODIUM SCRUBBING PERFORMANCE

(Source of Data: HW-72666 Section 4; HW-79762PT2; Ref. 13)

Bottom Interface; 25-40C; A/O = 0.2-0.25

<u>M D2EHPA</u>	<u>1AF pH</u>	<u>1SS pH</u>	<u>1SS Composition</u> <sup>(d)</sup>	<u>1S Column Ht., ft.</u>	<u>MNa in 1SP</u>	
					<u>Average</u>	<u>Minimum</u>
0.2	4.0-4.4	2.2-2.6	0.25M H <sub>3</sub> Cit.	6 <sup>(a)</sup>	0.004	<0.0001
0.2	4.0-4.4	2.9-3.0	0.25M H <sub>3</sub> Cit.	6-9 <sup>(a)</sup>	0.004	0.0005
0.2	4.6-4.7	1.7 <sup>(c)</sup>	0.25M H <sub>3</sub> Cit.	6 <sup>(a)</sup>	0.002	0.0002
0.2	4.6-4.7	2.6	0.25M H <sub>3</sub> Cit.	6 <sup>(a)</sup>	0.004	0.0003
0.4	3.7-3.8	2.3	0.6 M H <sub>3</sub> Cit.	9 <sup>(a, b)</sup>	--	≤0.006
0.4	4.6	2.3	0.6 M H <sub>3</sub> Cit.	9 <sup>(a, b)</sup>	0.04	0.036
0.2	4.3-4.5	3.0	0.5 M HAcOH	6 <sup>(a)</sup>	0.007	0.0023
0.3	4.0	2.4	0.5 M HAcOH	10	0.0008	<0.0001
0.3	4.5	2.4	0.5 M HAcOH	10	--	0.0002
0.2	4.3	3.1	0.5 M HCOOH	6 <sup>(a)</sup>	--	0.0019
0.2	4.2-4.5	3.2	1.0 M HCOOH	6 <sup>(a)</sup>	0.005	0.0024
0.3	4.5-4.9	2.4	1.0 M HCOOH	10	0.002	0.0012

(a) Part of dual-purpose 1A columns.

(b) Frequency well below the flooding threshold.

(c) Excessive strontium reflux occurred at this pH.

(d) H<sub>3</sub> Cit. = citric acid  
HAcOH = hydroxyacetic acid  
HCOOH = formic acid

at low solvent loading amounted to only 4 to 11% with the 1SS pH adjusted to 2.4<sup>(10)</sup>. Generally, higher scrub pH's can be used in conjunction with a low pH in the 1A Column since sodium extraction and, hence, the sodium scrubbing duty will be lower.

The runs described above were made in an organic continuous 1S Column. Comparable sodium scrubbing was obtained in a limited number of runs with the aqueous phase continuous<sup>(10)</sup>.

The path of cesium was followed with Cs-134 tracer in the runs using a 1M formic acid scrub. Only 1 to 3% of the cesium extracted in the 1A Column, and less than 0.1% was found in the scrubbed product<sup>(10)</sup>.

### 6.2.3 Nickel Scrubbing Results

Nickel behavior in separate 1A and 1S Columns was determined in one series of runs with tartrate-complexed PAW and with 1M formic acid, pH 2.4 scrub. The final run also contained 0.005M EDTA in the 1SS. The results, as shown in Table IV-35, indicated that appreciable nickel extracted from the tartrate feed and that its removal in the 1S Column was improved by EDTA addition. Nickel extraction from an HEDTA or EDTA system should be negligible.

DECLASSIFIED

DECLASSIFIED

4170

TABLE IV-35

NICKEL EXTRACTION AND SCRUBBING BEHAVIOR

(Source of Data: HW-79762PT2)

Cartridge ht. = 10 ft.; A/O = 0.2; Temp. = 25C

1AF pH	M EDTA in 1SS	% of 1AF Ni in		
		1AP	1SP	1BP(a)
5.5	0	--	--	5.0 <sup>(b)</sup>
4.9	0	92	12	4.4
4.5	0	23	2.8	2.4
4.6	0.005	32	1.4	0.8

(a) Nickel in the 1SP should be quantitatively stripped in the 1B column and appear in the 1BP.

(b) Average of 3 runs.

6.3 1B Column Performance

6.3.1 Capacity Studies

A summary of 1B Column capacity studies is presented in Table IV-36(5a,10). The amplitude-frequency product was chosen as the measure of pulse energy input to correct for amplitude variation.

TABLE IV-36

1B COLUMN CAPACITY SUMMARY

(Source of Data: HW-79762PT2; HW-72666 Section4)

Ampl. = 0.6 to 1 in.; Cartridge ht. = 9 to 10 ft.; 1BP pH ≤ 3; Temp. = 25C

Plate Spacing inches	Volume Velocity, gph/ft <sup>2</sup>	Ampl. x Frequency, in. /min.	
		Max. Demonstrated	Flooding
Bottom Interface			
2	200	--	63 to 92
2	390	64	--
2	590	53	--
4	390	--	54 to 60
Top Interface			
2	390	53	--
2	590	--	≥45
4	190	70	--
4	390	--	71 to 74
4	500	70	--
4	640	--	80
4	790	60	--

DECLASSIFIED

DECLASSIFIED

4171

The flooding threshold values were relatively insensitive to plate spacing, flow rate and LBX composition; and results from runs using both dilute nitric acid and 1M citric acid are included in the above table. With nitric acid, however, the stability of the LB Column was greatly decreased whenever the LBP pH exceeded 4<sup>(10)</sup>. This condition existed only when there was insufficient acid in the LBX to strip the strontium. The cause of this pH effect was not determined, but the milky appearance and poor settling characteristics suggested the presence of a third phase.

### 6.3.2 Strontium Stripping Performance (5a,10)

Optimum strontium HTU's ranged from 1.6 to 2.1 ft with either 0.03M HNO<sub>3</sub> or 1M citric acid used as LBX. The HTU's were estimated by using the strontium E<sub>g</sub> at the pH of the LBX. This procedure leads to conservatively high HTU's since the pH, and hence the strontium E<sub>a</sub><sup>0</sup>, increase toward the product end of the column. The effects of major variables on strontium HTU's and waste losses are presented in the following paragraphs.

Effect of LBX Composition and Flow Ratio - At optimum pulsing conditions, the main factor affecting strontium loss was the pH of the LBP. This, in turn, was determined by the amount of acid supplied in the LBX and on the amount used up in stripping strontium and sodium from the LBF. The sodium content in the LBF is a function of the scrubbing efficiency of the LS Column and can vary independently of the strontium concentration. Whenever the LBF contains an unusually large quantity of sodium, additional acid must be supplied to keep the LBP pH from increasing above a value which will inhibit or block strontium stripping. This pH limit was about 2.4 to 2.8, depending on the solvent concentration and the flow ratio. Three methods of supplying the additional acid were tested in PAW flowsheet development: increasing the HNO<sub>3</sub> concentration in the LBX, using a buffer acid, and increasing the LBX flow. All of these were successful, but increasing the LBX flow proved to be the simplest method<sup>(10)</sup>.

Buffer acids are currently favored for stripping high concentrations of strontium from the LBF because of their reservoir of exchangeable hydrogen ions. For example, 1M citric acid will give up 0.14M H<sup>+</sup> as the pH increases from 1.7 to 2.2. The same pH change with HNO<sub>3</sub> corresponds to an exchange of only 0.014M H<sup>+</sup>. Both citric and tartaric acid at 1 to 1.5M have been successfully used in pilot plant runs to obtain LBP product compositions of 0.04 to 0.06M Sr and 0.1 to 0.2M Na<sup>(5a)</sup>.

Effect of Interface Position - The interface position had little or no effect on strontium HTU's. Steady state operation, however, was gained much faster with the interface at the bottom because of the higher relative flow of the solvent phase. In addition, the LBP pH was more

DECLASSIFIED

responsive to adverse operating conditions because of the lower aqueous holdup. For high product purity, however, top interface operation may be preferred to divert interfacial solids to the LBW.

Effect of Flow Rate - Strontium HTU's were not appreciably affected by volume velocity. They ranged, typically, between 1.6 and 2.1 ft at flow rates from 200 to 580 gph/ft<sup>2</sup>.

Effect of Solvent Composition - There was no evidence that variation in solvent concentrations from 0.08M to 0.4M D2EHPA affected the results in any way other than caused by variation in the distribution ratios.

6.3.3 Decontamination from Calcium and Cerium

The decontamination factors for calcium and cerium in the LB Column are approximately equal to their respective extraction factors; i.e.,  $DF \approx E_B^O / (A/O)$ . Thus, the optimum decontamination performance will be obtained by operating at the highest pH and lowest LBX flow rate compatible with strontium recovery. Because of strontium and sodium transfer, the aqueous phase pH varies throughout the LB Column with the highest pH occurring at the product end. Although the LBP pH should be controlling as far as decontamination performance is concerned, in practice the pH (or acidity) of the LBX also has an important effect on the DF's, as illustrated in Table IV-37.

TABLE IV-37

CALCIUM AND CERIUM DECONTAMINATION PERFORMANCE

(Source of Data: HW-79762PT2)

PAW Flowsheet, A/O = 0.2 to 0.3

M HNO <sub>3</sub> in LBX	LBP pH	Ca DF		Ce DF	
		Ave. (a)	Max.	Ave. (a)	Max.
0.03	1.5-1.7	3.0	4.5	1000	3300
	1.8-2.0	5.8	8.5	ca. 1400	7000
	2.1-2.3	24	48	ca. 1000	2000
	2.4-2.6	54	82	ca. 2000	>4900
0.10	1.5	--	1.6	--	≥60
	2.0	--	2.2	--	660

(a) Average results for four or more runs.

High solvent loadings had an adverse effect on calcium decontamination in strontium crude purification runs with LBX solutions containing 1M citric acid (5a). The calcium DF's increased from 3 to an average of 40 when the calcium concentration in the LBP was decreased from 0.056M

DECLASSIFIED

4173

ISO-100

to 0.015M(5a). Calcium DF's of 10 to 40 have been obtained in the SSW under similar operating conditions with about 0.015M Ca in the LBF(5b).

Cerium decontamination factors ranged from 55 to 100 in the SSW LB Columns(5b). These values are considerably lower than those obtained in "cold" runs with dilute nitric acid, perhaps because of citrate complexing.

#### 6.3.4 Decontamination from Fe, Al, and Cr

Over-all iron decontamination factors (IAF to LBP) were  $> 10,000$  in ZAW flowsheet demonstration runs ( $< 0.005$  g/l Fe in the LBP)(13). Corresponding aluminum DF's were about 20,000 with HEDTA-complexed IAF and 2500 with tartrate-complexed feed. The aluminum DF in the LB Column alone averaged 160 for both ZAW feeds. DF's of these magnitudes probably cannot be maintained under plant conditions because of entrainment. For example, over-all iron DF's as low as 400 and 1300 have been measured in SSW runs(1) and 200 to 7000 in Csrex process demonstration runs(11).

Chromium behaves much like iron under process flowsheet conditions. When properly complexed, very little chromium will extract and that that does should remain in the solvent. Under Csrex process conditions, over-all chromium DF's ranged from 200 to 2000(11).

#### 6.4 LC Column Performance

##### 6.4.1 Capacity Studies

The flooding behavior of the LC Column was very similar to that of the LB Column. A summary of the capacity studies is presented in Table IV-38.

The stability of the LC Column (bottom interface) was improved by increasing the pulse amplitude to  $1.8 \pm 0.2$  in.; the maximum stable amplitude-frequency product was 68 in./min at 0.8 in. amplitude, 92 in./min at 2 in. amplitude, and 66 in./min at 4.7 in. amplitude. The plate spacing was 2 in., and the volume velocity was 390 gal/hr-ft<sup>2</sup> for this test.

##### 6.4.2 Total Rare Earth Stripping

The majority of the efficiency studies were made to demonstrate total stripping concepts, using Ce-144 tracer and 0.3 to 2M HNO<sub>3</sub> as LCX. The results of these studies should apply also to promethium-rare earth

DECLASSIFIED

stripping in the Ce(IV) partitioning flowsheet studies described in Section C 3.5.2. The effects of major variables on stripping efficiency are discussed in the following paragraphs.

TABLE IV-38  
1C COLUMN CAPACITY STUDIES

(Source of Data: HW-79762PT2)

Amplitude = 0.6 to 1 in.; Cartridge ht. = 10 ft.; 1CX = 0.3 to 2M HNO<sub>3</sub>

Plate Spacing, inches	Volume Velocity, gph/ft <sup>2</sup>	Temperature, Centigrade	Ampl. x Frequency, in./min.	Max. Demonstrated Flooding
Bottom Interface				
2	110	25	94	--
2	190	25	--	75 to 84
2	190	40	83	--
2	290	40	74	--
2	390	25	74	--
4	280	25	--	60 to ≥68
4	390	44	45	--
4	600	25	--	≥45 to 53
4	600	50	53	--
4	660	41	45	--
Top Interface				
2	390	25	--	64 to 66
2	570	25	57	--
2	770	25	--	≥30
4	390	25	60	--
4	390	40-50	--	55 to 80
4	600	25	--	≥45 to 53
4	600	25	45	--
4	710	25	--	≥40
4	800	25	--	44

Effect of Interface Position, Flow Rate, and Pulsing Conditions -

The cerium stripping efficiency was apparently diffusion controlled; those variables which increased the organic holdup time and intimacy of contact were the most effective in reducing cerium losses and HTU's. Optimum cerium HTU's of 1.5 to 2.2 feet (0.2 to 1.2% loss in the 10-ft-tall column) were obtained by operating with a bottom interface at volume velocities less than 400 gph/ft<sup>2</sup> and amplitude-frequency products within about 85% of the flooding threshold value. Cerium waste losses were increased two- to eight-fold typically by operation at flow rates of 600 gph/ft<sup>2</sup> or with top interface. A summary showing the effect of these variables is presented in Table IV-39<sup>(10)</sup>.

Effect of Pulse Amplitude - The effect of pulse amplitude was studied using an air-driven pulse generator to supply the variable amplitude<sup>(10)</sup>. The frequency was varied to maintain a constant dispersed phase holdup, as measured by static pressure. The results showed that increasing the pulse amplitude from 0.8 to 2 inches had a negligible effect on waste losses, but a further increase to ca. 3 inches increased the loss three-fold. The "threshold" amplitude of 2 inches, perhaps coincidentally, was the same as the plate spacing.

DECLASSIFIED

4175

00

TABLE IV-39  
CERIUM STRIPPING EFFICIENCY STUDIES

(Source of Data: HW-79762PT2)

Amplitude = 0.6 to 1 in.; Cartridge ht. = 10 ft.; 1CX = 1 to 2M HNO<sub>3</sub>; Temp. = 25C

Interface Position	Volume Velocity, gph/ft <sup>2</sup>	Ampl. x Frequency, in./min.			Approximate Ce HTU, feet
		In./Min	% of Flooding	% Ce Loss	
Top	390	45	68	23	7.1
Top	390	56	85	2.8	2.8
Top	390	60	91	1.7	2.4
Top	390	64	97	1.7	2.4
Top	580	45	ca. 75	24	7.1
Top	580	48	ca. 80	13	4.8
Top	580	52	ca. 87	6.2	3.6
Top	580	57	ca. 95	5.8	3.4
Bottom	280	50	74	24	7.1
Bottom	280	56	83	ca. 6	ca. 3.5
Bottom	280	62	91	ca. 1	ca. 2.1
Bottom	280	68	ca. 100	2.1	2.5
Bottom	390	33	ca. 43	32	9.1
Bottom	390	64	ca. 84	0.7	1.9
Bottom	390	74	ca. 97	0.2	1.5
Bottom	580	39	74	31	8.2
Bottom	580	45	85	4.9	3.3
Bottom	580	50	94	≤1.8	≤2.5

Effect of Temperature - Cerium HTU's were reduced 20 to 30% by increasing the temperature from 25 to 40 C. Optimum HTU's of 1.6 to 2.1 ft were obtained at 40 to 50 C (volume velocity = 390 gal/hr-ft<sup>2</sup>) in an aqueous continuous column with a 10-ft-tall cartridge of 4-in-spaced, 10% free area nozzle plates<sup>(12,13)</sup>.

Effect of LCX Composition and Flow Ratio - The concentration of HNO<sub>3</sub> in the LCX had little or no effect on waste losses or HTU provided that the flow ratio was adjusted to keep the extraction factor constant. The minimum flow ratio demonstrated to give good stripping performance was 0.09 with 2M HNO<sub>3</sub> plus 0.094M H<sub>2</sub>SO<sub>4</sub> in the LCX. Lowering the flow ratio to 0.06 increased the losses in the 10-ft-tall, top interface column from 0.6 to 2.0% at 50 C<sup>(12)</sup>. The sulfuric acid was added to stimulate the effect of persulfate decomposition products during normal partitioning runs.

#### 6.4.3 Cerium-Rare Earth Partitioning by Persulfate Oxidation<sup>(12)</sup>

Continuous separation of cerium from the other rare earths can be accomplished in the 1C Column by adding persulfate and silver catalyst to the LCX to oxidize cerium to highly extractable Ce(IV) according to the reactions discussed in Section C 3.5.3. A short scrub section must be added below the feed point to assure complete extraction of Ce(IV).

DECLASSIFIED

DECLASSIFIED

4176

750-100

The assumed mechanism for the separation of cerium from the other rare earths in a countercurrent solvent extraction column involves the following steps:

- (1) The rare earths, including cerium, are stripped from the solvent by the  $2M$   $HNO_3$  in the LCF (fast).
- (2) The cerium is oxidized in the aqueous phase to Ce(IV) by silver-catalyzed persulfate (relatively slow).
- (3) The Ce(IV) is re-extracted into the solvent phase (relatively fast).
- (4) The extracted Ce(IV) is reduced by the solvent to Ce(III) in an undesired side reaction (slow).

Factors that should improve the separation include:

- . Using a long aqueous phase residence time (low LCF flow rate and aqueous-continuous operation) to provide adequate time for cerium oxidation.
- . Using a short solvent phase resident time to minimize Ce(IV) reduction by the solvent.
- . Adding a scrub section below the LCF feed point to recover that small fraction of cerium that will be pulled below the feed point before it can be oxidized and re-extracted.
- . Operating the system at an elevated temperature to improve the kinetics of mass transfer and cerium oxidation.

Scouting runs confirmed the validity of these assumptions and demonstrated that scrub section heights of 2 to 4 ft were generally adequate to assure removal of over 95% of the cerium from the rare earth product. (In the absence of any scrub section, 20 to 30% of the cerium was found in the LCF.)

The remaining pilot plant demonstration runs used a 14-ft-tall column divided to give a 10 ft stripping section and a 4 ft scrub section. The plate spacing was graded, with 2-in. spacing in the scrub section and 4-in. in the stripping section, to improve dispersion characteristics. The rare earth feed (LCF) contained  $0.004M$  rare earths, including  $0.001M$  cerium, in  $0.3M$  D2EHPA- $0.15M$  TBP-hydrocarbon diluent. The LCF contained  $2M$   $HNO_3$  and varying amounts of persulfate and silver. The flow rates of the LCF and LCS (solvent scrub) streams were 320 and 64 gal/hr-ft<sup>2</sup>, respectively; the LCF flow was normally 10 to 20% of the LCF flow. Pulsing conditions were set at 80 to 90% of the estimated flooding frequency. The results were obtained:

DECLASSIFIED

DECLASSIFIED

4177

100-100

Effect of Interface Position - Moving the interface from the top of the column to the bottom increased the cerium loss to the LCP from  $\leq 3.7\%$  to  $79\%$  of the entering cerium. This result demonstrated that long aqueous phase residence times are required for quantitative cerium oxidation and re-extraction, since the immediate effect of the move was to decrease the aqueous phase residence time from 120 to 17 min. (The long solvent residence time obtained with the bottom interface also favors the reduction of extracted Ce(IV) by the solvent.)

Effect of LCX Flow Rate - The LCX flow rate also affects the aqueous phase residence time, but 3-fold rate variations (aqueous residence times of 80 to 200 min) did not appear to affect the cerium separation performance. The results may reflect the lack of sufficient runs to define the effect properly. Certainly, under some conditions, a high aqueous rate would not provide enough residence time for complete cerium oxidation; and an unusually low aqueous rate might not only permit destruction of the persulfate before it reached the feed point but also be inadequate to strip all of the trivalent rare earths from the LCF, as discussed in D 6.4.2.

Effect of Silver and Persulfate Concentrations - As discussed in C 3.5.3, most of the persulfate used up in the column will be lost by side reactions with water, solvent, and solution impurities; hence it is important to use low silver concentrations to increase the persulfate life and to maintain the desired reaction rate by starting with high persulfate concentrations. In the present application, the maximum persulfate concentration will be restricted by the stability of the resulting rare earth sulfates.

The validity of the above analysis was confirmed by the pilot plant results shown in Figure IV-61, where the amount of cerium left in the rare earth product is plotted as a function of silver and persulfate concentrations in the LCX. (The data for the full test range of LCX flow rates were included in the absence of any definite effect of such rates on cerium behavior.) The data show that optimum performance was obtained at  $0.3M$  persulfate concentration with as little as  $0.0012M$   $Ag^+$  present. Acceptable cerium losses were also obtained at  $50\text{ C}$  with  $0.18M$  persulfate and  $0.02$  to  $0.03M$  silver; however, the losses appeared to be quite sensitive to the silver concentration: high losses at  $0.04M$  silver were attributed to premature persulfate destruction, while high losses at  $0.01M$  silver were tentatively attributed to an inadequate oxidation rate. Runs with  $0.1M$  persulfate or less were completely unsuccessful.

The persulfate concentrations shown in Figure IV-61 were corrected for persulfate decomposition in the LCX storage tank. The persulfate loss during storage was minimized by adding silver to the column in a separate stream.

DECLASSIFIED

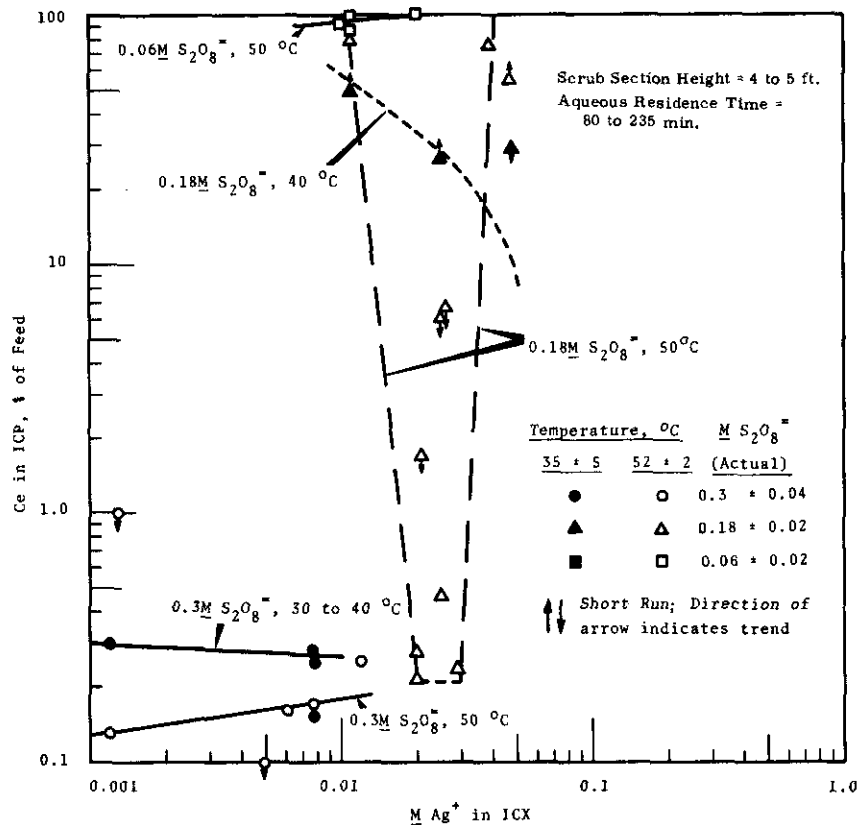


FIGURE IV-61

Effect of Silver and Persulfate Concentration  
on Cerium Loss to the 1CP  
(Source of Data: BNWL-173)

Effect of Temperature - The reaction rate of persulfate ion is highly dependent on temperature, as discussed in Section C 3.5.3. The poor performance observed at 40 C using 0.18M persulfate (illustrated in Figure IV-61) can thus be explained as an adverse effect of low temperature on the cerium oxidation rate. This effect could be overcome either by increasing the temperature to 50 C or by increasing the silver concentration to about 0.04M. The temperature effect at 0.3M persulfate was much less pronounced, and low cerium losses were obtained at temperatures ranging from 30 to 53 C.

Elevated temperature operation also favors rare earth stripping, as discussed in D 6.4.2.

#### Effect of Diluent and Solvent Pretreatment

Comparable performance was obtained with solvents containing either Soltrol-170 or NPH as diluents. Experiments described in

Sections C 3.5.3 and H 1.4, however, indicate that Ce(IV) is more stable in NPH solvent than in Soltrol solvents under radiation, and NPH has been recommended as the diluent to be used when partitioning Ce-144 from the other rare earths.

Several solvent washing procedures were tested during the pilot plant program, including washes with 2M HNO<sub>3</sub> containing either persulfate or permanganate to oxidize reducing impurities in the solvent; but the only treatment that appeared to be essential was sulfamic acid addition to destroy nitrous acid remaining from the standard HNO<sub>3</sub>-NaNO<sub>2</sub> cerium-removal step. About 0.02 to 0.04 g-mole of sulfamic acid per liter of solvent (added as a concentrated solution in dilute HNO<sub>3</sub>) was sufficient. No attempt was made to decant the small amount of associated aqueous phase before reusing the treated solvent.

#### ICP Solution Stability

Precipitates found in several ICP samples after prolonged standing were tentatively identified as the double sulfate salts of sodium or potassium and rare earths. Approximate threshold conditions for precipitate formation in 2M HNO<sub>3</sub> are shown in Table IV-40.

TABLE IV-40

THRESHOLD CONDITIONS FOR PRECIPITATION OF  
RARE EARTH SULFATES IN THE ICP

(Source of Data: BNWL-173)

1CP = 2M HNO<sub>3</sub>; 0 to 0.3M Ag<sup>+</sup>; 25 C

<u>Persulfate Cation</u>	<u>M of Persulfate Cation</u>	<u>M SO<sub>4</sub><sup>=</sup></u>	<u>Approximate RE Solubility, M</u>
Na <sup>+</sup>	0.58	0.58	≤0.03
	0.78	0.78	0.02±0.01
K <sup>+</sup>	0.4	0.4	0.45±0.013
	0.68±0.1	0.68±0.1	0.03
NH <sub>4</sub> <sup>+</sup>	0.72	0.72	>0.1

The data indicate that rare earths are much more stable in sulfate solutions derived from ammonium persulfate than in the corresponding sodium or potassium solutions and that the potassium system is slightly more stable than the sodium. Unfortunately, the potassium persulfate concentration at 25 C is limited to 0.26M by its solubility in 2M HNO<sub>3</sub> (Section H 3.1), and the use of ammonium salts in separations plants is avoided whenever possible because of the potential for plugging off-gas filters by the deposition of ammonium nitrate solids.

#### 6.4.4 Iron and Aluminum Contamination in the LCP

The LCP derived from ZAW process demonstration runs (Section D 6.1.3) contained 0.006 to 0.02% of the iron and 0.6 to 4% of the aluminum entering in the LAF<sup>(13)</sup>. The average aluminum contamination in the LCP was about 2- to 3-fold higher in runs using tartrate-complexed feed than with HEDTA-complexed feed. The material balances across the IC Column were poor, but evidently 40 to 100% of the aluminum in the LCF was stripped from the solvent by the ICX (2M HNO<sub>3</sub>, A/O = 0.2, 40 C).

### 7. Strontium Semiworks Process Demonstrations

Since 1961, the Strontium Semiworks (formerly the Hot Semiworks) has been used to recover and purify over 10 megacuries of Sr-90 from crude concentrates prepared in the Purex Plant by PbSO<sub>4</sub> precipitation techniques<sup>(1,2,5,8,15)</sup>. More recently, the same facility has been used to demonstrate the proposed B-Plant solvent extraction flowsheets presented in Section C 3.6 at approximately full-level fission product activity<sup>(14)</sup>. Highlights of the production and demonstration runs are presented in the following sections.

Two 4-in-diameter pulse columns, variously known as the 1A and 1B Columns<sup>(5b)</sup> or the HA and HC Columns<sup>(8)</sup>, were used as the principal solvent extraction contactors. The 1A Column is a dual-purpose column with a 15-ft-tall scrub section surmounting a 10-ft-tall extraction section. The 1B Column contains a 16-ft-tall cartridge and has recently been modified so that it also can be operated as a dual-purpose cerium-rare earth partitioning column with a 10-ft-tall stripping section above a 6-ft-tall scrub section<sup>(14)</sup>. The 1A extraction cartridge is made up of 23% free area stainless steel nozzle plates (3/16-in.-diameter holes); the 1A scrub and 1B cartridges contain 10% free area stainless steel nozzle plates (1/8-in. holes). All plates are spaced 4 in. apart. With the exception of plate spacing and height, the cartridge geometries were similar to the corresponding B-Plant cartridges.

#### 7.1 Strontium Crude Purification

A typical flowsheet used in the strontium crude purification runs is presented in Figure IV-62. Excellent performance as measured by strontium losses and the purity of the recovered product has been achieved in this process, particularly with NPH as the diluent. A summary of this experience is presented in Table IV-41. The columns were operated at ambient temperatures with the organic phase continuous in the 1A Column and the aqueous phase continuous in the 1B Column. Typical volume velocities were about 700 and 350 gph/ft<sup>2</sup> in the 1A and 1B Columns, respectively.

TABLE IV-41  
SUMMARY OF TYPICAL STRONTIUM SEMIWORKS EXPERIENCE  
IN PURIFYING STRONTIUM CRUDES

(Source of Data: G. L. Ritter, Isochem Inc., unpublished data)

Feed Material

Run No.	Ion/Sr-90 Mole Ratio					Isotope/Sr-90 Curie Ratio		
	Ca	Ba	Fe	Pb	Na	Ce- 144	ZrNb- 95	Ru- 106
SSW-2	0.86	0.034	6.8	0.86	--	2.0	0.20	0.03
SSW-6	1.63	0.22	5.7	0.21	150	0.35	0.28	0.014
SSW-7	1.1	0.051	7.5	1.3	110	0.48	0.098	0.017
SSW-8	1.2	0.17	11	2.1	750	0.45	0.013	0.010
SSW-9	0.80	<0.06	8.1	1.3	400	0.45	0.22	0.018
SSW-10	3.5	0.32	31	1.0	1300	1.2	0.04	0.035

A. Decontamination Factors

Run No.	Ca	Ba	Fe	Pb	Na	Ce- 144	ZrNb 95	Ru- 106
SSW-2	20	20	>1000	--	--	1650	8000	>750
SSW-6	4	50	320	16	--	3500	1950	35
SSW-7	11	3	7500	1300	--	480	120	34
SSW-8	16	30	450	160	120	2800	>150	>80
SSW-9	26	--	400	750	600	6900	1200	460
SSW-10	35	--	560	600	20	920	>50	>15

B. Recovery Performance

Run No.	Kilocuries Sr-90 Processed		% Sr-90 Lost	
	Feed	Product	To 1AW	To 1BW
SSW-2 <sup>(a)</sup>	975	905	2	7.5 <sup>(c)</sup>
SSW-6 <sup>(a)</sup>	1200	1100 <sup>(d)</sup>	4-2 <sup>(c)</sup>	10-3 <sup>(c)</sup>
SSW-7 <sup>(a)</sup>	940 <sup>(d)</sup>	890 <sup>(d)</sup>	4	5
SSW-8 <sup>(b)</sup>	940	885	<1	<1
SSW-9 <sup>(b)</sup>	550	510	<1	<1
SSW-10 <sup>(b)</sup>	890	910	7 <sup>(e)</sup>	0.4

(a) Soltrol-170 diluent.

(b) NPH diluent.

(c) Solvent changeout during run. Losses decreased as shown when new solvent was used.

(d) Includes 140 kilocurie rework from Run No. SSW-6.

(e) High loss because of unfavorable aqueous/organic ratio and Na and Ca feed content.

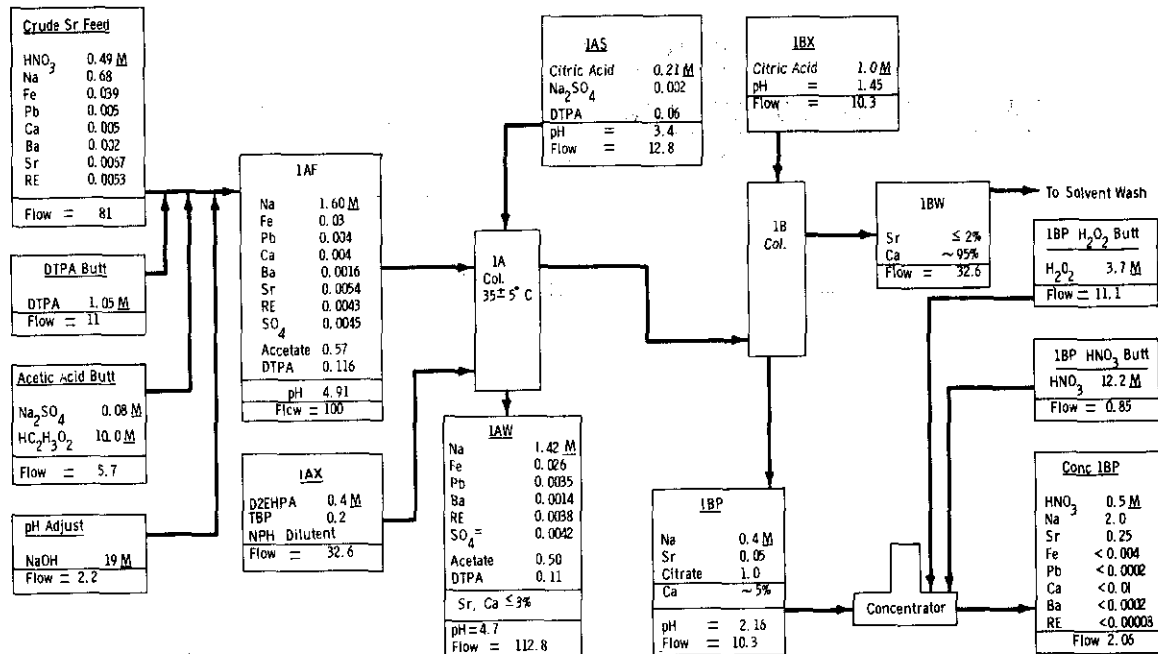


FIGURE IV-62

Typical Strontium Semiworks Chemical Flowsheet  
for Purification of Strontium  
(Source of Data: RL-SEP-20)

## 7.2 PAW Flowsheet Demonstration

### 7.2.1 1A - 1B Columns

A process test of an HEDTA-complexed PAW flowsheet similar to that shown in Fig. IV-48 was completed in October, 1965 (Pm Process Test No. 4) (14). Rare earth extraction and separation from strontium was excellent; however the low LAF and LAW pH's (3.6 and 3.2, respectively) prevented quantitative extraction of strontium. Extraction losses were about 25% for strontium, 1% for cerium, and 2% for promethium. The strontium loss was 1% in the 1B Column (using 0.04M HNO<sub>3</sub> as 1BX), and the decontamination factor from cerium was 1300. The rare earths were quantitatively stripped from the solvent by a batch contact with 3M HNO<sub>3</sub>. A detailed material balance summary is presented in Table IV-42.

The 1A and 1B Columns were operated at 40 to 50 C with the aqueous phase continuous; volume velocities were 820 and 440 gph/ft<sup>2</sup>, respectively. Relative flows of the LAF, IAS(ISS), IAX, and 1BX streams were 100, 25, 100, and 20. The solvent used in this and the remaining tests was 0.4M D2EHPA-0.2M TBP-NPH diluent.

TABLE IV-42

PAW FLOWSHEET DEMONSTRATION RUN SUMMARY

Pm Process Test No. 4

(Source of Data: G. L. Ritter<sup>(14)</sup>)MATERIAL BALANCE

Stream	Promethium		Cerium		Strontium	
	KCi	%	KCi	%	KCi	%
1AF	112	100	580	100	107	100
1AW	2	2	2	<1	22	20
1BP	< 0.1	0.1	0.3	< 0.1	75	70
1CP <sup>(a)</sup>	105	94	530	92	1	1
Total	107	96	532	92	98	91

DECONTAMINATION FACTORS

	<u>Strontium Product (1BP)</u>	<u>Rare Earth Product (1CP)<sup>(a)</sup></u>
Fe	> 3200	> 2000
Pb	50	25
ZrNb	200	100
Ru	>350	>250
U	> 60	> 40
Pu	> 17	> 11
Y	100	20
Np	>350	>250
Sr	--	150
Pm	750	--
Ce	1300	--
Ca	4.1	1.2
Na	> 14	> 9
Al	--	30

(a) Resulting from batch strip with 3M HNO<sub>3</sub>.

7.2.2 1C Column

Promethium Process Test No. 2 was the first full-level demonstration, and the most successful to date (June 1966), of the persulfate oxidized 1C Column flowsheet. The results fully verified the Cold Semi-works tests described in Section D 6.4.3. The steady-state loss of promethium in the cerium product (1CW) was 1% and that for cerium in the promethium-rare earth product (1CP) was 1% (12,14).

1AF for this run contained 0.0048M rare earths, including 0.0015M cerium, 0.06M HEDTA, and 0.2M hydroxyacetic acid. It was prepared from Purex waste that had been treated with a lead sulfate precipitation and a D2EHPA solvent extraction cycle to eliminate most of the impurities. The rare earths were extracted with 0.4M D2EHPA-0.2M TBP-NPH that had been used in previous SSW runs and was reused during the run after stripping the cerium out with a nitric acid-sodium nitrite solution and destroying the residual nitrite with sulfamic acid. A 1AS stream containing 0.025M HNO<sub>3</sub> was used as the 1A Column scrub to simulate the 1B Column treatment. The 1CX, after blending separate silver and persulfate streams, contained 2M HNO<sub>3</sub>, 0.2M K<sub>2</sub>S<sub>2</sub>O<sub>8</sub> and 0.02M AgNO<sub>3</sub>. Relative flow ratios 1AF:1AS:1AX:1CX:1CS were 1.05:0.25:1.0:0.2:0.2; 1A and 1C Column velocities were 840 and 510 gph/ft<sup>2</sup>, respectively. The columns were operated at ca. 40 C with the organic phase continuous in the 1A Column and the aqueous phase continuous in the 1C Column. An over-all material balance summary is presented in Table IV-43.

TABLE IV-43

OVER-ALL PROMETHIUM, CERIUM, AND STRONTIUM  
MATERIAL BALANCES FOR Pm PROCESS TEST NO. 2

(Source of Data: G. L. Ritter<sup>(14)</sup>)

Stream	Promethium		Cerium		Strontium	
	KCi	%	KCi	%	KCi	%
1AF(a)	171	100	908	100	58	100
1AW	14	8	16	1.8	47	81
1CP	151	88	16	1.8	1	2
1CW	7	4	858	95	0.8	1.4

(a) Ca. 1.2 watts/liter.

The steady-state 1A Column rare earth losses were 2 to 4-fold less than the over-all losses, which for both the 1A and 1C Columns reflect the effects of deliberate process upsets and the usual start-up and shut-down losses. Typical steady-state losses in the 1AW were 1 and 4% for cerium and promethium, respectively.

### 7.3 ZAW Flowsheet Demonstration

#### 7.3.1 1A-1B Columns

The 1A and 1B Column portion of the ZAW flowsheet presented in Fig. IV-49 was tested in June, 1966<sup>(14)</sup>. The only significant changes in the flowsheet were the use of slightly less tartrate in the feed (0.013 vice 0.025M) and more HNO<sub>3</sub> in the 1BX (0.03 vice 0.02M). The rare earths were batch stripped from the 1BW with 3M HNO<sub>3</sub>.

The feed was derived from a Purex head-end product to which large amounts of ferric and aluminum nitrate and other lesser amounts of other cold chemicals were added to simulate ZAW. The feed was adjusted to pH 4.0. The columns were operated at 40 to 45 C with volume velocities of 400 and 220 gph/ft<sup>2</sup> in the 1A and 1B Columns, respectively. The 1A Column was operated with the organic phase continuous, and the 1B Column was operated with the aqueous phase continuous. Material balances and decontamination factors are tabulated in Table IV-44.

The performance was excellent except for the high rare earth loss in the 1A Column. The promethium and cerium losses in the 1AW correspond to HTU's of 7.2 and 4.3 ft., respectively. For comparison, the cerium HTU in a Cold Semiworks demonstration runs under the same conditions was 4.0 ft (Table IV-30).

The behavior of americium-curium was also followed in this run. The over-all material balance was poor, but the results of this and earlier tests indicate that americium and curium will follow the trivalent rare earths. Americium comprised 36% of the Am-Cm in the feed and 41% in the product.

TABLE IV-44  
ZAW FLOWSHEET DEMONSTRATION RUN SUMMARY  
 (Source of Data: G. L. Ritter<sup>(14)</sup>)

Stream	MATERIAL BALANCE							
	Promethium		Cerium		Strontium		Americium	
	KCi	%	KCi	%	KCi	%	Ci	%
1AF	100	100	580	100	93	100	3.5	100
1AW	22	22	60	10	3	3	0.17	6
1BP	0.14	0.14	0.05	< 0.01	88	95	< 0.03	1
1CP(a)	75	75	540	93	0.6	0.6	1.9	55
1CW(a)	--	--	--	--	--	--	--	--
Total	97	97	614	106	92	98	2.1	60

Impurity	DECONTAMINATION FACTORS	
	Strontium Product	Rare Earth Product <sup>(a)</sup>
Fe	> 100,000	4,000
Pb	50	20
Al	> 13,000	120
U	> 120	> 36
Pu	> 320	> 100
Na	450	150
Ca	5.4	1.2
Cr	> 4,000	1,200
Ce	11,000	--
Pm	800	--
Sr	--	100
ZrNb	125	> 7.5

(a) Resulting from the batch strip with  $3M HNO_3$ .

8. References

1. S. J. Beard and P. W. Smith. Status of Fission Product Recovery at Hanford, RL-SA-40. August 16, 1965.
2. S. J. Beard, P. W. Smith, and J. S. Cochran. Large Scale Processing and Source Preparation of Separated Fission Products, RL-SA-59. December 6, 1965.
3. L. A. Bray, BNW. Personal communication, June 1965.
4. L. A. Bray. D2EHPA Extraction of Zirflex and Purex Acid Wastes, BNWL-CC-595.
5. Chemical Development Operation. Hot Semiworks Strontium-90 Recovery Program, HW-72666, July 17, 1963.
  - a. M. D. Alford and G. L. Richardson, Ibid, Section 4, "Cold Semiworks Studies".
  - b. C. R. Cooley and G. L. Richardson. Ibid, Section 5, "Hot Semiworks Studies".
6. A. P. Colburn. "Simplified Calculation of Diffusional Processes", Ind. Eng. Chem., vol. 33, pp. 459-467. 1941.
7. B. V. Coplan, J. K. Davidson, and E. L. Zebroski. "The 'Pump-Mix' Mixer Settler - A New Liquid-Liquid Extractor", Chem. Eng. Prog., vol. 50, pp. 403-408. 1954.
8. Fission Products Process Engineering. Specifications and Standards: Strontium Purification at the Strontium Semiworks, RL-SEP-20. February 15, 1965.
9. G. L. Richardson and A. M. Platt. "The Design and Operation of Industrial Scale Pulse Columns for Purex Service", Progress in Nuclear Energy, Series IV, Vol. 4; Technology, Engineering and Safety. Pergamon Press, New York. pp. 279-307. 1961.
10. G. L. Richardson. Solvent Extraction of Strontium, Cerium, and Rare Earths with D2EHPA. Part 2: Pilot Plant Studies, HW-79762 PT2. February 1964.
11. G. L. Richardson. The Csrex Process for Co-Extraction of Cesium, Strontium, and Rare Earths: Pilot Plant Studies, HW-81091. March 2, 1964.
12. G. L. Richardson. Continuous Separation of Cerium from Trivalent Rare Earths by Persulfate Oxidation and D2EHPA Solvent Extraction: Pilot Plant Studies, BNWL-173. November 1965.

13. G. L. Richardson. Solvent Extraction of Strontium and Rare Earths from Zirflex Acid Waste: Pilot Plant Studies. BNWL-CC-785. August 1966.
14. G. L. Ritter, Personal communication, Isochem Inc. 1966.
15. G. L. Ritter and J. S. Buckingham. Plant Scale Demonstration of Promethium Recovery and Purification Processes, RL-SA-53. September 17, 1965.
16. V. Rod. "Calculation of Extraction Columns with Longitudinal Mixing", British Chem. Eng., vol. 9, no. 5, pp 300-304. May 1964.
17. J. J. Shefcik. Performance of Turbomixer for Continuous Washing of Purex Organic, HW-51386. July 3, 1957.

E. BATCH D2EHPA EXTRACTION OF NEPTUNIUM AND PLUTONIUM  
FROM PUREX ACID SLUDGE SOLUTION

1. Introduction

A large fraction of the sludge now contained in the Purex self-boiling tanks was derived from Hanford Purex plant high-level waste produced before the start-up of Np-237 recovery operations in the Purex plant proper. Considerable Np-237 and also plutonium, the latter from normal small Purex process losses, have thus accumulated in the sludge.

This part of the manual is devoted to discussing the chemistry of the batch solvent (D2EHPA) extraction process which has been developed for recovering neptunium and plutonium from PAS solution<sup>(1)</sup>. Current interest in recovering Np-237 stems from its use in producing Pu-238, an isotopic power source useful in space vehicles.

Also to be noted is that much of the stored Redox process sludge contains amounts of Np-237 and plutonium judged worth recovering<sup>(2)</sup>. It is anticipated that this neptunium and plutonium will report largely to the HNO<sub>3</sub> leach solution used to recover Sr-90 from the Redox sludge. It is also anticipated, although not demonstrated experimentally, that the D2EHPA extraction process described in this section can be used satisfactorily to recover neptunium and plutonium from RAS solutions.

2. Process Concept

The concept of the batch extraction process for recovery of neptunium and plutonium from PAS solution is illustrated in Figure IV-63.

Core of the process is a sequence of extraction-strip batch contacts. The first series of contacts serves to recover neptunium and plutonium from the PAS solution by D2EHPA extraction followed by oxalic acid stripping. These first contacts also serve to free the plutonium and neptunium from the bulk of the radioactive and inert contaminants present in the PAS solution; uranium and iron are the principal contaminants after the first contacts.

To provide further decontamination from uranium, iron, and other contaminants, neptunium and plutonium are again extracted into the D2EHPA extractant. Feed for this final extraction contact is prepared by destroying oxalate in the first oxalic acid strip solution by reaction with HNO<sub>3</sub> and H<sub>2</sub>O<sub>2</sub>. A nine-fold reduction in volume at this stage also serves to concentrate the plutonium and neptunium. Plutonium and neptunium are again removed from the organic phase by stripping with oxalic acid. This final strip solution is treated with HNO<sub>3</sub> and H<sub>2</sub>O<sub>2</sub> and concentrated to yield a solution suitable for transmittal to the Hanford Purex plant for final separation and purification of the neptunium and plutonium. Present plans call for accumulation of the plutonium and neptunium from 9000 gallons of PAS solution in 5 gallons of final product solution.

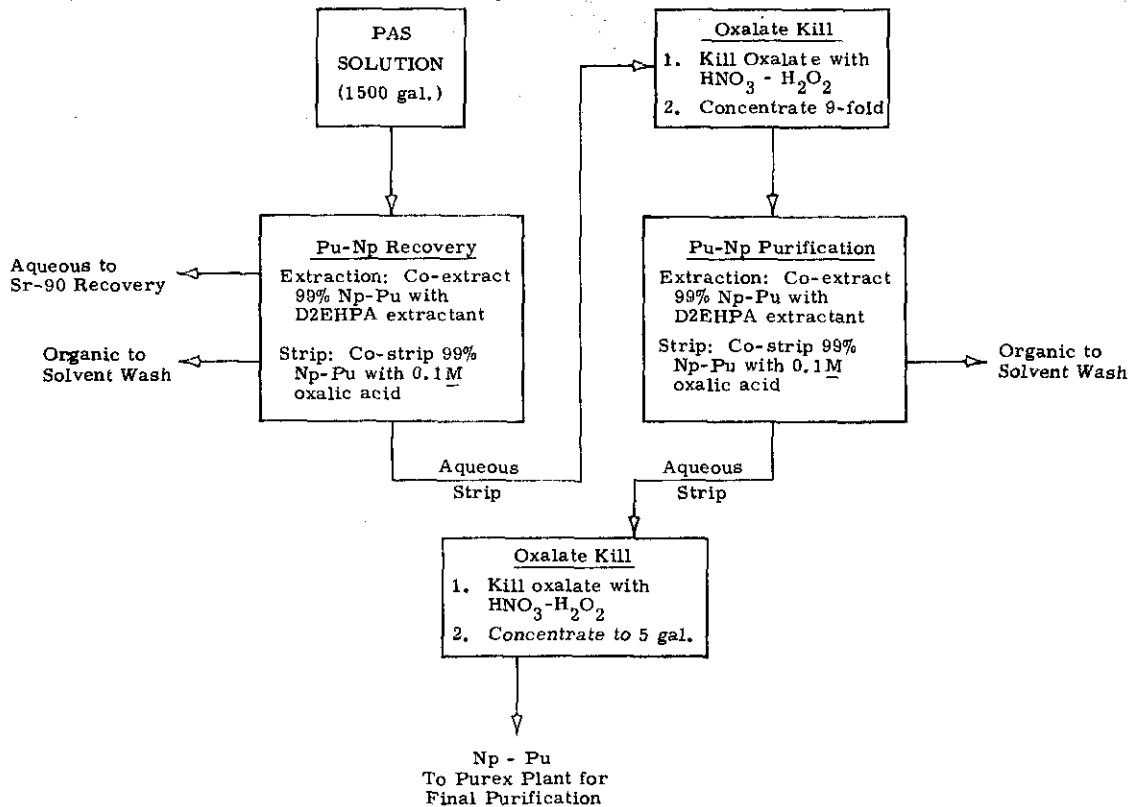


FIGURE IV-63

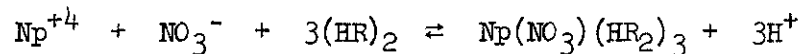
## D2EHPA Extraction of Np-Pu from PAS Solution

3. Extraction Step

The D2EHPA extraction of plutonium and neptunium from HNO<sub>3</sub> and HNO<sub>3</sub>-nitrate solutions has been investigated in great detail by Weaver and Horner<sup>(3)</sup>. Highlights of their findings are:

- a. The order of extraction of plutonium in different oxidation states is Pu(IV) > Pu(VI) >> Pu(III). Similarly, the order of extraction of neptunium is Np(IV) > Np(VI) >> Np(V).
- b. Extraction of Np(IV) from HNO<sub>3</sub> is inversely proportional to the square of the acidity above about 1M HNO<sub>3</sub>; below 1M HNO<sub>3</sub> it is directly proportional to acidity.
- c. Extraction of Pu(IV) from nitrate solutions is somewhat similar to that of Np(IV) but several times as high.
- d. Dilute oxalic acid is an effective reagent for stripping plutonium and neptunium from D2EHPA solutions.

In the range from  $10^{-4}$  to  $10^{-2}$  M D2EHPA in Amsco 125-82 diluent Weaver and Horner found that extraction of Pu(IV) from 1M  $\text{HNO}_3$  was proportional to the square of the uncomplexed D2EHPA concentration. On the other hand, Peppard and coworkers<sup>(4)</sup> find that in the D2EHPA (toluene) vs (perchlorate + nitrate) system the Np(IV) extracted species contains one nitrate group. They suggest the extraction reaction is:



where  $(\text{HR})_2$  is dimerized D2EHPA.

In PAS solution plutonium is present as Pu(IV) but neptunium is present, at least to some extent, in the inextractable Np(V) state. A key point in the extraction process, therefore, is the need to establish both elements in the quadrivalent state to permit extraction of both neptunium and plutonium into the same organic phase. Attempts to find a combination of oxidizing and/or reducing agents which would establish both neptunium and plutonium simultaneously in the quadrivalent state in PAS solution failed. A successful procedure consists of extracting Pu(IV) into the D2EHPA phase, and, after allowing the two phases to separate but without removing the organic phase, treating the aqueous phase with ferrous sulfamate and hydrazine to obtain Np(IV). Recontact of aqueous and organic phases then extracts the Np(IV). Satisfactory recovery of both actinides depends on the great affinity of D2EHPA for Pu(IV) so that serious back-extraction of plutonium does not occur during valence adjustment and extraction of neptunium.

This approach to recovery of neptunium and plutonium has been extensively tested in laboratory experiments with both synthetic and actual PAS solutions. Some typical results with actual PAS solutions are given in Table IV-45. These data demonstrate the extractant should be at least 0.1M D2EHPA to realize satisfactory recovery of both neptunium and plutonium.

TABLE IV-45  
D2EHPA EXTRACTION OF NEPTUNIUM AND PLUTONIUM FROM PAS SOLUTION

(Source of Data: W. W. Schulz, BNW, Unpublished Data)

PAS solutions obtained from stored waste contacted 30 min. at 25 C with an equal volume of indicated D2EHPA-TBP-diluent solution. Without phase separation, aqueous phase made indicated  $\text{N}_2\text{H}_4$  and ferrous sulfamate concentration and allowed to stand 30 min. at 25 C. Finally, aqueous and organic phases recontacted 30 min. at 25 C.

PAS Description		D2EHPA, M	TBP, M	FS <sup>(a)</sup> , M	$\text{N}_2\text{H}_4$ , M	% Not Extracted	
Sludge from Tank Number	PAS $\text{H}^+$ , M					Np	Pu
101	4.48 <sup>(b)</sup>	0.10	0.10	0.01	0.01	0.32	0.39
101	2.24	0.06	0.06	0.01	0.01	6.56	33.5
101	0.72	0.04	0.02	0.01	0.01	14.9	57.1
101	0.72	0.04	0.02	0.00	0.00	52.9	81.8
104	0.50	0.10	0.05	0.01	0.01	0.1	1.11
104	0.50	0.10	0.05	0.00	0.00	74.7	0.84

(a) Ferrous sulfamate

(b) Adjusted to 1.0M by addition of NaOH before extraction

Experiments with both synthetic and actual PAS solutions demonstrate ferrous sulfamate, either by itself or in combination with hydrazine, efficiently and rapidly reduces Np(V) to Np(IV). Hydrazine by itself is inadequate for this purpose. The combination of ferrous sulfamate with hydrazine appears preferable over ferrous sulfamate by itself to provide additional capacity for destroying nitrite ion and thereby preventing nitrite-catalyzed  $\text{HNO}_3$  oxidation of Fe(II). Concentrations of both reductants in the range of 0.01 to 0.05M have been found adequate for reduction of Np(V). Satisfactory reduction is achieved at 25 C in as little as 10 minutes.

#### 4. Strip Contact

Aqueous-soluble oxalate complexes of both Pu(IV) and Np(IV) are well-known<sup>(5)</sup>. Depending on conditions (acidity, oxalate concentration) one or more of the complexes  $[\text{M}(\text{C}_2\text{O}_4)_4]^{2+}$ ,  $[\text{M}(\text{C}_2\text{O}_4)_2]$ ,  $[\text{M}(\text{C}_2\text{O}_4)_3]^{2-}$ , and  $[\text{M}(\text{C}_2\text{O}_4)_4]^{4-}$  may be formed where M = Pu(IV) or Np(IV). Formation constants for these complexes are so high that, under proper conditions, dilute oxalic acid solutions quantitatively strip Pu(IV) and Np(IV) from the D2EHPA extractant. Data illustrating this point are presented in Table IV-46.

TABLE IV-46

#### OXALIC ACID STRIPPING OF PLUTONIUM AND NEPTUNIUM

(Source of Data: W. W. Schulz, BNW, Unpublished Data)

Initial organic contained either  $5 \times 10^{-5}$  M Pu(IV) or  $2 \times 10^{-5}$  M Np(IV) from extraction of PAS solution.

Organic Composition		Strip Conditions				$E_a^0$	
D2EHPA, M	TBP M	$\text{H}_2\text{C}_2\text{O}_4$ M	Time Min.	Temp. C	Vol. Ratio, Aq/Org	Pu	Np
0.1	0.05	0.1	30	25	1:1	0.0021	0.0011
0.1	0.05	0.25	30	25	1:1	0.0007	0.0004
0.1	0.05	0.1	30	50	1:1	0.17	--
0.1	0.05	0.1	30	50	1:2	1.0	--

Based on these data a single equal volume contact at 25 C with 0.1M  $\text{H}_2\text{C}_2\text{O}_4$  is specified in the chemical flowsheet (Figure IV-47) for stripping plutonium and neptunium. Pu(IV) is stripped less efficiently at 50 C than at 25 C according to these data. Higher temperatures favor oxalic acid stripping of iron (Section E-5) and should be avoided for this reason also.

If desirable for some reason, other complexants such as carbonate, citrate, EDTA, etc., could probably be used successfully to strip plutonium and neptunium from the D2EHPA phase. Oxalic acid, however, is smoothly and readily destroyed by reaction with  $\text{HNO}_3$  and/or  $\text{H}_2\text{O}_2$  (Section E8) and can be used without any danger of precipitating plutonium such as might occur during neutralization of alkaline solutions.

TABLE IV-47  
EXTRACTION CONTACT - DECONTAMINATION PERFORMANCE

(Source of Data: W. W. Schulz, BNW, Unpublished Data)

Synthetic (a) PAS solution, traced with various radioisotopes, contacted 60 minutes at 25 C with an equal volume of the indicated extractant.

Contaminant	0.1M D2EHPA, 0.1M TBP, NPH			0.04M D2EHPA, 0.02M TBP, Soltrol-170	
	E <sub>g</sub>	% Ext'd.	DF	E <sub>g</sub>	DF
Uranium	38.7	97.7	-	-	-
Iron	0.108	9.7	-	0.0220	46
Yttrium	5.46x10 <sup>-3</sup>	-	180	0.0169	60
Europium	1.03x10 <sup>-3</sup>	-	970	0.0053	185
Ruthenium	-	-	-	0.0027	360
Cerium	2.86x10 <sup>-4</sup>	-	-	1.79x10 <sup>-3</sup>	620
Chromium	-	-	-	<1.45x10 <sup>-3</sup>	>680
Americium	-	-	-	1.03x10 <sup>-4</sup>	9700
Strontium	-	-	-	<2.0 x10 <sup>-5</sup>	>4900
Manganese	-	-	-	<1.0 x10 <sup>-5</sup>	>10,000
Cesium	-	-	-	5.0 x10 <sup>-6</sup>	21,000

(a) 0.5M H<sup>+</sup>, 0.42M Na<sup>+</sup>, 0.36M Fe<sup>+3</sup>, 0.55M Al<sup>+3</sup>, 0.021M Cr<sup>+3</sup>, 0.012M Ni<sup>+2</sup>, 0.01M Mn<sup>+2</sup>, 0.032M UO<sub>2</sub><sup>+2</sup>, 0.004M Zr<sup>+4</sup>, 0.0017M Sr<sup>+2</sup>, 0.002M Ce<sup>+3</sup>, 0.026M SO<sub>4</sub><sup>-2</sup>, 0.057M PO<sub>4</sub><sup>-3</sup>, 3.6M NO<sub>3</sub><sup>-</sup>.

## 5. Decontamination Performance

Of the constituents of PAS solution only uranium and iron, besides plutonium and neptunium, extract into the D2EHPA solvent to any extent. Data illustrating this point are presented in Table IV-47.

Considerable decontamination from extracted iron and, especially, uranium is obtained across the oxalic acid strip step provided high oxalic acid concentrations and high temperatures are avoided. Some typical results for the strip step are shown in Table IV-48. The excellent decontamination performance observed in extraction-strip contacts (performed according to the flowsheet conditions shown in Figure IV-47 with actual PAS solutions substantiates the work with synthetic solutions<sup>(1)</sup>. For example, an oxalic acid strip solution derived from Tank 10<sup>4</sup> sludge was 0.0007M U and 0.0092M Fe; predicted values from experiments with synthetic PAS were 0.001M and 0.0094M, respectively. The oxalic acid solution from the Tank 10<sup>4</sup> sludge also contained less than 0.02 g/l of Zr, less than 5 ppm Mo, and only a trace (spectroscopic analysis) of Al, Si, and Mg.

TABLE IV-48  
STRIP CONTACT - DECONTAMINATION PERFORMANCE

(Source of Data: W. W. Schulz, BNW, Unpublished Data)

Indicated D2EHPA extractants contacted with synthetic PAS solution and then contacted 30 minutes with oxalic acid strip according to listed conditions.

Extractant		Strip			E <sub>g</sub>		% Stripped	
D2EHPA M	TBP M	H <sub>2</sub> C <sub>2</sub> O <sub>4</sub> M	Aqueous Organic	Temp. C	U	Fe	U	Fe
0.1	0.1	0.1	1:1	25	26.4	2.95	4.8	25.6
0.1	0.1	0.25	1:1	25	8.9	0.49	12.5	67.4
0.04	0.02	0.1	1:1	25	1.8	0.64	36.6	60.8
0.04	0.02	0.25	1:1	25	0.98	0.23	49.5	84.0
0.04	0.02	0.1	1:2	50	1.45	<0.014	25.4	~100

6. Purification Extraction - Strip Contacts

The primary extraction-strip contacts discussed in Sections E 3 and E 4 serve to recover the neptunium and plutonium and to free them from the bulk of the contaminants with which they are associated in PAS solution. Further purification and concentration are necessary and desirable, however, to provide a small volume of purified material to route to the Hanford Purex plant for final separation and purification.

The desired purification is accomplished by a further extraction-strip cycle using essentially the same flowsheet conditions employed in the primary contacts. Feed for the purification extraction contact is prepared by accumulating (after oxalate destruction) the neptunium and plutonium from several batches of PAS solution in 1M HNO<sub>3</sub> solution. It is estimated that this feed solution will also be about 0.09M Fe(NO<sub>3</sub>)<sub>3</sub>, and 0.01M UO<sub>2</sub>(NO<sub>3</sub>)<sub>2</sub>; smaller (<0.01M) amounts of other contaminants (Al, Zr, Y, etc.) may also be present.

Batch contact of the 1.0M HNO<sub>3</sub> feed with an equal volume of 0.1M D2EHPA-0.1M TBP-NPH solution serves to extract the Pu(IV). To recover the neptunium, the aqueous phase (without phase separation) is made 0.01 to 0.05M in both ferrous sulfamate and hydrazine to reduce Np(V) to Np(IV). Subsequent recontact of the aqueous and organic phases then extracts the Np(IV) without significant loss of Pu(IV) to the aqueous phase as illustrated by the data in Table IV-49<sup>(1)</sup>. Essentially all of the uranium and about 15% of the iron are co-extracted with the neptunium and plutonium.

TABLE IV-49

PURIFICATION CYCLE EXTRACTION CONTACT

Synthetic feed<sup>(a)</sup> contacted 30 minutes at 25C with an equal vol. of 0.1M D2EHPA, 0.1M TBP, NPH. Without phase separation, aqueous phase made 0.01M ferrous sulfamate and 0.01M hydrazine and allowed to stand 30 minutes at 25C. Aqueous and organic phases then recontacted 30 minutes at 25C.

Element	First Contact		Second Contact	
	E <sub>g</sub>	% Extracted	E <sub>g</sub>	% Extracted
Plutonium	1500	99.9	980	99.9
Neptunium	0.234	20.0	2620	99.9
Uranium	137	99.3	113	99.1
Iron	0.111	9.8	0.176	15.0

(a) 1.0M HNO<sub>3</sub>, 0.089M Fe(NO<sub>3</sub>)<sub>3</sub>, 0.01M UO<sub>2</sub>(NO<sub>3</sub>)<sub>2</sub>, 0.002M Zr(SO<sub>4</sub>)<sub>2</sub>, 0.08M Al(NO<sub>3</sub>)<sub>3</sub>, 4.1x10<sup>-4</sup>M Pu(NO<sub>3</sub>)<sub>4</sub>, 1.4x10<sup>-4</sup>M NpO<sub>2</sub>NO<sub>3</sub>.

To complete the purification cycle, the extracted plutonium and neptunium are stripped into an equal volume of 0.1M oxalic acid. Accompanying the plutonium and neptunium into the oxalic acid strip are about 84% of the extracted iron and 4% of the uranium. The oxalic acid solution is treated with  $\text{HNO}_3$  or  $\text{HNO}_3\text{-H}_2\text{O}_2$  to destroy the oxalate and then concentrated to about 5 gallons to yield a solution for shipment to the Purex plant for further purification. This concentrated product is expected to contain about 5 g/l Np and about 15 g/l Pu and to be also about 5.0M  $\text{HNO}_3$ , 0.1M  $\text{UO}_2(\text{NO}_3)_2$ , and 1 to 2M  $\text{Fe}(\text{NO}_3)_3$ . Small (<0.1M) amounts of aluminum and zirconium may also be present in some cases.

## 7. Solvent Treatment

The 0.1M D2EHPA extractant after each recovery extraction and strip contact is expected to contain about 2 to 5 g/l U and 1 to 3 g/l Fe. Smaller amounts of the other inert contaminants (i.e., Al, Zr, etc.) present in PAS solution will also likely be present in this used solvent. Radioactive contaminants will include Y-90 (from beta decay of Sr-90) and, from the younger sludges, small amounts of ZrNb-95 and RuRh-106.

Routine removal of the uranium and iron from the solvent is necessary to prevent over-loading the extractant and thereby impairing extraction recovery of neptunium and plutonium. Efficient removal of uranium and iron, as well as yttrium and zirconium, if present, can be readily accomplished by washing the D2EHPA solvent with a  $\text{Na}_2\text{CO}_3$ -sodium citrate (or sodium tartrate) solution as illustrated by the data in Table IV-50.

TABLE IV-50  
SOLVENT WASHING STUDIES

(Source of Data: W. W. Schulz, BNW, Unpublished Data)

0.1M D2EHPA, 0.1M TBP, NPH extractant from extraction and strip contacts with synthetic or actual PAS solution, washed for 15 minutes at 25C with indicated solution.

Wash Composition, M			Aqueous Organic	Eq		% Not Recovered		
$\text{Na}_2\text{CO}_3$	$\text{Na}_2\text{Tart. (a)}$	$\text{Na}_3\text{Cit. (b)}$		U	ZrNb-95	U	Y-90(c)	ZrNb-95
1.0	0.1	0.0	1/5	0.0062	-	3.7	-	-
1.0	0.1	0.0	1/3	0.0084	-	2.8	-	-
1.0	0.1	0.0	1/1	0.013	0.0008	0.9	-	0.09
1.5	0.0	0.1	1/5	0.0067	-	3.4	5.7	-
1.5	0.0	0.1	1/3	0.0063	-	2.1	7.0	-
1.5	0.0	0.1	1/1	0.011	0.0011	0.7	5.4	0.11

(a) Sodium Tartrate.

(b) Sodium Citrate.

(c) Solvent from contact with PAS from actual TK-101 sludge.

Sodium hydroxide solutions such as used in washing the mainline process D2EHPA extractant (Section C 6.3.1) could also be used to wash uranium from the 0.1M D2EHPA extractant. With NaOH solutions, however, uranium precipitates as the diuranate even in the presence of citrate or tartrate. Precipitation of uranium is avoided with  $\text{Na}_2\text{CO}_3$  washes because of the formation of soluble uranium carbonate complexes. Addition of citrate or tartrate to the  $\text{Na}_2\text{CO}_3$  solution prevents precipitation of hydrated iron oxide.

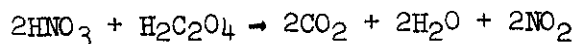
A second organic phase (Section C 2.6.1) formed when 0.1M D2EHPA-0.05M TBP-NPH solutions were contacted with 0.5 to 1.0M  $\text{Na}_2\text{CO}_3$  solutions<sup>(1)</sup>. When the TBP concentration was increased to 0.1M a third phase did not form if the initial  $\text{Na}_2\text{CO}_3$  concentration was 1.0M or greater. Because of this restriction on  $\text{Na}_2\text{CO}_3$  concentration, it is economically desirable to use only a small volume of wash solution in each batch wash. Removal of contaminants is adequate with 1.0 to 1.5M  $\text{Na}_2\text{CO}_3$  solution at an aqueous-to-organic flow ratio as low as 1 to 5 and this amount of carbonate is still sufficient to prevent precipitation of uranium.

Washing of the 0.1M D2EHPA extractant with  $\text{Na}_2\text{CO}_3$  solution converts it to the sodium form. Reconversion to the hydrogen form can be accomplished by washing the extractant with a small volume of  $\text{HNO}_3$ .

#### 8. Destruction of Oxalic Acid

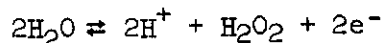
In the neptunium - plutonium recovery process, dilute oxalic acid solution is used to co-strip neptunium and plutonium from the D2EHPA phase in both the primary and purification extraction-strip cycles. Destruction of oxalic acid in these strip solutions is mandatory before satisfactory concentration and purification of the neptunium - plutonium fraction can be accomplished either in the D2EHPA purification cycle or, finally, in the Purex plant.

Many familiar oxidizing agents (e.g.,  $\text{KMnO}_4$ ,  $\text{Ce}(\text{SO}_4)_2$ , etc.) can be used to destroy oxalic acid. The use of most of these reagents would introduce metallic impurities into the neptunium - plutonium product. Nitric acid also reacts with oxalic acid according to the reaction

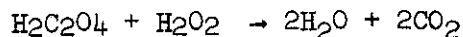


The reaction is first order with respect to oxalic acid. Typical data are presented in Figure IV-64. These data illustrate a major disadvantage of using  $\text{HNO}_3$  alone to destroy oxalic acid; namely, that the rate of reaction is intolerably slow at  $\text{HNO}_3$  concentrations below about 9M.

Hydrogen peroxide in acid solution is a powerful oxidizing agent; the potential for the couple



is -1.77 volts<sup>(6)</sup>. (The use of  $\text{H}_2\text{O}_2$  to oxidize citric acid in solutions containing Sr-90 is a well-established practice at Hanford as discussed in detail in Section C 4.3.5.) Oxidation of oxalic acid in accordance with the reaction



was studied as early as 1923 by Hatcher<sup>(7)</sup> who found ready oxidation occurred in various dilute acid ( $\text{HNO}_3$ ,  $\text{HCl}$ ) solutions at 20 C. Further applications (both uncatalyzed and catalyzed) of  $\text{H}_2\text{O}_2$  to oxidize oxalic acid have been alluded to in recent AEC project literature. As this manual was written,  $\text{H}_2\text{O}_2$  was under active laboratory consideration as the preferred reagent for destruction of oxalic acid in the strip solutions of the neptunium - plutonium recovery process.

### 9. Chemical Flowsheet

A chemical flowsheet for batch D2EHPA extraction of neptunium and plutonium from PAS solution is given in Figures IV-65 and IV-66.

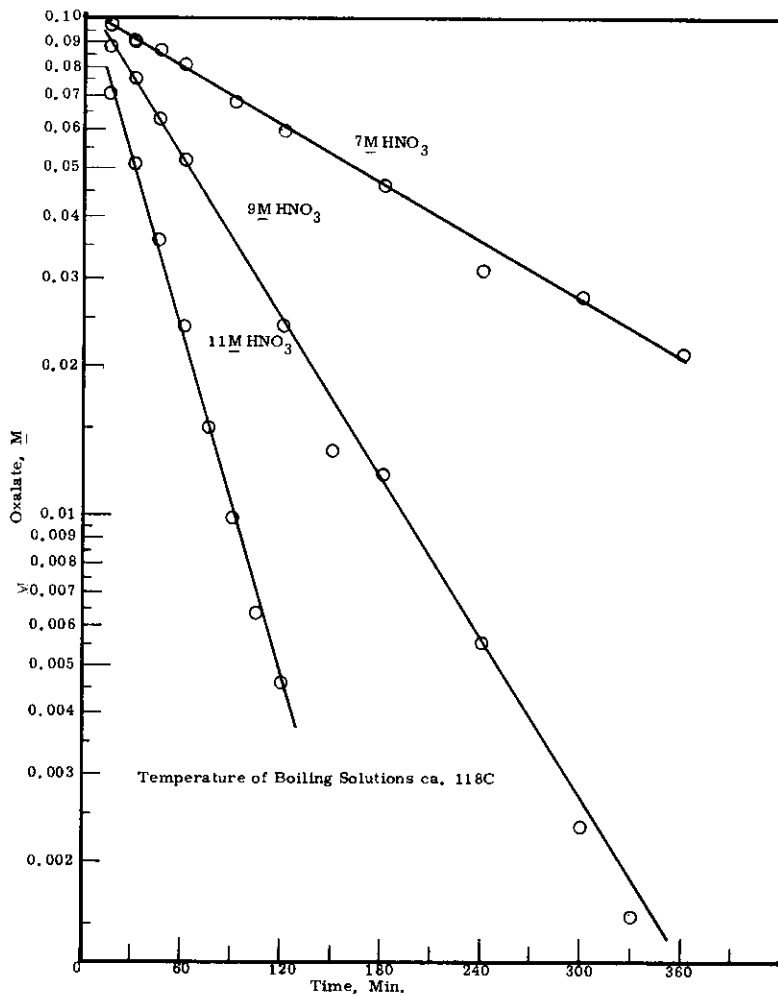


FIGURE IV-64

Kinetics of Destruction of Oxalic Acid with Nitric Acid  
(Source of Data: W. W. Schulz, BNW, Unpublished Data)

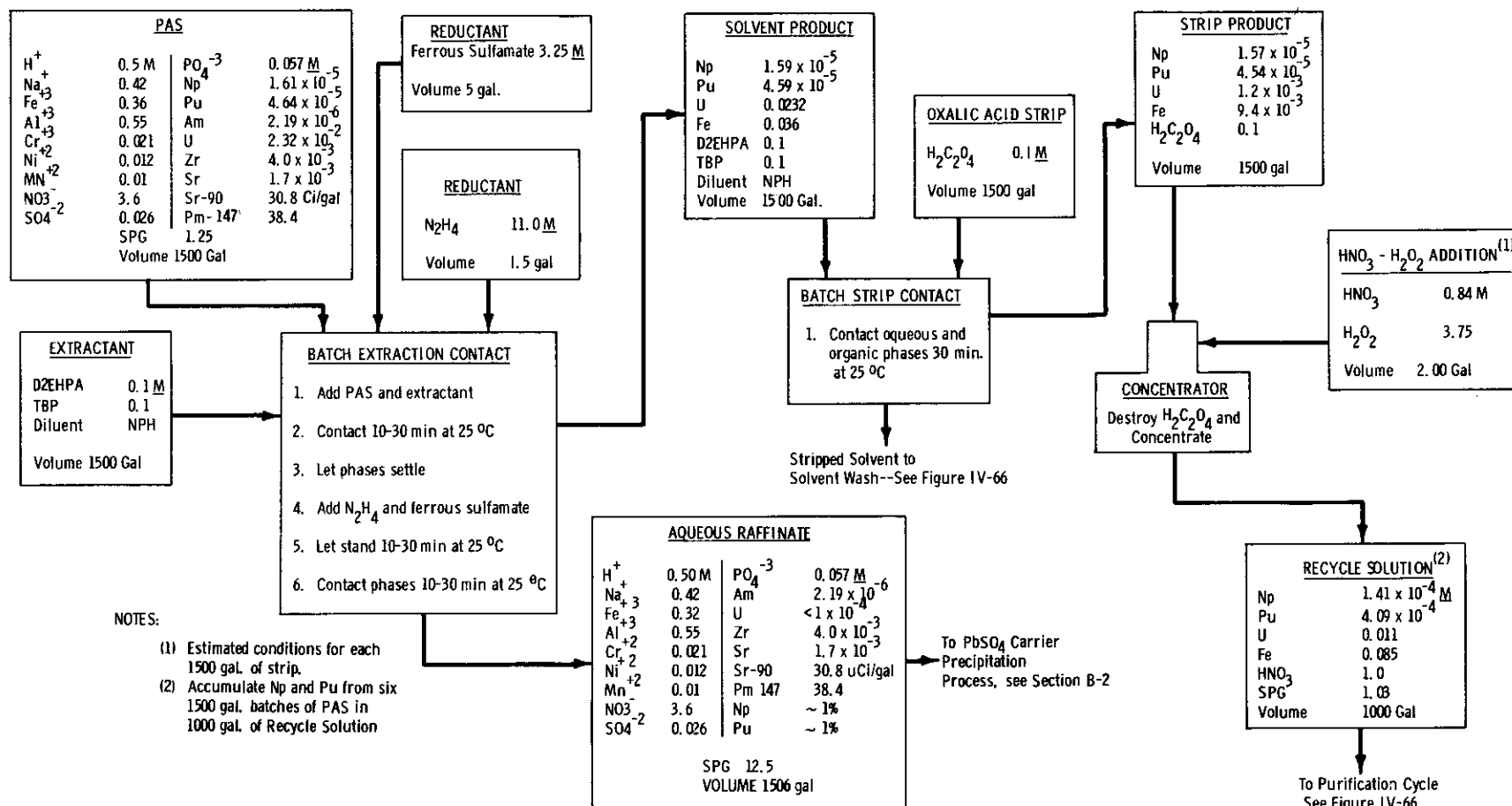


FIGURE IV-65

Chemical Flowsheet for Recovery of Neptunium and Plutonium from Purex Acid Sludge - Recovery Cycle

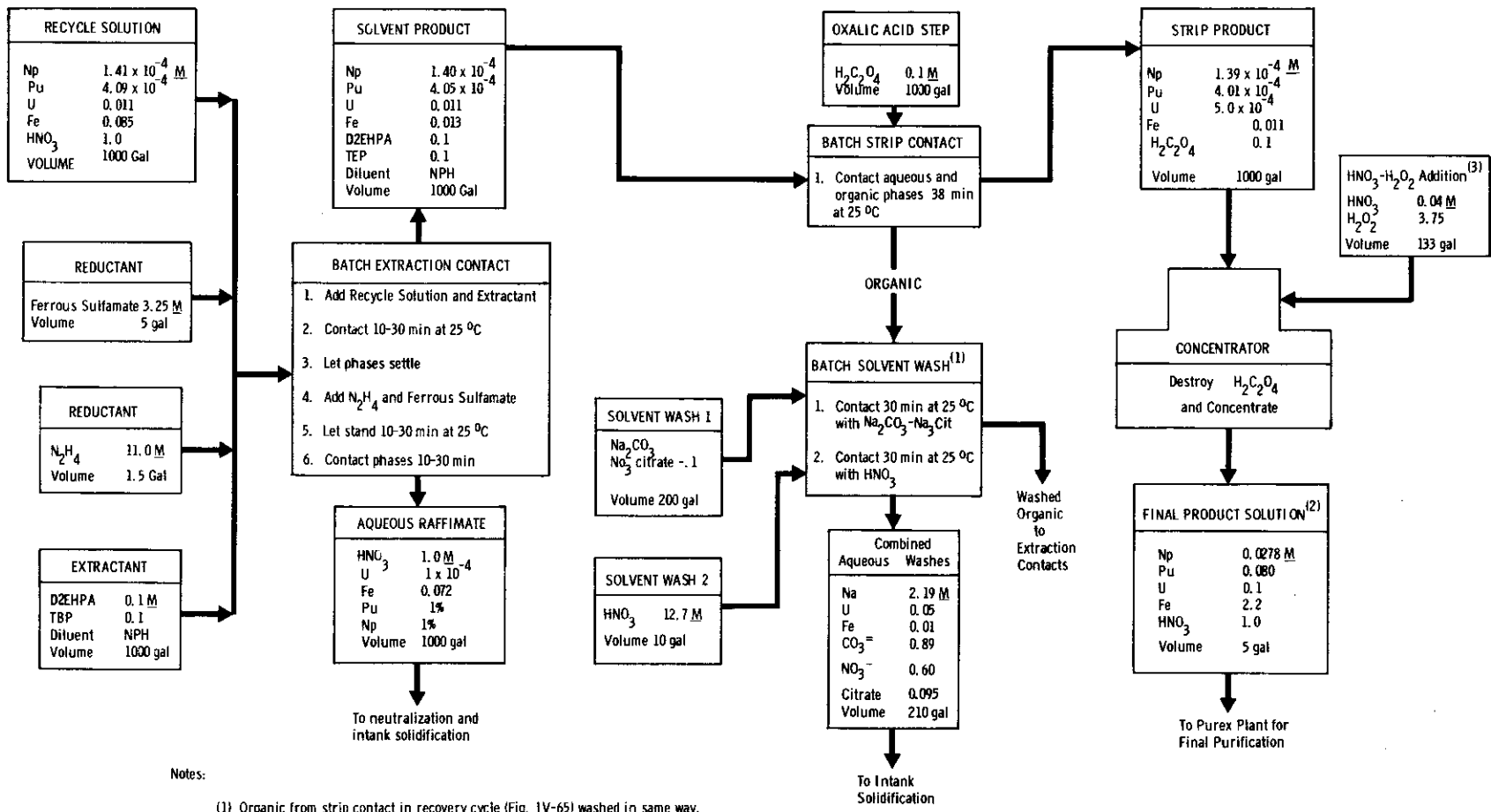


FIGURE IV-66

Chemical Flowsheet for Recovery of Neptunium and Plutonium from Purex Acid Sludge - Purification Cycle

10. References

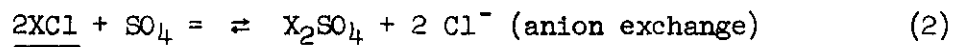
1. W. W. Schulz. Unpublished Data. Battelle-Northwest Laboratories. 1966.
2. J. W. Barnes and P. W. Smith. By-Product Recovery During Waste Processing - Engineering Study, RL-SEP-239. January 15, 1965.
3. B. Weaver and D. E. Horner. "Distribution Behavior of Neptunium and Plutonium between Acid Solutions and Some Organic Extractants", J. Chem. Eng. Data vol. 5, pp. 260 - 265. 1960.
4. D. F. Peppard and G. W. Mason. "Some Mechanisms of Extraction of M(II), (III), (IV), and (VI) Metals by Acidic Organophosphorous Extractants", Nucl. Sci. & Eng. vol. 16, pp. 382-388. 1963.
5. A. D. Gel'man, A. I. Moskvin, L. M. Zaitser, and M. P. Mefad'eva. Complex Compounds of Trans Uranium Elements, C. N. Turton and N. I. Turton, eds., New York; Consultants Bureau, 1962.
6. W. M. Latimer. Oxidation Potentials, Englewood Cliffs, New Jersey: Prentice Hall Inc., 1952.
7. W. H. Hatcher. "Hydrogen Peroxide as an Oxidizing Agent in Acid Solution", Trans. Roy. Soc. Canada vol. 17, pp. 119-124. 1923.

F. ION EXCHANGE PROCESSES1. General Principles of Ion Exchange

Ion exchangers are insoluble solid materials which carry exchangeable cations or anions. These ions can be exchanged for a stoichiometrically equivalent amount of other ions of the same sign when the ion exchanger is in contact with an electrolyte solution. Carriers of exchangeable cations are called cation exchangers, and carriers of exchangeable anions, anion exchangers. Typical reactions are



and



where X represents a structural unit of the ion exchanger, and solid phases are underlined.

Ion exchange is, with few exceptions, a reversible process. Thus, the calcium loaded on the cation exchanger in the example above can be eluted by passing a concentrated sodium salt solution through the exchanger.

Ion exchangers owe their characteristic properties to a peculiar feature of their structure. They consist of a framework which is held together by chemical bonds or lattice energy. This framework carries a positive or negative electric surplus charge which is compensated by ions of opposite sign, the so-called counter ions. The counter ions are free to move within the framework and can be replaced by other ions of the same sign. The framework of a cation exchanger may be regarded as a macromolecular or crystalline polyanion, that of an anion exchanger as a polycation. According to this simple model, the counter-ion content of the ion exchanger -- the ion-exchange capacity -- is a constant which is given solely by the magnitude of the framework charge and is independent of the nature of the counter ion<sup>(9)</sup>.

When an ion exchanger containing one species of counter ions is placed in a solution containing a second species, an exchange of counter ions takes place. After a certain time, determined by the mobilities of the counter ions, ion exchange equilibrium is attained. As a rule, the ion exchanger selects one species in preference to the other depending on ionic charge (valence), charge distribution, complex formation, and ion size. The selectivity is usually expressed as a mass action quotient, such as the following for the sodium-calcium exchange reaction presented above:

$$K_{\text{Na}}^{\text{Ca}} = \frac{(\text{CaX}_2)(\text{Na}^+)^2}{(\text{NaX})^2(\text{Ca}^{++})} \quad (3)$$

where the terms in parentheses are concentrations in consistent units (molarities or equivalent fractions, for example). The "K" defined by the above equation is not the thermodynamic equilibrium constant and can vary over a wide range depending on the temperature and the relative concentrations of the different counter ions in the system. The concept is quite useful, however, in predicting exchange equilibria when the value of K as a function of solution composition is known.

The use of binary exchange data to predict the equilibrium distribution is often complicated by the presence of more than two exchanging counter ions; however, Mercer and Ames<sup>(14)</sup> have shown that binary equilibrium data can be used to predict equilibrium concentrations of cesium and strontium on zeolites loaded from dilute solutions containing three or more cations. If the concentrations of the various cations on the zeolite are expressed in equivalent fractions, then the sum of all the cation equivalent fractions on the zeolite is unity:

$$A_z + B_z + C_z + \dots = 1 \quad (4)$$

To solve for  $A_z$ , the mass action expressions are substituted in place of  $B_z$  and  $C_z$  for the exchange of A with B and A with C, respectively. For example, where A and B are univalent and C is divalent, the following equation is obtained:

$$A_z + \frac{(B^+)}{K_B^A A^+} A_z + \frac{(C^{++})}{K_C^A A^{+2}} A_z^2 = 1, \quad (5)$$

where the concentrations of cations  $A^+$ ,  $B^+$ , and  $C^{++}$  in solution are expressed in equivalents/liter and the concentration of A on the zeolite,  $A_z$ , is expressed as the equivalent fraction. In column applications where the zeolite-containing column is loaded to  $\geq 50$  percent breakthrough and the breakthrough curve is steep, the zeolite is essentially in equilibrium with the feed; and  $A_z$  can be determined by solving the simple quadratic equation if  $K_B^A$  and  $K_C^A$  are known. ( $B_z$  and  $C_z$  can be solved by similar substitutions.) The calculation method is not restricted to zeolites but is applicable to any ion exchange media where suitable values of the mass action quotients are known or can be determined experimentally.

## 2. Ion Exchange Materials

### 2.1 Inorganic Cation Exchangers

Several naturally occurring and synthetic minerals exhibit a high cation exchange capacity and specificity for strontium and cesium. Among the most important members of this class are the zeolites. These are hydrated, crystalline aluminosilicates with the molecular structure  $(M, N_2)_x \cdot Al_2O_3 \cdot nSiO_2 \cdot mH_2O$ , where M is an alkaline earth and N an alkali metal. The zeolites have a relatively open three-dimensional framework structure with channels and interconnecting cavities in the aluminosilicate lattice. The zeolite lattice consists of  $SiO_4$  and  $AlO_4$  tetrahedra which have their oxygen atoms in common. Since aluminum is trivalent, the lattice carries a negative electric charge (one elementary charge per aluminum atom). This charge is balanced by alkali or alkaline earth cations, which do not occupy fixed positions but are free to move in the channels of the lattice framework. These ions act as counter ions and can be replaced by other cations. Specificity and exchange capacity are determined by the  $SiO_2/Al_2O_3$  ratio and by the crystalline structure. Increase in exchange capacity is gained from the lower silica/alumina ratios, greater acid stability from the higher ratios<sup>(23)</sup>.

Synthetic zeolites are prepared by gelling sodium silicate, sodium aluminate, and sodium hydroxide in fixed ratios followed by digestion to permit crystallization to 0.1 to 10 micron particle size. The zeolite crystals are then mixed with a clay binder, extruded, dried, and rotary-kiln fired at about 1200 F<sup>(23)</sup>. The synthetic zeolites have been most widely used as "molecular sieves" which, because of their very small and uniform pore structure, can sorb small molecules but completely exclude molecules larger than the pore openings. Typical pore openings range from 3 to 13 Å, depending on the zeolite type.

Selected properties of some of the more important zeolites studied at Hanford are presented in Table IV-51. One non-zeolite (Decalso) is included in this table because of its similarity to the zeolites in properties and applications. Decalso is an amorphous aluminosilicate gel, produced by Ionac Chemical Co., with the empirical formula  $Na_2O \cdot Al(OH)_3 \cdot 6Si(OH)_4 \cdot xH_2O$ . Unlike the zeolites, water forms an integral part of the Decalso structure; and dehydration of the loaded gel at temperatures above 100 C will prevent complete elution of the sorbed cation.

### 2.2 Organic Ion Exchangers

Ion exchange resins are typical gels. Their framework consists of an irregular, polymeric, three-dimensional network of hydrocarbon chains which carry active ionic groups such as  $-SO_3^-$  and  $-COO^-$  in cation exchangers and  $-N(CH_3)_3^+$  and  $-NH_3^+$  in anion exchangers. The framework of the resins, in contrast to that of the zeolites, is a flexible, random

TABLE IV-51  
 ZEOLITE PROPERTIES  
 (Ca. 20-50 mesh particles)

Source of Data: References (1) (12) (14) (23)

	Clinoptilolite	Linde					Norton "Zeolon"	Ionac "Decalso" <sup>(a)</sup>
		4A	4A XW	13 X	AW-400	AW-500		
Structural Type	Clinoptilolite	A	A	Faujasite	Erionite	Chabazite	Mordenite	gel 3 <sup>(a)</sup>
SiO <sub>2</sub> /Al <sub>2</sub> O <sub>3</sub> Ratio	8 - 10	2	2	2.5	6 - 7	4 - 5	10	
Total Exchange Capacity meq. /gm.	1.7	3.5	3.9	3.6	2.0	2.2	1.9	2.0(Cs)
Particle density, gm/cc (dry beads)	--	1.1	1.4	1.0	1.2	1.2	1.2	1.66
Packed density, gm/cc	0.7 - 0.8	0.7 - 0.8	0.8 - 0.9	0.6 - 0.7	0.8	0.8	0.8	0.7 - 0.8
Volumetric Exchange capacity, Eq. /l (b)	1.3	2.6	3.3	2.3	1.5	1.7	1.4	1.5(Cs)
Effective Pore Diameter, Å	<4	4	4	7-9	4	4-5	9-10	---
Internal Void Volume, %	--	45	45	51	--	--	41	---
Binder, Wt %	5-15	20	10	20	25	25	--	---
Water, lbs/100 lbs. absorbent at 25C	12	25	30	25	12	15	12	---
pH Tolerance Range	1 - 12	5 - 12	5 - 12	4 - 12	4 - 12	4 - 12	1 - 14	(5 - 13)
Maximum Temperature, degrees C (c)	(700)	550	550	--	550	550	(700)	100

(a) Not a zeolite. Empirical formula is Na<sub>2</sub>O·Al(OH)<sub>3</sub>·xH<sub>2</sub>O

(b) Based on average packed density.

(c) Adsorbed ions are difficult to remove if mineral is heated above indicated temperature.

network. The chemical, thermal, and mechanical stability and the ion-exchange behavior of the resins depend chiefly on the structure and the degree of crosslinking of the matrix and on the nature and number of the fixed ionic groups<sup>(9)</sup>.

The degree of crosslinking determines the mesh width of the matrix and thus the swelling ability of the resin and the mobilities of the counter ions in the resin. The latter, in turn, determine the rates of ion exchange. Highly cross-linked resins are resistant to swelling and chemical and radiation damage, but exchange kinetics are favored by lower crosslinkages.

Most of the commercial resins are based on a polystyrene matrix with a small proportion of divinylbenzene added to cross-link and stabilize the resin form. The degree of crosslinkage in cation resins is usually indicated by giving the proportion of divinylbenzene added; thus, an "X8" resin is one containing 8 weight percent divinylbenzene. Anion resins may also have a considerable amount of crosslinking through the amine structure. The polystyrene resins are produced in the shape of small spheres. The standard size is about 20-50 mesh, but smaller sizes are available. Since the rate controlling step in most ion exchange reactions is diffusion, decreasing the size of the resin particles materially decreases the time required for the resin to reach equilibrium with a contacting solution. Conversely, however, the pressure drop for solutions flowing through a bed of resin increases rapidly with a decreasing particle size (by a factor of about 11 on going from 20-50 mesh resin to 50-100 mesh)<sup>(6)</sup>.

Phenolic resins, produced by phenol-formaldehyde condensation, are another, less common class of resins. They are always in the form of granular particles and possess the combination of excellent physical durability and high porosity. They are not stable in nitric acid solutions, however,

Resins are available in both strong and weak acid and base forms. The strong acid and base resins are analogous to strong acids and bases such as HCl and NaOH and remain ionized over a wide pH range. Weak acid groups, such as  $-\text{COO}^-$ , are ionized only at high pH. Likewise, weak base groups such as  $-\text{NH}_3^+$  lose a proton to form uncharged  $-\text{NH}_2$  when the pH is high. Only strong acid and base resins will be used in B-Plant although the cesium selectivity of Duolite C-3 at high pH's is related to the weak-acid phenolic group.

Selected properties of current and candidate ion exchange resins used in chemical separations at Hanford are shown in Table IV-52.

TABLE IV-52  
ION EXCHANGE RESIN PROPERTIES

(20 - 50 mesh particles)

Source of Data: References (6)(7)(9)(11)

	<u>Dowex 50, 50W</u>	<u>Duolite C-3</u>	<u>Permutit SK</u>	<u>Amberlite IRA-401</u>
Type	Cation	Cation	Anion	Anion
Active Group	$-\text{SO}_3^-$	$-\text{CH}_2\text{SO}_3^-(-\text{OH})$	pyridinium	$-\text{CH}_2\text{N}(\text{CH}_3)_3^+$
Matrix	Polystyrene	Phenolic	Polystyrene	Polystyrene
Cross Linkage, %	8 <sup>(a)</sup>	--	~4	~4
Particle Density, g/cc (moist)	1.3	1.26 ( $\text{Na}^+$ )	~1.14 ( $\text{NO}_3^-$ )	1.1 ( $\text{NO}_3^-$ )
Bulk Density, g/cc (moist beads)	0.8	0.4	0.7	0.64
Total Capacity, meq/ml (wet)	1.7 ( $\text{H}^+$ )	1.2 ( $\text{Na}^+$ )	1.4 ( $\text{NO}_3^-$ )	1.2 ( $\text{NO}_3^-$ )
meq/g (dry)	5.0 ( $\text{H}^+$ )	2.9 ( $\text{H}^+$ )	4.3 ( $\text{NO}_3^-$ )	3.6 ( $\text{NO}_3^-$ )
Swelling Due to Exchange, % <sup>(b)</sup>	8	7	10	-9
% Water	53 ( $\text{H}^+$ )	60-80	45-55	49 ( $\text{NO}_3^-$ )
Maximum Temperature, °C <sup>(c)</sup>	150	60	60	60

(a) Available at 1 to 16% crosslinkage. Standard crosslinkage is 8% (X8).

(b) For exchange from  $\text{Na}^+$  to  $\text{H}^+$  form, cation exchange resins, and from  $\text{OH}^-$  to  $\text{Cl}^-$  for anion exchange resins.

(c) For thermal stability.

### 3. Engineering Concepts

#### 3.1 Loading

Most ion exchange operations, including the B-Plant ion exchange processes, are carried out by passing a feed solution downflow through a bed of ion-exchange material where the desired ion is removed by selective adsorption on the ion exchanger. The performance of an ion-exchange column is usually defined by a breakthrough curve where the ratio of the effluent concentration to the feed concentration of the ion being removed is plotted versus the feed throughput. When the equilibrium is favorable the ion initially on the bed will be displaced and move faster through the bed than the incoming ions, producing a self-sharpening boundary between the loaded and unloaded portions of the bed. The shape of this boundary reaches a steady-state within a short distance and remains unchanged as it moves down the column. The breakthrough curve is, therefore, determined by the steady-state shape of this boundary.

Logarithmic-probability coordinates are frequently used for plotting breakthrough curves. The use of the probability scale for plotting the concentration ratio,  $C/C_0$ , and the logarithmic scale for the feed throughput largely eliminates the S-shaped curvature obtained with linear scales and makes it possible to plot accurately those values which are either very small or very near to unity.

The equation for a straight line breakthrough curve on log-probability paper<sup>(20)</sup> is given by

$$C/C_0 = 1/2 [1 + P_i(A \ln n/n_0)] \quad (6)$$

where  $C/C_0$  = ratio of the effluent concentration to the feed concentration.

$$P_i(x) = \text{normal probability integral} = \frac{1}{\sqrt{2\pi}} \int_{-x}^x e^{-\frac{t^2}{2}} dt.$$

$A$  = slope of the line on log-probability paper, dimensionless.

$n$  = column volumes of feed solution.

$n_0$  = column volumes of feed at 50% breakthrough ( $C/C_0 = 0.5$ ).

This type of breakthrough curve is obtained in most, if not all, of the loading processes described in this section.

The slope,  $A$ , of the breakthrough curve is a measure of the process kinetics and is a complex function of the ion exchanger properties and operating conditions. It approximately corresponds to  $\sqrt{N}$  and  $\sqrt{\frac{N_R}{2}}$ , where  $N$  is the number of theoretical plates in the correlation method of Gluekauf<sup>(8)</sup> and  $N_R$  is the number of reaction units as defined by Heister and Vermeulen<sup>(18)</sup>:

$$N_R = \frac{k_F v}{F} \quad (7)$$

where  $k_F$  = reaction rate constant

$v$  = packed bed volume (column volume)

$F$  = volumetric flow rate

The ratio  $F/v$  represents the feed flow rate in column volumes per unit time; thus  $A$  should be inversely proportional to the square root of the flow rate in column volumes/hour.

A series of breakthrough curves are plotted in Figure IV-67 to illustrate the effect of variations in  $A$ . The use of the ratio  $n/n_0$  rather than  $n$  in this plot eliminates the capacity of the exchange material as a variable and is a convenient way to compare kinetic behavior at different operating conditions or with different ion exchange materials. Note that increasing values of  $A$  correspond to improved utilization of the column capacity.

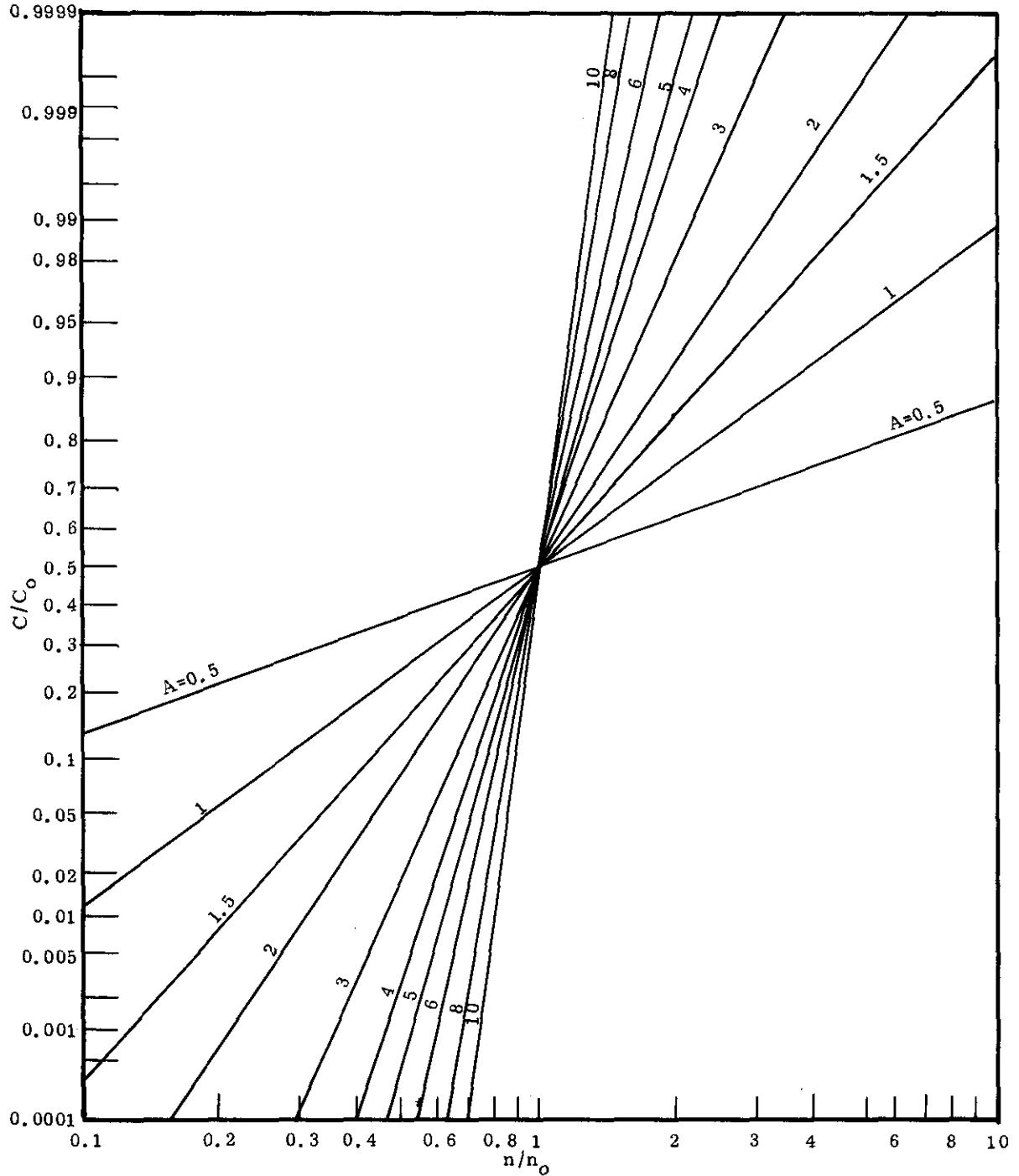


FIGURE IV-67

Logarithmic-Probability Plot of Breakthrough Curves  
Showing the Effect of the Parameter "A"

The area under the breakthrough curve from 0 to  $n$  column volumes is a measure of cumulative loss to the effluent stream; that is,

$$\text{Waste Loss Fraction} = \text{WLF} = \frac{1}{n} \int_0^n \frac{C}{C_0} \, dn \quad (8)$$

After substitution of the value of  $C/C_0$  from equation (6), this can be integrated to give

$$\text{WLF} = \frac{C}{C_0} - \frac{n_0}{2n} e^{1/2A^2} \left[ 1 + P_i \left( A \ln \frac{n}{n_0} - \frac{1}{A} \right) \right] \quad (9)$$

The effect of  $A$  on the waste loss fraction is shown as a function of  $n/n_0$  and  $C/C_0$  in Figures IV-68 and IV-69.

The capacity of the ion exchange bed in equilibrium with the feed solution can be expressed in terms of column volumes by the relationship

$$n_L = \frac{Qq\rho}{C_0} \quad (10)$$

where  $Q$  = maximum exchange capacity of the ion exchange material, meq/g.

$q$  = equivalent fraction of the adsorbing ion on the ion exchanger in equilibrium with the feed,

$C_0$  = concentration of adsorbing ion in the feed, meq/ml

$\rho$  = bulk density of the ion exchange bed, g/ml

Hence,  $n_L$  is equal to the equilibrium distribution ratio in volumetric concentration units and represents the minimum number of column volumes of feed solution required to fully load the bed (at  $A = \infty$ ).

The term  $n_L$  is often used interchangeably with  $n_0$ , the number of column volumes required to reach 50 percent breakthrough; however at low values of  $A$ , the two numbers differ considerably, as shown in the following derivation:

1. As  $n$  approaches infinity, the area above the breakthrough curve from  $C/C_0 = 0$  to  $C/C_0 = 1$  will approach  $n_L$  as a limit:

$$n_L = \lim_{n \rightarrow \infty} [n(1 - \text{WLF})]. \quad (11)$$

2. If the straight line breakthrough curve relationship on log-probability still applies as  $n$  approaches infinity, Equation (9) simplifies to

$$\text{WLF} = 1 - \frac{n_0}{n} e^{1/2A^2} \quad (12)$$

3. Thus,

$$n_L = n \left( 1 - 1 + \frac{n_o}{n} e^{1/2A^2} \right) = n_o e^{1/2A^2} \quad (13)$$

A plot of  $(n_L/n_o) - 1$  is presented in Figure IV-70. Note that the difference between  $n_L$  and  $n_o$  becomes less than 2 percent when  $A$  exceeds 5 and that  $n_L/n_o$  can be closely approximated by  $1 + 1/(2A^2)$  when  $A$  is larger than 3.

The breakthrough curve is fully defined when  $n_L$  and  $A$  are known or can be estimated by empirical relationships.  $A$  is usually determined from experimental breakthrough data;  $n_L$  is readily determined from equilibrium distribution ratio data. Plots of  $n/n_o$  vs  $A$  at several levels of  $C/C_o$  are presented in Figure IV-71 to aid in the construction of breakthrough curves.

### 3.1.1 Sample Calculation: Estimation of Cesium Breakthrough Curve

Equilibrium data for loading cesium on Linde AW-500 zeolite are presented in Figure IV-78. For Purex alkaline supernate (PSN), the cesium concentration in the feed ( $C_o$ ) is about 0.0008, the mole ratio of  $Cs^+/Na^+$  is about  $0.0008/4 = 0.0002$  and the corresponding cesium loading (neglecting the effect of trace amounts of competing potassium and rubidium) is about 0.061 mole of Cs/liter of AW-500. Then from Equation (10),

$$n_L = \frac{Qq_o}{C_o} = \frac{0.061}{0.0008} = 76.3$$

A correlation for estimating the slope of the breakthrough curve for Purex supernate solution and 20-50 mesh zeolite is presented in Section F 4.2.3 (Equation 23). Assume that the column is operated at a superficial velocity of 1.8 gal/min-ft<sup>2</sup> and a total flow rate of 1.5 column volumes/hr. Then

$$A = \frac{7.1 v^{0.125}}{R^{0.55}} = \frac{7.1 (1.8)^{0.125}}{(1.5)^{0.55}} = 6.1$$

The volume of feed required to reach the 50 percent breakthrough point is given by Figure IV-70 or Equation (13):

$$n_o = n_L e^{-1/2A^2} = 76.3 e^{-0.0134} = 75.3 \text{ column volumes.}$$

The volume of feed required to reach any other cesium breakthrough point can be estimated from Figure IV-71. Thus, at  $C/C_o = 0.01$  and  $A = 6.1$ , the value of  $n/n_o = 0.69$  and  $n = (0.69)(75.3) = 52$  column volumes. Similarly,  $n = 61$  column volumes at  $C/C_o = 0.1$ . These data, plotted on log-probability coordinates, will lie on a straight line.

The cumulative loss for a given breakthrough level can be determined from Figure IV-69. For example at 10 percent breakthrough and  $A = 6.1$ , the cumulative cesium loss is 0.7 percent. Alternatively, the column can be operated to 23 percent breakthrough without exceeding a cumulative loss of 2 percent.

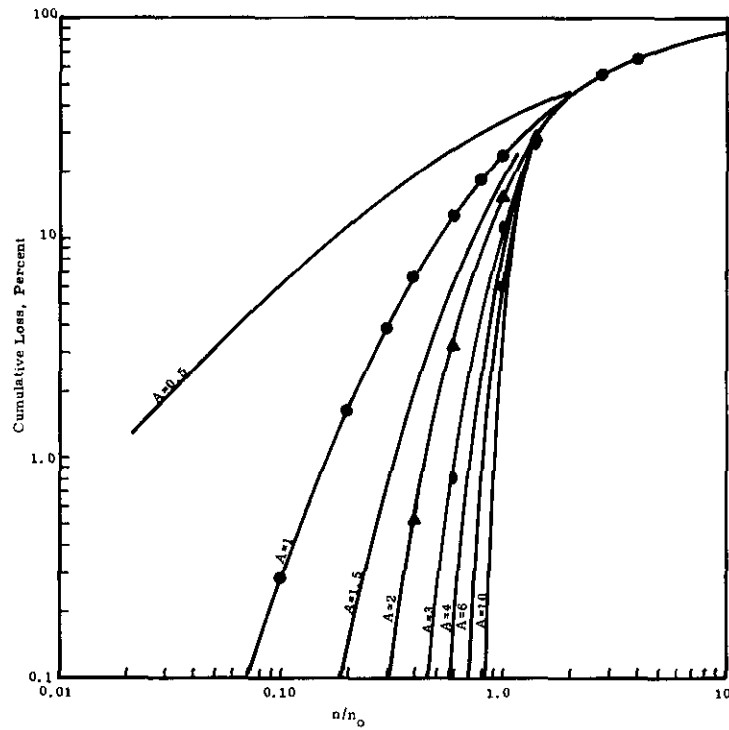


FIGURE IV-68

Cumulative Percent Breakthrough Loss  
As a Function of A and the Throughput Ratio,  $n/n_0$

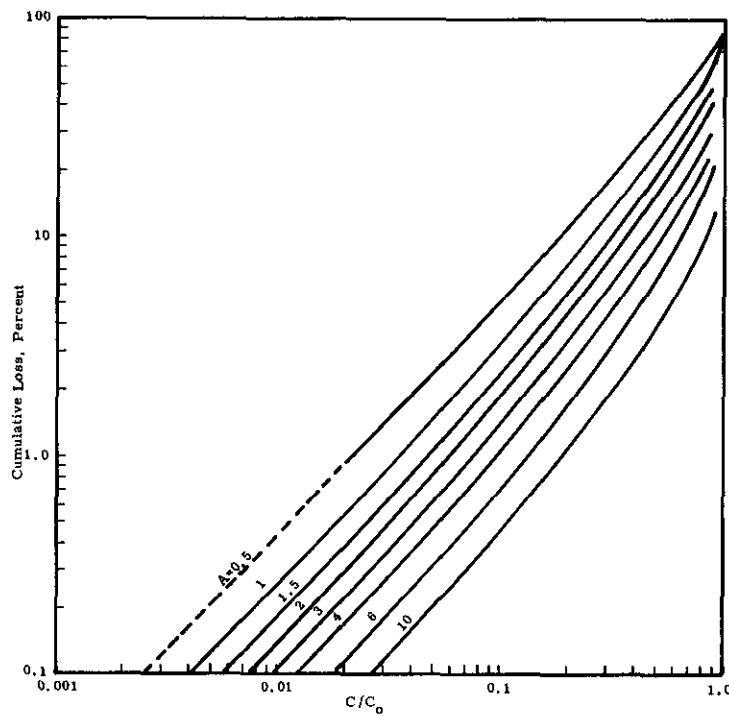


FIGURE IV-69

Cumulative Percent Breakthrough Loss  
As a Function of A and  $C/C_0$